UNIVERSITY OF CALIFORNIA, SAN DIEGO

Design and Synthesis of Archaea-Inspired Tetraether Lipids

A dissertation submitted in partial satisfaction of the requirements for the degree Doctor of Philosophy

in

Chemistry

by

Takaoki Koyanagi

Committee in charge:

Professor Jerry Yang, Chair
Professor Michael Burkart
Professor Michael Gilson
Professor Francesco Paesani
Professor Charles Perrin

2017

The dissertation of Takaoki Koyanagi is approved, and it is acceptable in quality and form for publication on microfilm and electronically:

_____

_____

_____

_____

_____

Chair

University of California, San Diego

2017

TABLE OF CONTENTS

LIST OF ABBREVIATIONS

a.u. = arbitrary units

°C = degrees Celsius

$CaCl_2$ = calcium chloride

CBz = carboxybenzyl

$CDCl_3$ = deuterated chloroform

δ = NMR chemical shift

d = doublet

DCM = dichloromethane

DHP = 3,4-dihydro-2H-pyran

DIBALH = diisobutylaluminum hydride

DLS = dynamic light scattering

DMF = dimethylformamide

DMP = Dess-Martin periodinane

DMSO = dimethylsulfoxide

DMT = dimethoxytrityl

DSC = differential scanning calorimetry

EDTA = ethylenediaminetetraacetic acid

EPC = L-α-phosphatidylcholine (egg,chicken)

EPR = enhanced permeation and retention

ESI = electron spray ionization

Et = ethyl

EtOac = ethylacetate

EtOH = ethanol

FDA = food and drug administration

g= grams

h= hours

HCl = hydrochloric acid

HBr = hydrobromic acid

HBS = hepes buffered saline

Hepes = 2-[4-(2-hydroxyethyl)piperazin-1-yl]ethanesulfonic acid

HPMA = poly[N-(2-hydroxypropyl) methacylamide]

Hz = Hertz (s^{-1})

J = NMR coupling constant

K = Kelvin, thousand

KOH = potassium hydroxide

λ_{abs} = absorbance wavelength

λ_{em} = emissions wavelength

λ_{ex} = excitation wavelength

L = liters

LAH = lithium aluminum hydride

m = meters, multiplet

*m*CPBA = meta chloroperoxybenzoic acid

Me = methyl

MeOH = methanol

MPS = mononuclear phagocyte system

mol = moles

MS = mass spectrometry

M_w = molecular weight

Nab = nanoparticle albumin bound

NaCl = sodium chloride

NIS = *N*-iodosuccinimide

NMR = nuclear magnetic resonance

NP = nanoparticle

PAcM = poly(N-acryloyl morpholine)

PBS = phosphate buffered saline

PDMA = poly(N,N-dimethylacrylamide)

PEG = polyethylene glycol

PMOX = poly(2-methyl-2-oxazoline)

POPC = 1-palmitoyl-2-oleoylphosphatidylcholine

PVP = poly(vinylpyrrolidone)

q = quartet

R = organic group

rt = room temperature

s = seconds, singlet

siRNA = small interfering ribonucleic acid

t = triplet

T = temperature

TBAB = tetra-n-butylammonium bromide

TBDMS = tert-butyldimethylsilyl

TEA = triethylamine

TFA = trifluoroacetic acid

THF = tetrahydrofuran

THP = tetrahydropyran

UV = ultraviolet

LIST OF FIGURES

LIST OF SCHEMES

LIST OF TABLES

ACKNOWLEDGEMENTS

I would like to thank Professor Jerry Yang for his support and his guidance to foster my development to write and publish scientific literature.

I would like to thank Dr. Geoffray Leriche for his countless scientific discussions guiding me to design and finish projects with ease. Without his help, my research would not have been completed in less than 4 years.

I would like to thank John Kim for watching over my dog, Dio, which allowed me to take time away from lab to decompress.

Chapter 2 is adapted, in part, from Takaoki Koyanagi, Geoffray Leriche, David Onofrei, Gregory P. Holland, Michael Mayer, and Jerry Yang. “Cyclohexane Rings Reduce Membrane Permeability to Small Ions in Archaea-Inspired Tetraether Lipids.” *Angew. Chem., Int. Ed.* 2016, *55*, 1890–1893. Copyright 2016 Wiley. Permission to use copyrighted images and data in the manuscript was also obtained from Geoffray Leriche, David Onofrei, Gregory P. Holland, Michael Mayer, and Jerry Yang. The dissertation author is the first author of this manuscript. Chapter 2 is also adapted, in part, from Takaoki Koyanagi, Geoffray Leriche, Alvin Yep, David Onofrei, Gregory P. Holland, Michael Mayer, and Jerry Yang. “Effect of Headgroups on Small-Ion Permeability across Archaea-Inspired Tetraether Lipid Membranes. *Chem.” - Eur. J.* 2016, *22*, 8074–8077. Copyright 2016 Wiley. Permission to use copyright images and data in the manuscript was also obtained from Geoffray Leriche,

Alvin Yep, David Onofrei, Gregory P. Holland, Michael Mayer, and Jerry Yang. The dissertation author is the first author of this manuscript. Chapter 2 is also adapted, in part, from Thomas B. H. Schroeder, Geoffray Leriche, Takaoki Koyanagi, Mitchell A. Johnson, Kathryn N. Haengel, Olivia M. Eggenberger, Claire L. Wang, Young Hun Kim, Karthik Diraviyam, David Sept, Jerry Yang, and Michael Mayer. “Effects of Lipid Tethering in Extremophile-Inspired Membranes on H+/OH− Flux at Room Temperature.” *Biophys. J.* 2016, *110*, 2430–2440. Copyright 2016 Elsevier. Permission to use copyright images and data in the manuscript was also obtained from Thomas B. H. Schroeder, Geoffray Leriche, Mitchell A. Johnson, Kathryn N. Haengel, Olivia M. Eggenberger, Claire L. Wang, Young Hun Kim, Karthik Diraviyam, David Sept, Jerry Yang, and Michael Mayer. The dissertation author is a co-author.

Chapter 3 is adapted, in part, from Takaoki Koyanagi, Kevin J. Cao, Geoffray Leriche, David Onofrei, Gregory P. Holland, Michael Mayer, David Sept, and Jerry Yang, “Hybrid Lipids Inspired by Extremophiles and Eukaryotes Afford Serum-Stable Membranes with Low Leakage.” *Chem. - Eur. J.* 2017, 23, 6757–6762. Copyright 2017 Wiley. Permission to use copyrighted images and data in the manuscript was obtained from Kevin J. Cao, Geoffray Leriche, David Onofrei, Gregory P. Holland, Michael Mayer, David Sept, and Jerry Yang. The dissertation author is the first author of this manuscript.

Chapter 4 is adapted, in part, from Takaoki Koyanagi, Jessica L. Cifelli, Geoffray Leriche, David Onofrei, Gregory P. Holland, and Jerry Yang, “Thiol-

triggered release of intraliposomal content from liposomes made of extremophile-inspired tetraether lipids." *Bioconjugate Chem.* 2017, ASAP. Copyright 2017 American Chemical Society. Permission to use copyrighted images and data in the manuscript was obtained from Jessica L. Cifelli, Geoffray Leriche, David Onofrei, Gregory P. Holland, and Jerry Yang. The dissertation author is the first author of this manuscript.

VITA

2007 Bachelor of Science, Illinois State University

2009 Masters of Science, Illinois State University

2010 Manufacturing Associate II, Spherotech inc.

2016 Medicinal Chemistry intern., Vertex Pharmaceuticals

2017 Doctor of Philosophy, University of California, San Diego

PUBLICATIONS

"Thiol-triggered release of intraliposomal content from liposomes made of extremophile-inspired tetraether lipids " **T. Koyanagi**, J. L. Cifelli, G. Leriche, D. Onofrei, G. Holland, J. Yang. *Bioconjugate Chemistry,* **2017**, 28, 2041-2045*.*

"Hybrid lipids inspired by extremophiles and eukaryotes afford serum stable membranes with low leakage" **T. Koyanagi**, K. Cao, G. Leriche, D. Onofrei, G. Holland, M. Mayer, D. Sept, J. Yang. *Chemistry – A European Journal,* **2017**, 23, 6757–6762*.*

"Characterization of drug encapsulation and retention in archaea-inspired tetraether liposomes" G. Leriche, J. L. Cifelli, A, K. C. Sibucao, J. P. Patterson, **T. Koyanagi** , N. C. Gianneschi, J. Yang. *Organic & Biomolecular Chemistry,* **2017**, *15,* 2157-2162*.*

"Effect of of headgroups on small ion permeability across Archaea-inspired lipid membranes" **T. Koyanagi**, G. Leriche, A. Yep, D. Onofrei, G. Holland, M. Mayer, J. Yang. *Chemistry – A European Journal,* **2016**, *22,* 8074-8077.

"Effects of Transmembrane Tethers in Extremophile-Inspired Lipid Membranes on H^+/OH^- Flux at Room Temperature" T. B. H. Schroeder, G. Leriche, **T.Koyanagi**, M. A. Johnson, K. N. Haengel, O. M. Eggenberger, C. L. Wang, Y. H. Kim, K. Diraviyam, D. Sept, J. Yang, M. Mayer. *Biophysical Journal*, **2016**, *110*, 2430-2440.

"Cyclohexane rings reduce membrane permeability to small ions in Archaea-inspired tetraether lipids" **T. Koyanagi**, G. Leriche, D. Onofrei, G. Holland, M. Mayer, J. Yang. *Angewandte Chemie, International Edition*, **2016**, *128*, 1890-1893.

"Solvent-free synthesis of monoacylaminals from the reaction of amides and aminals as precursors in carbinolamide synthesis" M. Sansone, **T. Koyanagi**, D. Przybyla, R. Nagorski. *Tetrahedron Letters,* **2010**, *51*, 6031-6033.

"(6R)-2-tert-Butyl-6-[(4R,5S)-3-isopropyl-4-methyl-5-phenyloxazolidin-2-yl]phenol" **T.Koyanagi**, K. Edler, R. Parrott II, S. Hitchcock, G. Ferrence. *Acta Crystallographica Section E*. **2010**, *E66*, 0898-0899.

PATENTS

"Bipolar Tetraether Lipids" J. Yang, **T. Koyanagi**, G. Leriche, M. Mayer: (**WO2017040702**)

ABSTRACT OF THE DISSERTATION

Design and Synthesis of Archaea-Inspired Tetraether Lipids

by

Takaoki Koyanagi

Doctor of Philosophy in Chemistry

University of California, San Diego, 2017

Professor Jerry C. Yang, Chair

Maintaining the correct ion homeostasis across membranes is a major challenge in both nature and artificial systems. Archaea, have evolved to solve membrane permeability problems to survive in extreme environments by incorporating unique structural features found in their lipid. Specifically, inclusion of phytanyl side chains, ether glycerol linkages, tethering of lipids,

cycloalkanes, and different polar lipid headgroups into their lipid membrane are believed to contribute to membrane stability.

We sought to gain a better understanding of the functional benefits attributed to these structural features to membrane stability to design a new class of synthetic Archaea inspired lipid membranes that can be used to overcome limitations (i.e. unstable in serum environment, high background leakage, and prone to hydrolysis) found in current lipid based technologies. Leakage experiments revealed liposomes made from **GMGTPC** (glycerol monoalkyl glycerol tetraether lipid with phosphatidylcholine headgroup) demonstrated a two order magnitude reduction in membrane leakage to small ions when compared with liposomes made from EggPC. Additionally, liposomes composed of **GMGTPC-CH** (cyclohexane integrated) lipid displayed an additional 40% decrease in membrane leakage to small ions when compared with liposomes made from **GMGTPC** lipids. Furthermore, leakage experiments revealed a higher degree of tolerance to headgroup modifications to membrane leakage for liposomes made from **GMGT** lipid analogs when compared with liposomes made from POPC.

After designing an optimal tetraether lipid scaffold that incorporates key Archaeal structural features for membrane leakage, we explored to integrate strategies employed by eukaryotes to improve membrane properties (i.e. addition of cholesterol). Liposomes made from the hybrid lipid, **GcGTPC-CH,** displayed a five-fold decrease in membrane leakage when compared with

liposomes made from **GMGTPC-CH,** while maintaining functional membrane properties similar to membranes made from diacyl lipids.

Lastly, we engineered a thiol responsive hybrid lipid, **GcGT(S-S)PC-CH**, that demonstrated similar membrane stability in serum as **GcGTPC-CH**. Gratifyingly, doxorubicin loaded liposomes composed of **GcGT(S-S)PC-CH** liposomes displayed a 4 or 20-fold increase in toxicity to HeLa cells when compared with liposomes made from **GcGTPC-CH** or Doxil, respectively.

This work represents a first step towards development of stimuli-responsive tetraether lipids that may offer advantages in membrane properties to be used in cancer therapy.

Chapter 1

Introduction

1.1 Introduction to Nano-Drug Delivery Systems

Drug delivery systems have been investigated for the process and administration of pharmaceutical compounds to improve therapeutic effect in a clinical setting.[1–8] To date, most nanomedicines in clinical developments are formulations or synthetic derivatives of previously FDA approved drugs which are more effective and more tolerable than with systemic delivery.[1,3,5,9–11] Some examples of improvements in therapeutic effects include controlling pharmacokinetics, reducing side effects, targeted delivery of drug, and reducing toxicity of the drug. [1,3,8,12–14] Several different delivery systems have been synthesized and investigated for tunable anti-cancer treatment to improve therapeutic effects.[3] The term “nanomedicine” was first used to represent nano-drug delivery systems that uses molecular tools and knowledge of human body for medical diagnosis and treatment in the 1990’s, with the first research published in 2000.[6,7] An illustration of historical timeline, designed by Shi *et. al,* depicting some selected major developments of nanomedicine beginning with the structural discovery of liposomes in the mid-1960s and continuing on to more recent development of polymers can be observed in Figure 1.1. Since 1995, at least 50 nanoparticle-based drugs (typically hydrophobic molecules)

have entered clinical practice.[5] In the brief time since discovery, research in nanomedicine has led to developments in imaging agents, *in vitro* diagnostics, therapeutics, and medical devices with over 200 nanomedicines that have been approved or under clinical investigations by the FDA.[4,15,16] Examples of popular nanomedicines under investigation includes protein nanoparticles, polymer drug conjugates, polymeric micelles and nanoparticles, dendrimers, and liposomes.[5]

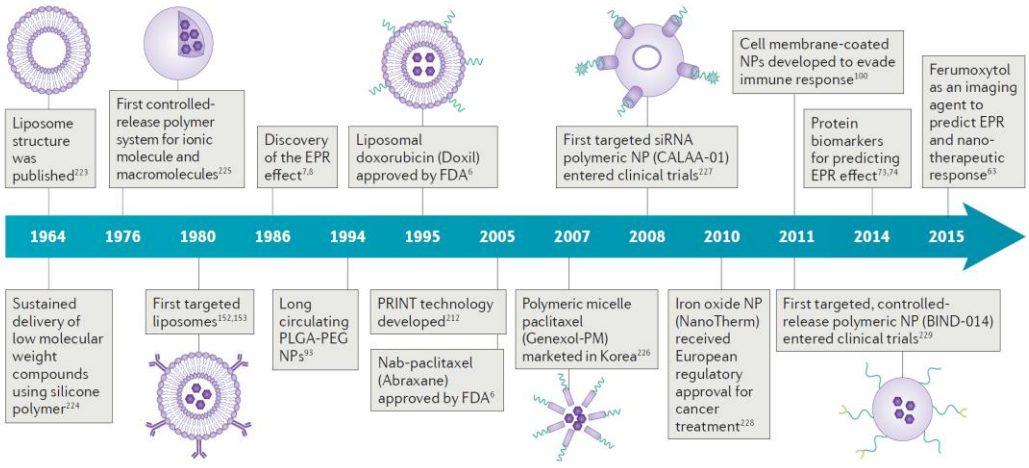

Figure 1.1. Historical timeline of major developments in the field of cancer nanomedicine. Reprinted by permission from Macmillan Publishers Ltd: [Nature Reviews Cancer] (Shi, J.; Kantoff, P. W.; Wooster, R.; Farokhzad, O. C. *Nat. Rev. Cancer* **2016**, *17* (1), 20–37.), copyright (2016)

1.1.1 Polymeric Nanoparticles for Drug Delivery

Protein nanoparticles are typically protein (albumin) bound drug-nanoparticles that improve solubility and *in vivo* delivery of poorly soluble drugs.[1,17,18] One example, Abraxane®,[18] is an albumin-bound formulation of

paclitaxel (FDA approved chemotherapeutic agent to treat solid tumors that is was originally extracted from the bark of the western yew tree, *Taxus brevifolia*).[19] Studies have shown, conjugation of paclitaxel to albumin prior to administration increases solubility and obtain desired PK of paclitaxel *in vivo*.[18] For example, Abraxane® has been shown to provide superior efficacy towards metastatic cancer with reduced toxicity and elimination of acute drug hypersensitivity when compared with Cremophor/ethanol-based formulation of Taxol, (drug marketed as Kolliphor® EL).[20] One concern, however, when using albumin is the potential infection and transmission of disease from donated plasma. To reduce the potential for disease transmission from HSA extracted from donated plasma, a recombinant human albumin (Recombumin®) has been developed by Novozymes.[21] Recombumin®, recombinant human albumin, has also been shown to be effective as: 1) an inhibitor for adsorption of the active molecules to the storage bottle, 2) a surfactant to aid in solubilization of the drug, and 3) a stabilizer of conformational structures of the molecules to remain active during storage.[21] Although, conjugation of paclitaxel to albumin prior to administration is relatively straightforward, protein nanoparticles are limited in versatility (restricted in use for formulation of hydrophobic drug molecules) and improved pharmacokinetic properties for other drugs are not guaranteed.

While polymer drug conjugates share similar advantages for formulation drugs as protein nanoparticles, they differ in the physical/chemical linkage used to attach drugs to polymers.[22] Systematic administration of synthetic drugs or biomolecules have been shown to be limited by the short half-life of the

molecules in circulation caused by renal clearance or enzymatic degradation.[5] For instance, chemical conjugation of drug, protein, or peptide to polyethyleneglycol (PEG) polymers has been shown to improve solubility, tunability of drug size, controllability of PK, and stability by reducing immune-mediated clearance and enzyme-mediated degradation.[11,22,23] Another example, Xyotax™, a drug conjugate formulation of paclitaxel that was under investigation as a treatment for cancer, evolved to Opaxio®, a nanomedicine that functionalizes paclitaxel to polyglutamic acid through ester bonds.[24] The polyglutamate functionalized paclitaxel showed large improvement in PK of systemic injections of paclitaxel alone with an added control of slow release of paclitaxel. The slow controlled release of paclitaxel was dictated by the rate of ester hydrolysis from the conjugated formulation in Opaxio.[25] This method of covalently attaching paclitaxel to the polyglutamic backbone allows for similar advantages discussed for protein nanoparticles, however, suffers from problems associated with challenges in drug efficacy from chemical modification of the drug.[26]

Polymeric micelles differ from other polymer conjugated drugs, which removes the additional challenges of covalently attaching drug molecules to the polymeric backbone.[26] Polymeric micelles passively encapsulate solubilized drugs inside a preformed polymeric micelle or nanoparticle.[27] Micelles are formed by the addition of amphiphillic surfactant or polymeric molecules to aqueous media that spontaneously associate to form core-shell structures.[27,28] Typical polymeric monomers used to form polymeric micelles include

poly(ethyleneoxide)-poly(benzyl-L-aspartate) and poly(N-isopropylacrylamide)-polystyrene.[29] An alternative formulation to aforementioned Abraxane® (protein nanoparticle formulation of palcitaxol), Genexol-PM® is a polymeric micelle formulation of paclitaxel devoid of Cremophor solvent that uses biodegradable amphiphillic diblock co-polymer poly(ethylene-glycol)-block-poly(D,L-lactide)(mPEG-DDLLA).[17] Genexol-PM® has been shown to be less toxic and increased tumor uptake when compared with solvent-formulated paclitaxel.[5] The observed increased drug uptake into tissues is believed to be promoted by an increased vascular permeability when compared with free drugs.[28] Despite the advantages discussed, however, the predominant hydrophobic character of micelle structures limits passive encapsulation of drugs to hydrophobic molecules and creates further disadvantages of low encapsulation efficiency.[27]

Dendrimers, the most recent polymeric technology under investigation as the next nanomedicine, are discrete nanostructures that are branched layers that grow outwards from the core.[2] Dendrimers are synthesized by starting with a core and grow stepwise (convergent or divergent polymerization) in concentric layers to increase in size, akin to globular proteins or onions.[30] Unlike traditional polymeric nanoparticles, dendrimers are the only known synthetic nanoparticle that allows for mathematically defined synthetic control and systematic engineering of nanostructures with total control that allows for a more versatile nanomedicine when conjugated with drugs.[2] For example, Vivagel® is an FDA approved topical antiviral dendrimeric formulations made with an anionic G4-poly(L-lysine)-type dendrimer displaying 32 naphthalene disulfonate groups on

the surface.[31] Additional advantages dendrimers have over other polymeric nanoparticles includes the ability to deliver 20-40% w/w of encapsulated or conjugated drugs, tunable size to make <10 nm dendrimer-drug conjugates, and mechanically robust enough to be freeze dried for storage.[2] However, due to the intricate design of the tunable branched polymers, difficult synthesis and high cost of production has been a barrier to be used successfully in cancer therapy.[29]

1.1.2. *Liposomes as Drug Delivery Systems*

Liposomes are self-assembled colloidal particles (shown in Figure 1.2) that are biocompatible, biodegradable, non-toxic, long circulating, targetable, and high drug loading drug delivery system that are typically made with phospholipid that occur naturally or prepared in a laboratory setting. The first structural characterization of liposomes was featured by Bangham and Horne in the mid-1960 using electron microscopy.[32–39] Liposomes were first studied by Bangham *et al.* as a platform to study biological membranes, however, liposomes began to garner interest as potential drug delivery system in the late 1960's.[32,33] The advantage of liposomes compared with other nano-drug delivery systems is their ability to tailor properties for delivering a range of cargo (hydrophilic and hydrophobic molecules), due to the ready access to a toolbox of commercial lipids with known biophysical properties.[40] Other lipid options include lipid extracted from organisms or synthesized through rational design

equipped with a variety of headgroups, linkers and hydrophobic tails.[41] The ability to mix and match different lipids to obtain the exact membrane property necessary for a liposomal delivery system with control over liposome macrostructures, biophysical characteristics and *in vivo* properties allows for a powerfully adaptable drug delivery system for a variety of applications.[33] Despite the promising drug delivery properties of liposomes, early results of liposomes as a drug delivery vehicle, however, was stifled by their colloidal and biological instability, inefficient and unstable encapsulation of drug molecules.[8,42]

The initial limitation liposomes faced was rapid clearance of large multilamellar liposomes by mononuclear phagocyte system (MPS). Traditionally, liposomes were made by creating a thin film of lipid on a glass container by first dissolving lipids in an organic solvent, continued by evaporation of the organic

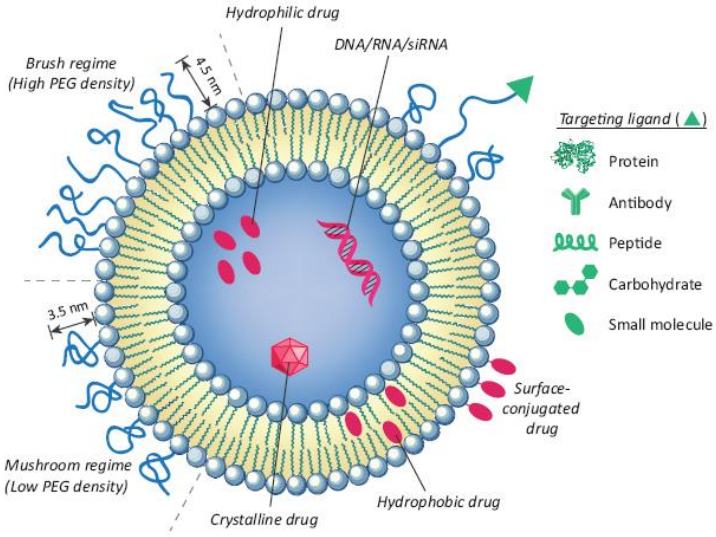

Figure 1.2. Illustration of liposomes used for nanomedicine. © {2014} {Melis Çağdaş, Ali Demir Sezer and Seyda Bucak}. Originally published in {Liposome as potential drug carrier systems for drug delivery, Chapter 1, Figure 1; open access} under {CC BY 3.0} license. Available from: {doi. 10.5772/58459}[135]

solvent.[35,43] The thin film was then hydrated in a buffer containing drugs and the lipids self-assemble into large multilamellar vesicles.[35,43] To improve evasion from MPS, liposomes formed with methods of extrusion, that further processes large multilamellar vesicles through a porous membrane or homogenization, allowed for production of smaller uniform liposomes with an average diameter of ~100 nm, which resulted in slower uptake by the MPS.[37] In addition to the reduced liposomal uptake by the MPS, liposomes smaller than 100 nm were observed to increase drug accumulation in cancer tissues owing to a phenomena coined the enhanced permeability and retention (EPR) effect.[38,44,45] Thus, liposomes with low background leakage that are <100 nm in diameter can be used to target tumor tissues while minimizing drug interaction with other tissues to reduce side effects compared with formulation of free drugs.[46–48]

The next improvement for liposomal technology that followed control of size distribution was the discovery of addition of free cholesterol to liposomal formulations to increase membrane stability.[49] In mammalian cells, sterols have been observed to be vital in regulating membrane fluidity.[50] While free cholesterol does not form bilayer structures on their own, due to their amphiphillic structure, cholesterol can integrate inside liposome bilayers.[51] The addition of cholesterol to liposomal formulation is believed to strengthen the mechanical bilayer properties and inhibit protein interactions with the liposomes. For example, addition of free cholesterol to liposomal formulations has been shown to reduce interaction with opsonins, a protein that has been observed to

tag liposomes, that signals macrophages to rapidly clear liposomal from the body.[52] Furthermore, liposome formed with the addition of 40 mol% of free cholesterol to longer saturated diacyl lipids, that are solid at room temperature, have been observed to eliminate phase transition by forcing bilayers into a stable gel-like state allowing for easier formation of liposomes without the need of external heating.[47]

The recent discovery that paved the road for liposomes to be used as drug carriers was the development of different liposomal drug encapsulation methods using passive or active loading.[53,54] When the drug is loaded passively, the hydrophilic drugs are introduced in the hydration solution during liposomal formation.[55] Using the method of freeze thaw technique, which uses a sequence of freezing and thawing of liposome suspensions, allows for an increase in unilamellar vesicles and a decrease in multilamellar vesicles promoted by transient hole formation by the development of ice crystals that increase drug penetration and liposome volume.[54] However, even with the application of freeze thaw technique that has been shown to increase encapsulation of drug inside the liposomes, only 5 – 20% of the drug molecule has been observed to retain inside the liposome after removal of free drug.[54] Another passive encapsulation technique, called ethanol injections, begins with a solution of lipid dissolved in ethanol that is then rapidly injected into an excess of drug solution using a thin needle to form unilamellar liposomes with a defined diameter (controlled by lipid concentration, injection rate, temperature and lipid

composition).[56] This strategy of forming liposomes was shown to be less favorable, due to the unresolved low encapsulation efficiency and reduced concentration of the drug caused by the presence of ethanol in liposomal solution.[57]

To address the low encapsulation efficiency of drugs inside liposomes, an alternative method termed active loading was established by Nicols, Deamer, and Bally.[58,59] The method of active loading differs from passive loading, in that, the drug is loaded after the liposomes have formed. The active loading process is performed by first achieving either an acidic (intraliposomal) or ammonium sulfate concentration gradient across the internal and external liposomal environment. Next, the liposomes encapsulated with either acid or ammonium sulfate is introduced to a solution of a weakly basic drug dissolved in a buffer containing media, typically PBS or HBS. As the neutral weak base, the drug permeates inside the liposomal membrane, the weak base becomes protonated inside the liposomes, thus, trapping the protonated molecule inside the liposome.[58–60] Anticancer drugs such as doxorubicin, idarubicin, or daunorubicin can be loaded in a drug to lipid ratio of 0.3 % w/w with an encapsulation efficiency of nearly 100% with excellent *in vitro* stability.[61]

The collective Improvements to liposomal formulations mentioned above allowed for the development and FDA approval of DOXIL® (doxorubicin, ALZA Corporation, USA), Myocet™ (doxorubicin, Enzon Pharmaceuticals, Inc., USA), DaunoXome (daunorubicin, NeXtar Pharmaceuticals, USA), and Marqibo®

(vincristine, Talon Therapeutics, USA), and DepoCyt® (cytarabine, Pacira, USA) for cancer therapy.[62,63] However, very few liposomal nanomedicines have recently been approved. We hypothesize that further exploration to generate more stable synthetic lipids with improved membrane properties can aid in the development of more FDA approved liposomal formulations.

1.2. Different Synthetic Methods to Improve Liposome Stability

1.2.1 Synthetic Diacyl Lipids to Improve Liposomal Stability

From the advent of liposomes, several research groups have advanced liposomal technology by synthesizing diacyl lipids with reduced passive leakage and improved serum stability. One of the largest milestone of synthetic diacyl lipid developed by Papahadjopoulos *et al.* began with the invention of steric stabilized liposomes by chemically conjugating hydrophilic polymers to diacyl lipids.[64] The most common chemical modification reported for diacyl lipid conjugation is by covalently attaching polyethylene glycol (PEG) to a phosphatidylethanolamine lipid through the formation of an amide bond. When sterically stabilized lipid derivative was added to liposomal formulation (5% w/w) to another non-functionalized commercial diacyl phospholipid, it was observed to protect the liposome surface from penetration and destruction by plasma proteins and also reduced macrophage uptake.[36,44,65]

Since the discovery of PEG functionalized diacyl lipids, the addition of PEG lipids to liposomal formulations has been a staple in current FDA approved drug delivery products due to the increased aqueous solubility, low cost of manufacturing, and biocompatibility.[25] Despite the favorable attributes gained by the addition of PEG functionalized diacyl lipids to liposomal formulations, the addition of PEG was not immunologically inert as first believed.[66,67] Studies have shown that even a low dose of PEGylated material can initiate an immune response to generate anti-PEG IgM antibodies in various species upon the first injection.[37,68] Subsequent injections resulted in the rapid clearance of the PEGylated therapeutic that require multiple doses within the window of the accelerated blood clearance effect of PEGylated therapeutics (3-28 days after first dose).[69] In some severe cases, the liposomes that were not taken up by the MPS or did not get excreted from the body, would accumulated in the epithelial cells causing toxic effects known as hand-foot syndrome and stomatitis.[70] To circumvent the negative effects of PEG while maintaining the beneficial effects of adding PEG to liposomes, several research groups have synthesized PEG alternatives such as PMOX,[71,72] PAcM,[73] PDMA,[74] polyglycerol,[69] PVP,[75] and HPMA[76] that have demonstrated increase circulation half-life while reducing the formation of anti-PEG IgM[71].

Another problem encountered in liposomal technology was the leaching of free cholesterol from liposomes during circulation by rapid transfer into biomembranes and lipoproteins, resulting in membrane destabilization of the liposomes. [77,78] To prevent the leaching and transfer of free cholesterol, Szoka's

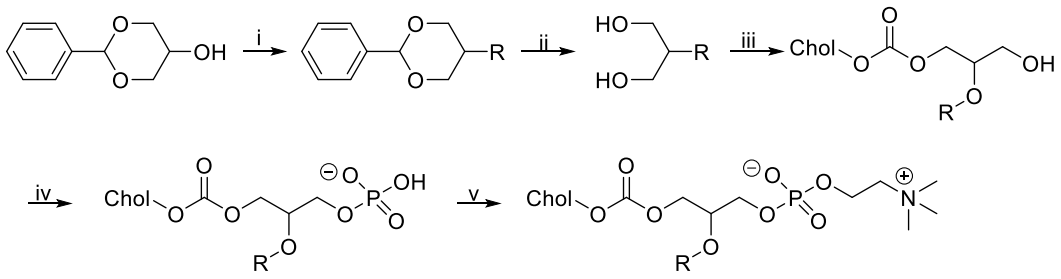

Scheme 1.1 Synthetic scheme for preparation of covalently attached cholesterol to daicyl lipids. Reagents and conditions: (i) (1) NaH (1.2 equiv.), toluene, r.t., 30 min; (2) iodoalkane (1.25 equiv.), reflux, overnight; (ii) HCl (conc.) in MeOH (10%), reflux, 5 h; (ii) cholesteryl chloroformate (1.05 equiv.), DIPEA (1.4 equiv.), DMAP (0.5 equiv.), $CHCl_3$, 0 °C, 0.5 h, and then r.t., overnight; (iv) $POCl_3$ (1.1 equiv.), pyridine (2 equiv.), THF, 0 °C, 2-3 h; (v) choline tetraphenyl borate (2 equiv.), TPS (2.5 equiv.), pyridine, 70 °C, 1 h, then r.t., 3 h. Reprinted with permission from (Huang, Z.; Szoka, F. C. *J. Am. Chem. Soc.* **2008**, *130* (46), 15702–15712.). Copyright (2008) American Chemical Society

group had synthesized a class of diacyl lipids that covalently attaches cholesterol to the glycerol backbone of the phophatidylcholine lipid (shown in Scheme 1.1).[79] The synthesis of cholesterol integrated diacyl lipids begins with an initial alkylation of 2-pheynyl-1,3-dioxane-5-ol, followed by a deprotection of the acetal resulting in the formation of the mono-functionalized glycerol diol. The synthesis of sterol modified diacyl lipid was completed after the addition of cholesterol to the lipid core *via* carbamate linkage and the addition of the phoshpotidylcholine headgroup to the remaining free alcohol of the glycerol. This new class of sterol modified phospholipids was shown to form stable liposomes, while having similar effects to free cholesterol when mixed to stabilize commercial diacyl liposomes showing reduced passive intraliposomal leakage.[80] By anchoring the cholesterol to the lipid membrane, it was shown to successfully reduce cholesterol transfer and increased *in vivo* liposome stability.[81] In addition to the decreased passive permeability of inner cargo, the

sterol modified liposomes had improved cellular uptake and slower clearance from the liver and spleen compared with traditional liposomes.[81]

Despite the promising synthetic progress for improved membrane properties for diacyl lipid on membrane leakage, diacyl lipids remained unstable in environments involving acid, enzymes, high lipid concentrated, and metal ions.[82–86]

1.2.2. Archaea Inspired Synthetic Tetraether Lipids for Robust Vesicles

1.2.2.1 Synthetic Strategy used to Design Archaeal Macrocyclic Tetraether Lipid Analogs

Archaea are extremophiles that thrive in harsh conditions such as high temperature, high acidity, high salinity, and high pressure.[87–89] The membranes found in these organisms have been observed to have a high degree of chemical and enzymatic stability.[90] One strategy that researchers have turned to in order to improve liposomal stability is by studying natural archaeal lipids.[82,91–98] Specifically, to investigate the essence of the organisms' inherent stability under extreme conditions, archaeal lipids have been extracted from archaeal biomass and characterized by many research groups.[99–102] In particular, De Rosa and Kates group have pioneered investigations into the biosynthesis and characterization of membrane lipids that have led to elucidation of a large number of unique structures of archaeal polar lipids (shown in Figure 1.3).[103,104] The unique structural features found in archaeal

lipids that differ from bacterial lipids includes: 1) ether linkages between fatty acids and the glycerol backbone that differ from bacterial lipids with ester linkages, 2) isoprenoid hydrocarbon chains that are highly methyl-branched in archaeal lipids, whereas, their bacterial counterpart have straight-chain fatty acids with and without double bonds, 3) lipid tails that are covalently tethered resulting in creating a membrane spanning lipids that form monolayer membranes that differs from bacterial lipids that form bilayers, and 4) cyclopentane and/or cyclohexane rings in the tethered region of the hydrophobic tails.[88,100] The ether linkages, isoprenoid chains, tethered tetraether lipid and integration of small rings have been suggested to play a significant role for the membrane stability or Archaea in extreme habitat.[90,105–107]

To investigate whether the inherent stability of Archaea is due to their lipid composition in the membrane, archaeal lipids have been extracted from *Sulfolobus acidocaldarius*, called polar lipid fraction E, to form liposomes to study membrane leakage.[82] These liposomes, coined archaeosomes, exhibited low permeability, tight membrane packing and improved stability compared with liposomes formed from diacyl lipids.[82,108,109] However, harvesting reproducible and large quantities of specific lipid compositions from cultured archaeal species can be challenging.[82,108,109] Instead, several groups have reported

model archaeal lipid analogs that incorporate key structural features that are believed to increase membrane stability of archaeal membranes.[97,110–126]

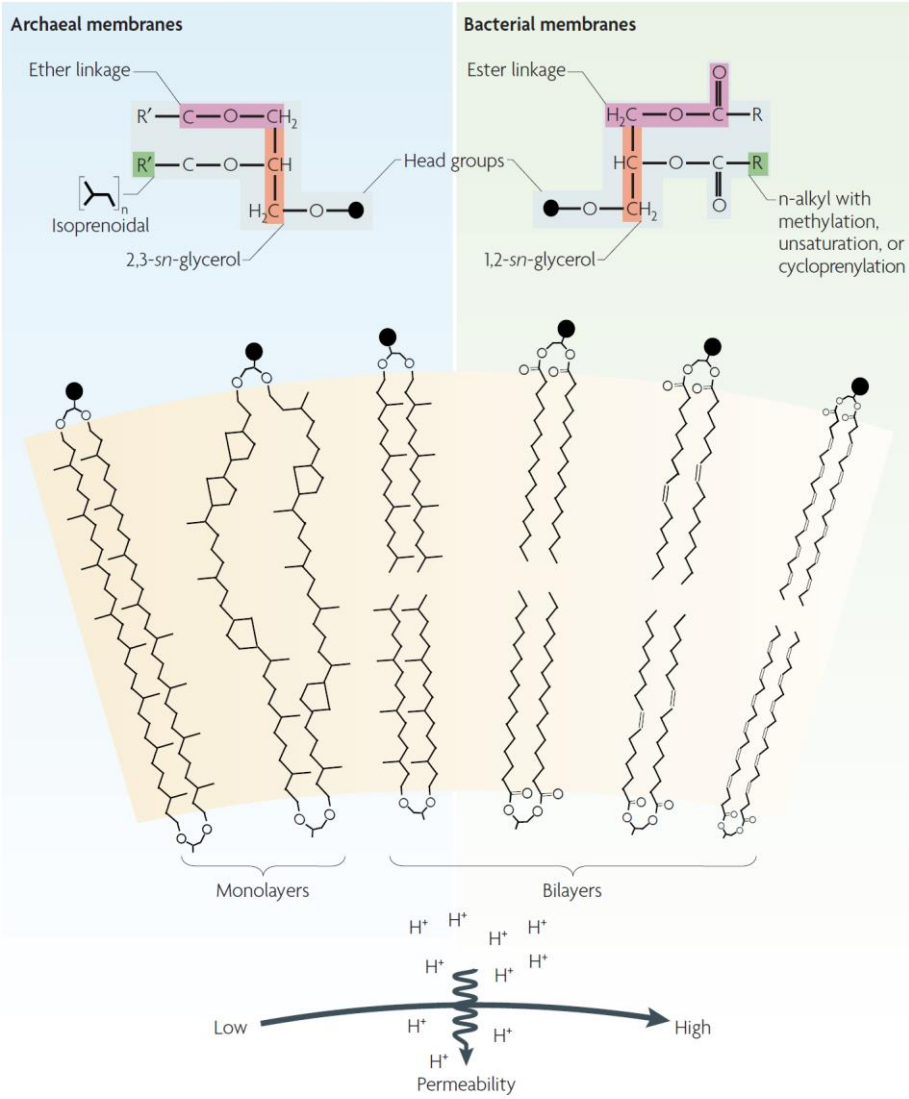

Figure 1.3. Membranes of the Archaea and Bacteria. Reprinted by permission from Macmillan Publishers Ltd: [Nature Reviews Microbiology] (Valentine, D. L. Nat. Rev. Microbiol. 2007, 5, 316–323.), copyright (2007)

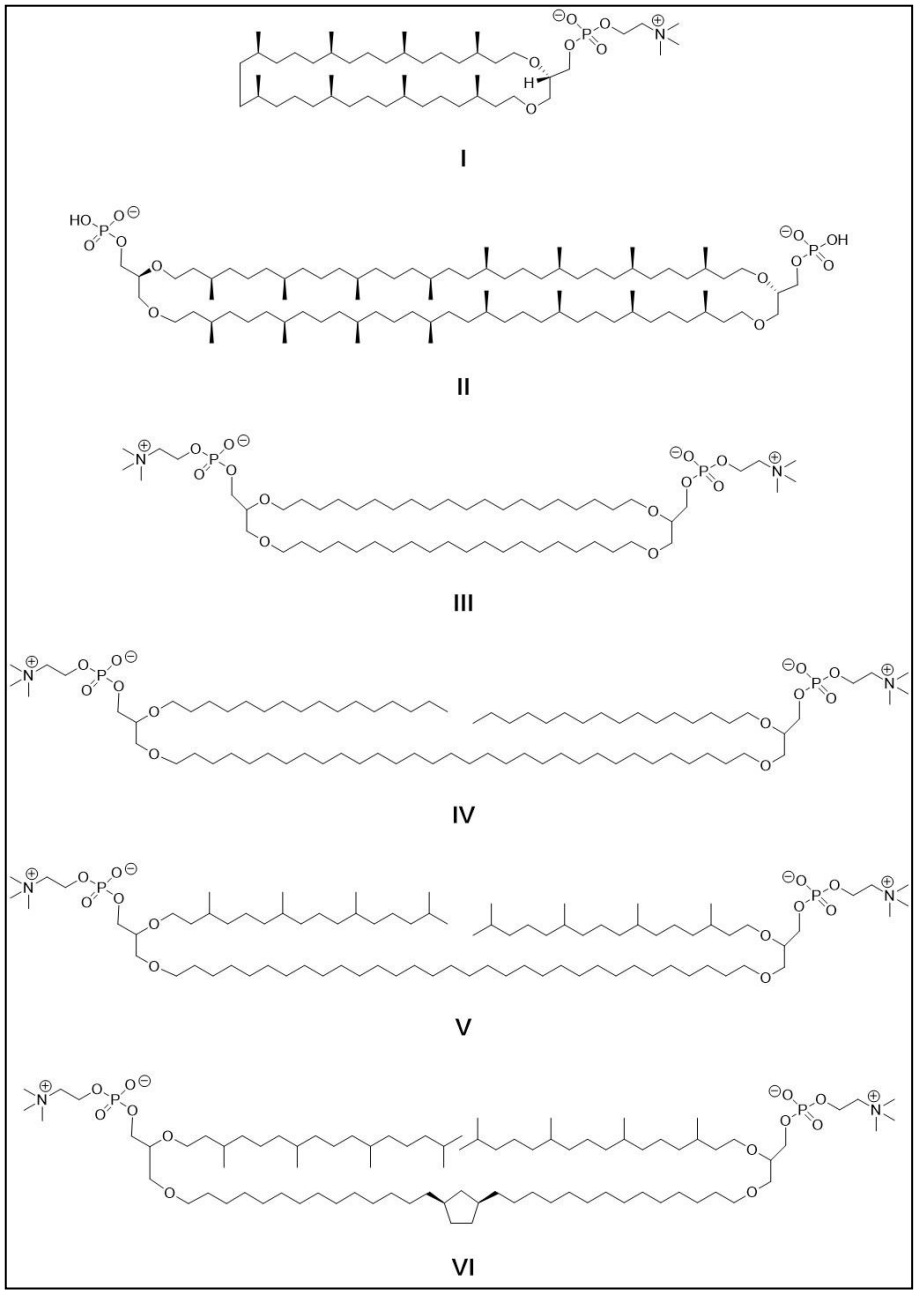

Figure 1.4. Sample representation set of synthetic archaeal lipid analogs in current research. Ref: **I**[114], **II**[113], **III**[117], **IV**[133], **V**[133], **VI**[119].

In the past, considerable effort has been invested in the development of Archaea inspired lipids with tetraether or tetraester[127,128] glycerol linkages. In this introduction, the synthesis of tetraether lipids will be the main focus considering the increased stability imparted by ether linkages when compared

with ester linkages.[129,130] In addition to the chemically promiscuous ester functional group, Yamauchi et al. has published research that demonstrates liposomes made with ordinary ester linked lipids were prone to aggregation and precipitation under high lipid concentration and in the presence of metal ions, resulting in loss of interior content within a few days.[83] Chemical structures of the most representative synthetic archaeal lipid analogues (shown in Figure 1.4) differ in their hydrophobic moiety. Previously synthesized examples of tetraether lipids that incorporate structural features found in Archaea possess either macrocyclic or hemicyclic membrane spanning hydrophobic chains as shown in Figure 1.4.

In nature, Archaeal lipids have been found to form 36-membered macrocyclic diether and 72-membered macrocyclic tetraether lipids.[88,131] To investigate the membrane leakage properties of these macrocyclic tetraether lipids, Kakinuma's group has successfully synthesized 36 (molecule **I**)[114] and 72-membered (molecule **II**)[113,115] macrocyclic lipids shown in Figure 1.4. The synthetic strategy used by the Kakinuma's group to design the 36-membered macrocyclic diether (**I**) involved the stereo-selective preparation of functionalized isoprenoid chains to the glycerol backbone through an ether linkage starting from a chiral (*R*)-3-hydroxy-2-methyl-propionate (shown in Scheme 1.2). The chirally pure C_{20} isoprenoid chains were synthesized by a series of elongation reactions to the C_5 unit consisting of protection, deprotection, displacement of the iodide by an enol-equivalent sulfur dioxide

analog and followed by the removal of the sulfone using Na(Hg). Following the formation of the C_{20} isoprenoid unit, alkylation by the glycerol backbone derived from 1-*O*-benzyl-*sn*-glycerol afforded the desired ether linkage affording the two half lipid scaffold. The key C-C bond connection necessary in the total synthesis of the 36-membered diether lipid was completed *via* intramolecular McMurry coupling of the oxidized alcohols catalyzed by low-valent titanium. The synthesis of the 36-membered diether was completed by an initial olefin reduction followed by the addition of the phosphatidylcholine headgroup to the remaining glycerol alcohol.

The total synthesis of 72-membered macrocyclic tetraether (**II**) was performed using the bifunctionalized C_{20} isoprenoid building block used in the 36-membered macrocyclic tetraether lipid synthesis (shown in Scheme 1.3). It is notable, to obtain the desired stereo-configuration of the glycerol backbone, the free alcohol of C_{20} isoprenoid building block was oxidized to an aldehyde and reacted with *sn*-1-*O*-benzylglycerol to form the acetal intermediate. Alkylation of the orthogonally protected C_{20} isoprenoid building block by the free hydroxyl group after the deprotected acetal afforded the acyclic diether lipid precursor which was later tethered together by the formation of β-hydroxysulfone. β-hydroxysulfone was successfully removed using a SmI_2 catalyzed reductive elimination, followed by the reduction of the olefin. Using

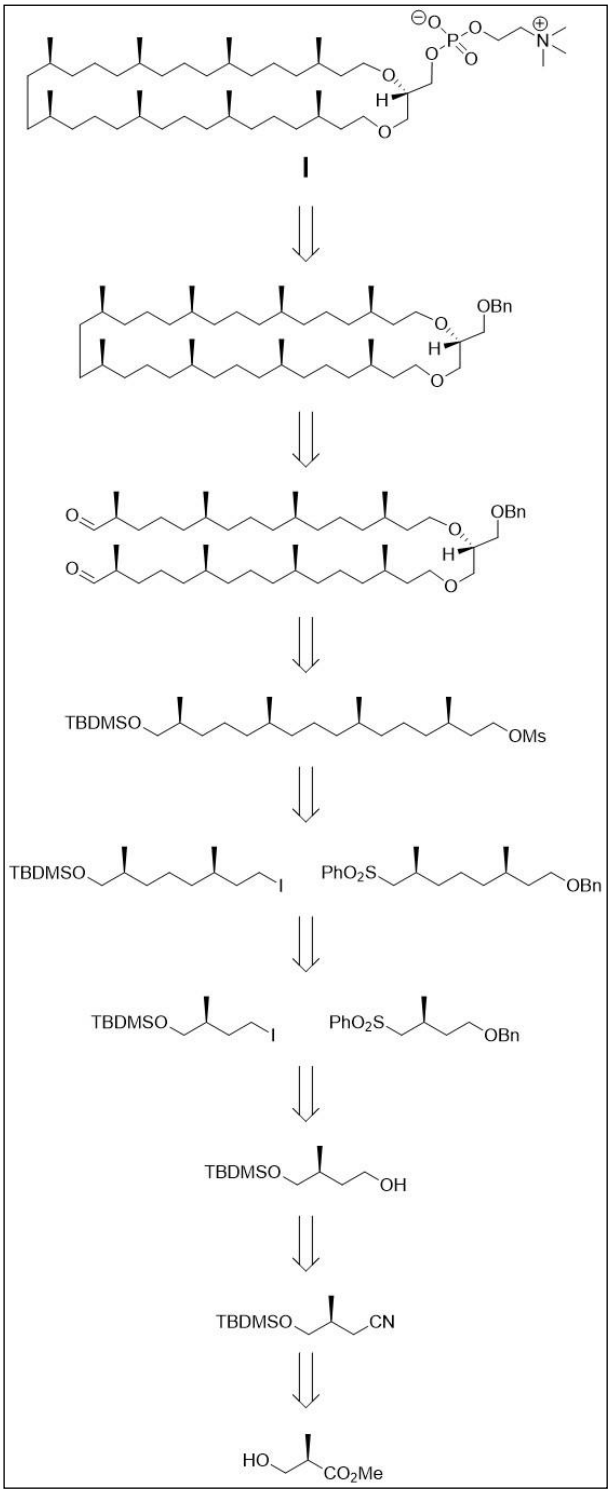

Scheme 1.2. Retrosynthetic strategy designed by the Kakinuma group to synthesize molecule **I.**[114]

techniques tested for the synthesis of the 36-membered diether lipids, the 72-

membered macro-cyclization was completed using McMurry coupling. The total synthesis of the 72-membered macrocyclic tetraether was completed following the reduction of the olefin and the addition of the phosphatidylcholine headgroup

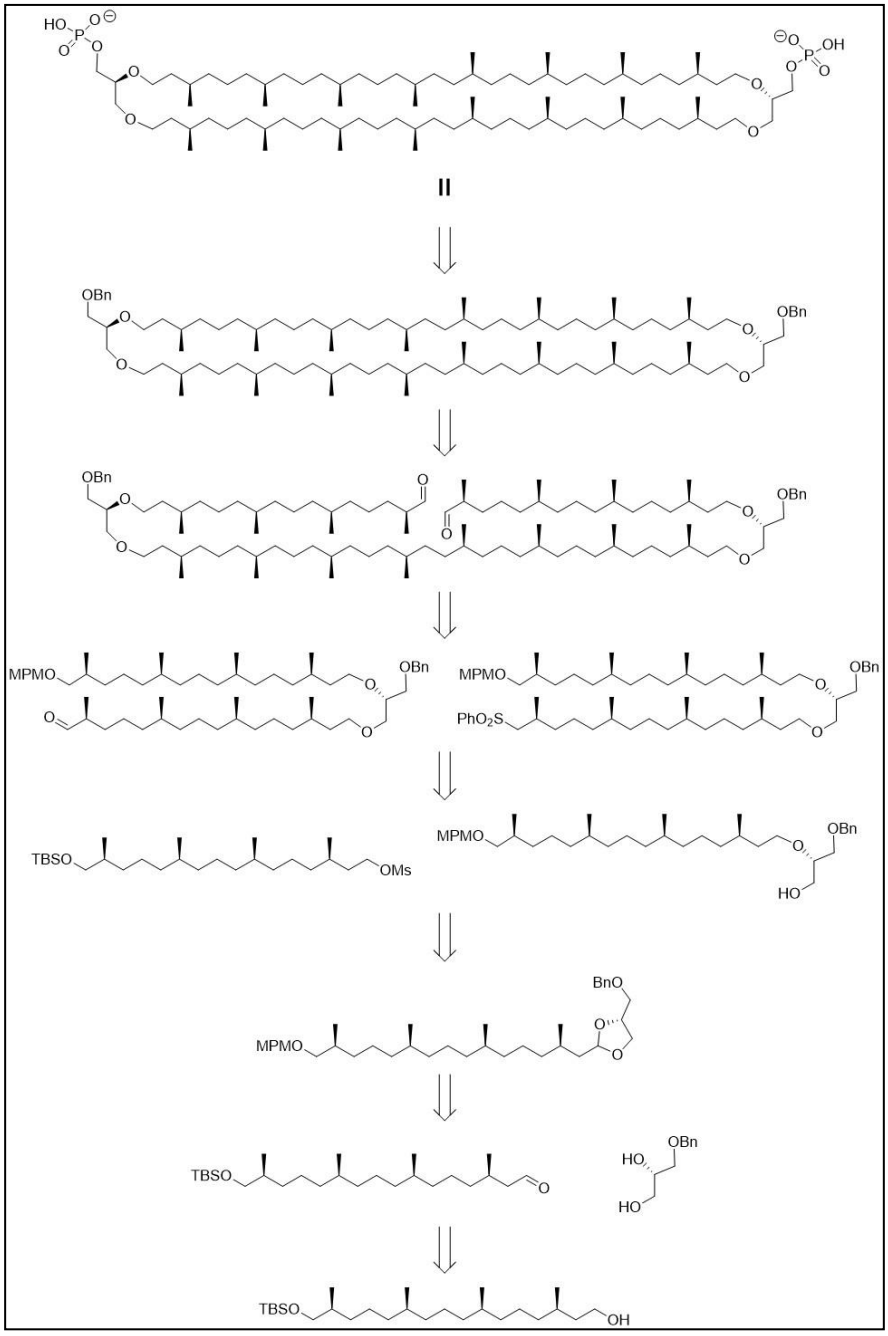

Scheme 1.3. Retrosynthetic strategy designed by the Kakinuma group to synthesize molecule **II.** [113]

to the remaining glycerol alcohols in 27 steps (longest linear reaction steps) with an overall yield of 1.7%.[115]

Total synthesis of the 72 membered macrocyclic archaeal lipid was elegantly performed by the Kakinuma group. However, to study the structure functional relationship of archaeal structures to membrane permeability in aqueous media requires a large amount of pure lipid. To address the synthetic challenges associated with synthesis of optically pure isoprenoid units involving low yield, Thompson's group designed a macrocyclic tetraether lipids equipped with saturated alkyl chains (**III**).[117] The synthetic strategy employed by the Thompson group begins with 2-phenyl-1,3-dioxan-5-ol as the masked glycerol backbone that participates in alkylating the terminal alkyne (shown in Scheme 1.4). The terminal alkyne of the alkylated glycerol is coupled together through an initial Glaser oxidation to form the hemicyclic tetraether lipid. This alkylation and coupling process was repeated to complete the macro-cyclization, followed by reduction of the alkynes and the addition of phosphatidylcholine headgroup to the free glycerol alcohol to complete the synthesis of a 48-membered macrocyclic tetraether lipid.[117] The saturated macrocyclic tetraether lipid was elegantly designed with fewer steps, however, without the branched methyl groups, the saturated macrocyclic tetraether lipid displayed a high phase transition temperature, which would cause complications when preparing liposomes.[132]

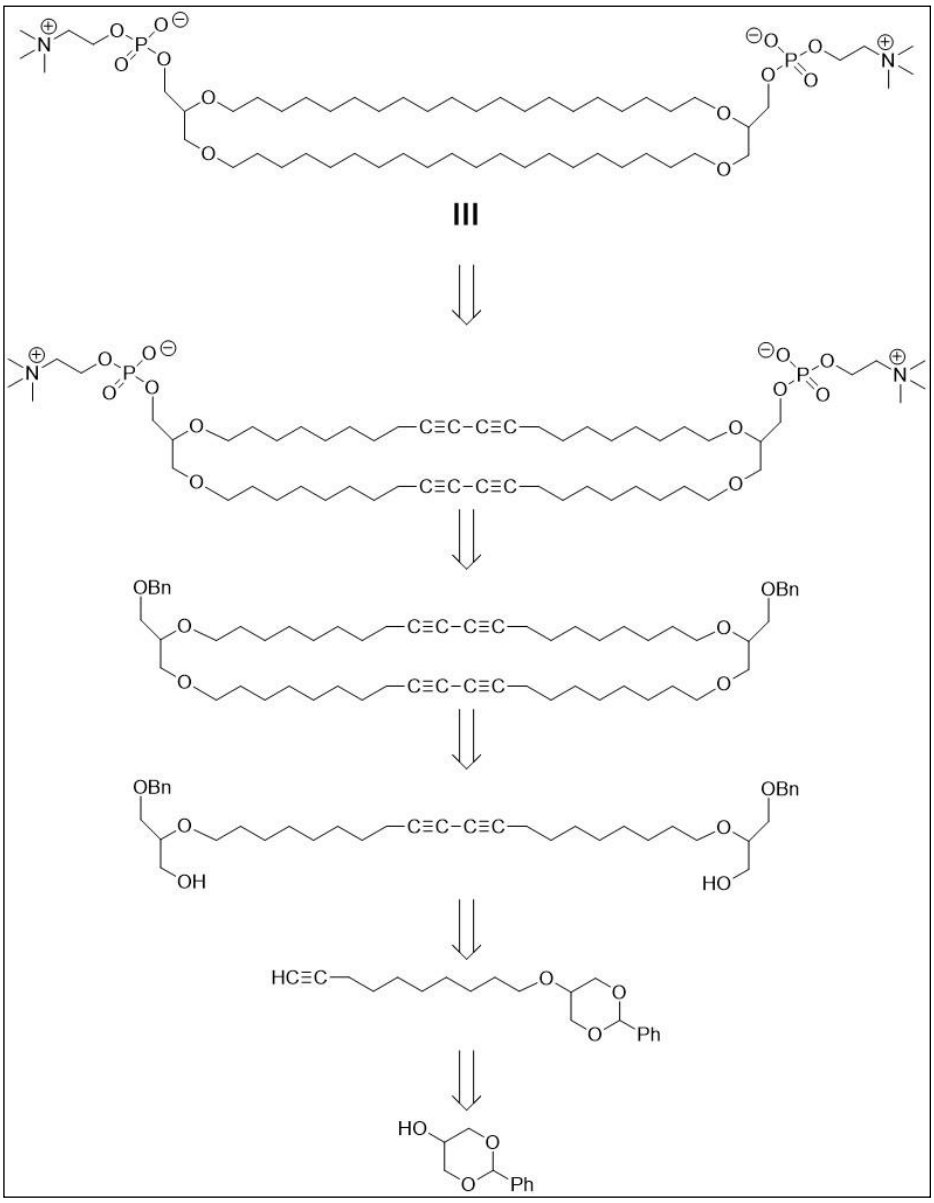

Scheme 1.4. Retrosynthetic strategy designed by the Thompson group to synthesize molecule **III.**[117]

1.2.2.2 Synthetic Strategy used to Design Archaeal Hemicyclic Tetraether Lipid Analogs

Scientists interested in studying structure functional relationships associated with structural features found in archaeal lipids on membrane permeability have focused their synthetic efforts on simpler model molecules that are hemicyclic, which still incorporate structures found in natural archaeal lipids and can be produce in a larger amounts. Thompson's group, one of the research groups that had shifted their research towards the simpler model molecules, designed a new set of hemicyclic tetraether lipids substituted with either a saturated alkyl or phytanyl group on the untethered portion on the lipid (shown in Figure 1.4). Both hemicyclic tetraether lipids (**IV** and **V**) were synthesized using a similar strategy as their synthesis of the macrocyclic tetraether lipid that differed in the initial alkylation of 2-phenyl-1,3-dioxan-5-ol with either an iodinated saturated alkyl chain or a iodine derivative of commercially available phytol (retrosynthetic strategy to synthesize phytanyl containing hemicyclic tetraether (**V)** shown in Scheme 1.5). The dimerization of the tethered region was completed using metathesis catalyzed by Grubb's reagent to form the hemicyclic tetraether lipids. Fascinatingly, without the branched alkane substituents, the saturated hemicyclic tetraether lipid, similar to the saturated macrocyclic tetraether lipid, still exhibited a high phase transition temperature (>85 °C)[133] which is not observed for natural archaeal lipids[89].

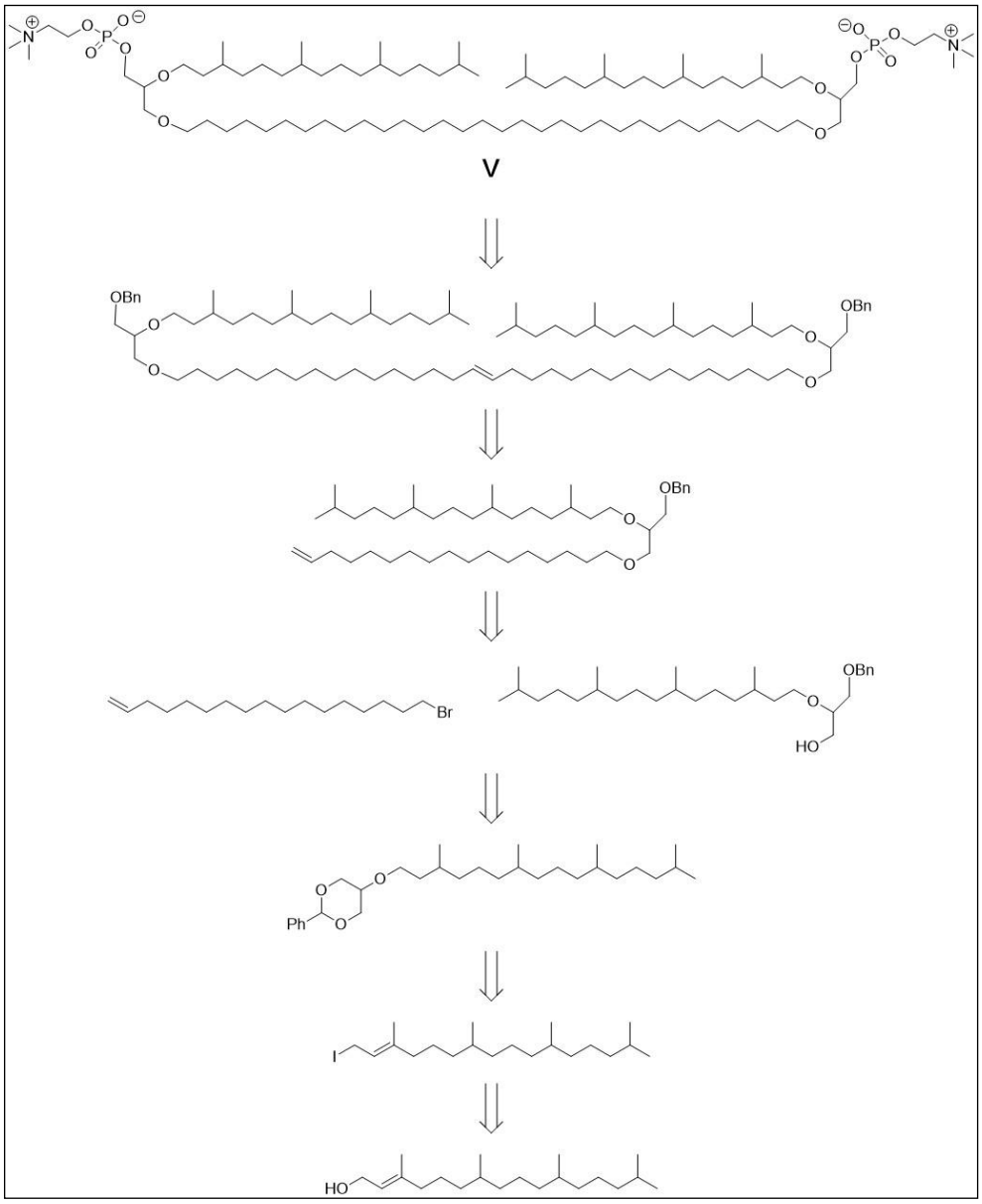

Scheme 1.5. Retrosynthetic strategy designed by the Thompson group to synthesize molecule **V.** [133]

To explore the structural benefits associated with incorporation of cyclopentane rings in the hydrophobic core of natural archaeal lipids, Benvegnu's group have successfully designed model hemicyclic lipids that incorporates a *cis*-1,3-cyclopentane in the lipid core. The synthetic strategy used to design molecule (**VI**) shown in Figure 1.4, began with the synthesis of

2 precursors, cyclopentane integrated hydrophobic chain and phytanyl affixed glycerol backbone (shown in Scheme 1.6). The cyclopentane integrated hydrophobic chain was elegantly synthesized by first a ring opening of norbornene *via* ozonolysis, followed by the reduction of the dialdehyde to form the diol. The newly formed alcohols were subsequently transformed to a phosphonium salt which were then couple through a Wittig reaction with two alkyl aldehydes to form the hydrophobic chain precursor. The diolefinated homologated hydrophobic chain was reduced/O-deprotected and the free primary alcohols were triflated. The glycerol backbone of the lipid, second piece of the tetraether lipid, was synthesized starting from solketal through a series of deprotection, protection and alkylation with iodophytyl. The hemi-cyclization of the lipid was performed through a round of alkylation of the phytanylated glycerol with the ditriflate of the cyclopentane integrated alkane. The synthesis of cyclopentane integrated hemicyclic tetraether (**VI**) was completed after the addition of phosphatidylcholine headgroup to the free alcohols of the glycerol backbone.

Despite the progress of the elegant synthesis of archaeal lipid analogues designed by many research groups, the relationship between structure and function of the tetraether lipids on membrane stability remains unclear due to the limited data available on their membrane permeability properties[83,84,86,97,122,134]. A systematic study that probes the effect of specific structural features found in the archaeal-inspired lipids on membrane leakage

could prove fortuitous in designing lipids with improved membrane properties for drug delivery.

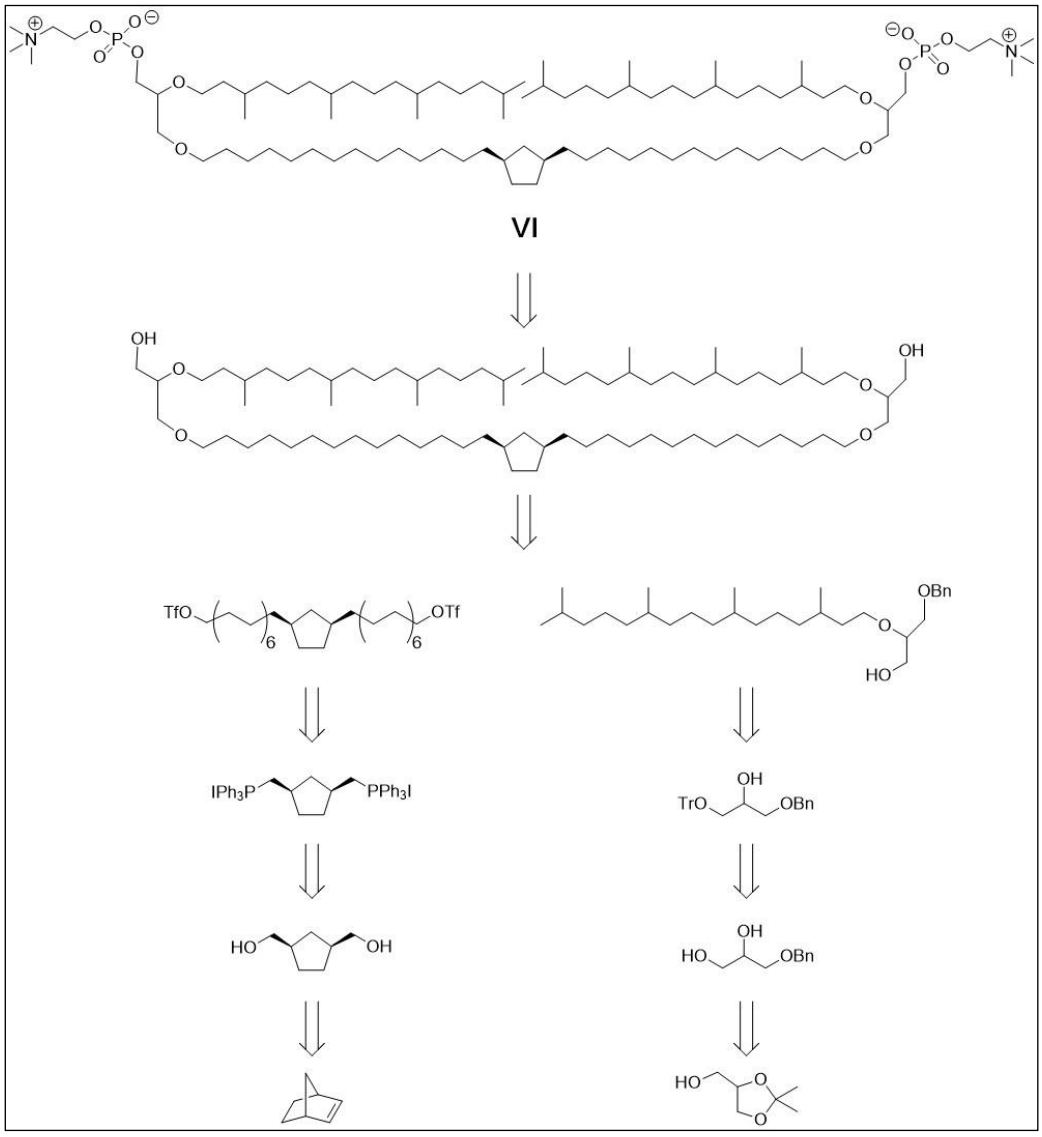

Scheme 1.6. Retrosynthetic strategy designed by the Benvegnu group to synthesize molecule **VI.** [119]

1.3 References

(1) Shi, J.; Kantoff, P. W.; Wooster, R.; Farokhzad, O. C. *Nat. Rev. Cancer* **2016**, *17* (1), 20–37.

(2) Kannan, R. M.; Nance, E.; Kannan, S.; Tomalia, D. A. *J. Intern. Med.* **2014**, *276* (6), 579–617.

(3) Caster, J. M.; Patel, A. N.; Zhang, T.; Wang, A. *Wiley Interdiscip. Rev. Nanomed. Nanobiotechnol.* **2016**, *9*.

(4) Etheridge, M. L.; Campbell, S. A.; Erdman, A. G.; Haynes, C. L.; Wolf, S. M.; McCullough, J. *Nanomedicine Nanotechnology, Biol. Med.* **2013**, *9* (1), 1–14.

(5) Min, Y.; Caster, J. M.; Eblan, M. J.; Wang, A. Z. *Chem. Rev.* **2015**, *115* (19), 11147–11190.

(6) Wagner, V.; Dullaart, A.; Bock, A.-K.; Zweck, A. *Nat. Biotechnol.* **2006**, *24* (10), 1211–1217.

(7) Wang, R.; Billone, P. S.; Mullett, W. M. *J. Nanomater.* **2013**, *2013* (April), 1–12.

(8) Allen, T. M.; Cullis, P. R. *Adv. Drug Deliv. Rev.* **2013**, *65* (1), 36–48.

(9) Barenholz, Y. *J. Control. Release* **2012**, *160* (2), 117–134.

(10) Mayer, M. I.; Weickum, R. J.; Jr, D. A. S.; Fileta, B. B.; Abdel-rahim, M. M.; Fant, G. V. **2001**, *35*, 1548–1551.

(11) Duncan, R. *Nat. Rev. Cancer* **2006**, *6* (9), 688–701.

(12) Malam, Y.; Loizidou, M.; Seifalian, A. M. *Trends Pharmacol. Sci.* **2009**, *30* (11), 592–599.

(13) Tiwari, G.; Sriwastawa, B.; Pandey, S.; Bannerjee, S.; Tiwari, R.; Bhati, L.; Pandey, P. *Int. J. Pharm. Investig.* **2012**, *2* (1), 2.

(14) Li, J.; Wang, X.; Zhang, T.; Wang, C.; Huang, Z.; Luo, X.; Deng, Y. *Asian J. Pharm. Sci.* **2014**, *10* (2), 81–98.

(15) Weissig, V.; Pettinger, T. K.; Murdock, N. *Int. J. Nanomedicine* **2014**, *9*, 4357–4373.

(16) Hare, J. I.; Lammers, T.; Ashford, M. B.; Puri, S.; Storm, G.; Barry, S. T. *Adv. Drug Deliv. Rev.* **2016**, *108*, 25–38.

(17) Werner, M. E.; Cummings, N. D.; Sethi, M.; Wang, E. C.; Sukumar, R.; Moore, D. T.; Wang, A. Z. *Int. J. Radiat. Oncol. Biol. Phys.* **2013**, *86* (3), 463–468.

(18) Miele, E.; Spinelli, G. P.; Miele, E.; Tomao, F.; Tomao, S. *Int. J. Nanomedicine* **2009**, *4*, 99–105.

(19) Wani, M. C.; Taylor, H. L.; Wall, M. E.; Coggon, P.; McPhail, a T. *J. Am. Chem. Soc.* **1971**, *93* (9), 2325–2327.

(20) Gelderblom, H.; Verweij, J.; Nooter, K.; Sparreboom, A. *Eur. J. Cancer* **2001**, *37* (13), 1590–1598.

(21) Mead, D.; Pearson, D.; Devine, M. *Innov. Pharm. Technol.* **2007**, No. 22, 42–44.

(22) Kopeček, J. *Adv. Drug Deliv. Rev.* **2013**, *65* (1), 49–59.

(23) Pasut, G.; Veronese, F. M. *Adv. Drug Deliv. Rev.* **2009**, *61* (13), 1177–1188.

(24) Singer, J. W. *J. Control. Release* **2005**, *109* (1–3), 120–126.

(25) Knop, K.; Hoogenboom, R.; Fischer, D.; Schubert, U. S. *Angew. Chemie - Int. Ed.* **2010**, *49* (36), 6288–6308.

(26) Kim, E. G.; Kim, K. M. *Biomol. Ther.* **2015**, *23* (6), 493–509.

(27) Nishiyama, N.; Kataoka, K. *Pharmacol. Ther.* **2006**, *112* (3), 630–648.

(28) Mourya, V. K.; Inamdar, N.; Nawale, R. B.; Kulthe, S. S. *Indian J. Pharm. Educ. Res.* **2011**, *45* (2), 128–138.

(29) Dikmen, G.; Genç, L.; Güney, G. **2011**, *5* (November 2016), 468–472.

(30) Namazi, H.; Adeli, M. *Biomaterials* **2005**, *26* (10), 1175–1183.

(31) Mccarthy, T. D.; Karellas, P.; Henderson, S. A.; Giannis, M.; David, F.; Keefe, O.; Heery, G.; Paull, J. R. A.; Matthews, B. R.; Holan, G.; Mccarthy, T. D.; Karellas, P.; Henderson, S. A.; Giannis, M.; Keefe, D. F. O.; Heery, G.; Paull, J. R. A.; Matthews, B. R. *Mol. Pharm.* **2005**, *2*, 312–318.

(32) Bangham, A. D.; Horne, R. W. *J. Mol. Biol.* **1964**, *8* (5), 660–668.

(33) Akbarzadeh, A.; Rezaei-Sadabady, R.; Davaran, S.; Joo, S. W.; Zarghami, N.; Hanifehpour, Y.; Samiei, M.; Kouhi, M.; Nejati-Koshki, K. *Nanoscale Res. Lett.* **2013**, *8* (1), 102.

(34) Immordino, M. L.; Dosio, F.; Cattel, L. *Int. J. Nanomedicine* **2006**, *1* (3), 297–315.

(35) Van der Meel, R.; Fens, M. H. A. M.; Vader, P.; Van Solinge, W. W.; Eniola-Adefeso, O.; Schiffelers, R. M. *J. Control. Release* **2014**, *195*, 72–85.

(36) Woodle, M. C. *Adv. Drug Deliv. Rev.* **1995**, *16* (2–3), 249–265.

(37) Ishida, T.; Harashima, H.; Kiwada, H. *Biosci. Rep.* **2002**, *22* (2), 197–224.

(38) Drummond, D. C.; Meyer, O.; Hong, K.; Kirpotin, D. B.; Papahadjopoulos, D. *Pharmacol. Rev.* **1999**, *51* (4), 691–743.

(39) Cullis, P. R.; Mayer, L. D.; Bally, M. B.; Madden, T. D.; Hope, M. J. *Adv. Drug Deliv. Rev.* **1989**, *3* (3), 267–282.

(40) Sipai Altaf Bhai, M.; Vandana, Y.; Mamatha, Y.; Prasanth, V. V. *J. Pharm. Sci. Innov.* **2012**, *1* (1), 13–21.

(41) Kohli, A. G.; Kierstead, P. H.; Venditto, V. J.; Walsh, C. L.; Szoka, F. C. *J. Control. Release* **2014**, *190*, 274–287.

(42) Chrai, S. S.; Murari, R.; Ahmad, I. *Biotech Trends* **2002**, 30–34.

(43) Berger, N.; Sachse, a; Bender, J.; Schubert, R.; Brandl, M. *Int. J. Pharm.* **2001**, *223* (1–2), 55–68.

(44) Allen, T. M.; Hansen, C.; Martin, F.; Redemann, C.; Yau-Young, A. *BBA - Biomembr.* **1991**, *1066* (1), 29–36.

(45) Proffitt, R. T.; Williams, L. E.; Presant, C. A.; Tin, G. W.; Uliana, J. A.; Gamble, R. C.; Baldeschwieler, J. D. *J Nucl Med* **1983**, *24* (1), 45–51.

(46) Loi, M.; Marchio, S.; Becherini, P.; Di Paolo, D.; Soster, M.; Curnis, F.;

Brignole, C.; Pagnan, G.; Perri, P.; Caffa, I.; Longhi, R.; Nico, B.; Bussolino, F.; Gambini, C.; Ribatti, D.; Cilli, M.; Arap, W.; Pasqualini, R.; Allen, T. M.; Corti, A.; Ponzoni, M.; Pastorino, F. *J. Control. Release* **2010**, *145* (1), 66–73.

(47) Mabrey, S.; Mateo, P. L.; Sturtevant, J. M. *Biochemistry* **1978**, *17* (12), 2464–2468.

(48) Pastorino, F.; Paolo, D. Di; Loi, M.; Becherini, P.; Caffa, I.; Zorzoli, A.; Marimpietri, D. **2009**, 1021–1027.

(49) Senior, J.; Gregoriadis, G. *Life Sci.* **1982**, *30* (I), 2123–2136.

(50) De Kruyff, B.; Demel, R. A.; Slotboom, A. J.; Van Deenen, L. L. M.; Rosenthal, A. F. *Biochim. Biophys. Acta - Biomembr.* **1973**, *307* (1), 1–19.

(51) Haines, T. H. *Prog. Lipid Res.* **2001**, *40* (4), 299–324.

(52) Oja, C. D.; Semple, S. C.; Chonn, A.; Cullis, P. R. *Biochim. Biophys. Acta - Biomembr.* **1996**, *1281* (1), 31–37.

(53) Woodle, M. C.; Papahadjopoulos, D. *Methods Enzymol.* **1989**, *171* (1984), 193–217.

(54) Mayer, L. D.; Hope, M. J.; Cullis, P. R.; Janoff, A. S. *BBA - Biomembr.* **1985**, *817* (1), 193–196.

(55) Szoka, F.; Papahadjopoulos, D. *Ann. Rev. Biophys. Bioeng.* **1980**, *9*, 467–508.

(56) Batzri, S.; Korn, E. D. *BBA - Biomembr.* **1973**, *298* (4), 1015–1019.

(57) Pons, M.; Foradada, M.; Estelrich, J. *Int. J. Pharm.* **1993**, *95* (1–3), 51–56.

(58) Bally, M. B.; Mayer, L. D.; Loughrey, H.; Redelmeier, T.; Madden, T. D.; Wong, K.; Harrigan, P. R.; Hope, M. J.; Cullis, P. R. *Chem. Phys. Lipids* **1988**, *47* (2), 97–107.

(59) Mayer, L. D.; Bally, M. B.; Cullis, P. R. *BBA - Biomembr.* **1986**, *857* (1), 123–126.

(60) Acta, B.; Bba, E.; Columbia, B.; November, R. **1985**, *816*, 294–302.

(61) Dos Santos, N.; Cox, K. A.; McKenzie, C. A.; Van Baarda, F.; Gallagher, R. C.; Karlsson, G.; Edwards, K.; Mayer, L. D.; Allen, C.; Bally, M. B. *Biochim. Biophys. Acta - Biomembr.* **2004**, *1661* (1), 47–60.

(62) Forssen, E. A. *Adv. Drug Deliv. Rev.* **1997**, *24* (2–3), 133–150.

(63) Swenson, C. E.; Perkins, W. R.; Roberts, P.; Janoff, A. S. *The Breast* **2001**, *10*, 1–7.

(64) Papahadjopoulos, D.; Allen, T. M.; Gabizon, A.; Mayhew, E.; Matthay, K.; Huang, S. K.; Lee, K. D.; Woodle, M. C.; Lasic, D. D.; Redemann, C. *Proc. Natl. Acad. Sci. U. S. A.* **1991**, *88* (24), 11460–11464.

(65) Woodle, M. C.; Newman, M. S.; Cohen, J. a. *J. Drug Target.* **1994**, *2* (5), 397–403.

(66) Owens, D. E.; Peppas, N. A. *Int. J. Pharm.* **2006**, *307* (1), 93–102.

(67) Richter, A. W.; Åkerblom, E. *Int. Arch. Allergy Immunol.* **1984**, *74* (1), 36–39.

(68) Ishida, T.; Ichihara, M.; Wang, X.; Kiwada, H. *J. Control. Release* **2006**, *115* (3), 243–250.

(69) Abu Lila, A. S.; Kiwada, H.; Ishida, T. *J. Control. Release* **2013**, *172* (1), 38–47.

(70) Uziely, B.; Jeffers, S.; Isacson, R.; Kutsch, K.; Wei-Tsao, D.; Yehoshua, Z.; Libson, E.; Muggia, F. M.; Gabizon, A. *J. Clin. Oncol.* **1995**, *13* (7), 1777–1785.

(71) Kierstead, P. H.; Okochi, H.; Venditto, V. J.; Chuong, T. C.; Kivimae, S.; Fréchet, J. M. J.; Szoka, F. C. *J. Control. Release* **2015**, *213*, 1–9.

(72) Gaertner, F. C.; Luxenhofer, R.; Blechert, B.; Jordan, R.; Essler, M. *J. Control. Release* **2007**, *119* (3), 291–300.

(73) Torchilin, V. P.; Trubetskoy, V. S.; Whiteman, K. R.; Caliceti, P.; Ferruti, P.; Veronese, F. M. *J. Pharm. Sci.* **1995**, *84* (9), 1049–1053.

(74) Kohori, F.; Sakai, K.; Aoyagi, T.; Yokoyama, M.; Yamato, M.; Sakurai, Y.; Okano, T. *Colloids Surfaces B Biointerfaces* **1999**, *16* (1–4), 195–205.

(75) Romberg, B.; Oussoren, C.; Snel, C. J.; Carstens, M. G.; Hennink, W. E.; Storm, G. *Biochim. Biophys. Acta - Biomembr.* **2007**, *1768* (3), 737–743.

(76) Duncan, R.; Vicent, M. J. *Adv. Drug Deliv. Rev.* **2010**, *62* (2), 272–282.

(77) Phillips, M. C.; Johnson, W. J.; Rothblat, G. H. *Biochim. Biophys. Acta* **1987**, *906* (2), 223–276.

(78) Hamilton, J. A. *Curr. Opin. Lipidol.* **2003**, *14* (3), 263–271.

(79) Huang, Z.; Szoka Jr., F. C. *J. Am. Chem. Soc.* **2008**, *130* (46), 15702–15712.

(80) Huang, Z.; Jaafari, M. R.; Szoka, F. C. *Angew. Chem., Int. Ed. Engl.* **2009**, *48* (23), 4146–4149.

(81) Kohli, A. G.; Kieler-Ferguson, H. M.; Chan, D.; Szoka, F. C. *J. Control. Release* **2014**, *176* (1), 86–93.

(82) Elferink, M. G. L.; de Wit, J. G.; Driessen, A. J. M.; Konings, W. N. *Biochim. Biophys. Acta, Biomembr.* **1994**, *1193* (2), 247–254.

(83) Yamauchi, K.; Doi, K.; Kinoshita, M.; Kii, F.; Fukuda, H. *Biochim. Biophys. Acta* **1992**, *1110* (2), 171–177.

(84) Yamauchi, K.; Doi, K.; Yoshida, Y.; Kinoshita, M. *Biochim. Biophys. Acta, Biomembr.* **1993**, *1146* (2), 178–182.

(85) Yamauchi, K.; Doi, K.; Kinoshita, M. *Biochim. Biophys. Acta - Biomembr.* **1996**, *1283* (2), 163–169.

(86) Arakawa, K.; Eguchi, T.; Kakinuma, K. *Chem. Lett.* **2001**, 5, 440–441.

(87) Koga, Y.; Nakano, M. *Syst. Appl. Microbiol.* **2008**, *31* (3), 169–182.

(88) Koga, Y. *Archaea* **2012**, *2012*, 789652.

(89) Blöcher, D.; Gutermann, R.; Henkel, B.; Ring, K. *BBA - Biomembr.* **1984**, *778* (1), 74–80.

(90) Chong, P. L.-G.; Ayesa, U.; Daswani, V. P.; Hur, E. C. *Archaea* **2012**, *2012*, 1–11.

(91) Gambacorta, A.; Gliozzi, A.; De Rosa, M. *World J. Microbiol. Biotechnol.* **1995**, *11* (1), 115–131.

(92) Whitfield, D. M.; Eichler, E. E.; Sprott, G. D. *Carbohydr. Res.* **2008**, *343*, 2349–2360.

(93) Benvegnu, T.; Lemiègre, L.; Cammas-Marion, S. *Recent Pat. Drug Deliv. Formul.* **2009**, *3* (3), 206–220.

(94) Le Gall, T.; Barbeau, J.; Barrier, S.; Berchel, M.; Lemiègre, L.; Jeftić, J.; Meriadec, C.; Artzner, F.; Gill, D. R.; Hyde, S. C.; Férec, C.; Lehn, P.; Jaffrès, P.-A.; Benvegnu, T.; Montier, T. *Mol. Pharm.* **2014**, *11* (9), 2973–2988.

(95) Gliozzi, A.; Relini, A.; Chong, P. L.-G. *J. Membr. Sci.* **2002**, *206*, 131–147.

(96) Bücher, C.; Grosse, X.; Rothe, H.; Fiethen, A.; Kuhn, H.; Liefeith, K. *Biointerphases* **2014**, *9* (1), 11002.

(97) Barbeau, J.; Cammas-Marion, S.; Auvray, P.; Benvegnu, T. *J. Drug Deliv.* **2011**, *2011*, 396068.

(98) Patel, G. B.; Agnew, B. J.; Deschatelets, L.; Fleming, L. P.; Sprott, G. D. *Int. J. Pharm.* **2000**, *194*, 39–49.

(99) Carballeira, N. M.; Reyes, M.; Sostre, A.; Huang, H.; Verhagen, M. F.; Adams, M. W. *J. bacteriol.* **1997**, *179* (8), 2766–2768.

(100) Valentine, D. L. *Nat. Rev. Microbiol.* **2007**, *5*, 316–323.

(101) Villanueva, L.; Damsté, J. S. S.; Schouten, S. *Nat. Rev. Microbiol.* **2014**, *12* (6), 438–448.

(102) De Rosa, M.; Gambacorta, A. *Prog. Lipid Res.* **1988**, *27* (3), 153–175.

(103) De Rosa, M.; Gambacorta, a; Gliozzi, a. *Microbiol. Rev.* **1986**, *50* (1), 70–80.

(104) Kates, M. In *Prog. Chem. Fats other Lipids*; Pergamon Press Ltd, 1978; pp 301–342.

(105) Koga, Y.; Morii, H. *Microbiol. Mol. Biol. Rev.* **2007**, *71* (1), 97–120.

(106) Gabriel, J. L.; Lee Gau Chong, P. *Chem. Phys. Lipids* **2000**, *105* (2), 193–200.

(107) Komatsu, H.; Chong, P. L. *Biochemistry* **1998**, *37* (1), 107–115.

(108) Chang, E. L. *Biochem. Biophys. Res. Commun.* 1994, pp 673–679.

(109) Uda, I.; Sugai, a; Itoh, Y. H.; Itoh, T. *Lipids* **2001**, *36* (1), 103–105.

(110) Montenegro, E.; Gabler, B.; Paradies, G.; Seemann, M.; Helmchen, G. *Angew. Chem.* **2003**, *42*, 2419–2421.

(111) Arakawa, K.; Eguchi, T.; Kakinuma, K. *Bull. Chem. Soc. Jpn.* **2001**, *74* (2), 347–356.

(112) Arakawa, K.; Eguchi, T.; Kakinuma, K. *J. Org. Chem.* **1998**, *63* (14), 4741–4745.

(113) Eguchi, T.; Ibaragi, K.; Kakinuma, K. *J. Org. Chem.* **1998**, *63* (8), 2689–2698.

(114) Eguchi, T.; Arakawa, K.; Terachi, T.; Kakinuma, K. *J. Org. Chem.* **1997**, *62* (7), 1924–1933.

(115) Eguchi, T.; Arakawa, K.; Kakinuma, K.; Rapp, G.; Ghosh, S.; Nakatani, Y.; Ourisson, G. *Chem. - A Eur. J.* **2000**, *6* (18), 3351–3358.

(116) Markowski, T.; Drescher, S.; Meister, A.; Hause, G.; Blume, A.; Dobner, B. *Eur. J. Org. Chem.* **2011**, 5894–5904.

(117) Patwardhan, A. P.; Thompson, D. H. *Org. Lett.* **1999**, *1* (2), 241–243.

(118) Svenson, S.; Thompson, D. *J. Org. Chem.* **1998**, *3263* (98), 7180–7182.

(119) Brard, M.; Lainé, C.; Réthoré, G.; Laurent, I.; Neveu, C.; Lemiègre, L.; Benvegnu, T. *J. Org. Chem.* **2007**, *72* (22), 8267–8279.

(120) Raguse, B.; Culshaw, P. N.; Prashar, J. K.; Raval, K. *Tetrahedron Lett.* **2000**, *41* (16), 2971–2974.

(121) Jacquemet, A.; Lemiègre, L.; Lambert, O.; Benvegnu, T. *J. Org. Chem.* **2011**, *76* (23), 9738–9747.

(122) Benvegnu, T.; Réthoré, G.; Brard, M.; Richter, W.; Plusquellec, D. *Chem. Commun. (Cambridge, U. K.)* **2005**, No. 44, 5536–5538.

(123) Lecollinet, G.; Auzély-Velty, R.; Benvegnu, T.; Plusquellec, D.; Mackenzie, G.; Goodby, J. W. *Chemical Communications*. 1998.

(124) Barbeau, J.; Belmadi, N.; Montier, T.; Le Gall, T.; Dalençon, S.; Lemiègre, L.; Benvegnu, T. *Tetrahedron Lett.* **2016**, *2*, 1–5.

(125) Lecollinet, G.; Auzély-Velty, R.; Danel, M.; Benvegnu, T.; Mackenzie, G.; Goodby, J. W.; Plusquellec, D. *J. Org. Chem.* **1999**, *64* (9), 3139–3150.

(126) Long, L.; Zhou, L.; Wang, L.; Meng, S.; Gong, A.; Du, F.; Zhang, C. **2013**, 8214–8220.

(127) Menger, F. M.; Chen, X. Y. *Tetrahedron Lett.* **1996**, *37* (3), 323–326.

(128) Cuccia, L. a; Morin, F.; Beck, A.; Hébert, N.; Just, G.; Lennox, R. B. *Chem. Eur. J.* **2000**, *6* (23), 4379–4384.

(129) Nacka, F.; Cansell, M.; Gouygou, J. P.; Gerbeaud, C.; Méléard, P.; Entressangles, B. *Colloids Surf. B. Biointerfaces* **2001**, *20* (3), 257–266.

(130) Snyder, W. R. *Biochim. Biophys. Acta (BBA)/Lipids Lipid Metab.* **1987**, *920* (2), 155–160.

(131) Damsté, J. S. S.; Rijpstra, W. I. C.; Hopmans, E. C.; Schouten, S.; Balk, M.; Stams, A. J. M. *Arch. Microbiol.* **2007**, *188* (6), 629–641.

(132) Thompson, D. H.; Wong, K. F.; Humphry-baker, R.; Wheeler, J. J.; Kim, J.; Rananware, S. B. *J. Am. Chem. Soc.* **1999**, *114*, 9035–9042.

(133) Febo-Ayala, W.; Morera-Félix, S. L.; Hrycyna, C. A.; Thompson, D. H. *Biochemistry* **2006**, *45* (49), 14683–14694.

(134) Yamauchi, K.; Sakamoto, Y.; Moriya, A.; Yamada, K.; Hosokawa, T.; Higuchi, T.; Kinoshita, M. *J. Am. Chem. Soc.* **1990**, *112* (8), 3188–3191.

(135) Melis Çağdaş, A. D. S. and S. B. (Ed.), P. A. D. S., Ed.; InTech, 2014; 2.

Chapter 2

Synthesis of Archaea Inspired Tetraether Lipids and Investigation of Structural Functional Relationship to Membrane Leakage

2.1 Introduction to Archaeal Lipid Structures and Structural Functional Relationship On Membrane Permeability

In nature, organisms respond to environmental stress by modifying their membrane lipid composition to remain viable.[1–4] For example, Archaea are extremophiles classified as either halophiles, thermophiles, or acidophiles depending on the environment they inhabit and have evolved mechanically and chemically robust membrane compositions that allows for their survival in high salinity, high temperature, or high acidity, respectively.[5] Archaeal membranes have been extensively studied in the hopes to unveil their unique structural benefits on membrane permeability that differs from their bacterial counterparts. A representative collection of lipid structures of archaeal lipids are shown in Figure 2.1 that highlight the unique structures found in macrocyclic tetraether lipids (i.e. isoprenoid alkyl chains, ether glycerol linkage, alkyl rings, and polar lipid headgroups). Notably, one structural feature shown in Figure 2.1 that has fascinated scientists, is how the integration of up to eight cyclopentane rings to

the lipid core affect membrane properties. For example, a hyperthermophillic Archaea, Crenarchaeota, have been observed to thrives in temperature above 80 °C and have different numbers of cyclopentane rings found in the lipids of the membrane depending on their growth temperature.[2,6,7] The increased number of cyclopentane rings is believed to tighten membrane packing as the environmental temperature rises.[8] In recent studies, Thaumarchaeota, a newly added category in the kingdom of Archaea, have been observed to incorporate cyclohexane rings into their lipids.[7] The reason for the incorporation of cyclohexane to the lipid tail has been enigmatic. One hypothesis proposed from molecular dynamic simulation calculation data suggests the addition of cyclohexane rings to the lipid core allows for a higher conformational freedom than cyclopentane that allow Thaumarchaeota to survive in colder marine environment.[9] In addition to the structural changes observed in the archaeal lipid tails for adaptation to environmental stress, changes in polar lipid headgroups have been observed as well.[10,11] For example, lipid compositions of archaeal membranes found in hot acid springs with pH < 3, have been found to have higher concentrations of polar lipid headgroups capable of increased hydrogen bonding.[12–14] This additional hydrogen bonding network has been hypothesized to function as an additional barrier to decrease membrane permeability towards protons. However, the difficulty of isolation of pure lipids with different polar lipid headgroups precludes testing this hypothesis.[15]

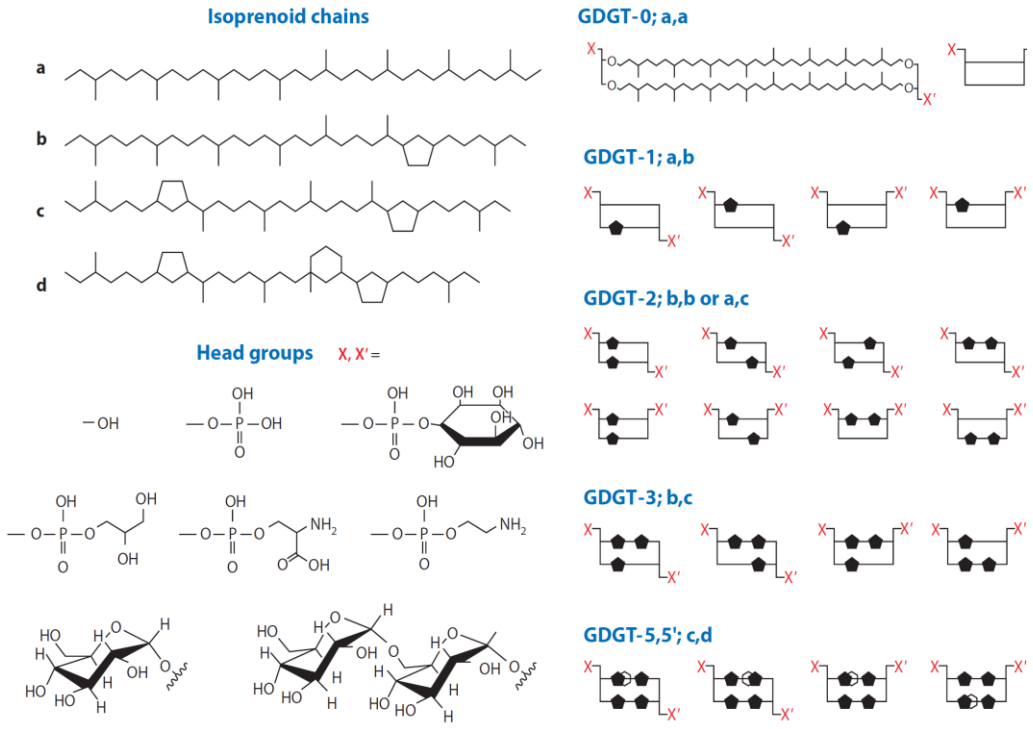

Figure 2.1. Tetraether lipids with varying hydrophobic core and polar lipid headgroups found in archaeal membranes. Reprinted by permission from Annual Reviews: [The Annual Review Earth and Planetary Sciences] (Pearson, A.; Ingalls, A. E. *Annu. Rev. Earth Planet. Sci.* **2013**, *41* (1), 359–384.), copyright (2013)

One approach, mention in chapter 1 of this dissertation, used to study structural/functional relationship of archaeal lipids on membrane leakage is by extracting natural lipids and forming vesicles. Specifically, liposomes made from polar lipid fraction E (PLFE) that are extracted from *Sulfolobus acidocaldarius* or *Thermoplasma acidophilum* exhibit low permeability towards small ions/molecules, tight membrane packing, and high stability in human bile containing solutions.[13,16] Another study showed a general trend of increased membrane stability of diacyl lipid membranes as the mole fraction of tetraether lipid increased.[17] Despite the favorable membrane properties attributed to

liposomes made by extracted lipids from Archaea, the structure-function relationship of archaeal lipid structures remains unclear because archaeosomes are made from mixtures of lipids.[18] A different strategy employed by scientists studying the structural-functional relationship of archaeal lipids, have turned their focus on synthesizing archaeal lipid analogs (as mentioned in section 1.2.2 of this thesis). While many groups have successfully synthesized archaeal lipid analogs, the structural functional relationship of these lipids on membrane permeability remains unclear. A systematic study that probes the structural effect of archaeal lipids on membrane permeability will be necessary to develop new classes of robust liposomes.

While archaeal tetraether lipids found in nature are typically macrocyclic (i.e., both transmembrane lipid tails are tethered), we designed Archaea-inspired tetraether lipids to be hemicyclic, analogous to the method employed by Thompson[19] and Benvegnu[20] groups. By synthesizing model hemicyclic tetraether lipids that incorporate structural features found in natural archaeal lipids, we can avoid problems of low yields associated with the increased number of steps that are required to synthesize useful quantities of the lipid molecules.[21] Using this strategy, we were able to synthesize sufficient amounts of lipids with varying hydrophobic core and polar lipid headgroups (Figure 2.2) necessary to form liposomes to study membrane leakage properties. To ensure stable liposomal formation, we initially designed our tetraether lipids with phosphocholine head groups because zwitterionic head groups are known to produce stable liposomes.[22] Next, after deciding on the lipid scaffold to be used

for synthesizing lipid analogs with different polar lipid head groups, we continued our investigation to study how structural changes affect membrane leakage.

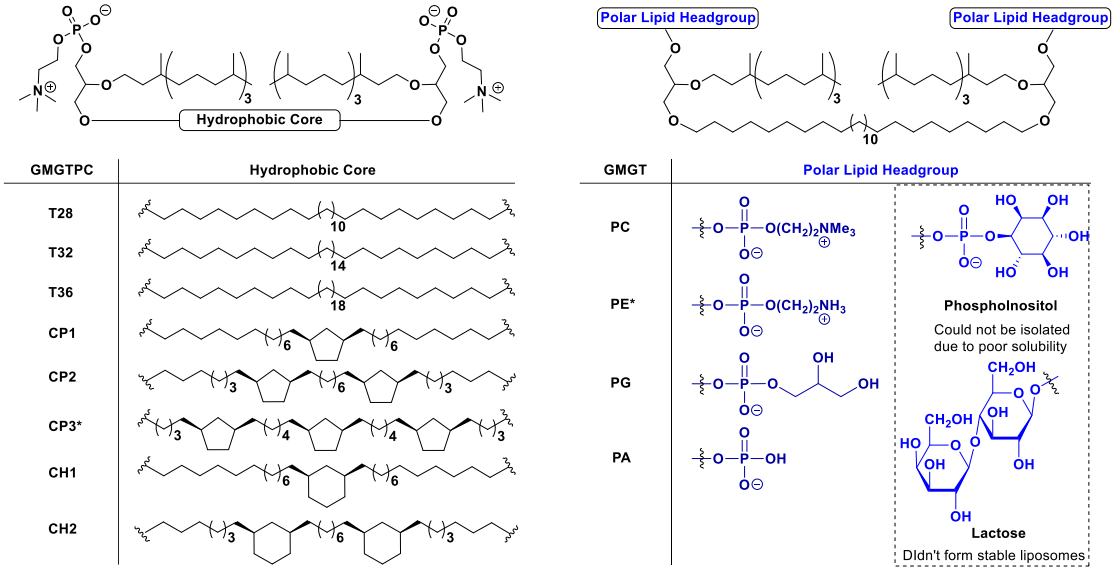

Figure 2.2. Structures of synthesized tetraether lipids.[41,67] *synthesized by Dr. Leriche

2.2 Synthesis of Archaea Inspired Tetraether Lipids

2.2.1 Synthesis of Archaea Inspired Tetraether Lipids with Varying Hydrophobic Core

The retrosynthesis of tetraether lipid analogs with varying hydrophobic core (shown in Scheme 2.1) began with an initial dissection between the polar lipid headgroup and the lipid scaffold to minimize the number of purification steps with charged species, thus, separating the molecule into two pieces (a phosphocholine moiety and a lipid scaffold diol) that can be covalently joined through alkylation. The construction of hemicyclic lipophilic diols can be formed through tethering of the hydrophobic core by alkylation of dibromoalkane by a

functionalized glycerol, which simplifies the molecule into two parts (phytanyl functionalized glycerol and dibromoalkane analogs carrying different hydrophobic cores). Beginning with the design of the functionalized glycerol, the architecture of the monobenzyl protected glycerol can be formed through a ring opening of the acetal using DIBAL-H and reduction of the olefin can be performed using standard hydrogenation conditions. The phytanyl appendage of the benzylidene acetal can be added to the commercially available 1,3-benzylideneglycerol by alkylation to iodophytol, which can be made from commercially available phytol. The other alkylation partner, the dibromoalkyl intermediate, can be formed through bromination of the alkyldiol analog. The alkyldiol analog, with varying alkyl lengths, can be formed through homologation using Wittig conditions followed by the removal of the benzyl protecting groups and reduction of the double bonds, which simplifies the molecule into the two Wittig reaction partners. One of the two Wittig partners, the aldehyde, can be synthesized by a selective monobenzyl protection of the diol followed by an oxidation of the free alcohol to the aldehyde. The other Wittig partner, the phosphonium salt, can be synthesized starting from a diol through a series of iodination of the diol, followed by the displacement of the newly formed diiodides by triphenylphosphine. With the synthetic strategy of tetraether lipid analogs (with varying hydrophobic cores) completed, I will next describe the specific chemical transformations used to accomplish the synthesis of a set of tetraether lipids with various hydrophobic cores.

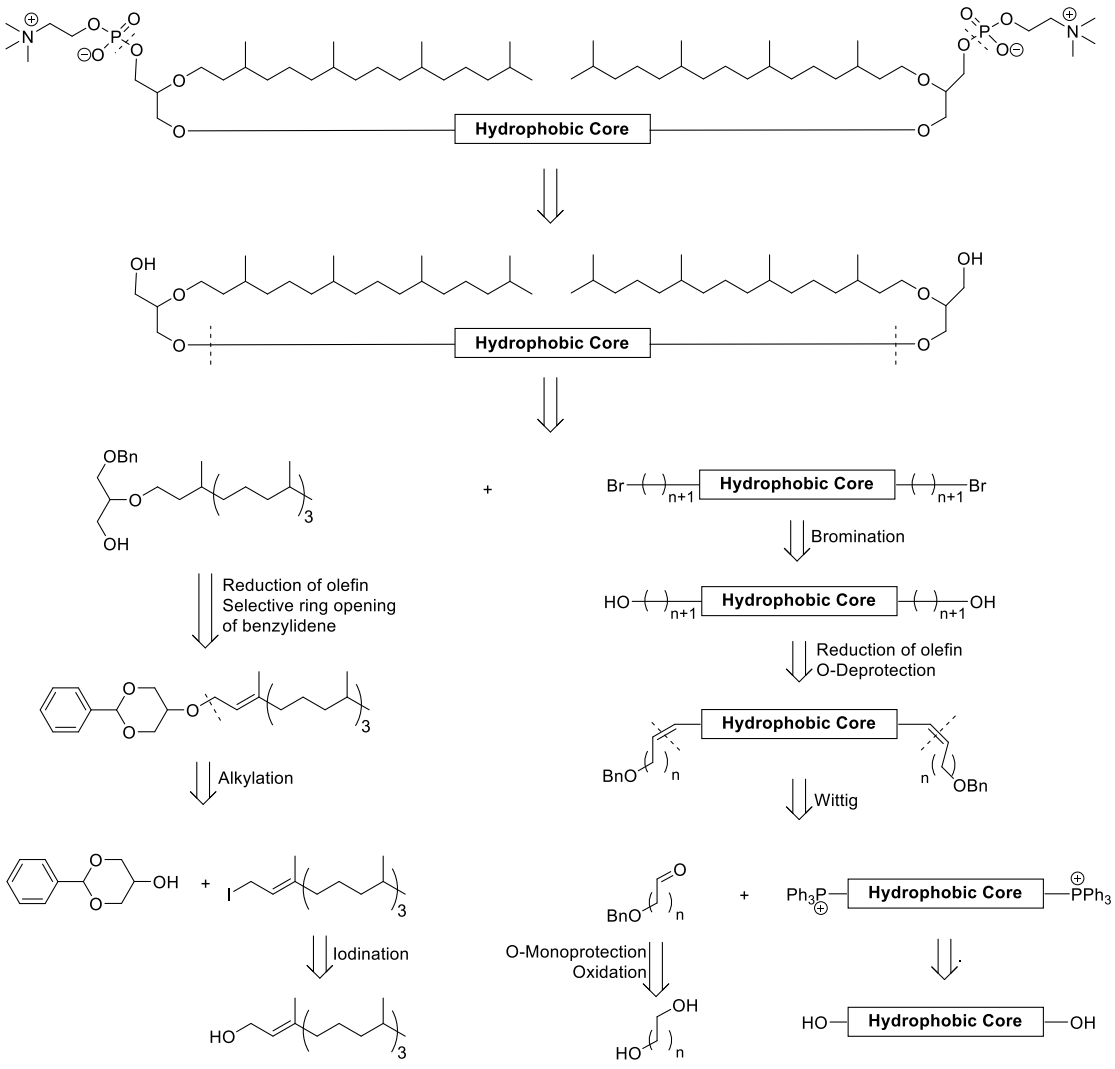

Scheme 2.1. Retrosynthetic strategy to synthesize tetraether lipid derivatives with different hydrophobic cores.

2.2.1.1 Synthesis of Phytanyl Functionalized Glycerol Backbone

The synthesis of phytanyl functionalized glycerol backbone **2.4,** used for all the Archaea inspired tetraether lipid analogs synthesized in this chapter, began by iodination of commercially available phytol (shown in Scheme 2.2) using standard conditions, resulting in the formation of iodinated phytol **2.1** in 70% yield. Next, iodinated phytol **2.1** was alkylated by commercially available 2-phenyl-1,3-dioxan-5-ol to generate the masked glycerol **2.2.** Following the addition of the phytanyl group, hydrogenation of the alkene **2.2** catalyzed by Wilkinson's catalyst afforded the reduced phytanyl substituted glycerol **2.3**, in 85% yield. Lastly, the synthesis of benzyl protected glycerol backbone **2.4** was completed by a selective ring opening of the acetal using DIBAL-H in 93% yield as a mixture of diastereomers.

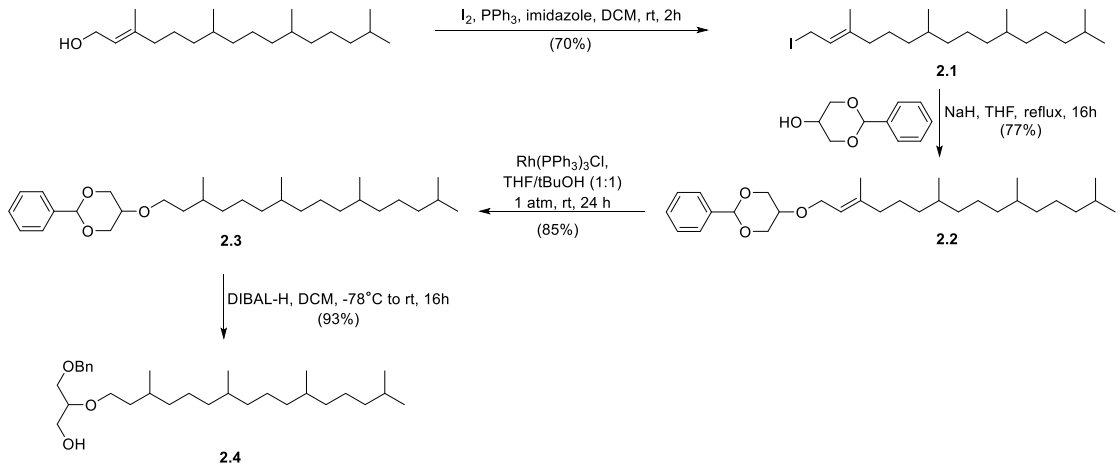

Scheme 2.2. Synthesis of glycerol scaffold **2.4**.

*2.2.1.2 Synthesis of **GMGTPC** T28, T32, T36*

The Synthesis of **GMGTPC** lipids with varying alkyl chain lengths of the tethered region began by the formation of an alkyldiol with the desired number of carbon chains. For example, 1,20-eicosanediol **2.5** was synthesized by the reduction of 1,20-eicosandioic acid by LAH for the T36 precursor, whereas, the 1,12-dodecanediol and 1,16-hexadecanediol were used for the synthesis of T28 and T32 precursors, respectively (shown in Scheme 2.3). Next, the alkyldiols of varying lengths were oxidized to form the respective alkyldialdehyde (**2.6-2.8**) using Albright-Onodera conditions. In parallel, Wittig coupling partner **2.10**, was generated by a series of reactions beginning with a selective THP monoprotection of 1,8-octanediol forming the mono-THP protected alcohol **2.9.** The free alcohol of **2.9** was transformed to the corresponding phosphonium salt **2.10** by an initial iodination of the free alcohol followed by a nucleophilic displacement of the iodide by triphenylphosphine (with an overall yield of 62% after 2 steps) which successively reacted with alkyldialdehyde (**2.6-2.8**) under Wittig conditions to afford the di-THP protected elongated olefin (**2.11-2.13**) as mostly the *cis* isomer. Notably, the mixture of conformational isomers of diolefin becomes inconsequential because the alkenes are subsequently reduced in the following step. The formation of Alkyldibromide (**2.17-2.19**) was completed by a series of Pd catalyzed hydrogenation steps to form the saturated THP protected diol (**2.14-2.16**), followed by a simultaneous deprotection of THP and bromination of diols using triphenylphosphine and carbontetrabromide. Next, the dibromoalkane was alkylated by glycerol moiety **2.4** by heating in THF to

reflux under basic conditions to generate the tethered benzyl-protected lipid precursor as a mixture of diastereomers (**2.20-2.22**). The removal of the benzyl protecting groups were accomplished by a Pd catalyzed hydrogenation, affording lipid scaffold diol (**2.23-2.25**). Upon the deprotection of the diol, the formation of **GMGTPC** T28, T32, and T36 (as a mixture of diastereomers) was completed by reacting diol (**2.23-2.25**) with 2-bromoethyl dichlorophosphate, ending with the displacement of the two bromides on the phosphatidylcholine precursor by trimethylamine.

*2.2.1.3 Synthesis of Cycloalkane Integrated **GMGTPC***

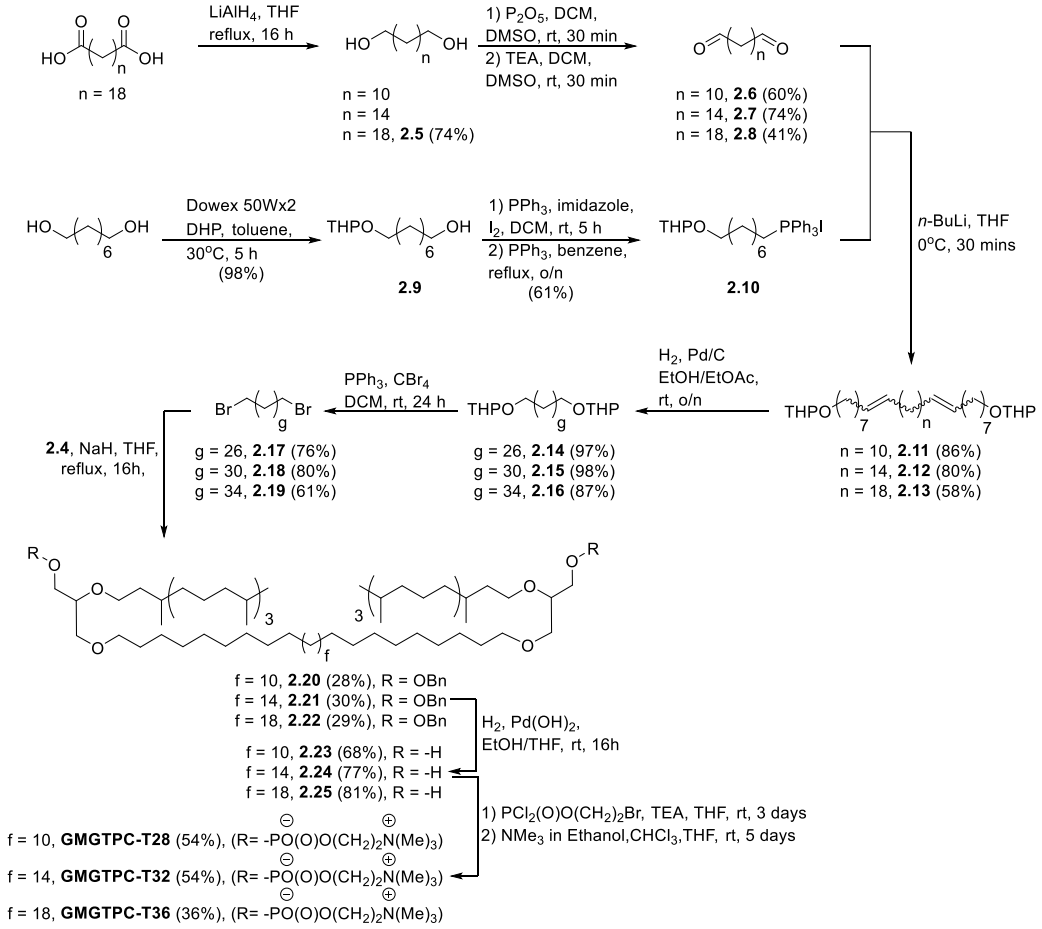

Scheme 2.3. Synthesis of **GMGTPC** T28, T32, T36.

We envisioned using three separate strategies for the synthesis of symmetrical *cis*-1,3-substituted 1, 2, or 3 cycloalkane-containing alkyldibromide. The first strategy to synthesize the tetraether lipid with one cycloalkane (shown in Scheme 2.4), began with the synthesis of the respective *cis*-1,3-cycloalkyl diphosphonium salts (**2.26** or **2.28**). The cyclohexane containing diphosphonium moiety **2.28** was formed by reduction of *cis*-1,3-cyclohexanedicarboxylic acid using LAH, followed by the transformation of the newly formed diol to the diphosphonium iodide derivative **2.28** using conditions from section 2.2.1.2. The cyclopentane containing diphosphonium moiety **2.26** was synthesized as previously reported by Benvegnu[23] group beginning with the formation of *cis*-1,3-cyclopentyldialdehyde by ozonolysis of norbornene, which was followed by the reduction of the dialdehyde using $NaBH_4$ to form the *cis*-1,3-cyclopentanediol. The formation of phosphonium salt **2.26** was completed by an initial iodination of diol followed by a nucleophilic substitution of the diiodides by triphenylphosphine. In parallel, the Wittig coupling partner **2.30**, was synthesized by a selective monobenzyl protection of dodecanediol **2.29**, followed by a DMP oxidation of the free alcohol to generate the monobenzyl protected aldehyde **2.30** (35% yield over 2 steps). The two Wittig partners, diphosphonium salt (**2.26** or **2.28**) and monoprotected aldehyde **2.30**, were coupled using Wittig conditions to form the elongated dibenzyl-protected olefin (**2.31** or **2.32**). The newly formed dibenzyl-protected olefin was simultaneously debenzylated and reduced using Pd catalyzed hydrogenation to form diol **2.33** or **2.34**. Subsequently, diol **2.33** or **2.34** was heated to reflux in

hydrobromic acid, which concluded the formation of dibromalkane **2.35** or **2.36**. The synthesis of **GMGTPC-CP1** or **GMGTPC-CH1** (as mixtures of diastereomers) was completed in a series of reactions beginning with alkylation of cycloalkane integrated dibromoalkane **2.35** or **2.36** by the phytanyl functionalized glycerol **2.4,** followed by the attachment of phosphocholine using synthetic conditions for the formation of **GMGTPC** (section 2.2.1.2).

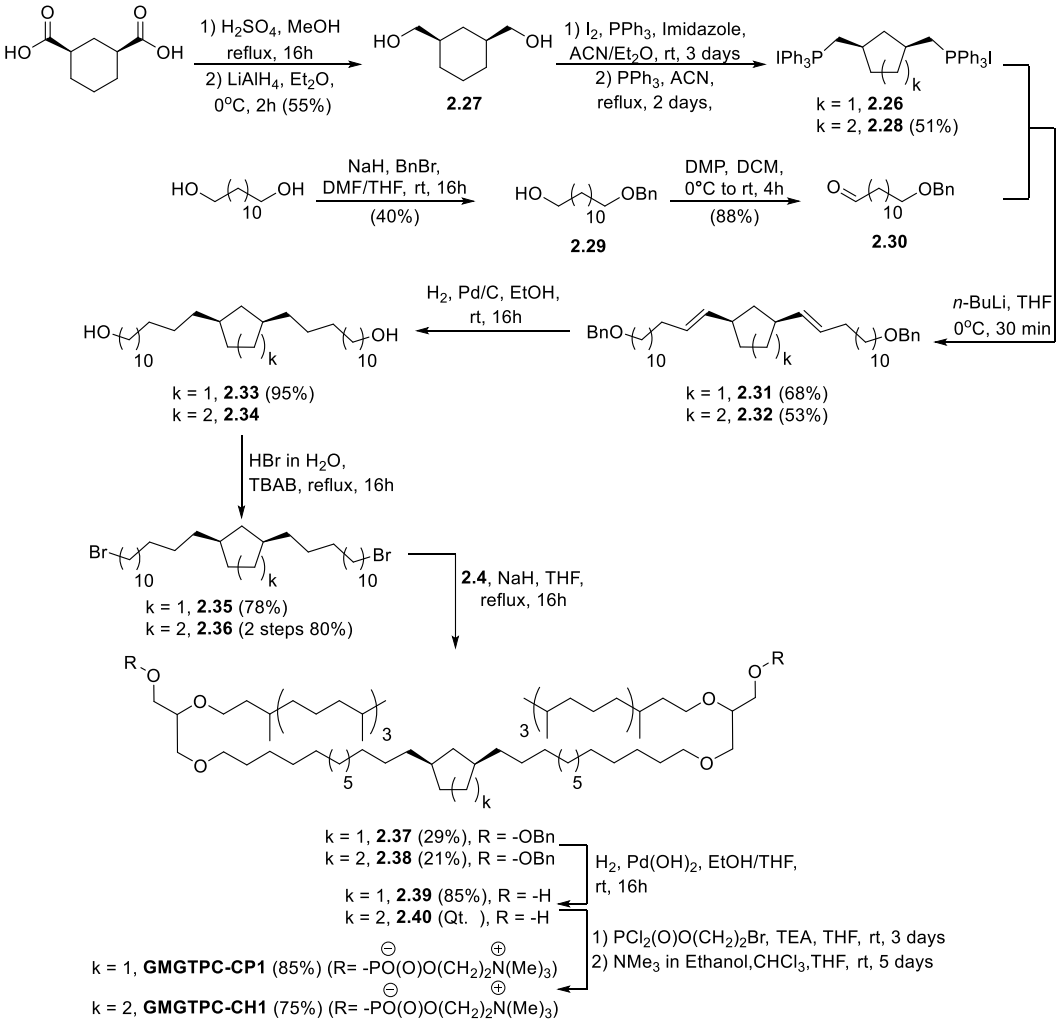

Scheme 2.4. Synthesis of **GMGTPC-CP1** and **GMGTPC-CH1**.

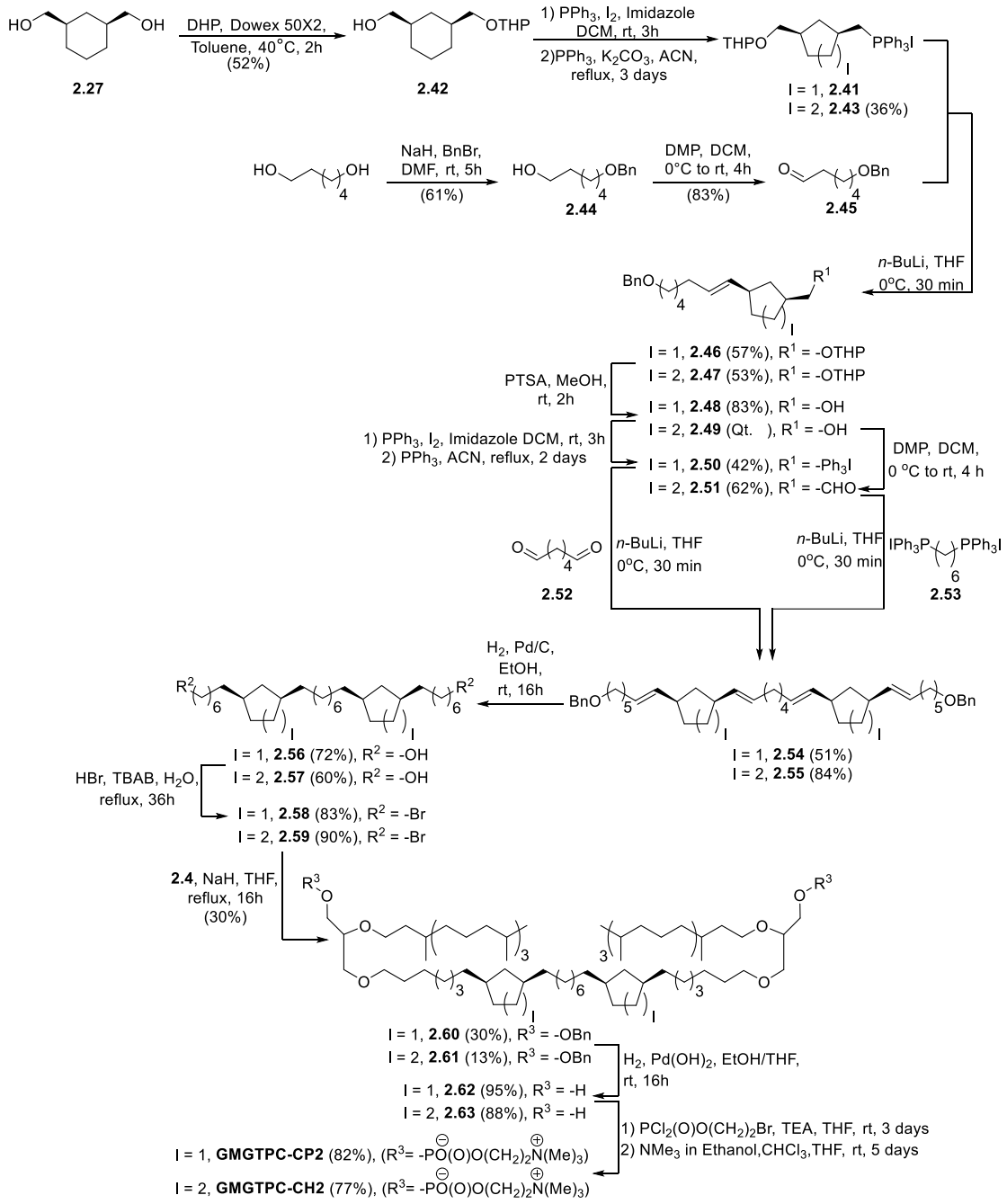

Scheme 2.5. Synthesis of **GMGTPC-CP2** and **GMGTPC-CH2**.

Our second strategy (shown in Scheme 2.5) to synthesize alkyldibromide analogues with 2 cycloalkanes began with a selective monoprotection of diol **2.27** (for **GMGTPC-CH2**) using THP, which was subsequently transformed to

the phosphonium iodide derivative **2.43** (19% yield over 2 steps). The cyclopentylphosphoniumiodide analog (for **GMGTPC-CP2**) **2.41** was synthesized as previously reported by Benvegnu group[24] using similar conditions as the cyclohexyl analog **2.43**. Aldehyde intermediate **2.45,** which was used in the subsequent Wittig reaction, was formed through a selective monobenzylation of 1,6-hexanediol to form the monoprotected alcohol **2.44,** which was followed by a DMP oxidation of the free alcohol to generate aldehyde **2.45** (51% yield over 2 steps). Homologation reaction involving the phosphonium iodide derivative **2.41** or **2.43** and monobenzylated aldehyde **2.45** was completed using Wittig conditions to afford the orthogonally protected olefin **2.46** or **2.47**. Next, setting the stage for the subsequent Wittig reaction, the THP protecting group on the orthogonally protected olefin **2.46** or **2.47** was selectively deprotected under acidic conditions affording monobenzylated olefin **2.48** or **2.49**. For the ensuing Wittig reaction involving the cyclohexyl analog, we explored two different synthetic strategies. For our first strategy, we envisioned converting the free alcohol of olefin **2.48** to the phosphonium derivative **2.50**. The phosphonium derivative **2.50** was next coupled with 1,6-hexandial **2.52** to generate the extended olefin **2.54** in 21% yield over two steps. For our second strategy, we switched the functional roles between the two Wittig coupling partners. Aldehyde **2.51** was formed by oxidation of the free alcohol of olefin **2.49** using DMP, which was coupled with 1,6-hexandiphosphonium iodide **2.53** to generate the extended olefin **2.55** in 52% yield over two steps. The increased yield observed for the second strategy is believed to originate from the

increased solubility of the crystalline 1,6-hexandiphosphonium iodide **2.53** compared with the less soluble oily phosphonium derivative **2.50**. Upon the completion of the homologation reactions to obtain the desired alkyl length **2.54** or **2.55**, the synthesis of diol **2.56** or **2.57** was completed by a Pd catalyzed hydrogenation resulting in debenzylation and reduction of the double bonds. The free diols were converted to the respective alkyldibromides **2.58** or **2.59** by heating in hydrobromic acid at reflux overnight, which was then alkylated by glycerol **2.4** to form the lipid precursor **2.60** or **2.61** as a mixture of diastereomers. The synthesis of **GMGTPC-CP2** or **GMGTPC-CH2** (as a mixture of diastereomers) was completed through a series of reactions involving deprotection of the diol and concluding with the addition of the phosphatidylcholine headgroups as described in section 2.2.1.2.

For our last strategy to synthesize the symmetrical alkyldibromide containing three *cis*-1,3-substituted cyclopentane (synthesized by Dr. Leriche) began with the formation of the central cyclopentane intermediate by coupling aldehyde **2.65,** formed by ozonlysis of monobenzyl-protected terminal alkene **2.64,** with diphosphonium substituted cyclopentane moiety **2.27** under Wittig conditions to generate the elongated olefin **2.66** (40% yield over 2 steps). Next, the elongated olefin was debenzylated and the alkene was reduced by a Pd catalyzed hydrogenation to form diol **2.67**, which was sequentially converted to diphosphonium salt **2.68** (using standard conditions; 49% yield over 2 steps). In parallel, unsymmetrical cyclopentane moiety **2.71** was formed in a similar series of reactions, beginning with ozonolysis of benzylprotected terminal olefin **2.69**

that was subsequently reacted with a THP protected monophosphonium cyclopentane **2.41** under Wittig conditions to form the extended olefin **2.71** (32% yield over 2 steps). Setting the stage for the next Wittig reaction, the THP protecting group of the orthogonally protected molecule **2.71** was selectively deprotected under acidic conditions to form alcohol **2.72** in quantitative yield. The free alcohol of the monobenzyl protected olefin **2.72** was oxidized using DMP, forming aldehyde **2.73** (70% yield), which was coupled with diphosphonium **2.68** in another Wittig reaction to form the elongated olefin **2.74** containing three *cis*-1,3 substituted cyclopentanes (as a mixture of syndiotactic and isotactic isomers; 77% yield). The key tethering fragment **2.76** was formed through a set of reactions beginning with debenzylation and reduction of alkenes through a Pd-catalyzed hydrogenation followed by bromination of the free diol **2.75** by heating to reflux in hydrobromic acid (52% yield over 2 steps). The synthesis of diastereomeric mixture **GMGTPC-CP-3** was completed through a series of reactions involving alkylation, deprotection of the diol, and addition of phosphatidylcholine headgroups using the same method described in section 2.2.1.2.

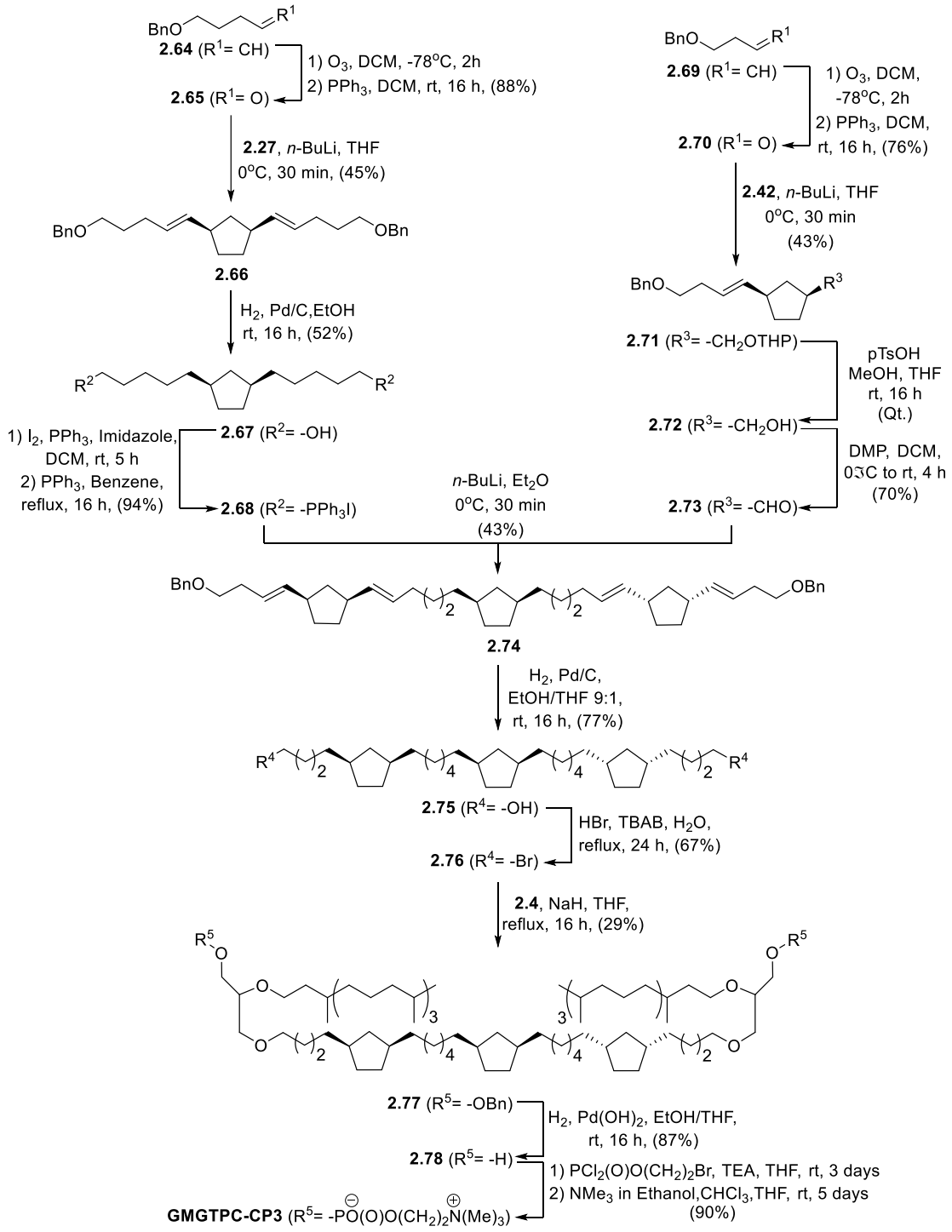

Scheme 2.6. Synthesis of **GMGTPC-CP3** designed and synthesized by Dr Leriche.

2.2.2 Synthesis of Archaea Inspired Tetraether Lipids with Varying Polar Lipid Headgroups

Our strategy to synthesize tetraether lipids with varying polar headgroup began with the preparation of benzyldiisopropylphosphoramidite analogs that would be coupled to diol **2.23** (shown in Figure 2.7)**.** The newly formed phosphite-triester adducts would then be oxidized to the corresponding phosphate-triesters followed by removal of protecting groups by hydrogenation with Pd to afford tetraether lipid analogs with varying polar lipid headgroups. In addition to tetraether lipids equipped with polar lipid headgroups with phosphate derivatives, we also explored the synthesis of lactose containing GMGT lipid, **GMGTLa**, using traditional glycosidation conditions to glycosylate diol **2.23**.

Starting with the synthesis of **GMGTPG** as the target compound**,** we began the synthesis by forming dibenzylprotected glycerol **2.80** from benzylation of 2-phenyl-1,3-dioxan-5-ol to form the masked glycerol **2.79** in quantitative yield. The formation of dibenzyl protected glycerol **2.80** was completed by a ring opening of acetal **2.79** using DIBAL-H in 96% yield. Next, phosphatidylglycerol tetraether lipid precursor **2.86** was generated in a series of reactions starting by coupling alcohol **2.80** with benzylalcohol functionalized tetraisopropylphosphanediamine **2.81,** forming prophosphoglycerol benzyldiisopropylphosphoramidite **2.82** that was sequentially reacted with diol **2.23**. Lastly, the formation of **GMGTPG** was completed after an oxidation of the phosphite intermediate with tert-butyl peroxide, forming phosphoramidite

intermediate **2.86**, followed by debenzylation using Pd catalyzed hydrogenation in 26% overall yield.

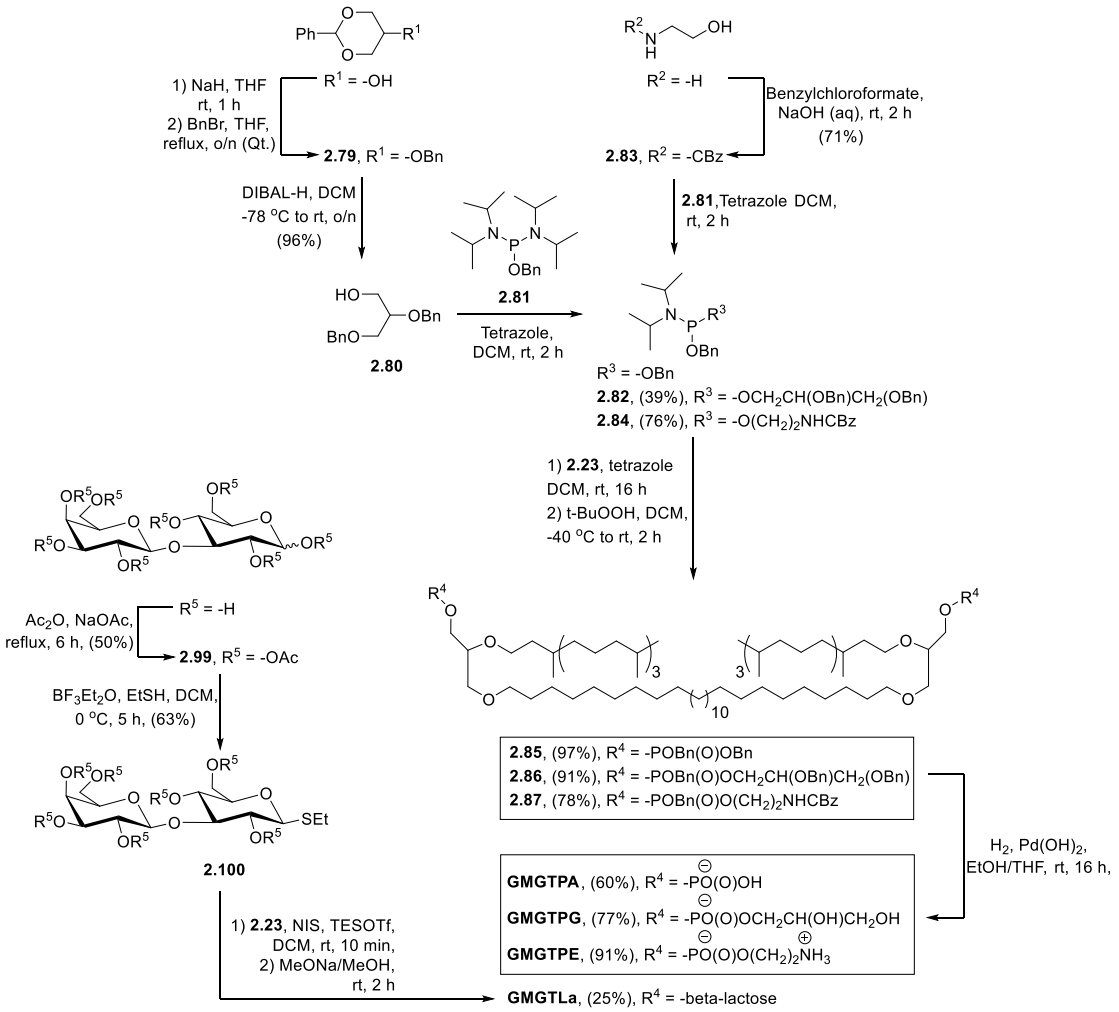

Scheme 2.7. Synthesis of **GMGT** lipids with different polar lipid headgroups.

Similarly, synthesis of **GMGTPE** (by Dr. Leriche) began by a selective CBz protection of the amine of ethanolamine, followed by the addition of the free alcohol of **2.83** to phosphoramidite **2.81** that afforded phosphoethanolamine precursor, benzyldiisopropylphosphoramidite intermediate **2.84**. The synthesis of **GMGTPE** was completed in a series of

reactions beginning with the union between diol **2.23** and **2.81**, followed by a tert-butyl peroxide propagated oxidation of the phosphite intermediate forming phosphate lipid precursor **2.87**, that concluded with deprotection of the amine and alcohol using Pd catalyzed hydrogenation in 38% overall yield.

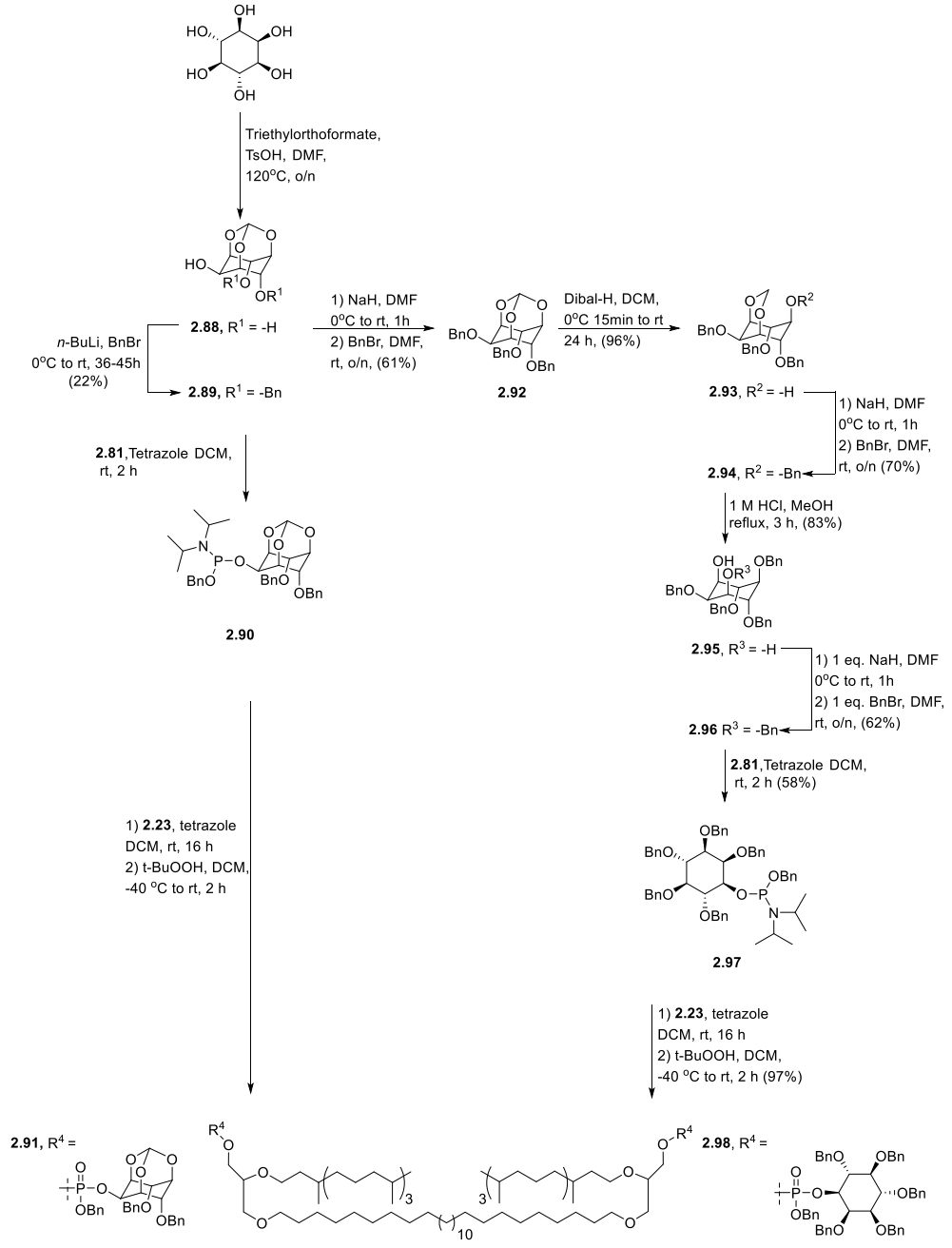

Scheme 2.8. Two strategies to synthesize **GMGTPI.**

Preparation of **GMGTPA** was performed in fewer steps by reacting diol **2.23** with the commercially available, dibenzyl diisopropylphosphoramidite, which was followed by oxidation of the phosphite intermediate using tert-butyl peroxide to form phosphate lipid intermediate **2.85** that was debenzylated by hydrogenation with Pd in 58% overall yield.

Notably, we were unsuccessful in synthesizing phosphatidylinositol **GMGTPI** lipid using the same synthetic strategy as mentioned above. Our initial attempt to synthesize **GMGTPI** began by selectively protecting all but one hydroxyl group on myo-inositol using orthoester and benzyl protection of alcohols. First, a selective orthoester formation[25] of myo-inositol using triethylorthoformate was accomplished to afford the selectively protected inositol **2.88** (shown in Scheme 2.8). The two adjacent axial alcohol groups were selectively benzyl-protected using *n*-BuLi to form the orthogonally protected inositol **2.89**. After all but one alcohol of the inositol was orthogonally protected, the free alcohol of **2.89** was reacted with phosphoramide **2.81** to afford the protected inositol phosphoramidite intermediate **2.90**. Similar to other GMGT lipid analogs synthesis, phosphoramidite intermediate **2.90** and diol **2.23** were coupled, which was followed by oxidation of the phosphite to phosphate affording inositol lipid precursor **2.91**. Up to this point, we were successful at synthesizing **GMGTPI** lipid precursor **2.91**. However, although several reactions conditions were attempted (shown in Table 2.1), we were unable to isolate **GMGTPI** after several deprotection conditions that were explored on Inositol lipid precursor **2.91**. Our initial deprotection condition for orthogonally protected

inositol lipid **2.91** was through a simultaneous acetal deprotection and benzyl deprotection using hydrogenation with Pd in the presence of TFA (shown in entry 1 of Table 2.1). However, under these conditions, we did not recover product or starting material. Perhaps a longer reaction time was required for the deprotection to occur, therefore, we next explored conditions involving longer reaction time while holding other conditions constant (entry 2 of Table 2.1). Interestingly, no product or starting material was observed for both reaction conditions which led us to believe that degradation of starting material and/or product may be taking place. Next, we tested the reaction conditions that focused solely on deprotection of the acetal under various solvent, time, and acid conditions (shown in entry 3-7 of Table 2.1). However, similar to results from entry 1-2 (Table 2.1), no product or starting material was present upon workup that further suggested the possibility of degradation. For the latter two conditions (entry 8.1-9.2 of Table 2.1), a sequential two-step deprotection of the acetal followed by debenzylation was attempted with different solvent ratios of DCM and MeOH. However, no starting material nor product was detected again. For the last deprotection condition (entry 10.1 and 10.2 of Table 2.1) we switched the two-step sequence order, hence, debenzylation followed by deprotection of the acetal. Nevertheless, no product nor starting material was detected upon workup.

Table 2.1. Reaction conditions screened to deprotect **GMGTPI** precursor **2.91**.

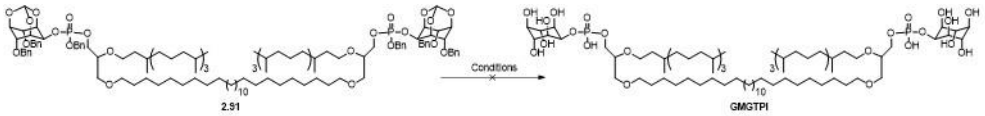

Entry	Reagent	Solvent	T (°C)	t (h)
1	$Pd(OH)_2$; 15% TFA	THF:MeOH (1/1)	25	3
2	$Pd(OH)_2$; 15% TFA	THF:MeOH (1/1)	25	16
3	4 M HCl	Dioxane	25	48
4	50% TFA	DCM:MeOH (4/1)	25	25
5	50% TFA	DCM:MeOH (1/1)	25	25
6	80% TFA	THF	25	24
7	80% TFA	THF	25	40
8.1	50% TFA	DCM:MeOH (4/1)	25	25
8.2	$Pd(OH)_2$	DCM:MeOH (4/1)	25	3
9.1	50% TFA	DCM:MeOH (1/1)	25	25
9.2	$Pd(OH)_2$	DCM:MeOH (1/1)	25	3
10.1	$Pd(OH)_2$	THF:MeOH (1/1)	25	3
10.2	50% TFA	THF:MeOH (1/1)	25	25

From the results observed from our first synthetic strategy that used two orthogonal protection of alcohol, which suggests a potential degradation problem caused during deprotection of the orthoester, we designed a second synthetic strategy to synthesize phosphatidylinositol **GMGTPI** that solely used benzyl-protected alcohols for **GMGTPI** lipid precursor molecule (shown in

Scheme 2.8). We began our second synthetic attempt by benzylation of all three free alcohols of the orthoester protected inositol intermediate **2.88** to form orthogonally protected inositol **2.92**. The orthoester of **2.92** was selectively opened[26] using DIBAL-H to afford acetal protected inositol **2.93**. The free alcohol of **2.93** was benzylated forming intermediate **2.94**, which was followed by deprotection of the acetal under acidic conditions to afford diol **2.95**. Lastly, using one equivalence of NaH and BnBr, the targeted benzyl-protected inositol with one free alcohol **2.96** was formed. The free alcohol on **2.96** was reacted with phosphoramidite **2.81** to form the phosphoramide inositol derivative **2.97**. Following the addition of **2.97** to lipid diol **2.23** and oxidation of the phosphite to phosphate, we successfully synthesized phosphatidylinositol lipid precursor **2.98**. Finally, the **GMGTPI** lipid precursor **2.98** was subjected to a Pd catalyzed hydrogenation to liberate the benzyl protected alcohol to generate the desired **GMGTPI**. However, during and after hydrogenation, spontaneous formation of white precipitate was observed. To purify and identify the precipitate, various solvent mixtures were employed (i.e. DCM, MeOH, EtOH, EtO_2, THF, ACN, BuOH, acetone, benzene, DMSO) to dissolve the solid. However, the white solid remained insoluble. Notably, similar to the results I observed during hydrogenation of **GMGTPI** lipid precursor **2.98**, formation of insoluble solid was also observed by Dr. Leriche during his deprotection reaction of CBz-protected phosphatidylserine tetraether lipid derivative, **GMGTPS**. We hypothesize the poor solubility of **GMGTPI** and **GMGTPS** may be due to the poor balance between the hydrophobic and hydrophilic nature of lipids preventing the

molecule to become solvated. Another possibility may be caused by the ability of the lipid to pack too well, as suggested by the high phase transition to liquid state observed for diacyl derivatives of phosphatidylinositol or phosphatidylserine.[27,28] The extraordinary rigid packing hypothesis may support the inability for solvents to solvate **GMGTPI** and **GMGTPS** lipids. Unfortunately, to study membrane properties, we must be able to form liposomes by creating thin lipid films by drying lipids dissolved in volatile solvent. However, because the crude lipid mixture was insoluble in organic solvents that were surveyed, we deemed the lipids unsuitable for further study in membrane leakage experiments.

In addition to lipids with phosphatidyl headgroups, the lactose conjugated lipid, **GMGTLa,** was synthesized using traditional glycosylation reactions.[23] The synthesis of **GMGTLa** began by acetylating all the alcohols of lactose using acetic anhydride to form protected lactose **2.99**. The anomeric carbon on the glucose portion of lactose was converted to thioether **2.100** by mercaptoethanol in ethereal trifluoroborate. Next, the thoiether of the protected lactose **2.100** was activated with *N*-iodosuccinmide (NIS) allowing for attack by the diol of lipid scaffold **2.23** to form the lactose lipid precursor. Lastly, de-acetylation of lactose using basic methanol completed the formation of lipid analog **GMGTLa** in 29% overall yield.

2.3 In vitro Assay of Synthetic Archaea Inspired Tetraether Lipids

2.3.1 Liposome Formation and Characterization

2.3.1.1 Liposome Formation and Characterization of Archaea Inspired Tetraether Lipids with Varying Hydrophobic Core

Liposomes were prepared from pure **GMGT** lipid analogs, with varying hydrophobic core, by dissolving the lipid in volatile organic solvents that was subsequently dried under vacuum. Next, the dried lipid films were hydrated (10 mg/mL) in 10 mM Bis-Tris buffer (including 4 mM 5,6-carboxyfluorescein (CF), 100 mM NaCl, pH 7.2 or pH 5.8) and extruded 25 times through a 200 nm polycarbonate membrane, followed by a second extrusion through a 100 nm membrane 51 times. This liposome preparation afforded liposomes of ~130 nm average hydrodynamic diameter as determined by dynamic light scattering (DLS, a more detailed description on liposome formation can be found in section 2.5.9 General Procedure for Liposome Formation). The average size of liposomes made with synthetic tetraether lipid analogs remained stable for at least 6 hours (see Figure 2.3A.).

After we confirmed the ability of synthetic **GMGT** lipid analogs to form stable liposomes, we examined whether **GMGT** lipid analogs displayed a phase transition using differential scanning calorimetry (DSC, detailed information can be found in section 2.5.1. Reagents and Instruments). Using 1,2-dimyristoyl-*sn*-glycero-3-phosphocholine (DMPC) as the positive control that displays a phase transition ~ 24 °C to validate our method (shown in Figure 2.3B, measurements taken by David Onofrei), we observed an absence of a lipid phase transition

from 5-65 ºC, which suggests that the **GMGTPC** lipid analogs were suitable for evaluation as liposomes to measure SFR to membrane leakage.

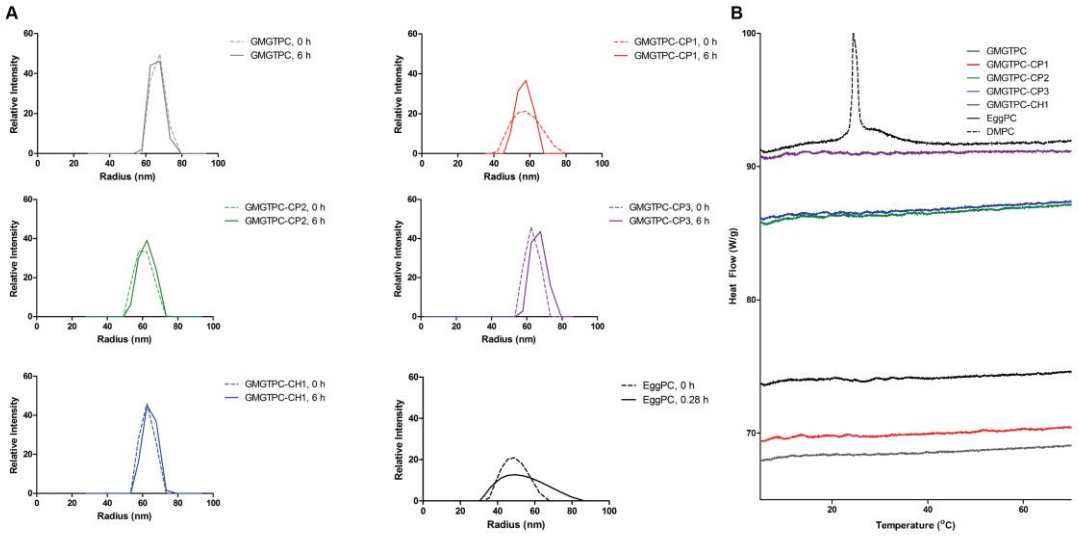

Figure 2.3. Physical characterization of lipids. A) DLS measurements of Liposomes made with **GMGTPC** lipid analogs or EggPC. (N = 10 for each trace); B) DSC measurements of synthetic GMGTPC lipid analogs and diacyl lipids. Measurement taken by David Onfrei.

2.3.1.2 Liposome Formation and Characterization of Archaea Inspired Tetraether Lipids with Varying Polar Lipid Headgroups

When we began our examination of the effect of changes in polar lipid headgroup on membrane leakage properties, pure **GMGTPC**, **GMGTPA** and **GMGTPG** readily formed stable liposomes (using liposome preparation described in section 2.5.9 General Procedure for Liposome Formation). However, we were unable to form stable liposomes from pure **GMGTPE** or **GMGTLa** lipids (similar results have been shown previously with standard diacylphospholipids with PE headgroups due to the relatively small headgroup size[29]). Since we were able to form stable liposomes comprised of 1:1 mixtures

between PC lipid analogs with lipid analogs equipped with PA, PG, or PE headgroups, we used these mixtures of lipids to evaluate the effects of changes in headgroup on relative membrane permeability (Figure 2.4). Regrettably, **GMGTLa** lipids did not form stable liposomes even when mixed with 1:1 with **GMGTPC**. Therefore, liposomal leakage assays were performed solely on **GMGTPC**, **GMGTPA**, **GMGTPG** and **GMGTPE** liposomes.

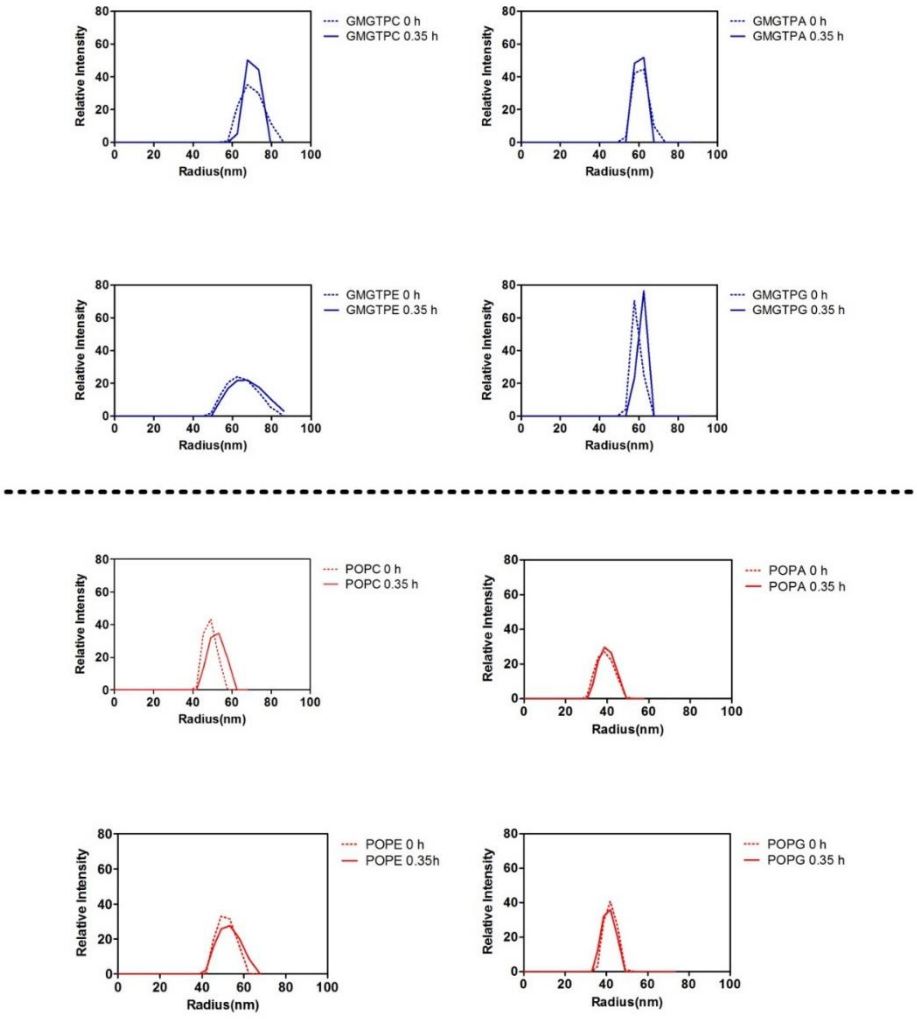

Figure 2.4. Hydrodynamic radius measured using Dynamic Light Scattering. PG, PE, PA liposomes were comprised of 1:1 mixture with PC lipids.

DSC measurements (by David Onofrei) of tetraether lipid headgroup analogs were taken to ensure suspensions of liposomal formulations made from **GMGTPC**, **GMGTPA**, **GMGTPG** or **GMGTPE** lipids in water maintained a liquid phase without an observed phase transition between 5 and 65 °C (see Figure 2.5). Similar to results obtained for **GMGT** lipid analogs with varying hydrophobic structures, no phase transition was observed and the lipids remained liquid within the window of temperature tested. In addition, morphology of liposomes made with **GMGT** lipids with varying headgroup were measured by DLS within the timeframe of the leakage assays and liposomes morphology remained static (shown in Figure 2.4), which suggests that liposome remained stable during leakage measurements and fusion or aggregation does not significantly contribute to the observed rate of small ion permeability measured.

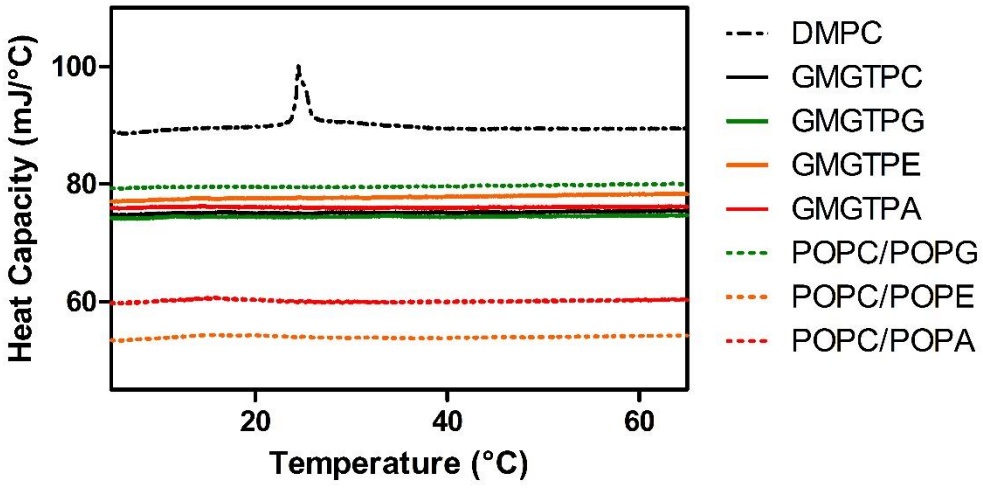

Figure 2.5. DSC measurements taken of synthetic GMGT lipid analogs and diacyl lipids. Measured by David Onofrei.

2.3.2 Small Ion Membrane Leakage Assay

2.3.2.1 Small Ion Membrane Leakage Assay Procedure

To study the effects of membrane properties attributed to changes in structure of synthetic lipids, we developed a modified pH equilibration assay that was previously reported by Kakinuma and coworkers.[30] In this assay, we encapsulated CF within the liposomes with an initial internal liposomal pH of 7.2, the liposomes were then incubated in a Bis-Tris buffered solution with an external pH of 5.8 and the change in fluorescence intensity of CF was monitored over time as the internal liposome pH equilibrated to pH 5.8 (a more detailed procedure can be found in section 2.5.10. General Procedure to Measure pH Equilibrium of CF). We chose to use pH 5.8 and 7.2 as external and internal liposomal pH, respectively, since CF exhibits a linear correlation between its fluorescence and environmental pH within this pH range.[32] To ensure the CF quenching monitored is attributed to leakage of small ions and not fusion induced leakage between liposomes, the addition of divalent cations in the buffer was avoided to prevent negatively charged lipid polar headgroups from inducing aggregation/fusion of liposomes.[31] While we expect all of the membranes to be most permeable to protons over any other ionic species under these experimental conditions, it is possible the intraliposomal buffer and other ions such as OH^-, Na^+, or Cl^- could also contribute to the observed rate of pH equilibration. We, therefore, consider the observed rates of pH equilibration from membranes composed of different lipids to represent an estimate of their

overall permeability to small ions rather than an estimate of the permeability of a single, specific ionic entity. The measured initial rates of pH equilibration, therefore, can be considered more generally as an estimate for membrane permeability to small ions rather than as an estimate of simply permeability to protons. Additionally, to minimize error in our leakage rate measurement from photobleaching and evaporation, we used initial rates (i.e., the first 15% change in CF fluorescence) to evaluate the rate of pH equilibration at room temperature.

For each assay, the relative fluorescence (F_{rel}) was normalized using equation (1) below. F_0 represents fluorescence at initial time T_0, F_A represents fluorescence measurements taken at different times, and F_{Nig} is the fluorescence measurement of the liposome solution including Nigericin after 600 second in Bis-Tris buffer at pH 5.8. Nigericin, a polyether ionophore known to form pores in membranes, was used as our positive control of complete pH exchange between the internal/external buffer systems. After the data was normalized, equation (2) was used to determine the initial rate (i.e., up to 15% decrease in CF fluorescence) of the decrease in CF fluorescence by combining individual measurements using GraphPad Prism 5 software.

$$F_{rel} = \left(1 - \frac{(F_0 - F_A)}{(F_0 - F_{Nig})}\right) X\ 100 \quad (1)$$

$$ln\ (F_{rel})\ =\ -kt \quad (2)$$

2.3.2.2 The Effect of Changes in Alkyl Chain Length of Tethered Lipid Region on Small Ion Membrane Permeability

To understand whether liposomes made with tetraether lipids showed improvement to small ion membrane leakage to liposomes made with diacyl lipids, we evaluated the observed initial rates of pH equilibration of liposomes composed of EggPC and **GMGTPC-T28** (shown in Figure 2.6A). Similar to previously reported trends comparing liposome permeability of lipids derived from Archaea vs. Bacteria,[16] **GMGTPC-T28** liposomes exhibited ~2 orders of magnitude reduction in rate of leakage of small ions when compared with liposomes formed from EggPC. This result could arise, in part, by a combination of the absence of the ester linkage found in EggPC, the presence of the branched alkane network provided by the phytanyl group in **GMGTPC-T28**, and the elimination of the small aqueous layer found in between the two lipid leaflets of a bilayer forming lipid (which, presumably, would not be present in a membrane composed of pure tethered **GMGTPC-T28** lipids).[16,34,35]

Next, to study the effects of changes in alkyl chain length of the tethered region of the lipid on small ion membrane permeability, small ion membrane permeability assay was administered to liposomes made from tetraether lipid analogs **GMGTPC-T28**, **GMGTPC-T32**, and **GMGTPC-T36** (shown in Figure 2.2). In contrast to the dramatic membrane leakage effect observed between liposomes made with EggPC and **GMGTPC-T28**, no significant statistical effect on membrane leakage was observed when alkyl chain lengths of the tethered

region changed from 28 to 36 (shown in Figure 2.6B and 2.6C). From this observation, because no statistical differences were observed for small ion membrane permeability between **GMGTPC-T28**, **GMGTPC-T32**, and **GMGTPC-T36**, we will refer to **GMGTPC-T28** simply as **GMGTPC**, which was used as our control lipid for the membrane leakage assays described later in this thesis.

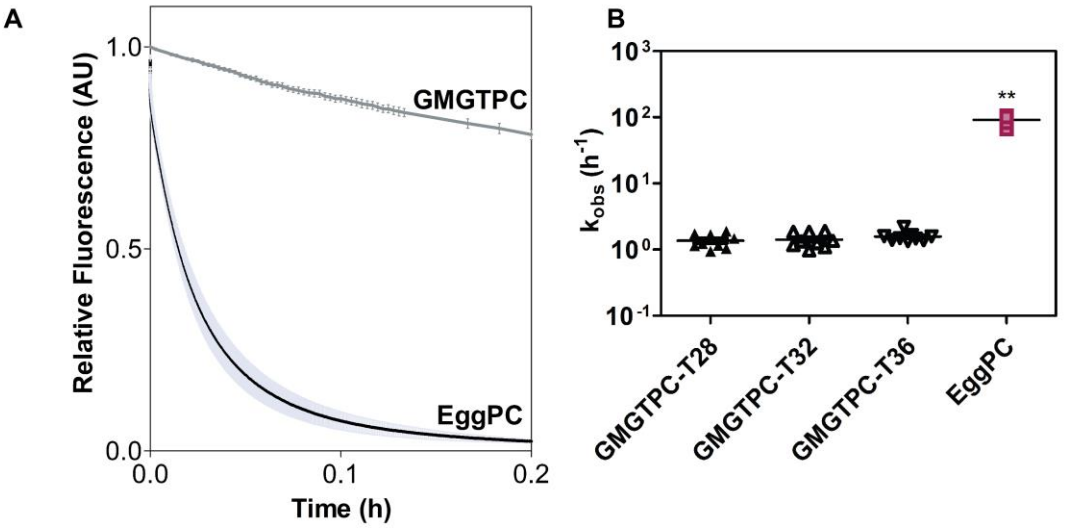

C

	GMGTPC-T28	GMGTPC-T32	GMGTPC-T36	EggPC
k_{obsd} (h^{-1})	1.4 ± 0.4	1.4 ± 0.4	1.6 ± 0.3	91.4 ± 12.7

Figure 2.6. Observed rate of pH equilibration from liposomes formed from EggPC or synthetic lipids. (A) Graph of changes in CF fluorescence from CF encapsulated **GMGTPC** or EggPC liposomes vs. time (h); (B) Comparison of the observed initial rates of decreased CF fluorescence from CF encapsulated liposomes comprised of different lipids; (C) Average observed initial rates of pH equilibration of liposomes comprised with different lipids. Standard errors of the mean are provided based on 9 measurements each. Statistical analyses were performed using a t-test with 95% confidence interval. ** indicate a p-value < 0.01.

2.3.2.3 The Effect of Integration of Alkyl Rings to the Tethered Lipid Region on Small Ion Membrane Permeability

The addition of cyclopentane rings in the hydrophobic region of natural archaeal lipids have been observed to increase packing and reduce membrane permeability.[7] To examine whether the presence of cyclopentane rings within the tethered transmembrane region of tetraether lipids found in many natural Crenarchaeota lipids is accompanied by a decrease in membrane permeability, we examined leakage properties of liposomes made with synthetic **GMGTPC** analogs functionalized with alkyl rings.[36-38] Specifically, to examine the effect of cyclopentane ring(s) integration to the tethered lipid tail on small ion membrane leakage, we evaluated the rate of pH equilibration of liposomes formed from **GMGTPC-CP1-3** (Figure 2.7A and 2.7B), which contained 1, 2, or 3 *cis*-1,3-cyclopentane rings in the hydrophobic core (shown in Figure 2.2). Interestingly, we found that the presence or number of cyclopentane rings had no significant observable effect on the rate of pH equilibration at room temperature compared to liposomes made with **GMGTPC** (which has zero rings within its tethered hydrophobic core) lipids. These results are in contrast to reported computational studies suggesting that cyclopentane rings[39] in tethered lipids increased lipid packing.[7,40] While the stereochemistry of the cyclopentane rings (*cis* versus *trans*) may account for the discrepancy between our experimental results, computational studies by our collaborators, conformational analysis[41] and X-ray studies[42] of polymers containing multiple 1,3-cyclopentane rings support that

the energy of inter-strand packing of these polymers is independent of the *cis* or *trans* configuration of the rings. Nevertheless, the results shown in Figure 2.7 demonstrate that any structural effects to the lipid through introduction of *cis* cyclopentane rings is not sufficient to significantly affect membrane leakage of small ions under the conditions used in these studies.

A

Lipid	k_{obsd} (h^{-1})
GMGTPC	1.4 ± 0.4
GMGTPC-CP1	1.2 ± 0.4
GMGTPC-CP2	1.3 ± 0.3
GMGTPC-CP3	1.4 ± 0.2

B

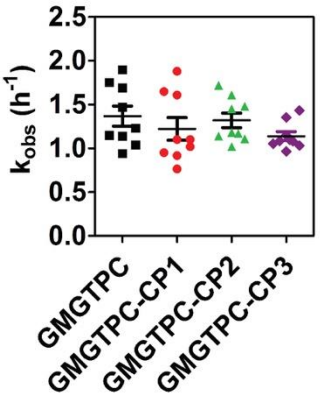

Figure 2.7. Comparison of observed initial rates of pH equilibration of liposomes comprising lipids with 0 - 3 cyclopentane ring(s). (A) Average observed initial rates of pH equilibration of CF (fluorescence intensity (monitored at λ(Ex/Em) = 485/517 nm) in liposomes comprised of **GMGTPC**, **GMGTPC-CP1**, **GMGTPC-CP2,** or **GMGTPC-CP3**. Standard errors of the mean are provided based on 9 measurements each. (B) Graph of the observed rates of CF fluorescence decrease for **GMGTPC**, **GMGTPC-CP1**, **GMGTPC-CP2,** or **GMGTPC-CP3**.

In order to examine the effects of incorporating cyclohexane rings into the tethered region on membrane leakage, we evaluated membrane leakage properties of **GMGTPC-CH1** and **GMGTPC-CH2** (Figure 2.2) comprising one or two *cis*-1,3-cyclohexane group(s). Interestingly, as shown in Figure 2.8, liposomes composed of **GMGTPC-CH1** lipids exhibited an additional ~40% reduction in the rate of small ion membrane leakage (k_{obsd} = 0.8 ± 0.1) compared with liposomes composed of lipids with no rings (**GMGTPC**) or with one or more cyclopentane rings (**GMGTPC-CP1-3**). When we compared the

structural effects of the addition of two *cis*-1,3- substituted cyclohexane rings, **GMGTPC-CH2** with **GMGTPC-CH1**, we observed smaller benefits of reduction in small ion membrane leakage when compared with **GMGTPC** (~28%), which suggests the addition of more cyclohexane rings to the lipid core does not translate into a cumulative advantage for **GMGTPC** liposomes. Presumably, the added benefit of integrating cyclohexane rings over cyclopentane rings may be due to the differences in flexibility of the cyclohexane ring compared with a cyclopentane ring, which may affect lipid packing and lead to reduced membrane permeability of small ions for **GMGTPC-CH1** liposomes.[43] These results could help support the structural benefits of cyclohexane ring incorporation found in lipids derived from Thaumarchaeota, which grow in a vast range of environmental conditions between pH 5-8 and temperature of 20-72°C.[2,32]

A

Lipid	k_{obsd} (h^{-1})
GMGTPC	1.4 ± 0.4
GMGTPC-CH1	0.8 ± 0.1
GMGTPC-CH2	1.0 ± 0.3

B

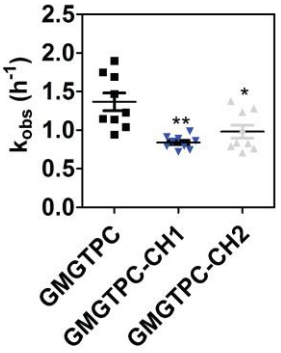

Figure 2.8. Comparison of observed initial rates of pH equilibration of liposomes comprised of lipids with 0, 1, or 2 cyclohexane ring(s). (A) Average observed initial rates of pH equilibration of CF (fluorescence intensity (monitored at λ(Ex/Em) = 485/517 nm) in liposomes comprised of **GMGTPC**, **GMGTPC-CH1**, **GMGTPC-CH2**. Standard errors of the mean are provided based on 9 measurements each. (B) Graph of the observed rates of CF fluorescence decrease for **GMGTPC**, **GMGTPC-CH1**, **GMGTPC-CH2**. Statistical analyses were performed using a t-test with 95% confidence interval. *, ** indicate a p-value < 0.1, 0.01, respectively.

2.3.2.4 The Effect of Changes in Polar Lipid Headgroups on Small Ion Membrane Permeability

Eukaryotes and prokaryotes often respond to environmental stress by modifying the membrane lipid composition.[1,33,34] Specifically, the ratio of polar lipid headgroups in mixtures in Archaea membranes have been observed to be dependent on specific growth conditions.[7] For instance, under acidic conditions, the lipid composition of Archaea will include a higher fraction of headgroups that can facilitate hydrogen bonding between the headgroups on adjacent lipids.[9,14] Several research groups have investigated the effect of changes in polar lipid headgroup on membrane properties using computational[35] and experimental studies[36] that suggest lipid headgroups affect membrane permeation of water, but have little effect on permeability of small organic molecules across membranes.[37] However, no systematic study on effects of headgroups on small ion permeability had previously been reported. To study whether changes in polar lipid headgroups translates to decrease in membrane leakage, small ion membrane leakage from liposomes comprised of 1:1 mixtures of **GMGT** lipid analogs equipped with either PA, PE, or PG polar lipid headgroups (shown in Figure 2.2) and **GMGTPC** were studied. Surprisingly, no statistically significant difference between the observed rate of leakage of small ions from liposomes composed of 1:1 mixtures of **GMGTPC** lipids with lipids containing **GMGTPE** or **GMGTPA** were observed compared to liposomes comprised of pure **GMGTPC** lipids (shown in Figure 2.9). Liposomes formed from 1:1 mixtures of

GMGTPC:**GMGTPG** lipids, however, exhibited a 1.5 fold increased rate of leakage compared with pure **GMGTPC** liposomes (shown in Table 2.2). Overall, the rate of small ion leakage from any two of the **GMGT** lipids differed by a factor of ≤ 1.6 as a function of headgroup.

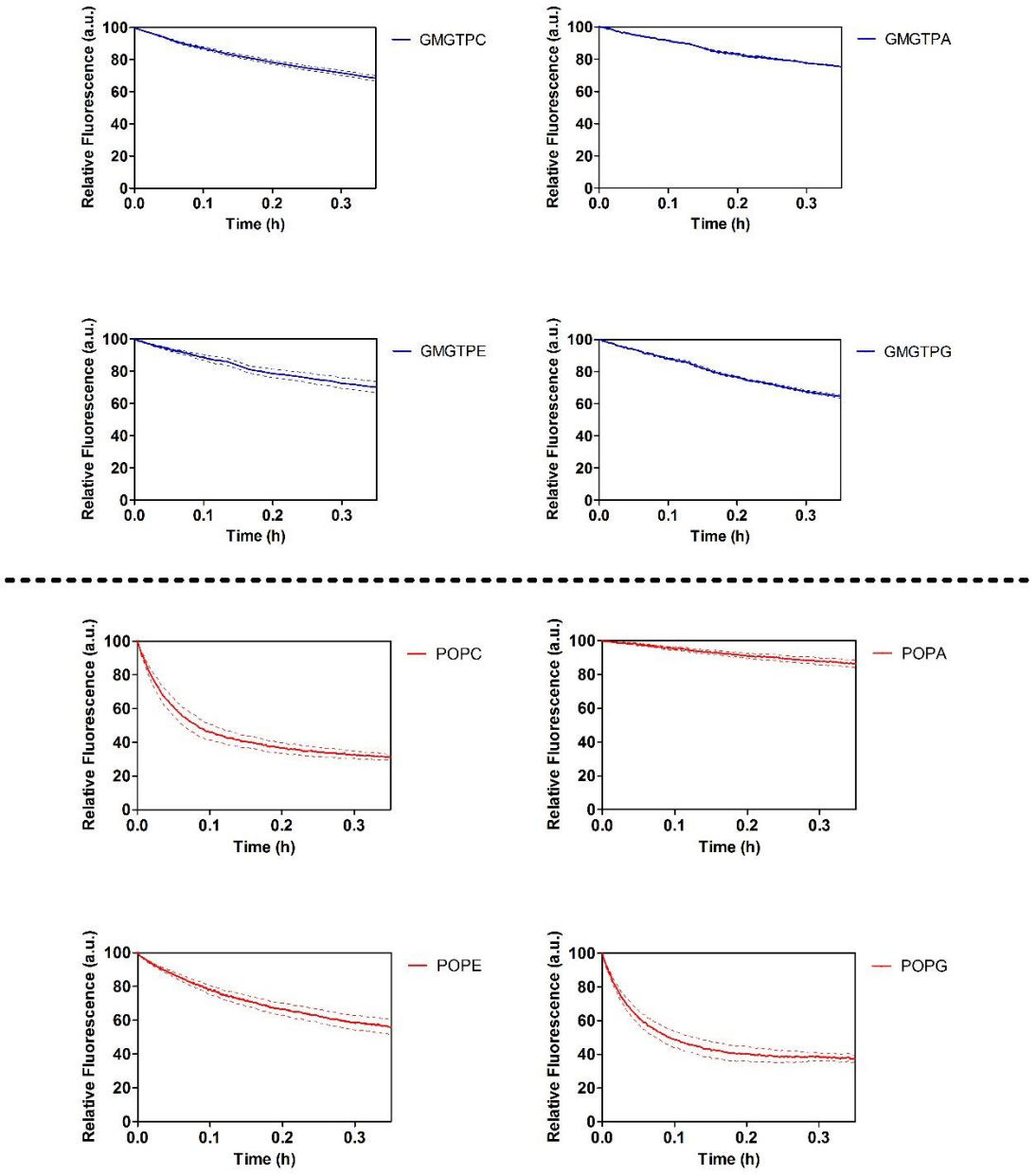

Figure. 2.9. pH equilibration of CF vs. time. dashed lines represents standard errors from 9 measurements.

We next examined how these results compared with the effect of headgroups on standard bilayer-forming diacylphospholipids, specifically, 1-palmitoyl-2-oleoyl-*sn*-glycerol (PO) lipids. To be able to compare membrane leakage results obtained from synthetic **GMGT** lipid analogs, we generated liposomes by mixing POPC lipids 1:1 with POPG, POPE, or POPA (i.e., the same four polar lipid headgroups examined for synthetic GMGT lipids) and compared their observed rate of leakage to liposomes comprised of pure POPC lipids. DSC measurements showed that liposomes comprised of 1:1 mixtures of POPC with POPA, POPE, or POPG maintained a liquid phase at room temperature and did not exhibit a phase transition between 5 and 65 °C (Figure 2.5). DLS measurement also confirmed that lipid fusion or aggregation is not expected to significantly contribute to the observed rate of membrane leakage (Figure 2.4).

When membrane leakage for liposomes made with PO series of lipids were monitored, a more dramatic effect of head groups on membrane leakage was observed compared with membrane leakage of liposomes made with synthetic tetraether lipid analogs. We observed significant differences in observed rates of leakage in respect to changes in polar lipid headgroups on liposomes made with PO lipid analogs (Figure 2.10). Similar leakage trend to **GMGTPG** lipids was observed with the addition of PG headgroup to diacyl lipids, showing an increase in membrane leakage of small ions by a factor of 2.5 compared with liposomal membrane leakage from PO lipid analogs with PC

headgroups only. In contrast to the case with **GMGTPE** or **GMGTPA** (which did not affect membrane leakage compared to **GMGTPC** lipids), the rate of leakage from POPE and POPA-containing membranes was a factor of 2.0 and 14.3 slower, respectively, compared with membranes formed from pure POPC lipids (shown in Figure 2.10). To illustrate the difference clearer, we normalize the effect of changes in polar lipid headgroups with the PC lipid on membrane leakage (shown in Figure 2.11), where we can see a greater dependence for liposomes made with PO lipid series than liposomes made with **GMGT** lipids on membrane leakage.

Table 2.2. Observed rate calculated for small ion permeability of liposomes using method of initial rates (15% completion; the observed rate was calculated by taking the mean of 9 kinetic rates per experiment. However, the observed rate of **GMGTPE** was calculated using 8 measured kinetic rates.1 experiment was determined to be an outlier using Q-test 95% confidence, and was omitted from the analysis).

Lipids	Observed Rate (h^{-1})	Std. Error of the Mean
GMGTPC	1.34	0.07
GMGTPC/PE	1.49	0.01
GMGTPC/PA	1.24	0.06
GMGTPC/PG	1.97	0.13
POPC	6.53	0.46
POPC/PE	3.37	0.31
POPC/PA	0.50	0.05
POPC/PG	16.21	1.14

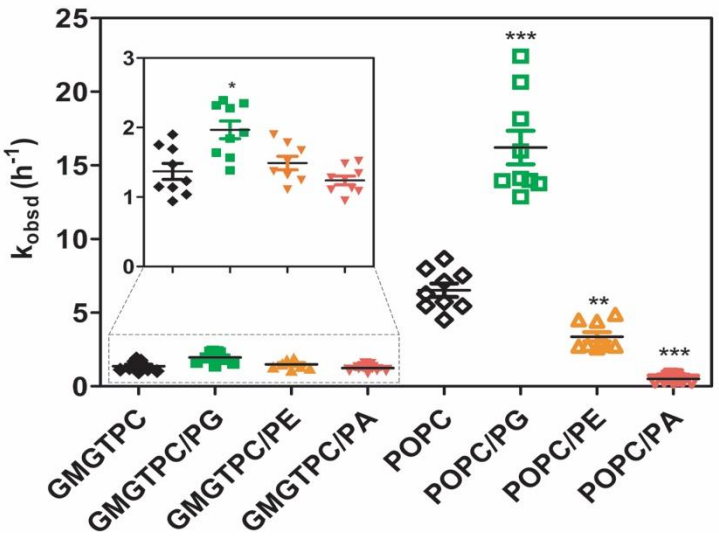

Figure 2.10. Observed initial rate of pH equilibration from liposomes formed from **GMGT** or PO series of lipids. Comparison of the observed initial rates of decreased CF fluorescence intensity (monitored at λ(Ex/Em) = 485/517 nm) from CF-encapsulated liposomes comprised of pure **GMGTPC** lipid or 1:1 mixtures of **GMGTPC** with **GMGTPG**, **GMGTPE**, or **GMGTPA** (the inset represents a zoomed in graph of the observed initial rates of leakage from the **GMGT** lipids); and pure POPC lipid or 1:1 mixtures of POPC with POPG, POPE, or POPA. Statistical significance was determined using a paired Student t-test. *, **, *** indicate a p-value of < 0.1, 0.01, 0.001, respectively, relative to the k_{obsd} of the analogous PC lipid.

The reduced permeation of small ions observed for liposomes containing POPC mixed with POPA or POPE (compared with pure POPC liposomes) could arise from increased intermolecular hydrogen bonding between headgroups of neighboring lipids. Such intermolecular hydrogen bonding may lead to exclusion of water molecules near the membrane surface and increased membrane packing, as suggested through X-ray diffraction[38], FT-IR[39] and computation[40] studies. For **GMGT** lipid analogs, we have shown leakage of small ions from tethered lipids was significantly reduced compared with bilayer-forming lipids,[41] presumably as a result of favorable lipid packing of hydrocarbon chains in neighboring lipids within the membrane. Such inherently tight membrane packing in **GMGT** lipid analogs, therefore, may not be as influenced by

membrane surface effects induced by the presence of PE or PA headgroups. On the other hand, for lipids with PG headgroups, the presence of multiple hydroxyl groups may lead to an increase in the number of water molecules in between lipid headgroups near the membrane surface, which could cause a decrease in lipid packing and an increase in membrane leakage.[36] We expect such an effect on leakage by PG headgroups would be more pronounced in PO lipids (which presumably are inherently more loosely packed) compared with **GMGT** lipid analogs as suggested by membrane permeability results observed in Figure 2.10 or 2.11.

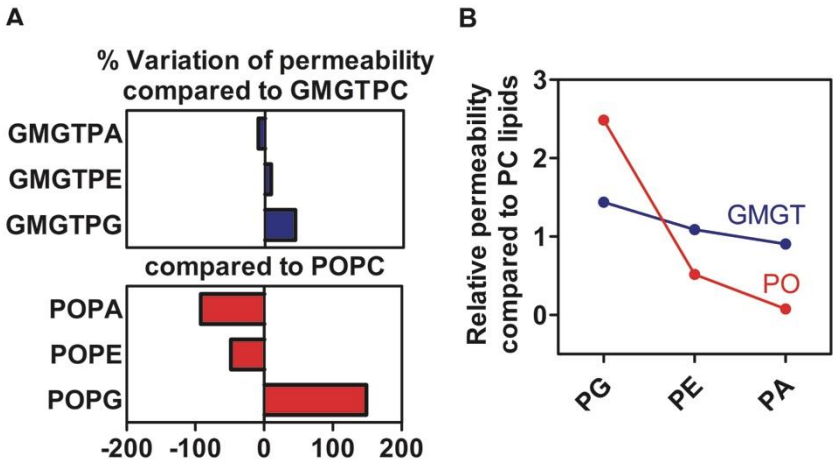

Figure 2.11. Relative effects of headgroups on small ion membrane leakage. A) Graph of the relative variation of leakage rate from membranes comprised of 1:1 mixtures of PC with PA, PE or PG lipids compared to membranes formed from pure PC lipids. Data represents the percent deviation of observed initial rates of membrane leakage compared to the observed initial rate of leakage from pure POPC or **GMGTPC** lipid membranes (zero percent). B) Graph showing the relative leakage rate of membranes comprised of 1:1 mixtures of PC with PA, PE, or PG lipids relative to the observed initial rate of leakage from membranes comprised of pure POPC or pure **GMGTPC** lipids (normalized to 1).

2.4 Conclusion

We have, thus, presented a systematic study of the effects on membrane leakage of some key structural features inspired from natural Archaea lipids. As anticipated, the incorporation of phytanyl groups, the presence of tethering, and the incorporation of ether glycerol backbones in tetraether lipids substantially reduced membrane permeability of small ions , ~2 orders of magnitude, when compared with commercially available EggPC lipids. Surprisingly, however, we found that incorporation of *cis*-1,3 substituted cyclopentane rings had no significant effect on membrane leakage of small ions in **GMGTPC** lipids. In contrast, incorporation of a 1 or 2 *cis*-1,3 cyclohexane ring significantly reduced small ion membrane leakage when compared with all other **GMGTPC** lipids studied, albeit, a cumulative leakage benefit of increasing the number of cyclohexane rings was not observed. Such differences in small ion membrane permeability between lipids containing cyclopentane versus cyclohexane rings could reflect differences in ring flexibility for cyclohexanes, as it relates to lipid packing.

When we focus our attention to the effects of changes in polar lipid headgroup on tetraether lipid analogs or diacyl lipids, we observed changes in polar lipid headgroups for liposomes containing tetraether lipids did not display a strong dependence on membrane leakage. Whereas, changes in polar lipid headgroups for liposomes made with diacyl PO lipids exhibited a strong effect on membrane leakage. Such large effects on small ion permeability exhibited

for diacyl lipids from headgroups modification may limit the utility of PO (and possibly other bilayer-forming) lipids in applications and studies where maintaining a consistent membrane permeability is important across various headgroups. On the other hand, membrane leakage from liposomes comprised of synthetic **GMGT** lipids was not heavily influenced by changes in polar lipid headgroups. These findings suggest that **GMGT** lipids may offer greater flexibility for tailoring the functionality presented in the lipid headgroups, without significantly compromising membrane permeability. Such versatility in the design of lipid headgroups may open up opportunities to use the cyclohexane integrated **GMGT** lipids in place of current diacyl lipid based technologies in a range of applications including the incorporation of receptor targeting molecules on lipids for development of liposomal drug delivery systems or the incorporation of ligands as well as charged headgroups to attract specific analytes or binding partners to the membrane surface for biophysical and drug delivery studies. This work represents an important step towards establishing some design principles inspired from nature for generating lipids with low membrane permeability for drug delivery applications.

2.5 Materials and Methods

2.5.1 Reagents and Instruments

All reagents were purchased from commercial sources and used without further purification. Diacyl lipids were purchased from Avanti Polar Lipids. Diacyl

lipids were stored under Argon at -20°C and used within 3 months of purchase. Glassware was dried at 115°C overnight. Air and moisture-sensitive reagents were transferred using a syringe or stainless steel cannula. Intermediates were purified over silica (60Å, particle size 40-63 μm) purchased from Dynamic Adsorbents, Inc. Reactions were monitored by thin-layer chromatography (TLC) using 0.25 mm silica gel plates (60F-254) from Dynamic Adsorbents, Inc. Deuterated solvents were purchased from Cambridge Isotope Laboratories, Inc. ^{1}H, ^{13}C, ^{31}P NMR spectra were obtained on either JEOL ECA 500 spectrometer or Varian 400 MHz/500MHz spectrometer. Chemical shifts are reported in ppm relative to residual solvent. The FID files were analyzed using NMRnotebook version 2.70 build 0.10 by NMRTEC.

Dynamic Light Scattering (DLS) measurements were performed on a Wyatt DynaPro NanoStar (Wyatt Technology, Santa Barbara, CA) instrument using a disposable cuvette (Eppendorf UVette 220 nm – 1,600 nm) and data processed using Wyatt DYNAMICS V7 software. Each analysis involved an average of 10 measurements. The data was exported for final plotting using GraphPad Prism 5 (GraphPad Software, Inc., La Jolla, CA).

Low resolution MS analysis was performed on a Micromass Quattro Ultima triple quadrupole mass spectrometer with an electrospray ionization (ESI) source. High resolution MS analysis was performed using Agilent 6230 Accurate-Mass TOFMS with an electrospray ionization (ESI) source by Molecular Mass Spectrometry Facility (MMSF) in the department of chemistry and biochemistry at University of California, San Diego.

Stopped-Flow fluorescence measurements were taken using Applied Photophysics SX-17MV stopped-flow. The slit was set at 4 nm and the PMU set to 600. The experiments were run using asymmetrical mixing; one solution comprised of the lipid solution in Bis-Tris buffer at pH 7.2 (0.1 mg/mL) and the other solution with either Bis-Tris buffer pH 7.2 / pH 5.8. The kinetic was measured when 25 µL of the liposome solution was mixed with 225 µl of Bis-Tris buffer pH7.2 / pH5.8 (0.01 mg/mL final liposome concentration) for 1000 seconds. The excitation was set at 485 nm and the fluorescence data was collected using a high pass cut-off filter at 505 nm. The data was exported for final plotting using GraphPad Prism 5 (GraphPad Software, Inc., La Jolla, CA).

Longer fluorescence decay measurements were taken on a Perkin Elmer Enspire© multimode plate reader (excitation 485 nm, emission 516 nm and 75 flashes; initially, each measurement was taken every second for 500 seconds, followed by every 60 seconds for 6 hours). Costar EIA/RIA plates were used (96 well half area, no lid, flat bottom, non-treated black polystyrene). The data were exported for final plotting using GraphPad Prism 5 (GraphPad Software, Inc., La Jolla, CA).

DSC experiments were performed in duplicate using a Thermal Analysis Q2000 DSC. Each experiment involved a 5 °C/min ramp from 0 °C to 70 °C under high purity N_2 at 50 mL/min. Samples were ~0.3 – 1.0 mg of lipid dissolved in water at ~5% by weight. TA Universal Analysis was used to extract T_m for these samples. All of the synthetic lipids did not exhibit a phase transition from

0 - 70 °C shown in Figure S7. DMPC was used as a positive control which showed a phase transition at 24 °C.

2.5.2 General Synthetic Procedures

2.5.2.1 Alcohol Oxidation Using Albright–Onodera Conditions

To a cold solution of the starting alcohol (1 eq) in a mixture of dry dichloromethane (DCM)/dimethyl sulfoxide (DMSO) (1:1) (0.15 M), phosphorus pentoxide (3 eq) was slowly added and reaction was stirred at room temperature for 30 minutes. Then, the reaction mixture was cooled using an ice-water bath and triethylamine (Et_3N) (10 eq) was slowly added. After 30 min of stirring at room temperature, the reaction mixture was cooled down again and 10% aqueous HCl was added. The resulting mixture was extracted with DCM, washed with water, dried over Na_2SO_4 and purified by column chromatography on silica gel.

Note: When a diol was used, the number of equivalents for P_2O_5 and Et_3N were 6 and 20 respectively.

2.5.2.2 Wittig Olefination

To a suspension of phosphonium salt (1 eq) in dry THF (0.07 M), butyllithium (1.2 eq) was added dropwise at 0°C. The reaction mixture was stirred for 15 min at 0°C, and the reactive aldehyde (1.1 eq) dissolved in dry tetrahydrofuran (THF) (0.09 M) was added dropwise. After 30 minutes of stirring

at room temperature, the reaction was quenched with water and solvent was removed under vacuum. The aqueous residue was extracted with DCM, washed successively with water and brine, dried over Na_2SO_4 and purified by column chromatography on silica gel.

Note: For double Wittig reactions, the amount of butyllithium was increased to 2.2 equivalents.

2.5.2.3 Bromination of Diol Using Hydrobromic Acid Solution

To a suspension of diol (0.02 M, 1 eq) in a solution of hydrobromic acid (48 wt. % in H_2O), tetrabutylammonium bromide (0.5 eq) was added and the reaction mixture was stirred at reflux for 24 hours. The solution was cooled down and extracted with DCM. The combined organic layers were washed with water until the aqueous layer remained at neutral pH, and dried over Na_2SO_4. Unless noted otherwise, the desired product was obtained after purification by column chromatography on silica gel using hexane/Ethyl Acetate (EtOAc) (99:1) as the eluent.

2.5.2.4 Formation of Tetraether Lipid Scaffold by S_N2 Reaction

To a cold solution of **2.4** (0.21 M, 2.5 eq) in dry THF, sodium hydride (2.7 eq) was added portionwise. The solution was stirred for 1 hour at room temperature and cooled down again. A solution of dibromoalkane (0.09 M, 1 eq) in dry THF was added and the reaction was stirred at reflux for 16 hours. The reaction was quenched with water and the solvent was removed under vacuum.

The aqueous residue was extracted with DCM, washed successively with water and brine, then dried over Na_2SO_4 and purified by column chromatography on silica gel.

2.5.2.5 Debenzylation of Lipid Scaffold by Hydrogenation

Benzylated lipid (1 eq) was dissolved in a degassed mixture of ethanol (EtOH)/THF (1:1) (0.01 M) and 20% $Pd(OH)_2$ (10% w/w) was added. The reaction was stirred under 1 atm H_2 at room temperature for 16 hours. The catalyst was removed by filtration through a pad of celite, and the resulting residue was purified by column chromatography on silica gel.

2.5.2.6 Formation of Phosphocholine Lipid

First, bromoethyldichlorophosphate was prepared following a reported protocol.[42] To a solution of bromoethyldichlorophosphate (8 eq) in dry THF (0.33 M), a solution of the diol (1 eq) and Et_3N (11 eq) in dry THF (0.04 M) was added dropwise. After stirring the mixture for 3 days in the dark at room temperature, toluene was added to precipitate triethylammonium chloride. Then, the solution was filtered through a small pad of celite and the filtrate concentrated. The resulting residue was dissolved in a mixture of THF/$NaHCO_3$ (sat) (2.8 mM) and the reaction was stirred for 16 hours at room temperature. THF was evaporated under vacuum and the resulting aqueous solution was acidified to pH 1 using a dilution solution of hydrochloric acid (1M) and extracted using several portions

of DCM/Methanol (MeOH) (8:2). The organic layers were combined, dried over Na_2SO_4 and concentrated under reduced pressure.

To a solution of the previous crude in a mixture of THF/chloroform ($CHCl_3$) (2:1) (0.03 M), Me_3N (33% in EtOH) (180 eq) was added and the reaction was stirred in a sealed tube at room temperature for 5 days. The reaction mixture was concentrated to dryness, purified on sephadex LH-20 using DCM/MeOH (1:1) as eluent and purified by column chromatography on silica gel.

2.5.3 Synthetic Procedure for Glycerol Scaffold

(E)-1-iodo-3,7,11,15-tetramethylhexadec-2-ene (**2.1**)

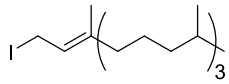

Compound **2.1** was synthesized following a reported protocol.[43]

(E)-2-phenyl-5-((3,7,11,15-tetramethylhexadec-2-en-1-yl)oxy)-1,3-dioxane (**2.2**)

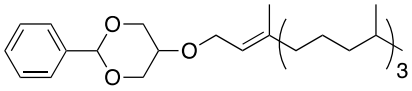

Compound **2.2** was synthesized following a reported protocol.[43]

2-phenyl-5-((3,7,11,15-tetramethylhexadecyl)oxy)-1,3-dioxane (**2.3**)

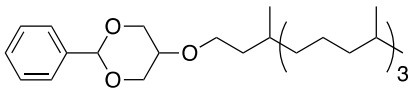

2.2 (0.50 g, 1.10 mmol) was dissolved in a degasiised solution of *tert*-butanol (tBuOH)/THF (1:1) (10 mL) and Wilkinson's catalyst ($Rh(PPh_3)_3Cl$) (0.02 g, 4% w/w) was added. The mixture was stirred under 1 atm H_2, at room temperature for 24 hours, and filtered through a small pad of alumina. The solvent was removed under vacuum and the crude product was purified by column chromatography on silica gel using hexane/EtOAc (95:5) as the eluent. Compound **2.3** was obtained as a yellow oil (0.43 g, 85%) and ^1H NMR spectrum matched previously reported data.[43]

3-(benzyloxy)-2-((3,7,11,15-tetramethylhexadecyl)oxy)propan-1-ol (**2.4**)

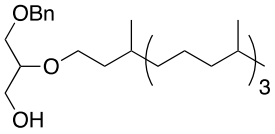

Compound **2.4** was synthesized following a reported protocol.[43]

*2.5.4 Synthetic Procedure for **GMGTPC** T28, T32, T34*

1,20-eicosanediol (**2.5**)

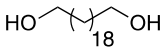

1,20-eicosanediol was synthesized from 1,20-eicosanedioic acid following a reported protocol.[44]

1,12-dodecanedial (**2.6**)

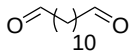

Dialdehyde **2.6** was synthesized from 1,12-dodecandiol (3.50 g, 17.3 mmol) according to the general procedure for Alcohol oxidation (Albright–Onodera conditions) (see section 2.5.2.1). **2.6** (2.06 g, 60%) was obtained as a white solid after purification by column chromatography on silica gel using hexane/EtOAc (95:5 to 90:10) as the eluent. ^{1}H NMR data matched previously reported data.[45]

1,16-hexadecanedial (**2.7**)

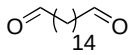

Dialdehyde **2.7** was synthesized from 1,16-hexadecanediol (342 mg, 1.32 mmol) according to the general procedure for Alcohol oxidation (Albright–Onodera conditions) (see section 2.5.2.1). 1,16-hexadecanedial (249 mg, 74%) was obtained as a white solid after purification by column chromatography on

silica gel using hexane/EtOAc (9:1 to 8:2) as the eluent. ^{1}H NMR data matched previously reported data.[46]

1,20-icosanedial (**2.8**)

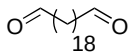

Dialdehyde **2.8** was synthesized from 1,20-eicosanediol (2.65 g, 8.44 mmol) according to the general procedure for Alcohol oxidation (Albright–Onodera conditions) (see section 2.5.2.1). 1,20-icosanedial (1.07 g, 41%) was obtained as a white solid after purification by column chromatography on silica gel using hexane/EtOAc (95:5 to 90:10) as the eluent.

Rf: 0.40 (hexane/EtOAc 9:1); ^{1}H NMR (500 MHz, $CDCl_3$-d_1) δ 9.72 (t, *J* = 1.9 Hz, 2H), 2.38 (ddd, J = 1.9, 7.2, 7.5 Hz, 4H), 1.61-1.56 (m, 4H), 1.29-1.21 (m, 28H); ^{13}C NMR (126 MHz, $CDCl_3$-d_1) δ 203.1, 44.1, 29.8, 29.8, 29.6, 29.5, 29.3; ESI-MS: 311.3 $[M+H]^+$; HRMS 311.2945 calcd for $[C_{20}H_{39}O_2]^+$, found 311.2945.

8-((tetrahydro-2H-pyran-2-yl)oxy)octan-1-ol (**2.9**)

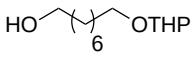

Compound **2.9** was synthesized following a reported protocol.[47]

triphenyl(8-((tetrahydro-2H-pyran-2-yl)oxy)octyl)phosphonium iodide (**2.10**)

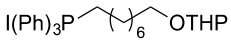

To a cold solution of triphenylphosphine (6.1 g, 23.5 mmol) and imidazole (1.6 g, 23.5 mmol) in DCM (45 mL), iodine (6.0 g, 23.5 mmol) was added. After stirring of the mixture at room temperature in the dark for 10 min, a solution of compound **2.9** (4.5 g, 19.6 mmol) in DCM (12 mL) was added. The reaction mixture was stirred for 2 hours at room temperature in the dark. The reaction mixture was washed with 10% $Na_2S_2O_3$ aqueous solution and extracted with DCM. The combined organic layers were washed with water, dried over Na_2SO_4, and purified by silica gel chromatography using hexane/EtOAc (8:2) as eluent. The resulting oil was carried out to the next step without further purification and characterization. To a solution of the purified crude in acetonitrile (ACN) (100 mL), potassium carbonate (3.2 g, 23.5 mmol) and triphenylphosphine (6.0 g, 23.5 mmol) were added. After stirring at reflux for two days, the reaction mixture was cooled down, evaporated and purified by column chromatography on silica gel using DCM/MeOH (100:0 to 95:5) as the eluent. Phosphonium salt **2.10** (9.1 g, 77%) was obtained as a white fluffy solid.

Rf: 0.78 (DCM/MeOH 95:5); ^{1}H NMR (500 MHz, $CDCl_3$-d_1) δ 7.76-7.63 (m, 15H), 4.45 (dd, *J* = 3.2, 4.4 Hz, 1H), 3.76 (ddd, *J* = 3.2, 7.4, 11.3 Hz, 1H), 3.60 (td, *J* = 6.9, 9.6 Hz, 1H), 3.54-3.48 (m, 2H), 3.42-3.38 (m, 1H), 3.26 (td, *J* = 6.9, 9.6 Hz, 1H), 1.74-1.40 (m, 12H), 1.23-1.15 (m, 6H); ^{13}C NMR (126 MHz, $CDCl_3$-d_1) δ 135.2 (d, *J*C-P= 3.0 Hz), 133.7 (d, *J*C-P = 10.0 Hz), 130.7 (d, *J*C-P = 12.5 Hz), 118.1 (d, *J*C-P= 86.0 Hz), 99.0, 67.6, 62.6, 30.8, 30.5, 30.3, 29.6, 29.1, 29.0,

26.1, 25.5, 23.3, 22.9, 22.6, 22.5, 19.8; ESI-MS: 475.3 $[M+Na]^+$; HRMS 475.2760 calcd for $[C_{31}H_{40}O_2P]^+$, found 475.2757.

*(8E,20E)-1,28-bis((tetrahydro-2H-pyran-2-yl)oxy)octacosa-8,20-diene (**2.11**)*

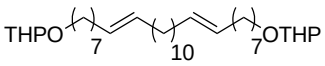

Compound **2.11** was synthesized by reaction of **2.6** (4.44 g, 7.37 mmol) and **2.10** (0.66 g, 3.4 mmol) according to the general procedure for Wittig olefination (see section 2.5.2.2). Olefin **2.11** (1.27 g, 61%) was obtained as a colorless oil after purification by column chromatography on silica gel using hexane/EtOAc (97:3 to 95:5) as the eluent.

Rf: 0.29 (hexane/EtOAc 97:3); ^{1}H NMR (500 MHz, $CDCl_3$-d_1) δ 5.34-5.26 (m, 4H), 4.53 (dd, J = 2.8, 4.4 Hz, 2H), 3.84-3.80 (m, 2H), 3.71-3.66 (m, 2H), 3.47-3.43 (m, 2H), 3.35-3.31 (m, 2H), 1.98-1.45 (m, 25H), 1.27-1.22 (m, 33H); ^{13}C NMR (126 MHz, $CDCl_3$-d_1) δ 130.5, 130.4, 130.1, 129.9, 99.0, 67.8, 62.4, 32.8, 32.7, 29.9, 29.9, 29.9, 29.8, 29.7, 29.7, 29.6, 29.5, 29.4, 29.3, 29.2, 27.2, 27.3, 26.4, 25.7, 19.8; ESI-MS: 613.6 $[M+Na]^+$; HRMS 613.5166 calcd for $[C_{38}H_{70}O_4Na]^+$, found 613.5167.

(8E,24E)-1,32-bis((tetrahydro-2H-pyran-2-yl)oxy)dotriaconta-8,24-diene (**2.12**)

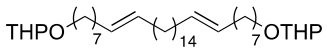

Compound **2.12** was synthesized by reaction of **2.7** (3.33 g, 5.53 mmol) and **2.10** (0.64 g, 3.40 mmol) according to the general procedure for Wittig olefination (see section 2.5.2.2). Olefin **2.12** (1.30 g, 80%) was obtained as a colorless oil after purification by column chromatography on silica gel using hexane/EtOAc (97:3 to 95:5) as eluent.

Rf: 0.41 (hexane/EtOAc 95:5); ^{1}H NMR (500 MHz, $CDCl_3$-d_1) δ 5.35-5.26 (m, 4H), 4.54 (dd, *J* = 2.8, 4.4 Hz, 2H), 3.86-3.80 (m, 2H), 3.72-3.66 (m, 2H), 3.49-3.43 (m, 2H), 3.37-3.31 (m, 2H), 1.99-1.92 (m, 8H), 1.83-1.65 (m, 4H), 1.57-1.46 (m, 12H), 1.33-1.22 (m, 40H); ^{13}C NMR (126 MHz, $CDCl_3$-d_1) δ 130.6, 130.4, 130.1, 129.9, 99.0, 67.8, 62.5, 32.8, 32.7, 31.0, 29.9, 29.9, 29.7, 29.6, 29.5, 29.4, 29.4, 29.3, 27.4, 26.4, 25.7, 19.9.

(8*E*,28*E*)-1,36-bis((tetrahydro-2*H*-pyran-2-yl)oxy)hexatriaconta-8,28-diene (**2.13**)

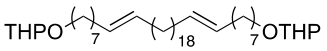

Compound **2.13** was synthesized by reaction of **2.8** (3.71 g, 6.16 mmol) and **2.10** (0.87 g, 2.80 mmol) according to the general procedure for Wittig olefination (see section 2.5.2.2). Olefin **2.13** (1.14 g, 58%) was obtained as a colorless oil after purification by column chromatography on silica gel using hexane/EtOAc (98:2 to 95:5) as eluent.

Rf: 0.47 (hexane/EtOAc 95:5); ^{1}H NMR (500 MHz, $CDCl_3$-d_1) δ 5.35-5.27 (m, 4H), 4.54 (dd, *J* = 2.9, 4.4 Hz, 2H), 3.86-3.81 (m, 2H), 3.72-3.67 (m, 2H), 3.48 (m, 2H), 3.36-3.32 (m, 2H), 1.99-1.92 (m, 8H), 1.83-1.65 (m, 4H), 1.58-1.46 (m, 12H), 1.32-1.22 (m, 48H); ^{13}C NMR (126 MHz, $CDCl_3$-d_1) δ 130.6, 130.4, 130.1, 130.0, 99.0, 67.8, 62.5, 32.8, 32,7, 31.0, 30.0, 29.9, 29.8, 29.8, 29.7, 29.6, 29.5, 29.4, 29.4, 29.3, 27.4, 27.4, 26.4, 25.7, 19.9.

1,28-bis((tetrahydro-2H-pyran-2-yl)oxy)octacosane (**2.14**)

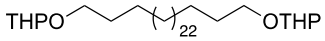

2.11 (1.27 g, 2.15 mmol) was dissolved in a degassed mixture of EtOH/EtOAc/pyridine (9:1:0.02) (55 mL) and 10% Pd/C (0.65 g, 50% w/w) was added. The reaction was stirred under 1 atm H_2 at room temperature for 16 hours. The catalyst was removed by filtration on celite after the solvent was heated to 40°C, and evaporation of the filtrate gave **2.14** (1.24 g, 97%) as a white solid without further purification.

^{1}H NMR (400 MHz, $CDCl_3$-d_1) δ 4.55 (dd, *J* = 2.8, 4.4 Hz, 2H), 3.87-3.83 (m, 2H), 3.70 (td, *J* = 6.9, 9.6 Hz, 2H), 3.49-3.44 (m, 2H), 3.35 (td, *J* = 6.9, 9.6 Hz, 2H), 1.84-1.76 (m, 2H), 1.72-1.66 (m, 2H), 1.58-1.46 (12H), 1.33-1.16 (m, 48H); ^{13}C NMR (100 MHz, $CDCl_3$-d_1) δ 99.0, 67.9, 62.5, 31.0, 29.9, 29.8, 29.7, 26.4, 25.7, 19.9; ESI-MS: 617.5 $[M+Na]^+$; HRMS 617.5479 calcd for $[C_{38}H_{74}O_4Na]^+$, found 617.5480.

1,32-bis((tetrahydro-2H-pyran-2-yl)oxy)dotriacontane (**2.15**)

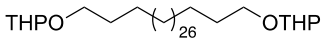

Compound **2.12** (1.30 g, 2.0 mmol) was dissolved in a degassed mixture of EtOH/EtOAc/pyridine (9:1:0.02) (55 mL) and 10% Pd/C (0.65 g, 50% w/w) was added. The reaction was stirred under 1 atm H_2 at room temperature for 16 hours. The catalyst was removed by filtration on celite after the solvent was heated to 40°C, and evaporation of the filtrate gave **2.15** (1.27 g, 98%) as a white solid which was used in the next step without further purification and characterization.

1,36-bis((tetrahydro-2H-pyran-2-yl)oxy)hexatriacontane (**2.16**)

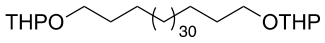

Compound **2.13** (1.10 g, 1.56 mmol) was dissolved in a degassed mixture of EtOH/EtOAc/pyridine (9:1:0.02) (55 mL) and 10% Pd/C (0.55 g, 50% w/w) was added. The reaction was stirred under 1 atm H_2 at room temperature for 16 hours. The catalyst was removed by filtration on celite after the solvent was heated to 40°C, and evaporation of the filtrate gave **2.16** (0.96 g, 87%) as a white solid which was used in the next step without further purification and characterization.

1,28-dibromooctacosane (**2.17**)

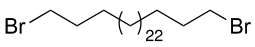

1,28-dibromooctacosane was synthesized following a reported protocol for conversion of tetrahydropyranylated alcohols to their corresponding bromides.[48] Carbon tetrabromide (1.80 g, 5.44 mmol) was added to a solution of **2.14** (1.08 g, 1.81 mmol) in dry DCM (30 mL). After stirring for 10 min, the solution was cooled down and triphenylphosphine (2.85 g, 10.88 mmol) was added. The mixture was stirred 24 hours at room temperature and purified by column chromatography on silica gel using DCM/hexane (1:1) as the eluent. Compound **2.17** (0.76 g, 76%) was obtained as a white solid.

Rf: 0.90 (DCM/hexane 1:1); ^{1}H NMR (500 MHz, $CDCl_3$-d_1) δ 3.39 (t, *J* = 6.9 Hz, 4H), 1.86-1.80 (m, 4H), 1.42-1.37 (m, 4H), 1.29-1.23 (m, 44H); ^{13}C NMR (126 MHz, $CDCl_3$-d_1) δ 34.3, 33.0, 29.9, 29.8, 29.8, 29.7, 29.0, 28.4.

1,32-dibromodotriacontane (**2.18**)

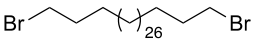

1,32-dibromodotriacontane was synthesized from protected diol **2.15** (1.27 g, 1.95 mmol) according to the general procedure for conversion of tetrahydropyranylated alcohols to their corresponding bromides (see section 2.5.2.3). Dibromoalkane **2.18** (0.95 g, 80%) was obtained as a white solid after purification by column chromatography on silica gel using hexane/DCM (1:1) as the eluent.

Rf: 0.90 (DCM/hexane 1:1); ^{1}H NMR (500 MHz, $CDCl_3$-d_1) δ 3.38 (t, *J* = 6.9 Hz, 4H), 1.86-1.80 (m, 4H), 1.40-1.24 (m, 56H); ^{13}C NMR (126 MHz, $CDCl_3$-d_1) δ 34.1, 33.1, 29.9, 29.8, 29.8, 29.7, 29.0, 28.4.

1,36-dibromohexatriacontane (**2.19**)

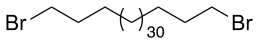

1,36-dibromohexatriacontane was synthesized from protected diol **2.16** (0.96 g, 1.36 mmol) according to the general procedure for conversion of tetrahydropyranylated alcohols to their corresponding bromides (see section 2.5.2.3). Dibromoalkane **2.19** (0.56 g, 61%) was obtained as a white solid after purification by column chromatography on silica gel using hexane/DCM (1:1) as the eluent.

Rf: 0.95 (DCM/hexane 1:1); ^{1}H NMR (500 MHz, $CDCl_3$-d_1) δ 3.38 (t, *J* = 6.9 Hz, 4H), 1.86-1.81 (m, 4H), 1.50-1.09 (m, 64H); ^{13}C NMR (126 MHz, $CDCl_3$-d_1) δ 34.2, 33.1, 29.9, 29.8, 29.8, 29.7, 29.0, 28.4.

18,51-bis((benzyloxy)methyl)-2,6,10,14,55,59,63,67-octamethyl-17,20,49,52-tetraoxaoctahexacontane (**2.20**)

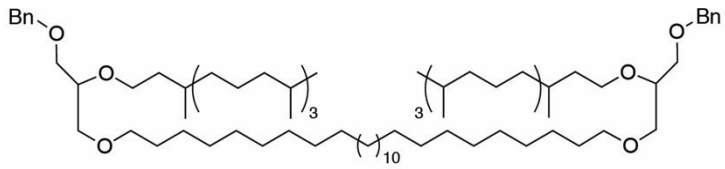

Compound **2.20** was synthesized by reaction of **2.4** (1.21 g, 2.62 mmol) and **2.17** (0.58 g, 1.05 mmol) according to the general procedure for formation of tetraether lipid scaffold by S_N2 reaction (see section 2.5.2.4). Compound **2.20** (0.39 g, 28%) was obtained as a colorless oil after purification by column chromatography on silica gel using hexane/EtOAc (98:2 to 95:5) as the eluent.

Rf: 0.26 (hexane/EtOAc 95:5); ^{1}H NMR (500 MHz, $CDCl_3$-d_1) δ 7.32-7.25 (m, 10H), 4.54 (s, 4H), 3.64-3.45 (m, 14H), 3.41 (t, *J* = 6.9 Hz, 4H), 1.67-1.48 (m, 10H), 1.36-1.02 (m, 90H), 0.86-0.82 (m, 30H); ^{13}C NMR (126 MHz, $CDCl_3$-d_1) δ 138.6, 128.5, 127.8, 127.7, 78.1, 73.5, 71.9, 70.9, 70.5, 69.1, 39.6, 37.7, 37.7, 37.6, 37.6, 37.5, 37.4, 37.3, 33.0, 30.0, 29.9, 29.9, 29.7, 28.2, 26.3, 25.0, 24.7, 24.6, 22.9, 22.8, 20.0, 19.9, 19.8.

18,55-bis((benzyloxy)methyl)-2,6,10,14,59,63,67,71-octamethyl-17,20,53,56-tetraoxadoheptacontane (**2.21**)

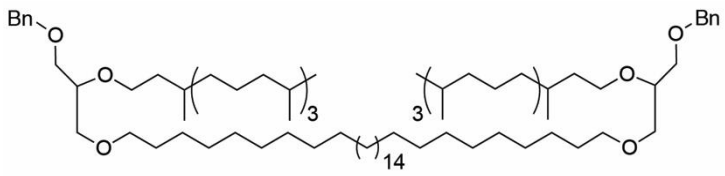

Compound **2.21** was synthesized by reaction of **2.4** (1.25 g, 2.69 mmol) and **2.18** (0.66 g, 1.08 mmol) according to the general procedure for formation of tetraether lipid scaffold by S_N2 reaction (see section 2.5.2.4). Compound **2.21** (0.42 g, 30%) was obtained as a colorless oil after purification by column chromatography on silica gel using hexane/EtOAc (98:2 to 95:5) as the eluent.

Rf: 0.37 (hexane/EtOAc 95:5); ^{1}H NMR (500 MHz, $CDCl_3$-d_1) δ 7.32-7.24 (m, 10H), 4.54 (s, 4H), 3.62-3.40 (m, 18H), 1.62-1.48 (m, 10H), 1.36-1.04 (m, 98H), 0.86-0.82 (m, 30H); ^{13}C NMR (126 MHz, $CDCl_3$-d_1) δ 138.6, 128.5, 127.8, 127.7, 78.2, 73.5, 71.9, 70.9, 70.5, 69.1, 39.6, 37.7, 37.7, 37.6, 37.5, 37.4, 37.3, 33.0, 29.9, 29.9, 29.7, 28.2, 26.3, 25.0, 24.7, 24.6, 22.9, 22.8, 20.0, 19.9, 19.8; ESI-MS: 1394.3 $[M+Na]^+$; HRMS 1394.2890 calcd for $[C_{92}H_{170}O_6Na]^+$, found 1394.2888.

18,59-bis((benzyloxy)methyl)-2,6,10,14,63,67,71,75-octamethyl-17,20,57,60-tetraoxahexaheptacontane (**2.22**)

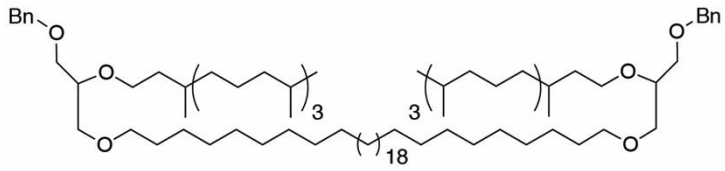

Compound **2.22** was synthesized by reaction of **2.4** (1.07 g, 2.32 mmol) and **2.19** (0.53 g, 0.79 mmol) according to the general procedure for formation of tetraether lipid scaffold by S_N2 reaction (see section 2.5.2.4). Compound **2.22** (0.33 g, 29%) was obtained as a colorless oil after purification by column chromatography on silica gel using hexane/EtOAc (98:2 to 95:5) as the eluent.

Rf: 0.35 (hexane/EtOAc 95:5); ^{1}H NMR (500 MHz, $CDCl_3$-d_1) δ 7.32-7.25 (m, 10H), 4.54 (s, 4H), 3.64-3.40 (m, 18H), 1.64-1.48 (m, 10H), 1.38-1.00 (m, 106H), 0.86-0.82 (m, 30H); ^{13}C NMR (126 MHz, $CDCl_3$-d_1) δ 138.6, 128.5, 127.8, 127.7, 78.1, 73.6, 71.9, 70.9, 70.5, 69.1, 39.6, 37.7, 37.7, 37.6, 37.6, 37.5, 37.4, 37.3, 33.0, 29.9, 29.9, 29.7, 28.2, 26.3, 25.0, 24.7, 24.6, 22.9, 22.9, 20.0, 19.9, 19.8; ESI-MS: 1450.4 $[M+Na]^+$; HRMS 1450.3516 calcd for $[C_{96}H_{178}O_6Na]^+$, found 1450.3518.

3-((28-(3-hydroxy-2-((3,7,11,15-tetramethylhexadecyl)oxy)propoxy)octacosyl) oxy)-2-((3,7,11,15-tetramethylhexadecyl) oxy)propan-1-ol (**2.23**)

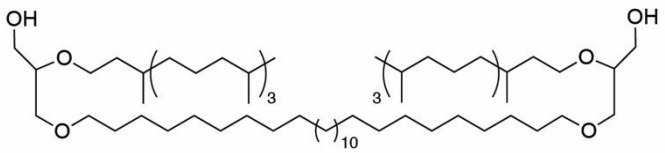

Compound **2.23** was synthesized by hydrogenation of **2.20** (0.39 g, 0.30 mmol) according to the general procedure for debenzylation of the lipid scaffold by hydrogenation (see section 2.5.2.5). Diol **2.23** (0.23 g, 68%) was obtained as a white solid after purification by column chromatography on silica gel using hexane/EtOAc (9:1 to 8:2) as the eluent.

Rf: 0.52 (hexane/EtOAc 8:2); ^{1}H NMR (500 MHz, $CDCl_3$-d_1) δ 3.71-3.39 (m, 18H), 2.16 (brs, 2H), 1.62-1.45 (m, 10H), 1.39-1.02 (m, 90H), 0.85-0.81 (m, 30H); ^{13}C NMR (126 MHz, $CDCl_3$-d_1) δ 78.5, 72.1, 72.1, 68.9, 63.3, 39.6, 37.7, 37.7, 37.6, 37.5, 37.5, 37.3, 37.2, 33.0, 30.0, 29.9, 29.8, 29.7, 28.2, 26.3, 25.0, 24.7, 24.6, 22.9, 22.8, 20.0, 19.9,19.8; ESI-MS: 1135.8 $[M+H]^+$.

3-((32-(3-hydroxy-2-((3,7,11,15-tetramethylhexadecyl)oxy)propoxy) dotriacontyl)oxy)-2-((3,7,11,15-tetramethylhexadecyl)oxy)propan-1-ol (**2.24**)

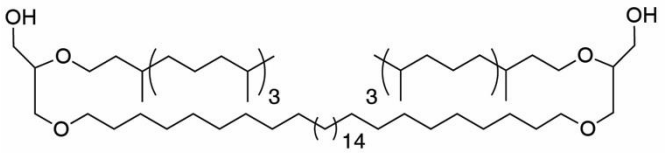

Compound **2.24** was synthesized by hydrogenation of **2.21** (0.42 g, 0.31 mmol) according to the general procedure for debenzylation of the lipid scaffold by

hydrogenation (see section 2.5.2.5). Diol **2.24** (0.28 g, 77%) was obtained as a white solid after purification by column chromatography on silica gel using hexane/EtOAc (9:1 to 8:2) as the eluent.

Rf: 0.70 (hexane/EtOAc 8:2); ^{1}H NMR (500 MHz, $CDCl_3$-d_1) δ 3.71-3.39 (m, 18H), 2.19 (brs, 2H), 1.61-1.47 (m, 10H), 1.38-1.03 (m, 98H), 0.86-0.81 (m, 30H); ^{13}C NMR (126 MHz, $CDCl_3$-d_1) δ 78.5, 72.1, 71.1, 68.8, 63.3, 39.6, 37.7, 37.7, 37.6, 37.5, 37.3, 37.2, 33.0, 30.0, 29.9, 29.8, 29.7, 28.2, 26.3, 25.0, 24.7, 24.6, 22.9, 22.8, 20.0, 19.9, 19.8.

3-((36-(3-hydroxy-2-((3,7,11,15-tetramethylhexadecyl)oxy)propoxy)hexa triacontyl)oxy)-2-((3,7,11,15-tetramethylhexadecyl)oxy)propan-1-ol (**2.25**)

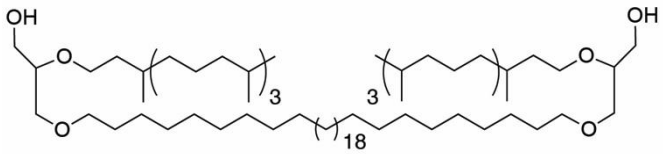

Compound **2.25** was synthesized by hydrogenation of **2.22** (0.33 g, 0.23 mmol) according to the general procedure for debenzylation of the lipid scaffold by hydrogenation (see section 2.5.2.5). Diol **2.25** (0.23 g, 81%) was obtained as a white solid after purification by column chromatography on silica gel using hexane/EtOAc (9:1 to 8:2) as the eluent.

Rf: 0.39 (hexane/EtOAc 8:2); ^{1}H NMR (500 MHz, $CDCl_3$-d_1) δ 3.71-3.39 (m, 18H), 2.22 (brs, 2H), 1.63-1.46 (m, 10H), 1.38-1.00 (m, 106H), 0.86-0.81 (m, 30H); ^{13}C NMR (126 MHz, $CDCl_3$-d_1) δ 78.5, 72.1, 71.1, 68.8, 63.3, 39.6, 37.7,

37.6, 37.5, 37.5, 37.3, 37.2, 33.0, 30.0, 29.9, 29.8, 29.7, 28.2, 26.3, 25.0, 24.7, 24.6, 22.9, 22.8, 20.0, 19.9, 19.8.

(octacosane-1,28-diylbis(oxy))bis(2-((3,7,11,15-tetramethylhexadecyl)oxy) propane-3, 1-diyl) bis(2-(trimethylammonio)ethyl) bis(phosphate) (**GMGTPC-T28**)

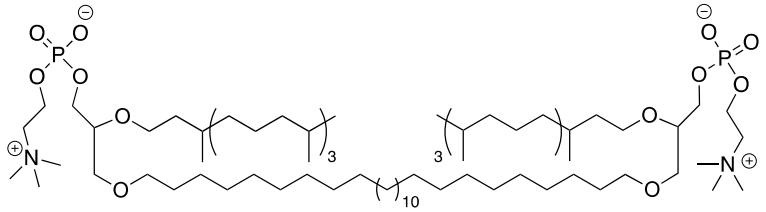

Lipid **GMGTPC-T28** was synthesized from diol **2.23** (0.23 g, 0.21 mmol) following the general procedure for formation of phosphocholine lipid (see section 2.5.2.6). Lipid **GMGTPC-T28** (0.16 g, 54%) was obtained as a white gum after purification by column chromatography on silica gel using DCM/MeOH/H_2O (70:30:5) as the eluent.

Rf: 0.33 (DCM/MeOH/H_2O 70:30:5); ^{1}H NMR (500 MHz, MeOD-d_4/$CDCl_3$-d_1 1:1) δ 4.00-3.96 (m, 4H), 3.63 (t, *J* = 5.5 Hz, 4H), 3.40-3.31 (m, 12H), 3.23-3.17 (m, 6H), 2.95 (s, 18H), 1.39-1.22 (m, 10H), 1.14-0.79 (m, 90H), 0.62-0.58 (30H); ^{13}C NMR (126 MHz, MeOD-d_4/$CDCl_3$-d_1 1:1) δ 77.8, 77.7, 77.7, 77.6, 71.3, 70.2, 68.6, 68.3, 66.0, 64.7, 64.6, 58.6, 58.5, 53.5, 39.0, 37.3, 37.1, 37.0, 36.8, 36.8, 36.7, 32.4, 29.5, 29.3, 29.1, 27.5, 25.6, 24.3, 24.0, 22.0, 21.9, 19.1, 19.0, 19.0, 18.9, 18.9; ^{31}P NMR (202 MHz, MeOD-d_4/$CDCl_3$-d_1 1:1) δ 0.16; ESI-MS: 1466.0 $[M+H]^+$; HRMS calcd 1466.2615 for $[C_{84}H_{175}N_2O_{12}P_2]^+$, found 1466.2597.

(dotriacontane-1,32-diylbis(oxy))bis(2-((3,7,11,15-tetramethylhexadecyl)oxy) propane-3,1-diyl) bis(2-(trimethylammonio)ethyl) bis(phosphate) (**GMGTPC-T32**)

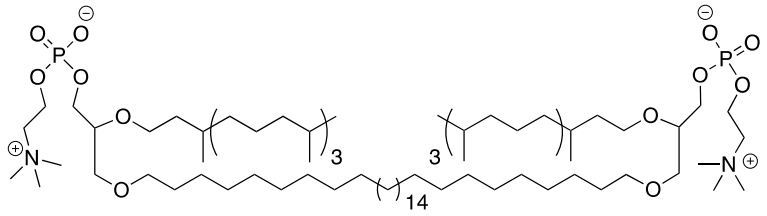

Lipid **GMGTPC-T32** was synthesized from diol **2.24** (0.28 g, 0.23 mmol) following the general procedure for formation of phosphocholine lipid (see section 2.5.2.6). **GMGTPC-T32** (0.19 g, 54%) was obtained as a white gum after purification by column chromatography on silica gel using DCM/MeOH/H_2O (70:30:5) as the eluent.

Rf: 0.40 (DCM/MeOH/H_2O 70:30:5); ^{1}H NMR (500 MHz, MeOD-d_4/$CDCl_3$-d_1 1:1) δ 3.93-3.88 (m, 4H), 3.56 (t, *J* = 5.5 Hz, 4H), 3.32-3.09 (m, 18H), 2.88 (s, 18H), 1.27-1.16 (m, 10H), 1.04-0.71 (m, 98H), 0.55-0.50 (m, 30H); ^{13}C NMR (126 MHz, MeOD-d_4/$CDCl_3$-d_1 1:1) δ 77.8, 77.7, 77.7, 77.6, 77.5, 71.4, 70.2, 68.7, 68.4, 66.0, 64.7, 58.6, 58.6, 53.6, 39.0, 37.3, 37.1, 37.1, 37.0, 36.9, 36.8, 36.7, 32.4, 29.5, 29.4, 29.3, 29.2, 27.6, 25.7, 24.4, 24.1, 24.0, 22.1, 22.0, 19.2, 19.1, 19.1, 19.0, 18.9; ^{31}P NMR (202 MHz, MeOD-d_4/$CDCl_3$-d_1 1:1) δ 0.16; ESI-MS: 1522.2 $[M+H]^+$; HRMS calcd 1522.3241 for $[C_{88}H_{183}N_2O_{12}P_2]^+$, found 1522.3261.

(hexatriacontane-1,36-diylbis(oxy))bis(2-((3,7,11,15-tetramethylhexadecyl)oxy) propane-3,1-diyl) bis(2-(trimethylammonio)ethyl) bis(phosphate) (**GMGTPC-T36**)

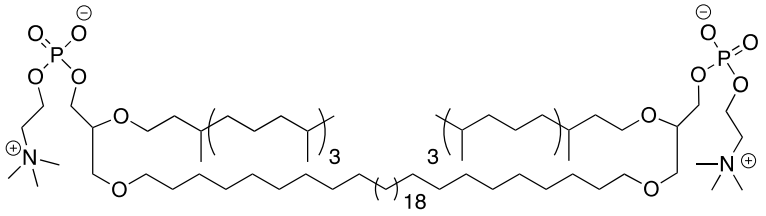

Lipid **GMGTPC-T36** was synthesized from diol **2.25** (0.23 g, 0.19 mmol) following the general procedure for formation of phosphocholine lipid (see section 2.5.2.6). **GMGTPC-T36** (0.10 g, 36%) was obtained as a white gum after purification by column chromatography on silica gel using DCM/MeOH/H_2O (70:30:5) as the eluent.

Rf: 0.36 (DCM/MeOH/H_2O 70:30:5); ^{1}H NMR (500 MHz, MeOD-d_4/$CDCl_3$-d_1 1:1) δ 3.95-3.90 (m, 4H), 3.56 (t, *J* = 5.5 Hz, 4H), 3.34-3.11 (m, 18H), 2.89 (s, 18H), 1.28-1.17 (m, 10H), 1.08-0.73 (m, 108H), 0.56-0.51 (m, 30H); ^{13}C NMR (126 MHz, MeOD-d_4/$CDCl_3$-d_1 1:1) δ 77.8, 77.7, 77.7, 77.6, 77.5, 71.4, 70.2, 68.7, 68.4, 66.0, 64.7, 58.6, 58.6, 53.6, 39.0, 37.3, 37.2, 37.1, 37.0, 36.9, 36.8, 36.7, 32.4, 29.6, 29.3, 29.2, 27.6, 25.7, 24.4, 24.1, 24.0, 22.1, 22.1, 19.2, 19.1, 19.1, 19.0, 19.0; ^{31}P NMR (202 MHz, MeOD-d_4/$CDCl_3$-d_1 1:1) δ 0.21; ESI-MS: 1578.2 $[M+H]^+$; HRMS calcd 1578.3867 for $[C_{92}H_{191}N_2O_{12}P_2]^+$, found 1578.3853.

*2.5.5 Synthetic Procedure for **GMGTPC-CP1** and **GMGTPC-CH1***

((1R,3S)-cyclohexane-1,3-diyl)dimethanol (**2.27**)

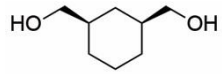

To a cold suspension of $LiAlH_4$ (10.4 g, 272.0 mmol) in dry Et_2O (300 mL), a solution of *cis*-1,3-cyclohexanedicarboxylic acid (10.9 g, 54.4 mmol) in dry Et_2O (230 mL) was added dropwise. After stirring at 0°C for 1.5 hours, 1M HCl solution was added slowly to quench the reaction. The reaction mixture was extracted with EtOAc and the combined organic layer was washed with water, brine and dried over Na_2SO_4. Diol **2.27** (4.4 g, 55%) was obtained as a white solid after solvent evaporation.

^{1}H NMR (500 MHz, $CDCl_3$-d_1) δ 3.38-3.40 (m, 4H), 2.04-2.00 (m, 3H), 1.88-1.73 (m, 4H), 1.55-1.47 (m, 2H), 1.32-1.22 (m, 1H), 0.89-0.81 (m, 2H), 0.65-0.58 (m, 1H).

(((1R,3S)-cyclopentane-1,3-diyl)bis(methylene))bis(triphenylphosphonium) iodide (**2.26**)

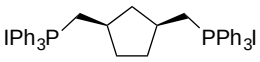

Compound **2.26** was synthesized following a reported protocol.[23]

*(((1R,3S)-cyclohexane-1,3-diyl)bis(methylene))bis(triphenylphosphonium) iodide (**2.28**)*

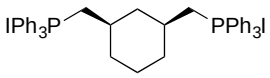

To a cold solution of triphenylphosphine (17.4 g, 66.5 mmol) and imidazole (4.5 g, 66.5 mmol) in mixture of dry ACN/Et_2O (1:3) (150 mL), iodine (16.8 g, 66.5 mmol) was added. After stirring of the mixture at room temperature in the dark for 10 min, a solution of compound **2.27** (4.4 g, 30.2 mmol) in dry Et_2O (30 mL) was added. The reaction mixture was stirred for 2 hours at room temperature in the dark. Reaction mixture was washed with 10% $Na_2S_2O_3$ aqueous solution and extracted with Et_2O. The combined organic layers were washed with water, dried over Na_2SO_4, and purified by silica gel chromatography using a mixture of hexane/EtOAc (8:2) as the eluent. The resulting oil was carried out to the next step without further purification and characterization. To a solution of the purified crude in ACN (80 mL), triphenylphosphine (23.7 g, 90.6 mmol) was added and the reaction mixture was stirred for 16 hours at reflux. After the reaction mixture was allowed to cool down to room temperature, the product was precipitated by adding toluene. Pure compound **2.28** (13.7 g, 51%) was obtained as a white solid after recrystallization from MeOH and Et_2O.

^{1}H NMR (500 MHz, MeOD-d_4) δ 7.89-7.72 (m, 30H), 3.52-3.36 (m, 4H), 1.88-1.70 (m, 3H), 1.64-1.57 (m, 1H), 1.45-1.42 (m, 1H), 1.33-1.30 (m, 2H), 1.20-1.12 (m, 2H), 1.03-0.94 (m, 1H); ^{13}C NMR (126 MHz, MeOD-d_4) δ 136.4, 135.0 (d, JC-P = 10.1 Hz), 131.7 (d, J C-P= 12.6 Hz), 120.5 (d, J C-P= 86.0 Hz), 34.7,

43.6, 43.6, 34.6, 34.5, 34.1, 29.4, 29.0, 29.2; ^{31}P NMR (202 MHz, MeOD-d_4) δ 22.78; ESI-MS: 317.5 $[M-2I]^{2+}$; HRMS calcd 317.1454 for $[C_{44}H_{44}P_2]^{2+}$, found 317.1452.

12-(benzyloxy)dodecan-1-ol (**2.29**)

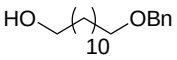

Compound **2.29** was synthesized following a reported protocol.[49]

12-(benzyloxy)dodecanal (**2.30**)

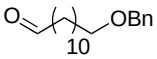

To a cold solution of **2.29** (1.44 g, 4.90 mmol) in dry DCM (45 mL), Dess-Martin Periodinane (DMP) (2.50 g, 5.89 mmol) was added portion-wise. The resulting mixture was allowed to reach room temperature over 1 hour. After 3 more hours of stirring at room temperature, the mixture was diluted with DCM, washed successively with 1M NaOH solution, water and brine. The organic layer was then dried over Na_2SO_4, concentrated under reduce pressure and purified by column chromatography on silica gel using hexane/EtOAc (95:5) as the eluent. Aldehyde **2.30** (1.25 g, 88%) was obtained as a colorless oil.

Rf: 0.47 (hexane/EtOAc 95:5); ^{1}H NMR (400 MHz, $CDCl_3$-d_1) δ 9.74 (t, *J* = 1.7 Hz, 1H), 7.33-7.25 (m, 5H), 4.48 (s, 2H), 3.44 (t, *J* = 6.7 Hz, 2H), 2.40 (tt, *J* =

1.7, 6.7 Hz, 2H), 1.62-1.55 (m, 4H), 1.35-1.25 (m, 14H); ESI-MS: 291.2 $[M+H]^+$; HRMS 291.2319 calcd for $[C_{19}H_{31}O_2]^+$, found 291.2322.

(1R,3S)-1,3-bis((E)-13-(benzyloxy)tridec-1-en-1-yl)cyclopentane (**2.31**)

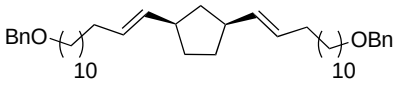

Compound **2.31** was synthesized by reaction of **2.30** (3.84 g, 13.24 mmol) and **2.26** (4.87 g, 5.57 mmol) according to the general procedure for Wittig olefination (see section 2.5.2.2). Olefin **2.31** (2.44 g, 68%) was obtained as a colorless oil after purification by column chromatography on silica gel using hexane/EtOAc (99:1) as the eluent.

Rf: 0.45 (hexane/EtOAc 99:1); ^{1}H NMR (500 MHz, $CDCl_3$-d_1) δ 7.35-7.26 (m, 10H), 5.37-5.27 (m, 4H), 4.50 (s, 4H), 3.46 (dd, *J* = 6.5, 6.8 Hz, 4H), 2.82-2.76 (m, 1.5H), 2.49-2.43 (m, 0.5H), 2.04-1.77 (m, 7H), 1.64-1.58 (m, 4H), 1.36-1.26 (m, 34H), 1.06-0.96 (m, 1H); ^{13}C NMR (126 MHz, $CDCl_3$-d_1) δ 138.9, 135.3, 135.2, 135.0, 134.9, 128.8, 128.8, 128.7, 128.5, 127.8, 127.6, 73.0, 70.7, 43.7, 42.3, 41.9, 38.4, 38.2, 33.0, 32.8, 32.7, 32.5, 32.4, 30.1, 30.0, 29.8, 29.7, 29.7, 29.5, 29.4, 27.7, 26.4; ESI-MS: 660.6 $[M+NH_4]^+$; HRMS calcd 660.5714 for $[C_{45}H_{70}O_2NH_4]^+$, found 660.5715.

(1R,3S)-1,3-bis((E)-13-(benzyloxy)tridec-1-en-1-yl)cyclohexane **(2.32)**

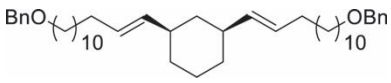

Compound **2.32** was synthesized by reaction of **2.30** (2.57 g, 2.89 mmol) and **2.28** (2.01 g, 6.93 mmol) according to the general procedure for Wittig olefination (see section 2.5.2.2). Olefin **2.32** (1.00 g, 53%) was obtained as a colorless oil after purification by column chromatography on silica gel using hexane/EtOAc (99:1) as the eluent.

Rf: 0.40 (Hexane/EtOAc 99:1); ^{1}H NMR (500 MHz, $CDCl_3$-d_1) δ 7.34-7.25 (m, 10H), 5.40-5.14 (m, 4H), 4.50 (s, 4H), 3.46 (t, *J* = 6.6 Hz, 4H), 2.35 (m, 1H), 2.06-1.92 (m, 5H), 1.78-1.52 (m, 8H), 1.38-1.26 (m, 33H), 1.02-0.81 (m, 3H); ^{13}C NMR (126 MHz, $CDCl_3$-d_1) δ 138.9, 136.3, 136.2, 135.9, 135.8, 134.0, 133.8, 128.5, 128.5, 128.1, 127.8, 127.6, 73.0, 70.7, 40.8, 40.5, 40.1, 40.0, 36.3, 36.2, 33.1, 32.9, 32.9, 32.8, 30.2, 30.0, 29.9, 29.8, 29.7, 29.5, 29.3, 27.7, 27.6, 26.4, 26.0, 25.9; ESI-MS: 657.5 $[M+H]^+$; HRMS calcd 679.5425 for $[C_{46}H_{72}O_2Na]^+$, found 679.5424.

13,13'-((1R,3S)-cyclopentane-1,3-diyl)bis(tridecan-1-ol) (**2.33**)

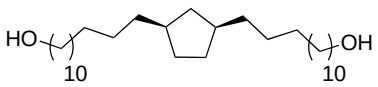

To a degassed solution of **2.31** (2.38 g, 3.71 mmol) in EtOH (220 mL), 10% Pd/C (0.60 g, 25% w/w) was added. The reaction was stirred under 1 atm H_2 at

room temperature for 24 hours. The solution was then filtered through celite, and the solvent was evaporated. Diol **2.33** (1.64 g, 95%) was obtained as a white solid and used without further purification.

Rf: 0.26 (hexane/EtOAc 95:5); ^{1}H NMR (500 MHz, MeOD-d_4/$CDCl_3$-d_1 1:1) δ 3.58 (t, *J* = 7.0 Hz, 4H), 1.92-1.68 (m, 5H), 1.58-1.51 (m, 4H), 1.39-1.21 (m, 44H), 1.18-1.11 (m, 2H), 0.67-0.59 (m, 1H); ^{13}C NMR (126 MHz, MeOD-d_4/$CDCl_3$-d_1 1:1) δ 62.4, 40.7, 40.1, 36.7, 32.5, 31.6, 29.9, 29.7, 29.6, 29.5, 28.7,

13,13'-((1R,3S)-cyclohexane-1,3-diyl)bis(tridecan-1-ol) (**2.34**)

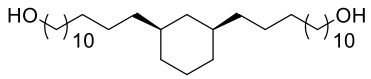

To a degassed solution of olefin **2.32** (0.95 g, 1.45 mmol) in EtOH (88 mL), 10% Pd/C (0.24 g, 25% w/w) was added. The reaction was stirred under 1 atm H_2 at room temperature for 24 hours. The solution was then filtered through celite, and the solvent was evaporated to yield a white solid which was used in the next step without further purification and characterization.

(*1R,3S)-1,3-bis(13-bromotridecyl)cyclopentane* (**2.35**)

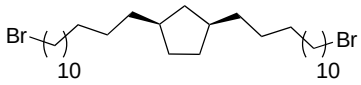

Dibromo alkane **2.35** (1.57 g, 78%) was obtained as a white solid from diol **2.33** (1.58 g, 3.39 mmol) following the general procedure for bromination of diol using hydrobromic acid solution (see section 2.5.2.3).

Rf: 0.81 (hexane/EtOAc 99:1); (500 MHz, $CDCl_3$-d_1) δ 3.41 (t, *J* = 7.0 Hz, 4H), 1.89-1.69 (m, 9H), 1.44-1.14 (m, 44H), 0.91-0.85 (m, 2H), 0.66-0.50 (m, 1H); ^{13}C NMR (126 MHz, $CDCl_3$-d_1) δ 40.9, 40.4, 39.0, 37.0, 37.0, 34.2, 33.2, 33.0, 31.9, 30.2, 29.9, 29.9, 29.8, 29.7, 29.0, 29.0, 28.9, 28.4.

28.6, 25.7; ESI-MS: 467.6 $[M+H]^+$.

(1R,3S)-1,3-bis(13-bromotridecyl)cyclohexane (**2.36**)

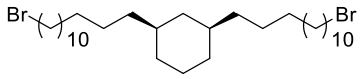

Dibromo alkane **2.36** (0.70 g, 80%) was obtained as a white solid from diol **2.34** (0.70 g, 1.45 mmol) following the general procedure for bromination of diol using hydrobromic acid solution (see section 2.5.2.3).

Rf: 0.80 (hexane/EtOAc 99:1); ^1H NMR (500 MHz, $CDCl_3$-d_1) δ 3.39 (t, *J* = 6.9 Hz, 4H), 1.86-1.80 (m, 4H), 1.69-1.66 (m, 3H), 1.43-1.37 (m, 4H), 1.29-1.05 (m, 43H), 0.87-0.69 (m, 3H), 0.49-0.42 (m, 1H); ^{13}C NMR (126 MHz, $CDCl_3$-d_1) δ 40.6, 37.9, 37.8, 34.2, 33.5, 32.9, 30.1, 29.9, 29.8, 29.7, 29.6, 29.5, 29.4, 28.9, 28.3, 27.0, 26.5.

(1R,3S)-1,3-bis(13-(3-(benzyloxy)-2-((3,7,11,15-tetramethylhexadecyl)oxy) propoxy)tridecyl)cyclopentane (**2.37**)

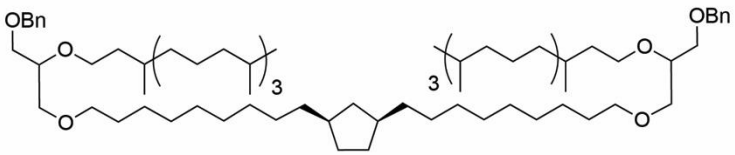

Compound **2.37** was synthesized by reaction of **2.4** (0.39 g, 0.84 mmol) and **2.35** (0.20 g, 0.34 mmol) according to the general procedure for formation of tetraether lipid scaffold by S_N2 reaction (see section 2.5.2.4). Compound **2.37** (0.13 g, 29%) was obtained as a colorless oil after purification by column chromatography on silica gel using hexane/EtOAc (99:1 to 95:5) as the eluent.

Rf: 0.27 (hexane/EtOAc 95:5); ^{1}H NMR (500 MHz, $CDCl_3$-d_1) δ 7.25-7.26 (m, 10H), 4.57 (s, 4H), 3.68-3.43 (m, 18H), 1.94-1.89 (m, 1H), 1.81-1.71 (m, 4H), 1.69-1.50 (m, 10H), 1.42-1.07 (m, 88H), 0.89-0.60 (m, 31H); ^{13}C NMR (126 MHz, $CDCl_3$-d_1) δ 138.6, 128.6, 128.5, 127.8, 127.8, 128.7, 100.1, 78.1, 73.5, 71.8, 70.9, 70.5, 69.0, 40.9, 40.3, 39.6, 39.0, 37.7, 37.7, 37.6, 37.6, 37.5, 37.5, 36.9, 33.0, 31.8, 30.2, 30.0, 29.9, 29.8, 29.7, 29.0, 28.1, 26.3, 25.0, 24.7, 24.6, 22.9, 22.8, 20.0, 19.9, 19.8.

(1R,3S)-1,3-bis(13-(3-(benzyloxy)-2-((3,7,11,15-tetramethylhexadecyl)oxy) propoxy)tridecyl)cyclohexane (**2.38**)

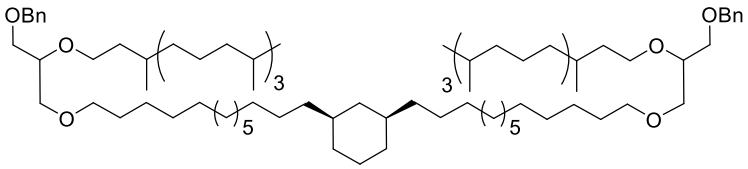

Compound **2.38** was synthesized by reaction of **2.4** (1.53 g, 3.32 mmol) and **2.36** (0.67 g, 1.11 mmol) according to the general procedure for formation of tetraether lipid scaffold by S_N2 reaction (see section 2.5.2.4). Compound **2.38** (0.32 g, 21%) was obtained as a colorless oil after purification by column chromatography on silica gel using hexane/EtOAc (98:2 to 95:5) as the eluent.

Rf: 0.35 (hexane/EtOAc 95:5); ^{1}H NMR (500 MHz, $CDCl_3$-d_1) δ 7.33-7.24 (m, 10H), 4.55 (s, 4H), 3.65-3.41 (m, 18H), 1.72-1.50 (m, 14H), 1.39-1.04 (m, 89H), 0.88-0.72 (m, 32H), 0.52-0.45 (m, 1H); ^{13}C NMR (126 MHz, $CDCl_3$-d_1) δ 138.6, 128.4, 127.7, 127.6, 78.1, 73.5, 71.8, 70.9, 70.4, 69.0, 40.7, 39.5, 38.0, 37.9, 37.8, 37.7, 37.6, 37.5, 37.4, 37.3, 37.2, 33.6, 33.0, 30.3, 29.9, 29.8, 29.7, 28.1, 27.1, 26.6, 26.3, 25.0, 24.7, 24.5, 22.9, 22.8, 20.0, 19.9, 19.8.

3,3'-((((1R,3S)-cyclopentane-1,3-diyl)bis(tridecane-13,1-diyl))bis(oxy))bis(2-((3,7,11,15-tetramethylhexadecyl)oxy)propan-1-ol) (**2.39**)

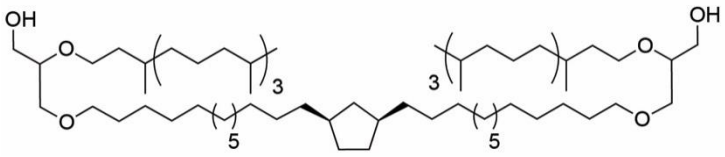

Compound **2.39** was synthesized by hydrogen-ation of **2.37** (0.28 g, 0.28 mmol) according to the general procedure for debenzylation of lipid scaffold by hydrogenation (see section 2.5.2.5). Diol **2.39** (0.28 g, 85%) was obtained as a colorless oil after purification by column chromatography on silica gel using hexane/EtOAc (9:1 to 8:2) as the eluent.

Rf: 0.43 (hexane/EtOAc 8:2); ^{1}H NMR (500 MHz, $CDCl_3$-d_1) δ 3.75-3.37 (m, 18H), 2.22 (t, *J* = 7.0 Hz, 2H), 1.91-1.48 (m, 17H), 1.43-1.01 (m, 86H), 0.88-0.84 (m, 30H), 0.75-0.59 (m, 1H); ^{13}C NMR (126 MHz, $CDCl_3$-d_1) δ 78.4, 72.1, 71.1, 68.9, 63.3, 40.9, 40.3, 39.6, 39.0, 37.7, 37.7, 37.6, 37.6, 37.5, 37.3, 37.3, 37.0, 33.2, 33.0, 31.8, 30.2, 30.0, 29.9, 29.8, 29.7, 29.0, 28.9, 28.2, 26.3, 25.0, 24.7, 24.6, 22.9, 22.8, 20.0, 19.9, 19.8; ESI-MS: 1175.9 $[M+H]^+$; HRMS calcd 1176.1818 for $[C_{77}H_{155}O_6]^+$, found 1176.1817.

3,3'-((((1R,3S)-cyclohexane-1,3-diyl)bis(tridecane-13,1-diyl))bis(oxy))bis(2-((3,7,11,15-tetramethylhexadecyl)oxy)propan-1-ol) (**2.40**)

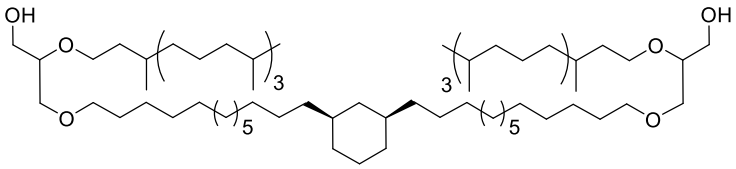

Compound **2.40** was synthesized by hydrogenation of **2.38** (0.32 g, 0.23 mmol) according to the general procedure for debenzylation of lipid scaffold by hydrogenation (see section 2.5.2.5). Diol **2.40** (0.28 g, Qt.) was obtained as a colorless oil after purification by column chromatography on silica gel using hexane/EtOAc (8:2) as the eluent.

Rf: 0.48 (hexane/EtOAc 8:2); ^{1}H NMR (500 MHz, $CDCl_3$-d_1) δ 3.71-3.39 (m, 18H), 2.11 (brs, 2H), 1.69-1.46 (m, 14H), 1.39-1.00 (m, 89H), 0.86-0.68 (m, 32H), 0.49-0.42 (m, 1H); ^{13}C NMR (126 MHz, $CDCl_3$-d_1) δ 78.4, 72.0, 71.1, 71.0, 68.8, 63.3, 63.2, 40.7, 39.6, 38.0, 37.9, 37.8, 37.7, 37.6, 37.5, 37.4, 37.3, 37.2, 33.6, 33.0, 30.3, 30.1, 30.0, 29.9, 29.8, 29.7, 28.2, 27.1, 26.6, 26.3, 25.0, 24.7, 24.5, 22.9, 22.8, 20.0, 19.9, 19.8; ESI-MS: 1190.2 $[M+H]^+$; HRMS calcd 1190.1975 for $[C_{78}H_{157}O_6]^+$, found 1190.1979.

((((1R,3S)-cyclopentane-1,3-diyl)bis(tridecane-13,1-diyl))bis(oxy))bis(2-((3,7,11,15-tetramethylhexadecyl)oxy)propane-3,1-diyl) bis(2-(trimethylammonio) ethyl) bis(phosphate) (**GMGTPC-CP1**)

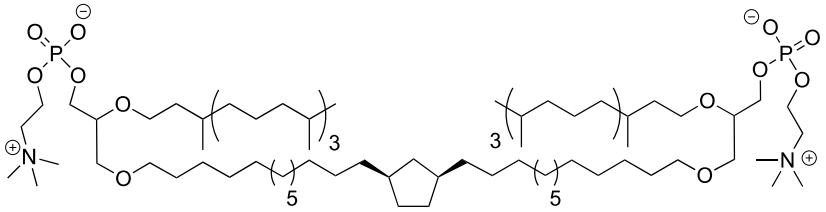

Lipid **GMGTPC-CP1** was synthesized from diol **2.39** (0.38 g, 0.32 mmol) following the general procedure for formation of phosphocholine lipid (see section 2.5.2.6). Lipid **GMGTPC-CP1** (0.42 g, 85%) was obtained as a white gum after purification by column chromatography on silica gel using DCM/MeOH/H_2O (70:30:5) as the eluent.

Rf: 0.32 (DCM/MeOH/H_2O 70:30:5); ^{1}H NMR (500 MHz, MeOD-d_4/$CDCl_3$-d_1 1:1) δ 3.91 (m, 4H), 3.56 (t, *J* = 5.5 Hz, 4H), 3.33-3.10 (m, 18H), 2.89 (s, 18H), 1.75-1.15 (m, 14H), 1.05-0.72 (m, 89H), 0.55-0.51 (m, 31H), 0.33-0.26 (m, 1H); ^{13}C NMR (126 MHz, MeOD-d_4/$CDCl_3$-d_1 1:1) δ 77.8, 77.8, 77.7, 71.4, 70.2, 68.7, 68.5, 66.1, 64.7, 64.7, 58.6, 58.6, 53.6, 40.4, 39.8, 39.0, 37.3, 37.1, 37.0, 36.9, 36.8, 36.7, 36.4, 32.4, 31.2, 29.6, 29.4, 29.3, 29.3, 29.2, 28.4, 27.6, 25.8, 24.4, 24.1, 24.0, 22.1, 22.0, 19.2, 19.1, 19.1, 19.0; ^{31}P NMR (202 MHz, MeOD-d_4/$CDCl_3$-d_1 1:1) δ 0.22; ESI-MS: 1505.9 $[M+H]^+$; HRMS calcd 1506.2928 for $[C_{87}H_{179}N_2O_{12}P_2]^+$, found 1506.2930.

((((1R,3S)-cyclohexane-1,3-diyl)bis(tridecane-13,1-diyl))bis(oxy))bis(2-((3,7,11, 15-tetramethylhexadecyl)oxy)propane-3,1-diyl)bis(2-(trimethylammonio)ethyl) bis(phosphate) (**GMGTPC-CH1**)

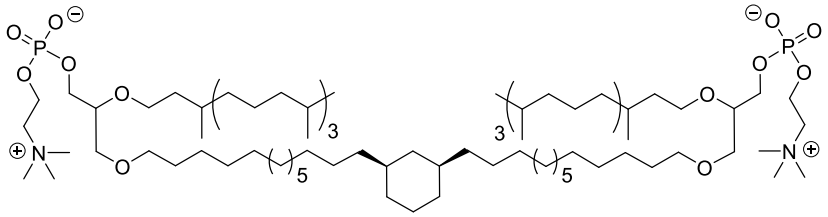

Lipid **GMGTPC-CH1** was synthesized from diol **2.40** (0.26 g, 0.22 mmol) following the general pro-cedure for formation of phosphocholine lipid (section 2.5.2.6). Lipid **GMGTPC-CH1** (0.25 g, 75%) was obtained as a white gum after purification by column chromatography on silica gel using DCM/MeOH/H_2O (70:30:5) as the eluent.

Rf: 0.55 (DCM/MeOH/H_2O 70:30:5); ^{1}H NMR (500 MHz, MeOD-d_4/$CDCl_3$-d_1 1:1) δ 3.90-3.86 (m, 4H), 3.53 (t, *J* = 5.6 Hz, 4H), 3.32-3.20 (m, 12H), 3.13-3.06 (m, 6H), 2.04 (s, 18H), 1.37-1.32 (m, 4H), 1.25-1.12 (m, 10H), 1.02-0.69 (m, 89H), 0.52-0.48 (m, 30H), 0.43-0.35 (m, 2H), 0.15-0.08 (m, 1H); ^{13}C NMR (126 MHz, MeOD-d_4/$CDCl_3$-d_1 1:1) δ 77.8, 77.7, 77.6, 71.3, 70.2, 68.6, 68.4, 66.0, 64.7, 64.6, 58.6, 58.5, 53.5, 40.2, 39.0, 37.5, 37.4, 37.3, 37.2, 37.1, 37.0, 36.9, 36.8, 36.7, 33.1, 32.4, 29.6, 29.5, 29.4, 29.3, 29.2, 29.1, 27.5, 26.5, 26.0, 25.7, 24.4, 24.0, 23.9, 22.1, 22.0, 19.2, 19.1, 19.0, 18.9, 18.8; ^{31}P NMR (202 MHz, MeOD-d_4/$CDCl_3$-d_1 1:1) δ 0.15; ESI-MS: 1520.4 $[M+H]^+$; HRMS calcd 1520.3084 for $[C_{88}H_{181}N_2O_{12}P_2]^+$, found 1520.3093.

*2.5.6 Synthetic Procedure for **GMGTPC-CP2** and **GMGTPC-CH2***

((1R,3S)-3-(((tetrahydro-2H-pyran-2-yl)oxy)methyl)cyclohexyl)methanol (**2.42**)

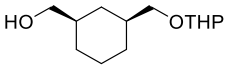

To a solution of 2.26 (5.8 g, 0.05 mol) in 255 mL of toluene, 14.6 mL of DHP and 8.9 g of Dowex 50WX2 resin was added and stirred at 30 °C for 5 hours. The resin was filtered, concentrated under reduce pressure and filtered through a plug of silica gel using hexane/EtOAc (4:1) as the eluent. THP protected **2.42** (5.3 g, 52%) was obtained as a colorless oil and used in the next step without purification.

triphenyl(((1S,3R)-3-(((tetrahydro-2H-pyran-2-yl)oxy)methyl)cyclopentyl)methyl) phosphonium iodide (**2.41**)

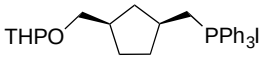

Compound **2.41** was synthesized following a reported protocol.[24]

iodotriphenyl(((1R,3S)-3-(((tetrahydro-2H-pyran-2-yl)oxy)methyl)cyclohexyl)methyl)-l5-phosphane **(2.43)**

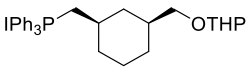

To a cold solution of triphenylphosphine (7.3 g, 27.9 mmol) and imidazole (1.9 g, 27.9 mmol) in DCM (54 mL), iodine (7.1 mg, 27.9 mmol) was added. After stirring of the mixture at room temperature in the dark for 10 min, a solution of compound **2.42** (5.3 g, 23.3 mmol) in DCM (14 mL) was added. The reaction

mixture was stirred for 2 hours at room temperature in the dark. The reaction mixture was washed with 10% $Na_2S_2O_3$ aqueous solution and extracted with DCM. The combined organic layers were washed with water, dried over Na_2SO_4, and purified by silica gel chromatography using DCM as the eluent. The resulting oil was carried out to the next step without further purification and characterization. To a solution of the purified crude in ACN (124 mL), triphenylphosphine (7.3 g, 27.9 mmol) was added. After stirring at reflux for two days, the reaction mixture was cooled down, evaporated and purified by column chromatography on silica gel using DCM/MeOH (100:0 to 98:2) as the eluent. Phosphonium salt **2.43** (5.1 g, 36%) was obtained as a yellow pale solid.

Rf: 0.46 (DCM/MeOH 95:5); ^{1}H NMR (500 MHz, $CDCl_3$-d_1) δ 7.86-7.64 (m, 15H), 4.40-4.34 (m, 1H), 3.91-3.63 (m, 2H), 3.50-3.32 (m, 3H), 3.04-3.2.92 (m, 1H), 1.77-1.37 (m, 16H; 2 extra H's from water at 1.6 ppm), 1.15-1.00 (m, 2H), 0.90-0.82 (m, 1H)

6-(benzyloxy)hexan-1-ol (**2.44**)

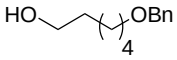

Compound **2.44** was synthesized following a reported protocol[49] and ^{1}H NMR data match previously reported data.[50]

6-(benzyloxy)hexanal (**2.45**)

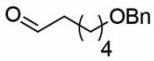

To a cold solution of **2.44** (2.15 g, 10.34 mmol) in dry DCM (100 mL), DMP (5.26 g, 12.40 mmol) was added portionwise. The resulting mixture was allowed to reach room temperature over 1 hour. After 3 more hours of stirring at room temperature, the mixture was diluted with DCM, washed successively with 1M NaOH solution, water and brine. The organic solution was dried over Na_2SO_4, concentrated under reduce pressure and purified by column chromatography on silica gel using hexane/EtOAc (95:5 to 90:10) as the eluent. Aldehyde **2.45** (1.77 g, 83%) was obtained as a colorless oil and ^{1}H NMR data match previously reported data.[51]

2-(((1S,3R)-3-((E)-7-(benzyloxy)hept-1-en-1-yl)cyclopentyl)methoxy)tetrahydro-2H-pyran (**2.46**)

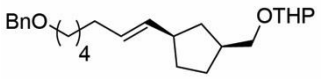

Compound **2.46** was synthesized by reaction of **2.45** (0.85 g, 4.14 mmol) and **2.41** (2.02 g, 3.45 mmol) according to the general procedure for Wittig olefination (see section 2.5.2.2). Olefin **2.46** (0.76 g, 57%) was obtained as a colorless oil after purification by column chromatography on silica gel using hexane/EtOAc (99:1 to 95:5) as the eluent.

Rf: 0.39 (hexane/EtOAc 95:5); ^{1}H NMR (500 MHz, $CDCl_3$-d_1) δ 7.34-7.25 (m, 5H), 5.39-5.24 (m, 2H), 4.58 (ddd, *J* = 1.9, 2.9, 4.2 Hz, 1H), 4.50 (s, 2H), 3.89-

3.84 (m, 1H), 3.65-3.60 (m, 1H), 3.51-3.45 (m, 3H), 3.31-3.26 (m, 1H), 2.79-2.71 (m, 0.8H), 2.45-2.42 (m, 0.2H), 2.28-2.20 (m, 1H), 2.08-2.89 (m, 3H), 1.86-1.67 (m, 4H), 1.65-1.23 (m, 12H), 1.03-0.90 (m, 1H); ^{13}C NMR (126 MHz, $CDCl_3$-d_1) δ 138.8, 135.2, 134.9, 128.8, 128.7, 128.5, 127.8, 127.6, 99.0, 73.0, 72.5, 72.4, 70.6, 62.4, 62.3, 43.7, 43.6, 39.7, 39.5, 38.5, 38.4, 38.4, 38.1, 37.9, 37.7, 32.9, 32.9, 32.6, 32.5, 30.9, 30.0, 29.9, 29.8, 29.6, 29.1, 29.0, 28.8, 27.6, 36.0, 25.9, 25.7, 19.8, 19.7; ESI-MS: 409.3 $[M+Na]^+$; HRMS calcd 409.2713 for $[C_{25}H_{38}O_3Na]^+$, found 409.2714.

2-(((1S,3R)-3-((E)-7-(benzyloxy)hept-1-en-1-yl)cyclohexyl)methoxy)tetrahydro-2H-pyran (**2.47**)

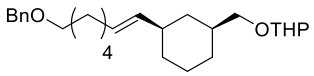

Compound **2.47** was synthesized by reaction of **2.45** (2.1 g, 10.1 mmol) and **2.43** (5.1 g, 8.5 mmol) according to the general procedure for Wittig olefination (see section 2.5.2.2). Olefin **2.47** (2.3 g, 68%) was obtained as a colorless oil after purification by column chromatography on silica gel using hexane/EtOAc (99:1 to 95:5) as the eluent.

Rf: 0.55 (hexane/EtOAc 95:5); ^{1}H NMR (500 MHz, $CDCl_3$-d_1) δ 7.31-7.24 (m, 5H), 5.31-5.11 (m, 2H), 4.53-4.52 (m, 1H), 4.48 (s, 2H), 3.85-3.79 (m, 1H), 3.53-3.42 (m, 4H), 3.18-3.12 (m, 1H), 2.31-2.22 (m, 1H), 2.05-1.97 (m, 2H), 1.94-

1.45 (m, 16.4H extra protons from water at 1.6 ppm), 1.38-1.22 (m, 4.3H), 1.01-0.69 (m, 2.5H)

((1S,3R)-3-((E)-7-(benzyloxy)hept-1-en-1-yl)cyclopentyl)methanol (**2.48**)

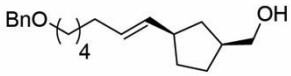

To a solution of **2.46** (740 mg, 1.92 mmol) in MeOH (32 mL), p-toluenesulfonic acid (18 mg, 0.3 mmol) was added. The solution was stirred 2 hours at room temperature, concentrated and purified by column chromatography on silica gel using hexane/EtOAc (9:1 to 8:2) as the eluent. Alcohol **2.48** (477 mg, 83%) was obtained as a colorless oil.

Rf: 0.41 (hexane/EtOAc 8:2); ^{1}H NMR (500 MHz, $CDCl_3$-d_1) δ 7.34-7.25 (m, 5H), 5.31-5.24 (m, 2H), 4.49 (s, 2H), 3,51-3.44 (m, 4H), 2.79-2.71 (m, 0.8H), 2.47-2.39 (m, 0.2H), 2.19-2.13 (m, 1H), 2.06-1.95 (m, 2H), 1.94-1.87 (m, 1H), 1.79-1.59 (m, 5H), 1.44-1.22 (m, 6H), 0.98-0.88 (m, 1H); ^{13}C NMR (126 MHz, $CDCl_3$-d_1) δ 138.8, 134.9, 134.7, 129.0, 128.8, 128.5, 127.8, 127.6, 73.0, 70.6, 67.7, 67.6, 43.6, 42.2, 42.0, 38.5, 37.6, 37.1, 32.9, 32.6, 32.4, 29.9, 29.8, 29.8, 29.5, 28.4, 28.2, 27.6, 26.0, 25.8; ESI-MS: 303.2 $[M+H]^+$; HRMS calcd 325.2138 for $[C_{20}H_{30}O_2Na]^+$, found 325.2137.

((1S,3R)-3-((E)-7-(benzyloxy)hept-1-en-1-yl)cyclohexyl)methanol (**2.49**)

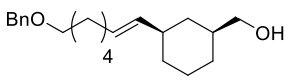

To a solution of **2.47** (2.3 g, 5.7 mmol) in MeOH (98 mL), p-toluenesulfonic acid (54 mg, 0.3 mmol) was added. The solution was stirred for 2 hours at room temperature, concentrated, washed with 40 mL of 1M NaOH three times, 40 mL of water, 40 mL of brine solution, dried over $MgSO_4$, then concentrated under vacuum. Alcohol **2.49** (2.0 g, Qt.) was obtained as a colorless oil. The crude product was used without further purification and used in the next step.

(((1S,3R)-3-((E)-7-(benzyloxy)hept-1-en-1-yl)cyclopentyl)methyl)triphenyl-phosphonium iodide (**2.50**)

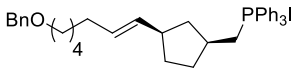

To a cold solution of triphenylphosphine (476 mg, 1.82 mmol) and imidazole (218 mg, 3.20 mmol) in DCM (11 mL), iodine (539 mg, 2.13 mmol) was added. After stirring of the mixture at room temperature in the dark for 10 min, a solution of compound **2.48** (460 mg, 1.52 mmol) in DCM (11 mL) was added. The reaction mixture was stirred for 2 hours at room temperature in the dark. The reaction mixture was washed with 10% $Na_2S_2O_3$ aqueous solution and extracted with DCM. The combined organic layers were washed with water, dried over Na_2SO_4, and purified by silica gel chromatography using DCM as the eluent. The resulting oil was carried out to the next step without further purification and characterization. To a solution of the purified crude in ACN (70

mL), triphenylphosphine (476 mg, 1.82 mmol) was added. After stirring at reflux for two days, the reaction mixture was cooled down, evaporated and purified by column chromatography on silica gel using DCM/MeOH (100:0 to 98:2) as the eluent. Phosphonium salt **2.50** (427 mg, 42%) was obtained as a yellow pale solid.

Rf: 0.46 (DCM/MeOH 95:5); ^{1}H NMR (500 MHz, $CDCl_3$-d_1) δ 7.79-7.62 (m, 15H), 7.25-7.17 (m, 5H), 5.20-5.13 (m, 2H), 4.40 (s, 2H), 3.77-3.64 (m, 2H), 3.38-3.35 (m, 2H), 2.57-2.49 (m, 0.8H), 2.24-2.13 (m, 1.2H), 1.91-1.80 (m, 2H), 1.74-1.66 (m, 1H), 1.62-1.13 (m, 11H); ^{13}C NMR (126 MHz, $CDCl_3$-d_1) δ 138.6, 138.5, 135.1, 133.8, 133.7, 133.6, 132.0, 132.0, 130.6, 130.5, 129.2, 129.1, 128.5 (*J*C-P = 12.5 Hz), 128.3, 127.6, 127.4, 118.4 (*J*C-P= 86.0 Hz), 72.8, 70.3, 42.8, 42.5, 42.4, 42.2, 42.1, 37.5, 34.5, 24.5, 34.3, 33.2, 33.1, 32.3, 32.0, 31.5, 29.6, 29.2, 29.1, 28.7, 27.3, 25.6, 25.6; ESI-MS: 547.4 $[M+H]^+$.

(1S,3R)-3-((E)-7-(benzyloxy)hept-1-en-1-yl)cyclohexane-1-carbaldehyde

(**2.51**)

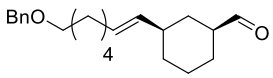

Alcohol **2.49** (2.0 g, 6.2 mmol) was dissolved in DCM (57 mL) then DMP reagent (3.1 g, 7.4 mmol) and mixed for 2 hours at 0 °C, followed by another 2 hours of mixing at room temperature. The solution was washed with 50 mL of 10 % sodium thiosulfate, 50 mL of 1 M NaOH, 50 mL of brine and purified by column

chromatography on silica gel using Hexane/EtOAc (95:5 to 4:1) as the eluent. Aldehyde **2.51** (1.2g, 62%) was obtained as a light yellow oil.

Rf: 0.38 (Hexane/EtOAc 95:5); ^{1}H NMR (400 MHz, $CDCl_3$-d_1) δ 9.57 (s, 1H), 7.34-7.25 (m, 5H), 5.29-5.26 (m, 1H), 5.18-5.14 (m, 1H), 4.48 (s, 2H), 3.44 (t, *J* = 6.6 Hz, 2H), 2.34-2.23 (m, 2H), 2.04-2.00 (m, 2H), 1.98-1.91 (m, 2H), 1.87-1.83 (m, 2H), 1.64-1.57 (m, 3H), 1.38-1.32 (m, 5.8H more protons may be attributed to grease), 1.19 -1.11 (m, 1H), 1.05-0.98 (m, 2H); ESI-MS: 337.2 $[M+Na]^+$.

adipaldehyde (**2.52**)

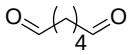

Dialdehyde **2.52** was synthesized following a reported protocol.[52]

1,6-bis(iodotriphenyl-l5-phosphaneyl)hexane (**2.53**)

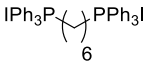

To a cold solution of triphenylphosphine (14.7 g, 55.9 mmol) and imidazole (3.8 g, 55.9 mmol) in DCM (134 mL), iodine (14.2 g, 55.9 mmol) was added. After stirring of the mixture at room temperature in the dark for 10 min, a solution of compound 1,6-hexanediol (3 g, 25.4 mmol) in DCM (134 mL) was added. The reaction mixture was stirred for 2 hours at room temperature in the dark. The reaction mixture was washed with 10% $Na_2S_2O_3$ aqueous solution and

extracted with DCM. The combined organic layers were washed with water, dried over Na_2SO_4, and purified by silica gel chromatography using DCM as the eluent. The resulting oil was carried out to the next step without further purification and characterization. To a solution of the purified crude in benzene (100 mL), triphenylphosphine (20 g, 76.2 mmol) was added. After stirring at reflux for 16 hours, the reaction mixture was cooled down, solids were collected by filtration. Diphosphonium salt **2.53** (16.4 g, 75%) was obtained as a yellow pale solid.

^{1}H NMR (400 MHz, $CDCl_3$-d_1) δ 7.76-7.51 (m, 30H), 3.54-3.47 (m, 4H), 1.75-1.67 (m, 4H), 1.60-1.52 (m, 4H); ^{13}C NMR (100 MHz, $CDCl_3$-d_1) δ 135.0, 134.9, 113.6 (*J*C-P = 10.0 Hz), 130.5 (*J*C-P = 12.5 Hz), 118.3, 117.4, 29.0 (*J*C-P = 17.0 Hz), 22.8, 22.3, 22.2, 22.1. ESI-MS: 304.4 $[M]^{2+}$.

(1E,7E)-1-((1R,3S)-3-((E)-7-(benzyloxy)hept-1-en-1-yl)cyclopentyl)-8-((1S,3R)-3-((E)-7-(benzyloxy)hept-1-en-1-yl)cyclopentyl)octa-1,7-diene (**2.54**)

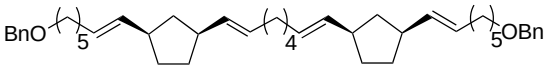

Compound **2.54** was synthesized by reaction of **2.50** (2.71 g, 4.02 mmol) and **2.52** (0.21 g, 1.83 mmol) according to the general procedure for Wittig olefination (see section 2.5.2.2). Olefin **2.54** (0.61 g, 51%) was obtained as a colorless oil after purification by column chromatography on silica gel using hexane/EtOAc (98:2) as the eluent. This product represents a possible mixture

of isotactic and syndiotactic isomers. For simplicity, only the isotactic isomer is shown in Figure 1 and throughout the supporting information.

Rf: 0.28 (hexane/EtOAc 98:2); ^{1}H NMR (500 MHz, $CDCl_3$-d_1) δ 7.34-7.25 (m, 10H), 5.36-5.26 (m, 8H), 4.48 (s, 4H), 3.44 (t, *J* = 6.9 Hz, 4H), 2.82-2.73 (m, 3H), 2.47-2.41 (m, 0.8H), 2.30-2.27 (m, 0.2H), 2.01-1.92 (m, 7H), 1.88-1.74 (m, 6H), 1.65-1.55 (m, 5H), 1.41-1.30 (m, 16H), 1.05-0.91 (m, 2H); ^{13}C NMR (126 MHz, $CDCl_3$-d_1) δ 138.8, 135.5, 135.4, 135.4, 135.3, 135.1, 135.0, 134.0, 133.8, 128.9, 128.7, 128.6, 128.6, 128.5, 127.8, 127.6, 73.0, 70.6, 43.7, 43.4, 42.3, 41.9, 38.4, 38.1, 33.0, 32.8, 32.6, 32.6, 32.5, 32.3, 29.9, 29.8, 29.8, 29.7, 29.6, 29.3, 27.6, 27.6, 26.0, 25.9.

(1E,7E)-1-((1R,3S)-3-((E)-7-(benzyloxy)hept-1-en-1-yl)cyclohexyl)-8-((1S,3R)-3-((E)-7-(benzyloxy)hept-1-en-1-yl)cyclohexyl)octa-1,7-diene (**2.55**)

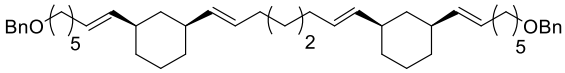

Compound **2.55** was synthesized by a reaction of **2.53** (1.3 g, 1.6 mmol) and **2.51** (1.1 g, 3.4 mmol) according to the general procedure for Wittig olefination (see section 2.5.2.2). Olefin **2.55** (0.89 g, 84%) was obtained as a colorless oil after purification by column chromatography on silica gel using hexane/EtOAc (98:2) as the eluent. This product represents a possible mixture of isotactic and syndiotactic isomers. For simplicity, only the isotactic isomer is shown.

Rf: 0.56 (hexane/EtOAc 98:2); ^{1}H NMR (500 MHz, $CDCl_3$-d_1) δ 7.36-7.28 (m, 10H), 5.38-5.17 (m, 8H), 4.52 (s, 4H), 3.49 (t, *J* = 6.6 Hz, 4H), 2.39-2.30 (m, 3H), 2.09-1.96 (m, 8.6H), 1.79-1.55 (m, 12.4H), 1.43-1.34 (m, 14H), 1.04-0.86 (m, 6H); ^{13}C NMR (126 MHz, $CDCl_3$-d_1) δ138.8, 136.3, 136.3, 136.0 135.9, 135.9, 135.8, 128.3, 128.2, 128.2, 128.1, 127.8, 127.8, 127.6, 73.0, 73.0, 70.5, 40.5, 40.0, 39.9, 36.3, 36.1, 33.0, 32.9, 32.8, 32.7, 32.7, 30.0, 29.9, 29.8, 29.7, 29.7, 29.6, 29.6, 29.4, 27.6, 27.5, 26.0, 25.9, 25.8. ESI-MS: 696.5 $[M + NH_4]^+$; HRMS calcd 701.5268 for $[C_{48}H_{70}O_2\ Na]^+$, found 701.5270.

1-((1R,3S)-3-(heptyl-7-ol)cyclopentyl)-8-((1S,3R)-3-(heptyl-7-ol)cyclopentyl) octane (**2.56**)

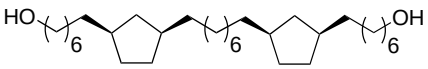

To a degassed solution of olefin **2.54** (0.85 g, 1.31 mmol) in EtOH (76 mL), 10% Pd/C (0.21 g, 25% w/w) was added. The reaction was stirred under 1 atm H_2 at room temperature for 24 hours. The solution was then filtered through celite, and the solvent was evaporated. Diol **2.56** (0.45 g, 72%) was obtained as a white solid.

^{1}H NMR (500 MHz, MeOD-d_4/$CDCl_3$-d_1 9:1) δ 3.34 (t, *J* = 6.9 Hz, 4H), 1.71-1.66 (m, 2H), 1.56-1.47 (m, 8H), 1.35-1.29 (m, 4H), 1.14-0,98 (m, 40H), 0.96-0.80 (m, 6H), 0.43-0.37 (m, 2H); ^{13}C NMR (126 MHz, MeOD-d_4/$CDCl_3$-d_1 9:1) δ 62.2, 40.6, 40.0, 38.6, 38.6, 32.9, 32.4, 31.5, 29.8, 29.6, 29.4, 28.6, 28.5, 25.6.

7,7'-((1R,1'R,3S,3'S)-octane-1,8-diylbis(cyclohexane-3,1-diyl))bis(heptan-1-ol) (**2.57**)

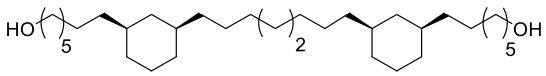

To a degassed solution of olefin **2.55** (0.89 g, 1.3 mmol) in EtOH (25.4 mL) and EtOAc (3.2 mL), 10% Pd/C (0.22 g, 25% w/w) was added. The reaction was stirred under 1 atm H_2 at room temperature for 24 hours. The solution was then filtered through celite, and the solvent was evaporated. Diol **2.57** (0.40 g, 60%) was obtained as a white solid. The crude solid was not further purified and used in the next step.

1-((1R,3S)-3-(7-bromoheptyl)cyclopentyl)-8-((1S,3R)-3-(7-bromoheptyl) cyclopentyl)octane (**2.58**)

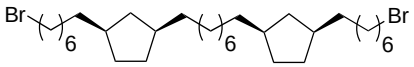

Dibromo alkane **2.58** (0.47 g, 83%) was obtained as a white solid from diol **2.56** (0.45 g, 0.94 mmol) following the general procedure for bromination of diol using hydrobromic acid solution (see section 2.5.2.3).

Rf: 0.75 (hexane); ^{1}H NMR (500 MHz, $CDCl_3$-d_1) δ 3.38 (t, *J* = 6.9 Hz, 4H), 1.90-1.66 (m, 13H), 1.42-1.00 (m, 40H), 0.87-0.83 (m, 1H), 0.63-0.56 (m, 2H); ^{13}C NMR (126 MHz, $CDCl_3$-d_1) δ 40.9, 40.3, 40.3, 39.0, 38.9, 36.9, 36.8, 34.3, 33.2, 33.0, 31.8, 30.2, 29.9, 29.0, 29.0, 28.9, 28.8, 28.7, 28.4.

1,8-bis((1S,3R)-3-(7-bromoheptyl)cyclohexyl)octane (**2.59**)

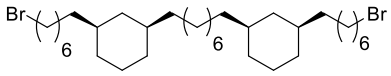

Dibromo alkane **2.59** (0.45 g, 90%) was obtained as a white solid from diol **2.57** (0.40 g, 0.79 mmol) following the general procedure for bromination of diol using hydrobromic acid solution (see section 2.5.2.3).

Rf: 0.89 (DCM/hexane 1:1); ^{1}H NMR (500 MHz, $CDCl_3$-d_1) δ 3.39 (t, *J* = 6.9 Hz, 4H), 1.86-1.80 (m, 4H), 1.70-1.63 (m, 7.6H), 1.50-1.46 (m, 0.4H), 1.41-1.37 (m, 4H), 1.30-1.10 (m, 38H), 0.78-0.69 (m, 4H), 0.50-0.43 (m, 2H); ^{13}C NMR (126 MHz, $CDCl_3$-d_1) δ 40.7, 38.0, 34.3, 33.7, 33.1, 30.3, 30.0, 30.0, 29.0, 28.4, 27.1, 27.0, 26.6.

1-((1R,3S)-3-(7-(3-(benzyloxy)-2-((3,7,11,15-tetramethylhexadecyl)oxy)propoxy) heptyl)cyclopentyl)-8-((1S,3R)-3-(7-(3-(benzyloxy)-2-((3,7,11,15-tetramethyl-hexadecyl)oxy)propoxy)heptyl)cyclopentyl)octane (**2.60**)

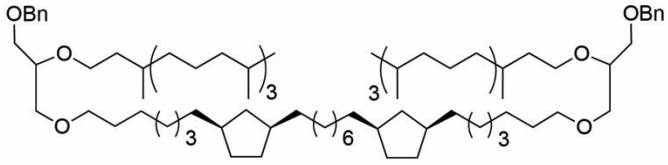

Compound **2.60** was synthesized by reaction of **2.4** (1.10 g, 2.35 mmol) and **2.58** (0.47 g, 0.78 mmol) according to the general procedure for formation of tetraether lipid scaffold by S_N2 reaction (see section 2.5.2.4). Product **2.60** (0.32

g, 30%) was obtained as a colorless oil after purification by column chromatography on silica gel using hexane/EtOAc (99:1 to 95:5) as the eluent.

Rf: 0.50 (hexane/EtOAc 95:5); ^{1}H NMR (500 MHz, $CDCl_3$-d_1) δ 7.32-7.25 (m, 10H), 4.53 (s, 4H), 3.63-3.92 (m, 18H), 1.88-1.85 (m, 2H), 1.76-1.66 (m, 6H), 1.62-1.47 (m, 10H), 1.37-1.01 (m, 84H), 0.85-0.81 (m, 30H), 0.73-0.56 (m, 2H); ^{13}C NMR (126 MHz, $CDCl_3$-d_1) δ 138.6, 128.5, 127.8, 127.7, 78.1, 73.6, 71.9, 70.9, 70.5, 69.1, 40.9, 40.3, 39.6, 39.0, 37.7, 37.7, 37.6, 37.6, 37.5, 37.4, 37.3, 37.0, 36.9, 33.3, 33.0, 31.8, 30.2, 30.1, 30.0, 30.0, 29.9, 29.8, 29.0, 28.9, 28.2, 26.4, 25.0, 24.7, 24.6, 23.0, 22.9, 20.0, 19.9, 19.8.

1-((1R,3S)-3-(7-(3-(benzyloxy)-2-((3,7,11,15-tetramethylhexadecyl)oxy)propoxy)heptyl)cyclohexyl)-8-((1S,3R)-3-(7-(3-(benzyloxy)-2-((3,7,11,15-tetramethylhexadecyl)oxy)propoxy)heptyl)cyclohexyl)octane (**2.61**)

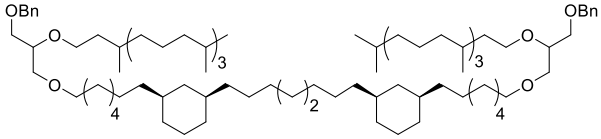

Compound **2.61** was synthesized by reaction of **2.4** (0.98 g, 2.12 mmol) and **2.59** (0.45 g, 0.71 mmol) according to the general procedure for formation of tetraether lipid scaffold by S_N2 reaction (see section 2.5.2.4). Product **2.61** (0.130 g, 13%) was obtained as a colorless oil after purification by column chromatography on silica gel using hexane/EtOAc (99:1 to 95:5) as the eluent.

Rf: 0.33 (hexane/EtOAc 95:5); ^{1}H NMR (500 MHz, $CDCl_3$-d_1) δ 7.32-7.24 (m, 10H), 4.54 (s, 4H), 3.62-3.40 (m, 18H), 1.71-1.59 (m, 10H), 1.55-1.48 (m, 8H), 1.38-1.02 (m, 84H), 0.86-0.82 (m, 30H), 0.78-0.70 (m, 4.2H), 0.51-0.44 (m, 1.8H); ^{13}C NMR (126 MHz, $CDCl_3$-d_1) δ 138.6, 128.5, 127.8, 127.7, 78.1, 73.6, 71.9, 71.0, 70.5, 69.1, 40.8, 39.6, 38.0, 38.0, 37.9, 37.7, 37.7, 37.6, 37.6, 37.5, 37.4, 37.3, 33.6, 33.0, 30.3, 30.2, 30.0, 30.0, 29.9, 29.8, 28.2, 27.1, 27.1, 26.6, 26.4, 25.0, 24.7, 24.7, 24.6, 22.9, 22.8, 20.0, 19.9, 19.8 ESI-MS: 1413.8 [M + NH_4]$^{+}$; HRMS calcd 1418.2890 for [$C_{94}H_{170}O_6$ Na]$^{+}$, found 1418.2907.

3-((7-((1R,3S)-3-(8-((1R,3S)-3-(7-(3-hydroxy-2-((3,7,11,15-tetramethylhexadecyl) oxy)propoxy)heptyl)cyclopentyl)octyl)cyclopentyl)heptyl)oxy)-2-((3,7,11,15-tetramethylhexadecyl)oxy)propan-1-ol (**2.62**)

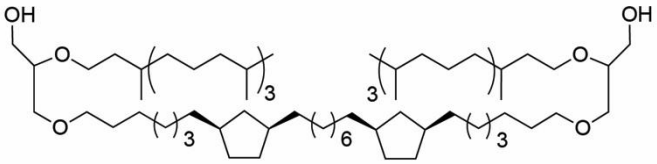

Compound **2.62** was synthesized by hydrogenation of **2.60** (0.22 g, 0.16 mmol) according to the general procedure for debenzylation of lipid scaffold by hydrogenation (see section 2.5.2.5). Diol **2.62** (0.18 g, 95%) was obtained as a colorless oil after purification by column chromatography on silica gel using hexane/EtOAc (95:5 to 85:15) as the eluent.

Rf: 0.41 (hexane/EtOAc 80:20); ^{1}H NMR (500 MHz, $CDCl_3$-d_1) δ 3.71-3.40 (m, 18H), 1.90-1.85 (m, 2H), 1.74-1.47 (m, 20H), 1.38-1.01 (m, 82H), 0.86-0.81 (m, 30H), 0.63-0.56 (m, 1H); ^{13}C NMR (126 MHz, $CDCl_3$-d_1) δ 78.5, 72.1, 71.1, 68.9, 40.9, 40.3, 39.6, 39.0, 37.7, 37.7, 37.6, 37.5, 37.4, 37.3, 37.0, 36.9, 33.2, 33.0, 31.9, 30.2, 30.1, 30.0, 30.0, 29.9, 29.7, 29.0, 28.9, 28.8, 28.2, 26.3, 25.0, 24.7, 24.6, 23.0, 22.9, 20.0, 19.9, 19.8; ESI-MS: 1187.8 $[M+H]^+$.

3-((7-((1R,3S)-3-(8-((1R,3S)-3-(7-(3-hydroxy-2-((3,7,11,15-tetramethylhexadecyl)oxy)propoxy)heptyl)cyclohexyl)octyl)cyclohexyl)heptyl)oxy)-2-((3,7,11,15-tetramethylhexadecyl)oxy)propan-1-ol (**2.63**)

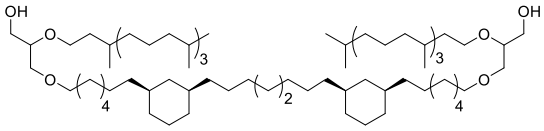

Compound **2.63** was synthesized by hydrogenation of **2.61** (0.130 g, 0.09 mmol) according to the general procedure for debenzylation of lipid scaffold by hydrogenation (see section 2.5.2.5). Diol **2.63** (0.10 g, 88%) was obtained as a colorless oil after purification by column chromatography on silica gel using hexane/EtOAc (95:5 to 85:15) as the eluent.

Rf: 0.40 (hexane/EtOAc 80:20); ^{1}H NMR (500 MHz, $CDCl_3$-d_1) δ 3.64-3.35 (m, 18H), 2.20-2.15 (m, 1.8H), 1.74-0.89 (m, 102.2H), 0.81-0.64 (m, 34H), 0.42-0.40 (m, 2H); ^{13}C NMR (126 MHz, $CDCl_3$-d_1) δ 78.5, 72.0, 71.1, 71.1, 68.8, 63.3, 63.3, 40.7, 39.6, 38.0, 37.9, 37.7, 37.6, 37.6, 37.5, 37.5, 37.3, 37.3, 33.6, 33.0, 33.0, 30.3, 30.2, 30.0, 29.9, 29.8, 29.7, 28.2, 27.1, 27.0, 26.6, 26.3, 25.0, 24.7,

24.5, 22.9, 22.8, 19.9, 19.9, 19.8; ESI-MS: 1217.1 $[M+H]^+$; HRMS calcd 1238.1951 for $[C_{80}H_{158}O_6\,Na]^+$, found 1238.1950.

3-((7-((1S,3R)-3-(8-((1S,3R)-3-(7-(3-((oxido(2-(trimethylammonio)ethoxy) phosphoryl)oxy)-2-((3,7,11,15-tetramethylhexadecyl)oxy)propoxy)heptyl) cyclopentyl)octyl)cyclopentyl)heptyl)oxy)-2-((3,7,11,15-tetramethylhexadecyl)oxy) propyl-(2-(trimethylammonio)ethyl) phosphate (**GMGTPC-CP2**)

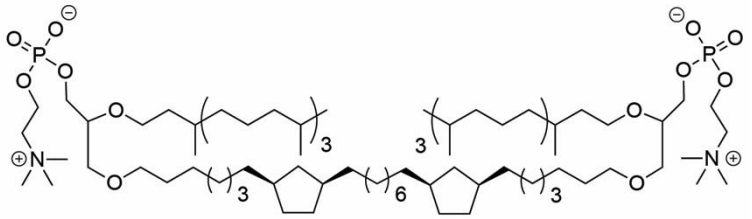

Lipid **GMGTPC-CP2** was synthesized from diol **2.62** (0.17 g, 0.14 mmol) following the general procedure for formation of phosphocholine lipid (see section 2.5.2.6). Lipid **GMGTPC-CP2** (0.15 g, 82%) was obtained as a white gum after purification by column chromatography on silica gel using DCM/MeOH/H_2O (70:30:5) as the eluent.

Rf: 0.50 (DCM/MeOH/H_2O 70:30:5); ^{1}H NMR (500 MHz, MeOD-d_4/$CDCl_3$-d_1 1:1) δ 3.90-3.87 (m, 4H), 3.53 (t, *J* = 5.5 Hz, 4H), 3.32-3.06 (m, 18H), 2.86 (s, 18H), 1.58-1.34 (m, 10H), 1.28-1.13 (m, 10H), 1.03-0.70 (m, 82H), 0.53-0.48 (m 30H), 0.30-0.24 (m, 2H); ^{13}C NMR (126 MHz, MeOD-d_4/$CDCl_3$-d_1 1:1) δ 77.8, 77.7, 77.6, 77.6, 71.3, 70.2, 68.6, 68.4, 66.0, 64.7, 64.6, 58.6, 58.5, 53.5, 40.3,

39.8, 39.0, 38.4, 38.3, 37.3, 37.1, 37.0, 37.0, 36.9, 36.8, 36.7, 36.4, 36.3, 32.6, 32.4, 31.2, 29.5, 29.4, 29.3, 29.2, 29.1, 28.3, 27.5, 25.7, 24.4, 24.0, 24.0, 22.1, 22.0, 19.1, 19.1, 19.0, 19.0, 18.9; ^{31}P NMR (202 MHz, MeOD-d_4/$CDCl_3$-d_1 1:1) δ 0.20; ESI-MS: 1518.2 $[M+H]^+$; HRMS calcd 1518.2928 for $[C_{88}H_{179}N_2O_{12}P_2]^+$, found 1518.2923.

3-((7-((1S,3R)-3-(8-((1S,3R)-3-(7-(3-((oxido(2-(trimethylammonio)ethoxy)phosphoryl)oxy)-2-((3,7,11,15-tetramethylhexadecyl)oxy)propoxy)heptyl)cyclohexyl)octyl)cyclohexyl)heptyl)oxy)-2-((3,7,11,15-tetramethylhexadecyl)oxy)propyl (2-(trimethylammonio)ethyl) phosphate (**GMGTPC-CH2**)

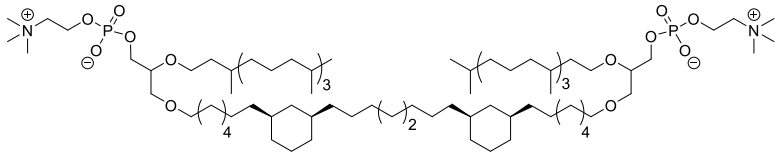

Lipid **GMGTPC-CH2** was synthesized from diol **2.63** (0.10 g, 0.08 mmol) following the general procedure for formation of phosphocholine lipid (see section 2.5.2.6). Lipid **GMGTPC-CH2** (0.10 g, 77%) was obtained as a white gum after purification by column chromatography on silica gel using DCM/MeOH/H_2O (70:30:5) as the eluent.

Rf: 0.12 (DCM/MeOH/H_2O 70:30:5); ^{1}H NMR (400 MHz, MeOD-d_4/$CDCl_3$-d_1 1:1) δ 3.93-3.84 (m, 4H), 3.52 (t, *J* = 5.6 Hz, 4H), 3.30-3.06 (m, 18H), 2.84 (s, 18H), 1.39-1.11 (m, 19H), 1.06-0.64 (m, 86H), 0.56-0.07 (m, 34H); ^{13}C NMR

(100 MHz, MeOD-d_4/$CDCl_3$-d_1 1:1) δ 71.3, 70.2, 68.6, 68.3, 66.0, 64.6, 64.6, 59.4, 58.5, 58.5, 53.5, 42.8, 40.2, 38.9, 37.3, 37.2, 37.0, 36.9, 36.8, 36.7, 36.7, 33.0, 32.3, 29.6, 29.5, 29.3, 29.2, 29.2, 29.1, 27.5, 26.5, 25.9, 25.7, 24.3, 24.0, 24.0, 22.0, 21.9, 19.1, 19.1, 19.0, 19.0, 18.9; ^{31}P NMR (161 MHz, MeOD-d_4/$CDCl_3$-d_1 1:1) δ 0.20; ESI-MS: 1546.2 $[M+H]^+$; HRMS calcd 1546.3241 for $[C_{90}H_{183}N_2O_{12}P_2]^+$, found 1546.3235.

*2.5.7 Synthetic Procedure for **GMGTPC-CP3***

((pent-4-en-1-yloxy)methyl)benzene (**2.64**)

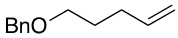

Compound **2.64** was synthesized following a reported protocol.[53]

4-(benzyloxy)butanal (**2.65**)

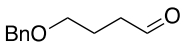

To a solution of **2.64** (6.63 g, 37.6 mmol) in DCM (300 mL) at -78 °C ozone was bubbled until the solution turned blue. Then, oxygen was bubbled for 10 min and triphenylphosphine (10.8 g, 41.4 mmol) was added portionwise at -78 °C. The reaction mixture was allowed to warm up slowly to room temperature and stirred overnight. The solvent was removed under reduced pressure and the resulting solid was purified by column chromatography on silica gel using

hexane/EtOAc (90:10 to 80:20) as the eluent. Aldehyde **2.65** (5.85 g, 88%) was obtained as a colorless oil and ^{1}H NMR data match previously reported data.[54]

(1R,3S)-1,3-bis((E)-5-(benzyloxy)pent-1-en-1-yl)cyclopentane (**2.66**)

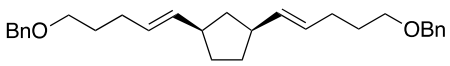

Compound **2.66** was synthesized by reaction of **2.27** (13.1 g, 14.9 mmol) and **2.65** (5.9 g, 32.9 mmol) according to the general procedure for Wittig olefination (see section 2.5.2.2). Olefin **2.66** (2.8 g, 45%) was obtained as a colorless oil after purification by column chromatography on silica gel using hexane/EtOAc (98:2) as the eluent.

Rf: 0.45 (hexane/EtOAc 95:5); ^{1}H NMR (500 MHz, $CDCl_3$-d_1) δ 7.36-7.28 (m, 10H); 5.41-5.29 (m, 4H); 4.52 (s, 4H); 3.51-3.48 (m, 4H), 2.86-2.77 (m, 1.7H), 2.50-2.45 (m, 0.3H); 2.19-2.08 (m, 4H), 1.93-1.78 (m, 3H), 1.73-1.67 (m, 4H), 1.41-1.34 (m, 2H), 1.08-0.99 (m, 1H); ^{13}C NMR (126 MHz, $CDCl_3$-d_1) δ 138.8, 136.0, 135.9, 135.7, 135.5, 128.5, 127.9, 127.8, 127.6, 73.1, 73.0, 70.0, 69.9, 43.6, 43.4, 42.2, 41.8, 38.4, 38.1, 32.9, 32.8, 32.4, 32.3, 30.1, 29.8, 29.2, 24.3.

5,5'-((1R,3S)-cyclopentane-1,3-diyl)bis(pentan-1-ol) (**2.67**)

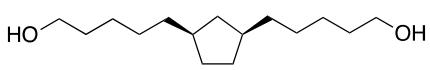

To a degassed solution of **2.66** (2.75 g, 6.58 mmol) in EtOH/THF (9:1) (75 mL), 10% Pd/C (0.69 g, 25% w/w) was added. The reaction was stirred under 1 atm

H_2 at room temperature for 16 hours. The solution was then filtered through celite, and the solvent was evaporated. Diol **2.67** (0.83 g, 52%) was obtained as a white solid after purification by column chromatography on silica gel using hexane/EtOAc (75:25 to 50:50) as the eluent.

Rf: 0.42 (hexane/EtOAc 1:1); ^{1}H NMR (500 MHz, $CDCl_3$-d_1) δ 3.49 (t, *J* = 6.9 Hz, 4H), 3.23 (brs, 2H), 1.84-1.79 (m, 1H), 1.73-1.61 (m, 4H), 1.48-1.42 (m, 4H), 1.25-1.04 (m, 14.2H), 0.57-0.51 (m, 0.8H); ^{13}C NMR (126 MHz, $CDCl_3$-d_1) δ 62.6, 40.1, 38.8, 36.8, 36.7, 33.0, 32.7, 31.6, 28.6, 28.5, 26.1; ESI-MS: 265.1 $[M+Na]^+$; HRMS calcd 265.2138 for $[C_{15}H_{30}O_2Na]^+$, found 265.2141.

(((1R,3S)-cyclopentane-1,3-diyl)bis(pentane-5,1-diyl))bis(triphenylphosphonium) iodide (**2.68**)

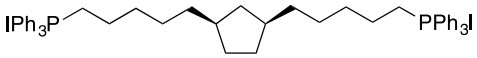

To a cold solution of triphenylphosphine (1.98 g, 7.55 mmol) and imidazole (0.52 g, 7.55 mmol) in DCM (18 mL), iodine (1.92 g, 7.55 mmol) was added. After stirring of the mixture at room temperature in the dark for 10 min, a solution of compound **2.67** (0.83 g, 3.43 mmol) in DCM (18 mL) was added. The reaction mixture was stirred for 2 hours at room temperature in the dark. The reaction mixture was washed with 10% $Na_2S_2O_3$ aqueous solution and extracted with DCM. The combined organic layers were washed with water, dried over Na_2SO_4, and purified by silica gel chromatography using a mixture of hexane/EtOAc (8:2) as eluent. The resulting oil was carried out to the next step without further

purification and characterization. To a solution of the purified crude in benzene (15 mL), triphenylphosphine (2.70 g, 10.29 mmol) was added. After stirring at reflux for 16 hours, the reaction mixture was cooled down, evaporated and purified by column chromatography on silica gel using DCM/MeOH (1:0 to 9:1) as the eluent. diphosphonium salt **2.68** (3.19 g, 94%) was obtained as a white solid.

^{1}H NMR (500 MHz, $CDCl_3$-d_1) δ 7.74-.61 (m, 30H), 3.48-3.42 (m, 4H), 1.76-1.71 (m, 1H), 1.57-1.50 (m, 12H), 1.16-0.85 (10.2H), 0.43-0.37 (m, 0.8H); ^{13}C NMR (126 MHz, $CDCl_3$-d_1) δ 135.2, 133.6 (d, *JC-P* = 10.0 Hz), 130.6 (d, *JC-P* = 12.5 Hz), 117.9 (d, *JC-P* = 85.7 Hz), 53.6, 40.2, 39.7, 38.3, 38.2, 36.0, 32.8, 31.5, 30.6, 30.5, 28.0, 23.2, 22.8, 22.5, 22.5; ESI-MS: 366.3 $[M\text{-}2I]^{2+}$; HRMS calcd 366.2001 for $[C_{51}H_{58}P_2]^{2+}$, found 366.2003.

((but-3-en-1-yloxy)methyl)benzene (**2.69**)

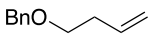

Compound **2.69** was synthesized following a reported protocol.[55]

3-(benzyloxy)propanal (**2.70**)

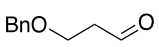

Compound **2.70** was synthesized following a reported protocol.[56]

2-(((1S,3R)-3-((E)-4-(benzyloxy)but-1-en-1-yl)cyclopentyl)methoxy)tetrahydro-2H-pyran (**2.71**)

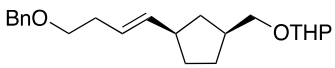

Compound **2.71** was synthesized by reaction of **2.41** (4.41 g, 7.52 mmol) and **2.70** (1.45 g, 9.02 mmol) according to the general procedure for Wittig olefination (see section 2.1). Olefin **2.71** (1.10 g, 43%) was obtained as a colorless oil after purification by column chromatography on silica gel using hexane/EtOAc (98:2 to 95:5) as the eluent.

Rf: 0.33 (hexane/EtOAc 95:5); ^{1}H NMR (500 MHz, $CDCl_3$-d_1) δ 7.32-7.24 (m, 5H), 5.49-5.30 (m, 2H), 4.57 (dd, *J* = 2.9, 4.2 Hz, 1H), 4.50 (s, 2H), 3.87-3.83 (m, 1H), 3.63-3.59 (m, 1H), 3.49-3.44 (m, 3H), 3.29-3.24 (m, 1H), 2.79-2.71 (m, 0.8H), 2.44-2.22 (m, 3.3H); 1.98-1.90 (m, 1H), 1.84-1.66 (m, 4H), 1.59-1.40 (m, 5H), 1.34-1.24 (m, 1H), 1.00-0.89 (m, 1H); ^{13}C NMR (126 MHz, $CDCl_3$-d_1) δ 138.7, 138.6, 137.1, 136.9, 128.4, 127.7, 127.6, 124.7, 124.4, 98.9, 72.9, 72.9, 72.4, 72.3, 72.2, 70.4, 70.3, 62.3, 62.2, 43.7, 43.6, 41.7, 39.7, 39.4, 38.6, 38.5, 38.2, 38.0, 37.7, 37.5, 33.1, 32.8, 32.8, 32.3, 30.8, 29.0, 28.9, 28.7, 28.4, 25.6, 19.7, 19.6.

((1S,3R)-3-((E)-4-(benzyloxy)but-1-en-1-yl)cyclopentyl)methanol (**2.72**)

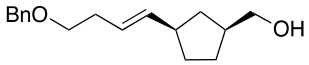

To a solution of **2.71** (1.10 g, 3.20 mmol) in a mixture of MeOH (150 mL) and THF (30 mL), p-toluenesulfonic acid (30 mg, 0.16 mmol) was added and the solution was stirred for 16 hours at room temperature. Then, the solvent was evaporated and the resulting residue was dissolved in EtOAc. The organic solution was washed successively with 1M NaOH solution, water, brine and dried over Na_2SO_4 to yield the alcohol **2.72** (0.84 g, Qt.) as a colorless oil.

^{1}H NMR (500 MHz, $CDCl_3$-d_1) δ 7.33-7.24 (m, 5H), 5.49-5.30 (m, 2H), 4.50 (s, 2H), 3.48-3.44 (m, 4H), 2.80-2.71 (m, 0.8H), 2.40-2.28 (M, 3.3H), 2.17-2.10 (m, 1H), 1.93-1.88 (m, 1H), 1.78-1.69 (m, 2H), 1.44-1.23 (m, 2H), 0.96-0.88 (m, 1H); ^{13}C NMR (126 MHz, $CDCl_3$-d_1) δ 138.5, 138.4, 136.9, 136.7, 128.4, 127.7, 127.6, 124.7, 124.5, 72.9, 72.8, 70.3, 70.2, 67.3, 67.2, 43.5, 42.1, 41.9, 38.5, 37.5, 36.9, 33.0, 32.7, 32.2, 28.4, 28.3, 28.2; ESI-MS: 283.1 $[M+Na]^+$; HRMS calcd 283.1669 for $[C_{17}H_{24}O_2Na]^+$, found 283.1668.

(1S,3R)-3-((E)-4-(benzyloxy)but-1-en-1-yl)cyclopentane-1-carbaldehyde (**2.73**)

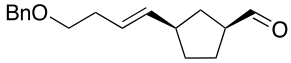

To a cold solution of **2.72** (0.84 g, 3.23 mmol) in dry DCM (30 mL), DMP (1.64 g, 3.88 mmol) was added portionwise. The resulting mixture was allowed to reach room temperature over 1 hour. After 3 more hours of stirring at room

temperature, the mixture was diluted with DCM, washed successively with 1M NaOH solution, water and brine. The organic solution was dried over Na_2SO_4, concentrated under reduce pressure and purified by column chromatography on silica gel using hexane/EtOAc (90:10 to 75:25) as the eluent. Aldehyde **2.73** (0.59 g, 70%) was obtained as a colorless oil.

Rf: 0.63 (hexane/EtOAc 75:25); ^{1}H NMR (500 MHz, $CDCl_3$-d_1) δ 9.64 (d, *J* = 2.5 Hz, 1H), 7.34-7.30 (m, 5H), 5.52-5.38 (m, 2H), 4.55 (s, 2H), 3.54-3.50 (m, 2H), 2.92-2.80 (m, 1.8H), 2.60-2.33 (m, 2.2H), 2.07-1.98 (m, 2H), 1.89-1.90 (m, 2H), 1.63-1.51 (m, 1H), 1.38-1.27 (m, 1H); ^{13}C NMR (126 MHz, $CDCl_3$-d_1) δ 203.6, 203.4, 138.6, 138.5, 135.3, 135.1, 128.4, 127.7, 127.6, 126.0, 125.7, 73.0, 72.9, 70.1, 70.0, 51.5, 51.3, 43.7, 38.7, 33.9, 33.8, 33.4, 33.1, 33.0, 32.7, 28.4, 25.9, 25.7; ESI-MS: 281.1 $[M+Na]^+$; HRMS calcd 281.1512 for $[C_{18}H_{22}O_2Na]^+$, found 281.1514.

(1S,3R)-1-((E)-6-((1R,3S)-3-((E)-4-(benzyloxy)but-1-en-1-yl)cyclopentyl)hex-5-en-1-yl)-3-((E)-6-((1S,3R)-3-((E)-4-(benzyloxy)but-1-en-1-yl)cyclopentyl)hex-5-en-1-yl)cyclopentane (**2.74**)

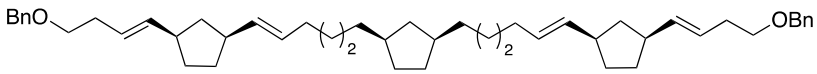

Compound **2.74** was synthesized by reaction of **2.68** (2.41 g, 2.44 mmol) and **2.73** (1.40 g, 5.43 mmol) according to the general procedure for Wittig olefination (see section 2.5.2.2). Olefin **2.74** (0.80 g, 43%) was obtained as a colorless oil after purification by column chromatography on silica gel using

hexane/EtOAc (98:2) as the eluent. This product represents a possible mixture of isotactic and syndiotactic isomers. For simplicity, only the isotactic isomer is shown.

Rf: 0.32 (hexane/EtOAc 95:5); ^{1}H NMR (500 MHz, $CDCl_3$-d_1) δ 7.33-7.25 (m, 10H), 5.49-5.23 (m, 8H), 4.51 (s, 4H), 3.48-3.44 (m, 4H), 2.82-2.75 (m, 3H), 2.50-2.28 (m, 5H), 2.02-1.70 (m, 15H), 1.38-1.24 (m, 16H), 1.14-0.96 (m, 4.2H), 0.66-0.58 (m, 0.8H); ^{13}C NMR (126 MHz, $CDCl_3$-d_1) δ 138.7, 137.6, 137.4, 137.4, 137.2, 135.3, 135.1, 134.8, 129.0, 128.9, 128.9, 128.6, 127.8, 127.7, 124.6, 124.3, 124.2, 73.1, 73.0, 70.5, 70.4, 43.7, 43.7, 42.3, 41.9, 41.8, 40.9, 40.3, 40.3, 39.0, 38.6, 38.5, 38.4, 38.3, 38.2, 36.9, 36.8, 36.7, 33.2, 33.0, 32.9, 32.8, 32.8, 32.5, 32.4, 31.8, 30.4, 30.1, 28.6, 28.5, 28.4, 27.7.

4-((1R,3S)-3-(6-((1R,3S)-3-(6-((1R,3S)-3-(4-hydroxybutyl)cyclopentyl)hexyl) cyclopentyl)hexyl)cyclopentyl)butan-1-ol (**2.75**)

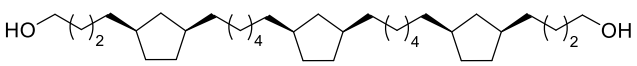

To a degassed solution of olefin **2.74** (0.77 g, 1.16 mmol) in EtOH/THF (8:2) (45 mL), 10% Pd/C (0.28 g, 25% w/w) was added. The reaction was stirred under 1 atm H_2 at room temperature for 24 hours. The solution was then filtered through celite, and the solvent was evaporated to yield a white solid which was used in the next step without further purification and characterization.

((1S,3R)-1-(6-((1R,3S)-3-(4-bromobutyl)cyclopentyl)hexyl)-3-(6-((1S,3R)-3-(4-bromobutyl)cyclopentyl)hexyl)cyclopentane (**2.76**)

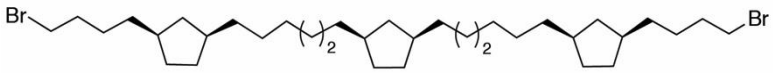

Dibromo alkane **2.76** (0.38 g, 67%) was obtained as a white solid from diol **2.75** (0.46 g, 0.89 mmol) following the general procedure for bromination of diol using hydrobromic acid solution (see section 2.5.2.3). The purification was accomplished by column chromatography on silica gel using hexane/DCM (1:1) as the eluent.

Rf: 0.86 (hexane/DCM); ^{1}H NMR (500 MHz, $CDCl_3$-d_1) δ 3.38 (dd, *J* = 6.6, 6.9 Hz, 4H), 1.90-1.67 (m, 19H), 1.43-1.02 (m, 40H), 0.87-0.59 (m, 3H); ^{13}C NMR (126 MHz, $CDCl_3$-d_1) δ 40.9, 40.8, 40.3, 40.1, 39.0, 38.9, 38.7, 37.0, 37.0, 36.9, 36.0, 35.9, 34.2, 33.3, 33.2, 31.8, 31.8, 31.7, 30.2, 28.9, 28.9, 27.5, 27.4.

(1*S*,3*R*)-1-(6-((1*R*,3*S*)-3-(4-(3-(benzyloxy)-2-((3,7,11,15-tetramethylhexadecyl)oxy)propoxy)butyl)cyclopentyl)hexyl)-3-(6-((1*S*,3*R*)-3-(4-(3-(benzyloxy)-2-((3,7,11,15-tetramethylhexadecyl)oxy)propoxy)butyl)cyclopentyl)hexyl) cyclopentane (**2.77**)

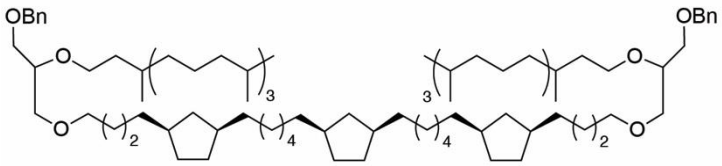

Compound **2.77** was synthesized by reaction of **2.4** (0.85 g, 1.84 mmol) and **2.76** (0.38 g, 0.60 mmol) according to the general procedure for formation of

tetraether lipid scaffold by S_N2 reaction (see section 2.5.2.4). Compound **2.77** (0.24 g, 29%) was obtained as a colorless oil after purification by column chromatography on silica gel using hexane/EtOAc (98:2 to 95:5) as eluent.

Rf: 0.29 (hexane/EtOAc 95:5); ^{1}H NMR (500 MHz, $CDCl_3$-d_1) δ 7.32-7.25 (m, 10H), 4.55 (s, 4H), 3.63-3.40 (m, 18H), 1.91-1.68 (m, 15H), 1.65-1.49 (m, 10H), 1.39-1.03 (m, 80H), 0.87-0.83 (m, 30H), 0.75-0.59 (m, 3H); ^{13}C NMR (126 MHz, $CDCl_3$-d_1) δ 138.6, 128.5, 127.8, 127.7, 78.1, 73.5, 71.9, 71.0, 70.5, 69.1, 40.9, 40.9, 40.3, 40.3, 39.6, 39.0, 38.9, 37.7, 37.7, 37.6, 37.6, 37.5, 37.4, 37.3, 37.0, 36.9, 36.8, 36.7, 33.2, 32.0, 31.8, 31.8, 30.2, 30.1, 30.0, 29.0, 28.9, 28.2, 25.4, 25.4, 25.0, 24.7, 24.6, 22.9, 22.8, 20.0, 19.9, 19.8; ESI-MS: 1408.9 $[M-H]^-$.

3-(4-((1R,3S)-3-(6-((1R,3S)-3-(6-((1R,3S)-3-(4-(3-hydroxy-2-((3,7,11,15-tetra methylhexadecyl)oxy)propoxy)butyl)cyclopentyl)hexyl)cyclopentyl)hexyl)cyclop entyl)butoxy)-2-((3,7,11,15-tetramethylhexadecyl)oxy)propan-1-ol (**2.78**)

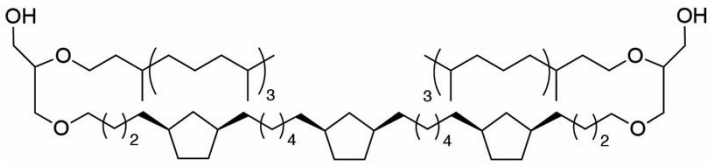

Compound **2.78** was synthesized by hydrogen-ation of **2.77** (0.24 g, 0.17 mmol) according to the general procedure for debenzylation of lipid scaffold by hydrogenation (see section 2.5.2.5). Diol **2.78** (0.18 g, 87%) was obtained as a colorless oil after purification by column chromatography on silica gel using hexane/EtOAc (9:1 to 8:2) as the eluent.

Rf: 0.38 (hexane/EtOAc); ^{1}H NMR (500 MHz, $CDCl_3$-d_1) δ 3.70-3.39 (m, 18H), 2.24 (brs, 2H), 1.90-1.47 (m, 25H), 1.37-1.00 (m, 80H), 0.85-0.81 (m, 30H), 0.72-0.58 (m, 3H); ^{13}C NMR (126 MHz, $CDCl_3$-d_1) δ 78.5, 72.0, 71.1, 68.8, 40.9, 40.8, 40.3, 40.2, 39.6, 39.0, 38.9, 37.7, 37.6, 37.6, 37.5, 37.5, 37.3, 37.3, 37.0, 36.9, 36.9, 36.7, 36.6, 33.2, 33.2, 33.0, 31.8, 31.8, 30.2, 30.1, 30.0, 28.9, 28.9, 28.2, 25.4, 25.3, 25.0, 24.7, 24.6, 22.9, 22.8, 20.0, 19.9, 19.8; ESI-MS: 1226.6 $[M-H]^-$.

3-(4-((1S,3R)-3-(6-((1S,3R)-3-(6-((1S,3R)-3-(4-(3-((oxido(2-(trimethylammonio) ethoxy)phosphoryl)oxy)-2-((3,7,11,15-tetramethylhexadecyl)oxy)propoxy)butyl) cyclopentyl)hexyl)cyclopentyl)hexyl)cyclopentyl)butoxy)-2-((3,7,11,15-tetramethylhexadecyl)oxy)propyl (2-(trimethylammonio)ethyl) phosphate (**GMGTPC-CP3**)

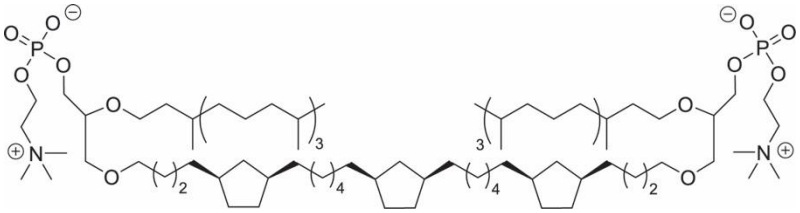

Lipid **GMGTPC-CP3** was synthesized from diol **2.78** (0.18 g, 0.14 mmol) following the general procedure for formation of phosphocholine lipid (see section 2.5.2.6). Lipid **GMGTPC-CP3** (0.20 g, 90%) was obtained as a white gum after purification by column chromatography on silica gel using DCM/MeOH/H_2O (70:30:5) as the eluent.

Rf: 0.59 (DCM/MeOH/H_2O 70:30:5); ^1H NMR (500 MHz, MeOD-d_4/$CDCl_3$-d_1 1:1) δ 3.91-3.86 (m, 4H), 3.53 (t, *J* = 5.4 Hz, 4H), 3.29-3.07 (m, 18H), 2.85 (m, 18H), 1.56-1.31 (m, 15H), 1.28-1.12 (m, 10H), 1.02-0.69 (m, 80H), 0.52-0.45 (m, 30H), 0.38-0.24 (m, 3H); ^{13}C NMR (126 MHz, MeOD-d_4/$CDCl_3$-d_1 1:1) δ 77.8, 77.7, 77.6, 77.5, 71.3, 70.2, 68.6, 68.4, 66.0, 66.0, 64.7, 58.6, 58.6, 53.5, 48.8, 39.8, 39.7, 39.0, 38.4, 38.3, 37.3, 37.1, 37.0, 37.0, 36.9, 36.8, 36.7, 36.4, 36.3, 36.2, 36.1, 32.6, 32.4, 31.2, 31.1, 29.5, 29.5, 29.4, 28.3, 28.2, 27.5, 24.8, 24.7, 24.4, 24.0, 24.0, 22.0, 21.9, 19.1, 19.0, 19.0, 18.9, 18.9; ^{31}P NMR (202 MHz, MeOD-d_4/$CDCl_3$-d_1 1:1) δ 0.16; ESI-MS: 1558.2 $[M-H]^-$; HRMS calcd 1558.3241 for $[C_{91}H_{183}N_2O_{12}P_2]^+$, found 1558.3241.

*2.5.8 Synthetic Procedure for **GMGT** Analogs with Varying Polar Lipid Headgroups*

5-(benzyloxy)-2-phenyl-1,3-dioxane (**2.79**)

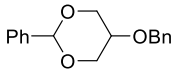

Compound **2.79** was prepared following a previously reported protocol.[57]

2,3-bis(benzyloxy)propan-1-ol (**2.80**)

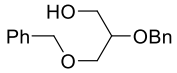

A solution of **2.79** (2.4 g, 1.3 mmol) in dry DCM was cooled to -78°C. DIBAL-H in DCM (1 M, 3.4 mL) was added dropwise to the cooled solution and reacted

for 16 h at rt. After the reaction was complete, a small amount of MeOH was used to quench the remaining DIBAL-H followed by the addition of aqueous NaOH (5 M, 15 mL). The solution was then extracted 3 times using diethylether (Et_2O) and then washed with water. The extracted organic layer was dried using anhydrous $MgSO_4$ and the solvent was removed using vacuum. The crude oil was purified over silica using hexane/EtOAc (4/6) as the eluent. Alcohol **2.80** (2.2 g, 96%) was obtained as a clear oil and NMR spectra matched previously reported data.[58]

1-(benzyloxy)-N,N,N',N'-tetraisopropylphosphanediamine (**2.81**)

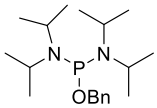

Compound **2.81** was synthesized following a previously reported protocol.[59]

benzyl (2,3-bis(benzyloxy)propyl) diisopropylphosphoramidite (**2.82**)

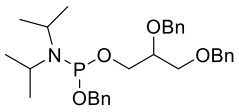

To a solution of **2.81** (0.9 g, 2.7 mmol) in 7 mL of degassed DCM, a solution of tetrazole (0.45 M in acetonitrile, 3 mL) was added dropwise. To the reaction mixture, a solution of **2.80** (0.4 g 1.4 mmol) in 7 mL of degassed DCM was added dropwise and reacted for 2 h at rt. The reaction was diluted with DCM and then washed with saturated aqueous $NaHCO_3$ solution, brine and then dried

over $MgSO_4$. The solvent was evaporated under vacuum and purified over silica using hexane/EtOAc/triethylamine (90:10:3) as the mobile phase. Phospharamidite **2.82** was obtained (252 mg, 39%) as a clear oil.

^{1}H NMR (500 MHz, $CDCl_3$-d_1) δ 7.43-7.29 (m, 15H), 4.82-4.70 (m, 4H), 4.61-4.59 (m, 2H), 3.90-3.65 (m, 7H), 1.28-1.24 (m, 12H); ^{13}C NMR (126 MHz, $CDCl_3$-d_1) δ; 139.7 (dd, *J* = 7.2, 3.2 Hz), 138.9, 138.5, 128.5, 128.4, 128.4, 127.9, 127.8, 127.7, 127.6, 127.6, 127.4, 127.1, 78.1 (dd, *J* = 7.7, 4.0 Hz), 73.5, 72.4, 70.6, 65.4 (dd, *J* = 17.9, 2.9 Hz), 63.2 (dd, *J* = 15.7, 9.6 Hz), 43.1 (dd, *J* = 12.2, 1.6 Hz), 24.8 (*J* = 7.2, 5.1 Hz); ^{31}P NMR (126 MHz, $CDCl_3$-d_1) δ 148.38.

benzyl (2-hydroxyethyl)carbamate (**2.83**)

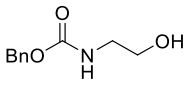

Compound **2.83** was prepared using a previously reported protocol.[60]

benzyl (2-(((benzyloxy)(diisopropylamino)phosphanyl)oxy)ethyl)carbamate (**2.84**)

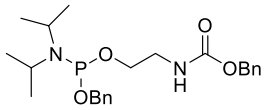

Compound **2.84** was prepared using previously reported protocol.[61]

tetrabenzyl((octacosane-1,28-diylbis(oxy))bis(2-((3,7,11,15-tetramethylhexadecyl)oxy)propane-3,1-diyl)) bis(phosphate) (**2.85**)

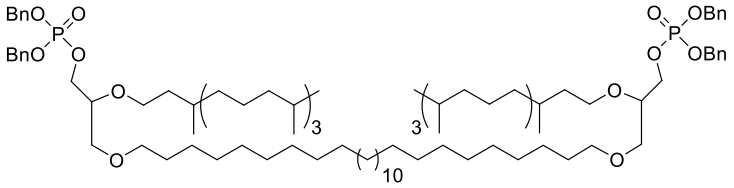

A solution of **2.23** (45 mg, 0.04 mmol) in 1 mL of degassed dichloromethane (DCM) and tetrazole (0.45 M in acetonitrile, 711 µL) was prepared. Then, a solution of dibenzyl-*N,N*-diisopropylphosphor-amidite (55 mg, 0.2 mmol) in 1 mL of degassed DCM was added dropwise and the reaction mixture was stirred at room temperature (rt) for 16 h. After the reaction was then cooled to -40°C, a tert-Butyl hydroperoxide solution (5-6 M in decane, 160 µL) was added and the reaction mixture was allowed to warm up to rt over 2 h. The solvent was evaporated over vacuum and the resulting residue was purified over silica using ethyl acetate/hexane (EtOAc/Hexane) (1/1) as the mobile phase. Benzylated lipid **2.85** was obtained as a clear oil (62 mg, 95%).

Rf = 0.81 (hexane/EtOAc 5:5); ^{1}H NMR (500 MHz, $CDCl_3$-d_1) δ 7.33-7.24 (m, 20H), 5.04-5.02 (m, 8H), 4.12-3.98 (m, 4H), 3.54-3.53 (m, 6H), 3.42-3.37 (m, 8H), 1.61-1.48 (m, 10H), 1.25-1.20 (m, 90H), 0.85-0.80 (m, 30H); ^{13}C NMR (126 MHz, $CDCl_3$-d_1) δ 135.9 (dd, *J* = 7.2, 2.5 Hz), 128.6, 128.5, 127.9, 71.8, 69.8, 69.3, 69.2, 69.1, 69.0, 67.1, 39.4, 37.6, 37.6, 37.5, 37.4, 37.3, 37.1, 37.0, 32.8, 29.9, 29.8, 29.7, 29.7, 29.6, 28.0, 26.1, 24.9, 24.5, 24.4, 22.8, 22.7, 19.8, 19.7,

19.7, 19.7, 19.6, 19.6; ^{31}P NMR (202 MHz, $CDCl_3$) δ 0.29; HRMS: 1678.2529 calcd for $[C_{102}H_{176}O_{12}P_2Na]^+$ found 1678.2554.

(**2.86**)

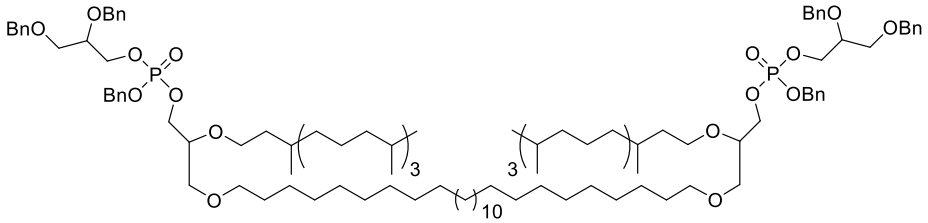

A solution of **2.23** (47 mg, 0.04 mmol) and tetrazole (0.45 M in acetonitrile, 800 µL) in 1.5 mL of degassed DCM was prepared. Then, a solution of **2.82** (84 mg, 0.17 mmol) in 1.5 mL of degassed DCM was added dropwise and the reaction mixture was stirred at rt for 16 h. After the reaction was then cooled to -40°C, a tert-Butyl hydroperoxide solution (5-6 M in decane, 169 µL) was added and the reaction mixture was allowed to warm up to rt over 2 h. The solvent was evaporated and purified over silica using EtOAc/hexane (1/1) as the mobile phase. Protected lipid **2.86** was obtained as a clear oil (75 mg, 91%).

Rf = 0.80 (hexane/EtOAc 5:5); ^{1}H NMR (500 MHz, $CDCl_3$-d_1) δ 7.34-7.25 (m, 30H), 5.04-5.03 (m, 4H), 4.66-4.59 (m,4H), 4.49 (d, *J* = 3.5 Hz, 4H), 4.22-4.17 (m, 2H), 4.14-4.07(m, 4H), 4.03-3.98 (m, 2H), 3.78-3.75 (m, 2H), 3.56-3.49 (m, 10H), 3.41-3.33 (m, 8H), 1.53-1.48 (m, 10H), 1.33-1.08 (m, 90H), 0.85-0.80 (m, 30H); ^{13}C NMR (126 MHz, $CDCl_3$-d_1) δ 138.3, 138.2, 136.1 (d, *J* = 7.2 Hz), 128.9, 128.7, 128.7, 128.6, 128.5, 128.1, 128.0, 127.9, 127.8, 73.6, 72.5, 72.0, 70.0,

69.4, 69.3, 69.2, 67.3, 67.1 (d, *J* = 7.2 Hz), 39.6, 37.8, 37.7, 37.6, 37.6, 37.5, 37.3, 37.2, 33.0, 30.0, 30.0, 29.9, 29.9, 29.8, 28.2, 26.3, 25.0, 24.7, 24.6, 23.0, 22.9, 20.0, 19.9, 19.9, 19.8, 19.8, 19.7; ^{31}P NMR (202 MHz, $CDCl_3$) δ -0.22; HRMS: 1984.4384 calcd for $[C_{122}H_{201}O_{16}P_2]^+$ found 1984.4389.

(**2.87**)

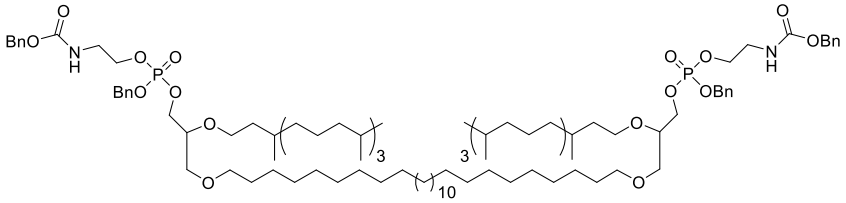

A solution of **2.23** (43 mg, 0.04 mmol) in 1 mL of degassed DCM and tetrazole (0.45 M in acetonitrile, 680 µL) was prepared. Then, a solution of **2.84** (65 mg, 0.15 mmol) in 1 mL of degassed DCM was added dropwise and the reaction mixture was stirred at rt for 16 h. After the reaction was then cooled to -40 °C, a tert-Butyl hydroperoxide solution (5-6 M in decane, 140 µL) was added and the reaction mixture was allowed to warm up to room temperature over 2 h. The solvent was evaporated and purified over silica using ethyl EtOAc/hexane (1/1) as the mobile phase. Compound **2.87** was obtained as a clear oil (54 mg, 78%).

Rf = 0.70 (hexane/EtOAc 25:75) ^{1}H NMR (500 MHz, $CDCl_3$-d_1) δ 7.35-7.31 (m, 20H), 5.07-5.04 (m, 8H), 4.15-3.98 (m, 8H), 3.56-3.33 (m, 18H), 1.56-1.45 (m, 10H), 1.34-1.03 (m, 90H), 0.85-0.81 (m, 30H); ^{13}C NMR (126 MHz, $CDCl_3$-d_1) δ 156.5, 136.6, 135.9 (dd, *J* = 6.5, 2.1 Hz), 128.8, 128.8, 128.7, 128.3, 128.2,

128.2, 128.2, 72.0, 69.6, 69.2, 69.1, 67.5, 67.4, 67.1, 67.1, 67.0, 66.9, 41.6, 41.5, 39.5, 37.8, 37.7, 37.6, 37.6, 37.5, 37.2, 37.1, 33.0, 30.0, 29.9, 29.8, 29.8, 29.7, 28.1, 26.3, 25.0, 24.7, 24.5, 22.9, 22.8, 19.9, 19.8, 19.7, 19.7; ESI-MS: 1852.99 $[M+Na]^+$; HRMS: 1852.3170 calcd for $[C_{108}H_{186}N_2O_{16}P_2Na]^+$ found 1852.3171.

(octacosane-1,28-diylbis(oxy))bis(2-((3,7,11,15-tetramethylhexadecyl)oxy)propane-3,1-diyl) bis(hydrogen phosphate) (**GMGTPA**)

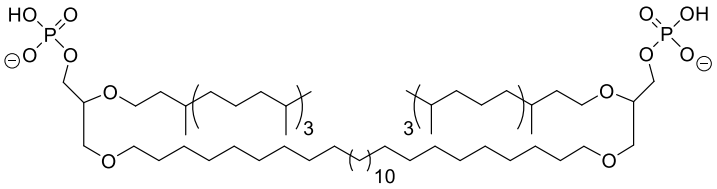

Benzylated lipid **2.85** (62 mg, 0.04 mmol) was dissolved in a degassed mixture of 3 mL of ethanol/tetrahydrofuran (EtOH/THF) (1:1) and 20% $Pd(OH)_2$ (10% w/w) was added. The reaction was stirred under hydrogen atmosphere (1 atm) at rt for 6 hours. The catalyst was removed by filtration through a pad of celite, and the resulting residue was purified by column chromatography on Sephadex LH 20 (DCM/MeOH 70:30). **GMGTPA** was obtained as a clear oil (29 mg, 60%).

^{1}H NMR (500 MHz, MeOD-d_4/$CDCl_3$-d_1 1:1) δ 3.94-3.92 (m, 4H), 3.67-3.56 (m, 8H), 3.49-3.30 (m, 6H), 1.65-1.47 (m, 10H), 1.35-1.04 (m, 90H), 0.87-0.82 (m, 30H); ^{13}C NMR (126 MHz, MeOD-d_4/$CDCl_3$-d_1 1:1) δ 72.5, 71.3, 69.8, 69.6, 65.7, 65.7, 40.1, 38.4, 38.2, 38.2, 38.1, 38.0, 37.8, 37.8, 33.5, 30.6, 30.4, 30.3,

28.7, 26.9, 25.6, 25.2, 25.1, 23.2, 23.1, 203, 20.2, 20.1, 20.1, 20.0; ^{31}P NMR (202 MHz, MeOD-d_4/$CDCl_3$-d_1 1:1) δ 1.18; ESI-MS: 1317.95 $[M+Na]^+$; HRMS: 1294.0686 calcd for $[C_{74}H_{151}O_{12}P_2]^-$ found 1294.0682.

(**GMGTPG**)

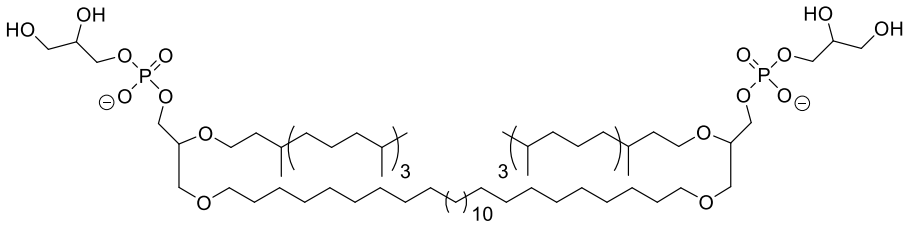

Benzylated lipid **2.86** (79 mg, 0.04 mmol) was dissolved in 3 mL of a degassed mixture of EtOH/THF (1:1) and 20% $Pd(OH)_2$ (10% w/w) was added. The reaction was stirred under hydrogen atmosphere (1 atm) at rt for 6 hours. The catalyst was removed by filtration through a pad of celite, and the resulting residue was purified by column chromatography on Sephadex LH 20 (DCM/MeOH 70:30). **GMGTPG** was obtained as a clear oil (44 mg, 77%).

^{1}H NMR (500 MHz, $CDCl_3$-d_1) δ 3.98-3.02 (m, 28H), 1.23-1.13 (m, 10H), 1.05-0.73 (m, 90H), 0.54-0.49 (m, 30H); ^{13}C NMR (126 MHz, $CDCl_3$-d_1) δ 71.4, 70.4, 70.3, 69.7, 68.8, 68.5, 67.3, 67.3, 65.7, 65.7, 62.0, 62.0, 61.5, 39.0, 37.2, 37.0, 37.0, 36.9, 36.7, 36.7, 32.4, 29.5, 29.3, 29.1, 27.6, 25.7, 24.4, 24.1, 24.0, 22.1, 22.0, 19.1, 19.1, 19.0, 18.9; ^{31}P NMR (202 MHz, MeOD-d_4/$CDCl_3$-d_1 1:1) δ 0.54; ESI-MS: 720.56 $[M-2H]^{2-}$; HRMS: 1442.1422 calcd for $[C_{80}H_{163}O_{16}P_2]^-$ found 1442.1428.

(**GMGTPE**)

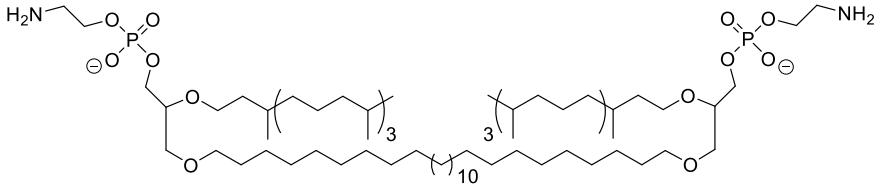

Benzylated lipid **2.87** (54 mg, 0.03 mmol) was dissolved in 6 mL of a degassed mixture of (EtOH)/THF (2:1) and 20% Pd/C (10% w/w) was added. The reaction was stirred under hydrogen atmosphere (1 atm) at rt for 6 hours. The catalyst was removed by filtration through a pad of celite, and the resulting residue was purified by column chromatography on Sephadex LH 20 (DCM/MeOH 70:30). **GMGTPE** was obtained as a clear oil (37 mg, 91%).

^{1}H NMR (500 MHz, MeOD-d_4/$CDCl_3$-d_1 1:1) δ 4.09-3.99 (m, 4H), 3.93-3.84 (m, 4H), 3.66-3.54 (m, 8H), 3.48-3.40 (m, 6H), 3.18-3.09 (m, 4H), 1.59-1.48 (m, 10H), 1.35-1.04 (m, 90H), 0.87-0.82 (m, 30H); ^{13}C NMR (126 MHz, MeOD-d_4/$CDCl_3$-d_1 1:1) δ 71.3, 70.1, 68.6, 68.4, 64.7, 64.7, 61.1, 61.1, 60.1, 60.1, 42.5, 40.1, 40.1, 39.0, 37.3, 37.1, 37.1, 37.0, 36.9, 36.8, 36.7, 36.7, 32.4, 29.6, 29.5, 29.4, 29.3, 29.1, 27.6, 25.7, 24.4, 24.1, 24.0, 22.1, 22.0, 19.1, 19.1, 19.0, 19.0, 18.9, 10.4; ^{31}P NMR (202 MHz, MeOD-d_4/$CDCl_3$-d_1 1:1) δ 1.10; ESI-MS: 1382.15 $[M+Na]^+$; HRMS: 1382.1676 calcd for $[C_{78}H_{163}N_2O_{12}P_2]^+$ found 1382.1673.

(1R,3s,5r,6R,7S,8s,9S)-2,4,10-trioxaadamantane-6,8,9-triol (**2.88**)

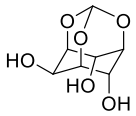

Compound **2.88** was synthesized as previously reported.[25]

(1r,3r,5R,6r,7S,8R,9S)-8,9-bis(benzyloxy)-2,4,10-trioxaadamantan-6-ol (**2.89**)

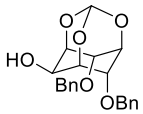

Compound **2.89** was synthesized as previously reported.[62]

benzyl ((1s,3s,5R,6s,7S,8R,9S)-8,9-bis(benzyloxy)-2,4,10-trioxaadamantan-6-yl) diisopropylphosphoramidite (**2.90**)

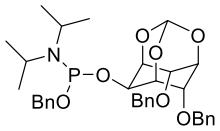

To a solution of **2.81** (1.26 g, 3.7 mmol) in 9.5 mL of degassed DCM, a solution of tetrazole (0.45 M in acetonitrile, 4.1 mL) was added dropwise. To the reaction mixture, a solution of **2.89** (0.69 g 1.9 mmol) in 9.5 mL of degassed DCM was added dropwise and reacted for 2 h at rt. The reaction was diluted with DCM and then washed with saturated aqueous $NaHCO_3$ solution, brine and then dried over $MgSO_4$. The solvent was evaporated under vacuum and purified over silica using hexane/EtOAc/triethylamine (90:10:3) as the mobile phase. Phospharamidite **2.90** was obtained (937 mg, 83%) as a clear oil.

Rf = 0.53 (hexane/EtOAc/TEA 80:20:3) ^{1}H NMR (500 MHz, $CDCl_3$-d_1) δ 7.32-7.20 (m, 20H should be 15H, but $CDCl_3$ peak adds integration), 5.51 (s, 1H), 4.78-4.67 (m, 2H), 4.63-4.60 (m, 1H), 4.57-4.50 (m, 4H), 4.44-4.42 (m, 1H), 4.36-4.35 (m, 1H), 4.33-4.31 (m, 2H), 4.28-4.26 (m, 1H), 3.72-3.64 (m, 2H), 1.15 (dd, *J* = 10.7, 6.8 Hz); ^{13}C NMR (126 MHz, $CDCl_3$-d_1) δ 139.1 (d, *J* = 7.3 Hz), 137.3, 127.9, 127.9, 127.3, 127.2, 127.1, 126.9, 126.7, 103.0, 73.9, 72.0 (d, *J* = 4.6 Hz), 71.7 (d, *J* = 4.6 Hz), 71.0, 67.7, 65.2 (d, *J* = 17.5 Hz), 62.0 (d, *J* = 16 Hz), 42.8 (d, *J* = 12.3 Hz), 24.3 (d, *J* = 7.3 Hz), 24.1 (d, *J* = 7.3 Hz); ^{31}P NMR (202 MHz, $CDCl_3$-d_1) δ 146.

2.91

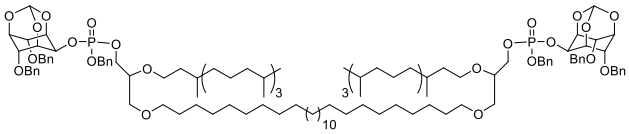

A solution of **2.23** (100 mg, 0.09 mmol) in 3 mL of degassed DCM and tetrazole (0.45 M in acetonitrile, 1600 µL) was prepared. Then, a solution of **2.90** (214 mg, 0.35 mmol) in 1 mL of degassed DCM was added dropwise and the reaction mixture was stirred at rt for 16 h. After the reaction was then cooled to -40 °C, a tert-Butyl hydroperoxide solution (5-6 M in decane, 356 µL) was added and the reaction mixture was allowed to warm up to room temperature over 2 h. The solvent was evaporated and purified over silica using EtOAc/hexane (1/1) as the mobile phase. Compound **2.91** was obtained as a clear oil (190 mg, 99%).

Rf = 0.72 (hexane/EtOAc 65:35); ^{1}H NMR (500 MHz, $CDCl_3$-d_1) δ 7.35-7.14 (m, 30H), 5.38 (s, 1.9H), 5.03-5.00 (m, 4H), 4.84-4.83 (m, 2H), 4.52-4.43 (m, 8H), 4.36-4.32 (m, 4H), 4.27-4.25 (m, 6H), 4.09-3.98 (m, 4H), 3.49-3.29 (m, 12H), 3.26-3.24 (m, 2H), 1.45-1.38 (m, 10H), 1.29-0.95 (m, 98H extra protons may be from grease), 0.76-0.72 (m, 30H); ^{13}C NMR (126 MHz, $CDCl_3$-d_1) δ 137.1, 135.3, 135.2, 128.5, 128.5, 128.3, 127.8, 127.7, 127.6, 102.9, 73.5, 71.6, 71.5, 70.7, 70.7, 70.6, 69.7, 69.7, 69.6, 69.4, 68.9, 68.8, 68.0, 68.0, 67.9, 67.6, 67.3, 67.2, 49.3, 39.2, 37.4, 37.3, 37.3, 37.2, 37.1, 36.8, 36.8, 32.6, 29.6, 29.5, 29.5, 29.4, 29.3, 27.8, 25.9, 24.6, 24.3, 24.2, 22.4, 22.3, 19.5, 19.4, 19.3, 19.3, 19.2; ^{31}P NMR (202 MHz, $CDCl_3$-d_1) δ -0.2; ESI-MS: 2203.42 $[M+Na]^+$; HRMS: 2202.4212 calcd for $[C_{130}H_{204}O_{22}P_2Na]^+$ found 2202.4196.

(1R,3s,5r,6R,7S,8s,9S)-6,8,9-tris(benzyloxy)-2,4,10-trioxaadamantane (**2.92**)

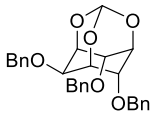

Compound **2.92** was prepared as previously reported.[26]

(1R,5S,6R,7s,8S,9s)-6,8,9-tris(benzyloxy)-2,4-dioxabicyclo[3.3.1]nonan-7-ol (**2.93**)

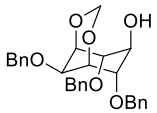

Compound **2.93** was prepared as previously reported.[26]

(1R,5S,6R,7s,8S,9s)-6,7,8,9-tetrakis(benzyloxy)-2,4-dioxabicyclo[3.3.1]nonane (**2.94**)

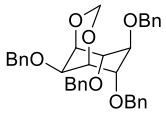

Compound **2.94** was prepared as previously reported.[26]

(1R,2r,3S,4R,5r,6S)-2,4,5,6-tetrakis(benzyloxy)cyclohexane-1,3-diol (**2.95**)

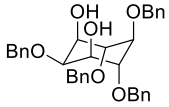

To a solution of **2.94** (2.5 g, 4.5 mmol) in MeOH (92 mL) concentrated HCl (8.3 mL) was added and heated at reflux for 3 hours. The solution was cooled to room temperature, MeOH was evaporated and purified over silica using EtOAc/hexane (6/4) as the mobile phase. Diol **2.95** was afforded (2.0 g, 83%) as a clear oil.

Rf = 0.67 (hexane/EtOAc 2:3) NMR spectrum agreed with previously published spectrum.[63]

(1S,2S,3R,4S,5S,6S)-2,3,4,5,6-pentakis(benzyloxy)cyclohexan-1-ol (**2.96**)

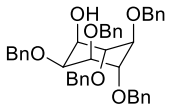

To a solution of **2.95** (2.0 g, 3.7 mmol) in 25 mL of THF, NaH (0.12 g, 5.2 mmol) was added at 0 °C and stirred for 1 hour. BnBr (0.430 mL, 3.7 mmol) was added

to the reaction mixture and stirred at room temperature overnight. THF was evaporated and then extracted with 40 mL of EtOAc three times, washed with brine, dried over MgSO4 and solvent was removed under vacuum. The crude liquid was purified over silica using EtOAc/hexane (1/4) as the mobile phase. Benzyl protected **2.96** (1.44 g, 62%) was obtained as a white powder.

Rf = 0.17 (hexane/EtOAc 1:4) NMR spectrum agreed with previously published spectrum.[64]

benzyl ((1S,2R,3R,4S,5S,6R)-2,3,4,5,6-pentakis(benzyloxy)cyclohexyl) diisopropylphosphoramidite (**2.97**)

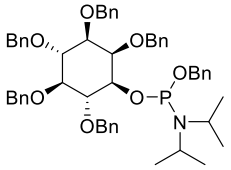

To a solution of **2.81** (1.35 g, 4.0 mmol) in 10.2 mL of degassed DCM, a solution of tetrazole (0.45 M in acetonitrile, 4.4 mL) was added dropwise. To the reaction mixture, a solution of **2.96** (0.91 g 1.4 mmol) in 10.2 mL of degassed DCM was added dropwise and reacted for 2 h at rt. The reaction was diluted with DCM and then washed with saturated aqueous $NaHCO_3$ solution, brine and then dried over $MgSO_4$. The solvent was evaporated under vacuum and purified over silica using hexane/EtOAc/triethylamine (90:10:3) as the mobile phase. Phospharamidite **2.97** was obtained (1.0 g, 58%) as a clear oil.

Rf = 0.63 (hexane/EtOAc/TEA 80:20:3) ^{1}H NMR (500 MHz, $CDCl_3$-d_1) δ 7.44-7.22 (m, 38.9H extra protons from $CDCl_3$), 4.97-4.53 (m, 12H), 4.44-4.43 (m, 1H), 4.15-4.07 (m, 2H), 3.77-3.64 (m, 3H), 3.50-3.31 (m, 2H), 1.19-1.11 (m, 12H)

(**2.98**)

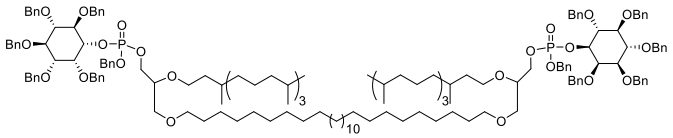

A solution of **2.23** (100 mg, 0.09 mmol) in 3 mL of degassed DCM and tetrazole (0.45 M in acetonitrile, 1600 µL) was prepared. Then, a solution of **2.97** (306 mg, 0.35 mmol) in 1 mL of degassed DCM was added dropwise and the reaction mixture was stirred at rt for 16 h. After the reaction was then cooled to -40 °C, a tert-Butyl hydroperoxide solution (5-6 M in decane, 352 µL) was added and the reaction mixture was allowed to warm up to room temperature over 2 h. The solvent was evaporated and purified over silica using EtOAc/hexane (1/1) as the mobile phase. Compound **2.98** was obtained as a clear oil (215 mg, 97%).

Rf = 0.72 (hexane/EtOAc 65:35) ^{1}H NMR (500 MHz, $CDCl_3$-d_1) δ 7.33-7.14 (m, 60.6H extra proton may be from $CDCl_3$), 5.00-4.53 (m, 24H), 4.33-3.90 (m, 12.8H extra proton may be from EtOAc), 3.48-3.23 (m, 18H), 1.56-1.41 (m, 10H), 1.33-0.97 (m, 98.1H extra protons can be from grease and EtOAc), 0.80-0.73 (m, 30H); ^{13}C NMR (126 MHz, $CDCl_3$-d_1) δ 139.0, 139.0, 138.8, 138.7, 138.7, 138.3, 136.1, 136.1, 136.0, 128.7, 128.6, 128.5, 128.5, 128.4, 128.3, 128.2,

128.1, 128.0, 127.9, 127.9, 127.8, 127.7, 127.6, 127.6, 127.5, 83.3, 81.5, 80.8, 80.7, 80.6, 80.3, 80.3, 80.2, 78.9, 78.8, 78.8, 76.7, 76.6, 76.2, 76.0, 75.7, 75.6, 75.3, 75.2, 72.9, 72.9, 72.9, 72.0, 71.9, 70.0, 69.9, 69.5, 69.5, 69.4, 69.3, 69.2, 69.1, 67.3, 67.3, 60.5, 39.5, 37.8, 37.7, 37.6, 37.6, 37.5, 37.3, 37.2, 33.0, 30.0, 29.9, 29.8, 29.7, 28.1, 26.3, 25.0, 24.7, 24.5, 22.9, 22.8, 21.2, 19.9, 19.9, 19.8, 19.7, 19.6, 14.4; HRMS: 2722.7342 calcd for $[C_{170}H_{244}O_{22}P_2Na]^+$ found 2722.7398.

(3R,4S,5R,6R)-6-(acetoxymethyl)-4-(((2S,3R,4S,5S,6R)-3,4,5-triacetoxy-6-(acetoxymethyl)tetrahydro-2H-pyran-2-yl)oxy)tetrahydro-2H-pyran-2,3,5-triyl triacetate (**2.99**)

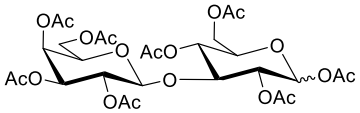

Molecule **2.99** was synthesized as previously reported.[65]

(2R,3S,4S,5R,6S)-2-(acetoxymethyl)-6-(((2R,3R,4S,5R,6S)-3,5-diacetoxy-2-(acetoxymethyl)-6-(ethylthio)tetrahydro-2H-pyran-4-yl)oxy)tetrahydro-2H-pyran-3,4,5-triyl triacetate (**2.100**)

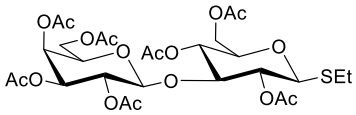

Molecule **2.100** was prepared as previously reported.[66]

(2S,3R,4S,5R,6R)-2-(((2R,3R,4S,5R,6R)-2-(3-((28-(3-(((2S,3S,4R,5S,6S)-3,5-dihydroxy-6-(hydroxymethyl)-4-(((2R,3S,4R,5S,6S)-3,4,5-trihydroxy-6-(hydroxymethyl)tetrahydro-2H-pyran-2-yl)oxy)tetrahydro-2H-pyran-2-yl)oxy)-2-((3,7,11,15-tetramethylhexadecyl)oxy)propoxy)octacosyl)oxy)-2-((3,7,11,15-tetramethylhexadecyl)oxy)propoxy)-3,5-dihydroxy-6-(hydroxymethyl)tetrahydro-2H-pyran-4-yl)oxy)-6-(hydroxymethyl)tetrahydro-2H-pyran-3,4,5-triol (**GMGTLa**)

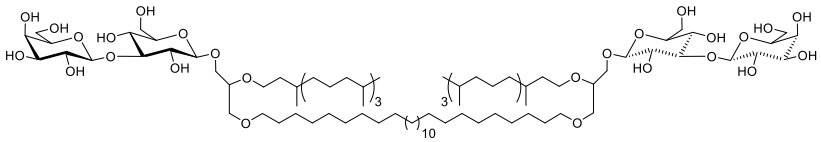

To a solution of 2.23 (80 mg, 0.07 mmol) in 13.8 mL of DCM, **2.100** (140 mg, 0.21 mmol) was added and cooled to 0 ºC. Next, N-iodosuccinimide (63 mg, 0.28 mmol) and triethylsilyltriflate (75 mg, 0.28 mmol) was added and stirred for 15 minutes at room temperature. Triethylamine (0.138 mL) was added to quench the reaction and the reaction mixture was washed with 10% (aq) NaS_2O_3, water, saturated NH_4Cl (aq), and dried over Na_2SO_4. The volatile solvent was removed via vacuum and purified using SiO_2 using EtOAc/hexane (2/3) as the mobile phase. The clear oil obtained was next dissolved in a solution mixture of dry MeOH (23 mL) and DCM (5 mL), then 0.5 M MeONa/MeOH (2.5 mL) was added and stirred for 2 hours at room temperature. To quench the reaction, 495 µL of AcOH (glacial) and 4.95 mL of MeOH were added to the reaction mixture. The volatile organic solvents were removed via vacuum and

the crude product was purified using Sephadex LH-20 (DCM/MeOH: 70/30) to obtain 24 mg of clear oil in 25% yield.

^{1}H NMR (500 MHz, MeOD-d_4/$CDCl_3$-d_1 1:1) δ 4.03-3.92 (m, 3H), 3.62-3.11 (m, 38H), 3.08-2.95 (m, 5H), 1.46-0.49 (m, 144H); ^{13}C NMR (126 MHz, MeOD-d_4/$CDCl_3$-d_1 1:1) δ 103.5, 103.0, 103.0, 95.4, 80.8, 79.6, 75.3, 74.7, 74.5, 73.2, 72.9, 71.4, 70.9, 70.0, 68.7, 68.6, 68.3, 61.0, 60.7, 39.0, 37.0, 37.0, 36.9, 36.6, 32.4, 29.3, 29.1, 27.6, 25.7, 24.4, 24.0, 24.0, 22.0, 21.9, 19.1, 19.1, 19.0, 18.9

2.5.9 General Procedure for Liposome Formation

10 mg/mL liposome solution was prepared by first dissolving 5 mg of lipid of interest into a 5 mL round bottom flask in a DCM/MeOH (7/3) solution. A thin lipid film was achieved by evaporating the solvent using a rotary evaporator (BUCHI RE111) then dried further over a hi-vacuum pump (Welch 1402) for 4 hrs. The thin lipid film was then hydrated, in a 4 mM Carboxyfluorescein (CF) solution prepared in buffer A, by vortexing the solution for 30 seconds followed by sonication in a water bath sonicator (Branson 2510) for 30 mins. After sonication, the lipid mixture underwent 5 freeze thaw cycles that consisted of 2 mins at -78°C followed by 2 mins at 50°C. The lipid solution was then extruded (Avanti mini-extruder) through 200 nm polycarbonate membrane 25 times followed by another extrusion with a 100 nm polycarbonate membrane 51 times.

The lipid solution was then stored at 4°C in Protein Lo-Bind Eppendorf tube. Liposome radius is shown in Figure S8 below.

2.5.10 General Procedure to Measure pH Equilibrium of CF

In order to obtain the fast rate of pH induced decrease of CF for EggPC, a stopped-flow assay was necessary. Before each assay, 10 µL of the stock extruded lipid solution was diluted in 500 µL of Bis-Tris buffer pH 7.2. Free CF was removed using a PD miniTrap^{TM} G-25 Sephadex^{TM} column from GE Healthcare ending 100 times dilution from the stock extruded solution (0.1 mg/mL). The reaction cell was cleaned using Bis-Tris buffer pH 7.2 (15 drives) until a steady signal was obtained before running any experiments. After a steady fluorescence signal was achieved and free CF was removed from the liposome solution, 25 µl of the lipid solution was mixed with 225 µL of Bis-Tris buffer pH 7.2 to obtain the relative maximum fluorescence at pH 7.2 (5 acquisitions). The reaction cell was again cleaned until a steady signal was observed and repeated with Bis-Tris buffer pH 5.8 (5 acquisitions). To confirm 100% change of fluorescence at pH 5.8 from the assay, the relative fluorescence at 1000 seconds was confirmed by comparison to the relative fluorescence of liposomes in Bis-Tris buffer pH 5.8 doped with 1 µL of a solution of Nigericin in Ethanol (100 µM) using the plate reader.

To obtain the pH equilibration observed rate of each lipid, the decrease in fluorescence of CF was followed using Perkin Elmer Enspire© multimode plate reader. Before each assay, 10 µL of the stock extruded lipid solution was diluted in 500 µL of buffer A. Free CF was removed using a PD miniTrap™ G-25 Sephadex™ column from GE Healthcare ending in 100 times dilution from the stock extruded solution (0.1 mg/mL). 45 µL of purified liposome solution was next added into three 0.5 mL Protein Lo-Bind tubes for each lipid solution. In one tube, 405 µL of Bis-Tris buffer pH 7.2 was added. In the second tube, 405 µL of Bis-Tris buffer pH 5.8 was added with 1 µL of 100 µM solution of Nigericin in Ethanol. In the third tube, right before starting the measurement, 405 µL of Bis-Tris buffer pH 5.8 was added. 125 µL was added to each well of the plate three times for each tubes resulting in three measurements with three replicates with a total of 9 measurements per lipid solution.

2.6 Acknowledgements

Chapter 2 is adapted, in part, from Takaoki Koyanagi, Geoffray Leriche, David Onofrei, Gregory P. Holland, Michael Mayer, and Jerry Yang. “Cyclohexane Rings Reduce Membrane Permeability to Small Ions in Archaea-Inspired Tetraether Lipids.” *Angew. Chem., Int. Ed.* 2016, *55*, 1890–1893. Copyright 2016 Wiley. Permission to use copyrighted images and data in the manuscript was also obtained from Geoffray Leriche, David Onofrei, Gregory P. Holland, Michael Mayer, and Jerry Yang. The dissertation author is the first

author of this manuscript. Chapter 2 is also adapted, in part, from Takaoki Koyanagi, Geoffray Leriche, Alvin Yep, David Onofrei, Gregory P. Holland, Michael Mayer, and Jerry Yang. “Effect of Headgroups on Small-Ion Permeability across Archaea-Inspired Tetraether Lipid Membranes. *Chem.” - Eur. J.* 2016, *22*, 8074–8077. Copyright 2016 Wiley. Permission to use copyright images and data in the manuscript was also obtained from Geoffray Leriche, Alvin Yep, David Onofrei, Gregory P. Holland, Michael Mayer, and Jerry Yang. The dissertation author is the first author of this manuscript. Chapter 2 is also adapted, in part, from Thomas B. H. Schroeder, Geoffray Leriche, Takaoki Koyanagi, Mitchell A. Johnson, Kathryn N. Haengel, Olivia M. Eggenberger, Claire L. Wang, Young Hun Kim, Karthik Diraviyam, David Sept, Jerry Yang, and Michael Mayer. “Effects of Lipid Tethering in Extremophile-Inspired Membranes on H+/OH− Flux at Room Temperature.” *Biophys. J.* 2016, *110*, 2430–2440. Copyright 2016 Elsevier. Permission to use copyright images and data in the manuscript was also obtained from Thomas B. H. Schroeder, Geoffray Leriche, Mitchell A. Johnson, Kathryn N. Haengel, Olivia M. Eggenberger, Claire L. Wang, Young Hun Kim, Karthik Diraviyam, David Sept, Jerry Yang, and Michael Mayer.

2.7 References

(1) Jain, S.; Caforio, A.; Driessen, A. J. M. *Front. Microbiol.* **2014**, *5*, 641.

(2) Villanueva, L.; Damsté, J. S. S.; Schouten, S. *Nat. Rev. Microbiol.* **2014**, *12* (6), 438–448.

(3) Van Meer, G.; Voelker, D. R.; Feigenson, G. W. *Nat. Rev. Mol. Cell Biol.* **2008**, *9* (2), 112–124.

(4) Koga, Y.; Morii, H. *Microbiol. Mol. Biol. Rev.* **2007**, *71* (1), 97–120.

(5) Woese, C. R.; Magrum, L. J.; Fox, G. E. *J. Mol. Evol.* **1978**, *11* (3), 245–252.

(6) Valentine, D. L. *Nat. Rev. Microbiol.* **2007**, *5*, 316–323.

(7) Chong, P. L.-G.; Ayesa, U.; Daswani, V. P.; Hur, E. C. *Archaea* **2012**, *2012*, 1–11.

(8) Gabriel, J. L.; Lee Gau Chong, P. *Chem. Phys. Lipids* **2000**, *105* (2), 193–200.

(9) Chong, P. L. G. *Chem. Phys. Lipids* **2010**, *163* (3), 253–265.

(10) Konings, W. N.; Albers, S. V; Koning, S.; Driessen, A. J. M. *Antonie van Leeuwen* **2002**, *81*, 61–72.

(11) Boyd, E. S.; Hamilton, T. L.; Wang, J.; He, L.; Zhang, C. L. *Front. Microbiol.* **2013**, *4* (APR), 1–15.

(12) Baker-Austin, C.; Dopson, M. *Trends Microbiol.* **2007**, *15* (4), 165–171.

(13) Elferink, M. G. L.; de Wit, J. G.; Driessen, A. J. M.; Konings, W. N. *Biochim. Biophys. Acta, Biomembr.* **1994**, *1193* (2), 247–254.

(14) Shimada, H.; Nemoto, N.; Shida, Y.; Oshima, T.; Yamagishi, A. *J. Bacteriol.* **2008**, *190* (15), 5404–5411.

(15) Wang, X.; Lv, B.; Cai, G.; Fu, L.; Wu, Y.; Wang, X.; Ren, B.; Ma, H. *Sci. Rep.* **2012**, *2* (2), 892.

(16) Chang, E. L. *Biochem. Biophys. Res. Commun.* **1994**, *202* (2), 673–679.

(17) Patel, G. B.; Agnew, B. J.; Deschatelets, L.; Fleming, L. P.; Sprott, G. D. *Int. J. Pharm.* **2000**, *194*, 39–49.

(18) Uda, I.; Sugai, a; Itoh, Y. H.; Itoh, T. *Lipids* **2001**, *36* (1), 103–105.

(19) Svenson, S.; Thompson, D. *J. Org. Chem.* **1998**, *3263* (98), 7180–7182.

(20) Brard, M.; Lainé, C.; Réthoré, G.; Laurent, I.; Neveu, C.; Lemiègre, L.; Benvegnu, T. *J. Org. Chem.* **2007**, *72* (22), 8267–8279.

(21) Eguchi, T.; Ibaragi, K.; Kakinuma, K. *J. Org. Chem.* **1998**, *63* (8), 2689–2698.

(22) WJ, Z.; CE, C. *Cell and Model Membrane Interactions*; Ohki, S., Ed.; Plenum Press: New York, 1991.

(23) Lecollinet, G.; Auzély-Velty, R.; Danel, M.; Benvegnu, T.; Mackenzie, G.; Goodby, J. W.; Plusquellec, D. *J. Org. Chem.* **1999**, *64* (9), 3139–3150.

(24) Brard, M.; Richter, W.; Benvegnu, T.; Plusquellec, D. *J. Am. Chem. Soc.* **2004**, *126* (32), 10003–10012.

(25) Godage, H. Y.; Riley, A. M.; Woodman, T. J.; Thomas, M. P.; Mahon, M. F.; Potter, B. V. L. *J. Org. Chem.* **2013**, *78*, 2275–2288.

(26) Gilbert, I. H.; Holmes, A. B.; Young, R. C. *Tetrahedron Lett.* **1990**, *31* (18), 2633–2634.

(27) Lewis, R. N.; McElhaney, R. N. *Biophys. J.* **2000**, *79*, 1455–1464.

(28) Nagle, J. F. *J. Membr. Biol.* **1976**, *27* (3), 233–250.

(29) Sipai Altaf Bhai, M.; Vandana, Y.; Mamatha, Y.; Prasanth, V. V. *J. Pharm. Sci. Innov.* **2012**, *1* (1), 13–21.

(30) Arakawa, K.; Eguchi, T.; Kakinuma, K. *Bull. Chem. Soc. Jpn.* **2001**, *74* (2), 347–356.

(31) Wilschut, J.; Papahadjopoulos, D. *Nature*. 1979, pp 690–692.

(32) Archaea, B.; Organismal, H. *Group* **1983**, 103–112.

(33) Gliozzi, A.; Relini, A.; Chong, P. L.-G. *J. Membr. Sci.* **2002**, *206*, 131–147.

(34) Andersson, A.-S. *J. Biol. Chem.* **1996**, *271* (12), 6801–6809.

(35) Mathai, J. C.; Tristram-Nagle, S.; Nagle, J. F.; Zeidel, M. L. *J. Gen. Physiol.* **2007**, *131* (1), 69–76.

(36) Jansen, M.; Blume, A. *Biophys. J.* **1995**, *68* (3), 997–1008.

(37) Spooner, M. J.; Gale, P. A. *Chem. Commun.* **2015**, *51* (51), 4883–4886.

(38) Boggs, J. M. *Biochim. Biophys. Acta* **1987**, *906* (3), 353–404.

(39) Hubner, W.; Blume, A. *Chem. Phys. Lipids* **1998**, *96* (1–2), 99–123.

(40) Murzyn, K.; Róg, T.; Pasenkiewicz-Gierula, M. *Biophys. J.* **2005**, *88* (2), 1091–1103.

(41) Koyanagi, T.; Leriche, G.; Onofrei, D.; Holland, G. P.; Mayer, M.; Yang, J. *Angew. Chem., Int. Ed.* **2016**, *55*, 1890–1893.

(42) Chang Chung, Y.; Hong Chiu, Y.; Wei Wu, Y.; Tai Tao, Y. *Biomaterials* **2005**, *26* (15), 2313–2324.

(43) Febo-Ayala, W.; Morera-Félix, S. L.; Hrycyna, C. A.; Thompson, D. H. *Biochemistry* **2006**, *45* (49), 14683–14694.

(44) Gao, Y.; Vlahakis, J. Z.; Szarek, W. A.; Brockhausen, I. *Bioorg. Med. Chem.* **2013**, *21* (5), 1305–1311.

(45) Shirouzu, T.; Watari, K.; Ono, M.; Koizumi, K.; Saiki, I.; Tanaka, C.; van Soest, R. W. M.; Miyamoto, T. *J. Nat. Prod.* **2013**, *76* (7), 1337–1342.

(46) Mangaleswaran, S.; Argade, P. N. *J. Or* **2001**, No. 17, 5259–5261.

(47) Babu, K. V.; Sharma, G. V. M. *Tetrahedron Asym.* **2008**, *19* (5), 577–583.

(48) Mioskowski, C.; Heitz, M.-P.; Wagner, A. *Tetrahedron Lett.* **1989**, No. 5, 557–558.

(49) *WO 2009/135977*.

(50) Shimojo, M.; Matsumoto, K.; Hatanaka, M. *Tetrahedron* **2000**, *56* (47), 9281–9288.

(51) Pan, X.; Lacôte, E.; Lalevée, J.; Curran, D. P. *J. Am. Chem. Soc.* **2012**, *134* (12), 5669–5674.

(52) Trigo, G. G.; Muñoz, E. M.; Llama-Hurtado, E. *J. Heterocycl. Chem.* **1984**, *21* (5), 1479–1483.

(53) Lowik, D. W. P. M.; Liskamp, R. M. J. *Eur. J. Org. Chem.* **2000**, *2000* (7), 1219–1228.

(54) Prabhakar, P.; Rajaram, S.; Reddy, D. K.; Shekar, V.; Venkateswarlu, Y. *Tetrahedron Asym.* **2010**, *21* (2), 216–221.

(55) Qin, L.; Ren, X.; Lu, Y.; Li, Y.; Zhou, J. *Angew. Chem., Int. Ed. Engl.* **2012**, *51* (24), 5915–5919.

(56) Flowers, C. L.; Vogel, P. *Chem. - A Eur. J.* **2010**, *16* (47), 14074–14082.

(57) Marinier, A.; Deslongchamps, P. *Tetrahedron Lett.* **1988**, *29* (48), 6215–6218.

(58) Bartoli, S.; De Nicola, G.; Roelens, S. *J. Org. Chem.* **2003**, *68* (21), 8149–8156.

(59) Iwashita, M.; Makide, K.; Nonomura, T.; Misumi, Y.; Otani, Y.; Ishida, M.; Taguchi, R.; Tsujimoto, M.; Aoki, J.; Arai, H.; Ohwada, T. *J. Med. Chem.* **2009**, *52* (19), 5837–5863.

(60) Yar, M.; Fritz, S. P.; Gates, P. J.; McGarrigle, E. M.; Aggarwal, V. K. *Eur. J. Org. Chem.* **2012**, 1, 160–166.

(61) Rzepecki, P. W.; Prestwich, G. D. *J. Org. Chem.* **2002**, *67* (16), 5454–5460.

(62) Devaraj, S.; Shashidhar, M. S.; Dixit, S. S. *Tetrahedron* **2005**, *61* (3), 529–536.

(63) Conway, S. J.; Gardiner, J.; Grove, S. J. a; Johns, M. K.; Lim, Z.-Y.; Painter, G. F.; Robinson, D. E. J. E.; Schieber, C.; Thuring, J. W.; Wong, L. S.-M.; Yin, M.-X.; Burgess, A. W.; Catimel, B.; Hawkins, P. T.; Ktistakis, N. T.; Stephens, L. R.; Holmes, A. B. *Org. Biomol. Chem.* **2010**, *8* (1), 66–76.

(64) Elie, C. J. J.; Verduyn, R.; Dreef, C. E.; Brounts, D. M.; van der Marel, G. A.; van Boom, J. H. *Tetrahedron* **1990**, *46* (24), 8243–8254.

(65) Šardzík, R.; Noble, G. T.; Weissenborn, M. J.; Martin, A.; Webb, S. J.; Flitsch, S. L. *Beilstein J. Org. Chem.* **2010**, *6*, 699–703.

(66) Contour, M. O.; Defaye, J.; Little, M.; Wong, E. *Carbohydr. Res.* **1989**, *193*, 283–287.

(67) Koyanagi, T.; Leriche, G.; Yep, A.; Onofrei, D.; Holland, G. P.; Mayer, M.; Yang, J. *Chem. - Eur. J.* **2016**, *22* (24), 8074–8077.

Chapter 3

Combining Structural Strategies Used by Eukaryotes and Archaea to Enhance Membrane Properties of Archaea Inspired Tetraether Lipids

3.1. Introduction

Leakage across membranes is a problem for applications in drug delivery.[1–3] For example, liposomes made from commercially available diacyl lipids were shown to be unstable towards hydrolysis and leaky, especially in the presence of serum.[3] The problem of content leakage and membrane instability has prompted many researchers to steer away from liposomal delivery systems and towards technologies based on covalent attachment of drugs to polymeric backbones of nanoparticles, as discussed in chapter 1 of this dissertation.[4–9] However, unlike drug-polymer conjugates that are typically limited to chemically adhering only one type of drug or cell-targeting functional group to a polymeric backbone, the potential versatility of liposomes include encapsulation of different types of drugs, facile addition of steric barrier functionalized lipid, and simple addition of peptide lipid conjugates for cell-mediated drug delivery without the need for multiple-chemical modification continues to make liposomal

delivery systems an attractive incentive for further development of membranes with low permeability.[1,10–13]

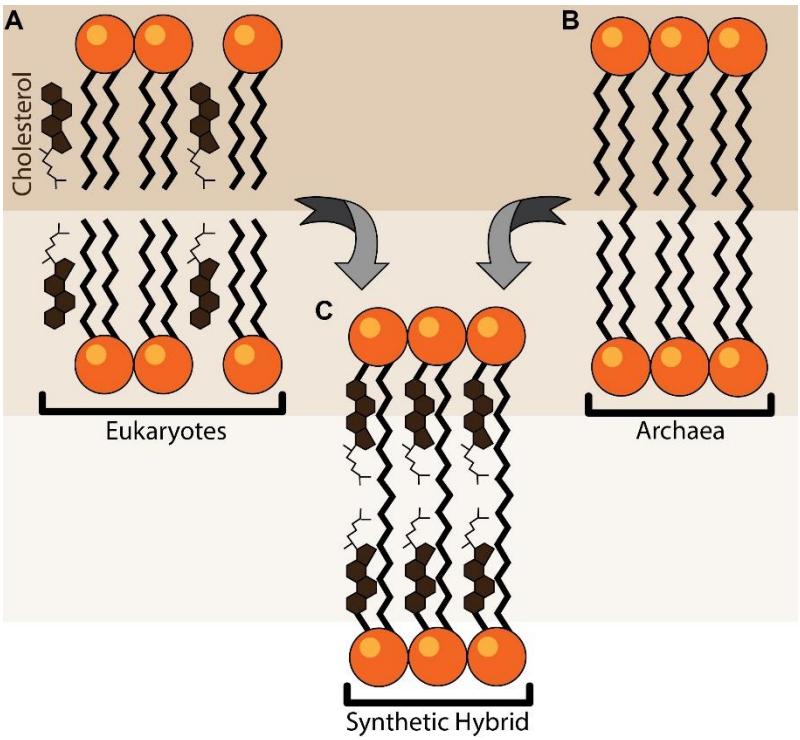

Figure 3.1. Comparison of strategies to improve membrane integrity used by eukaryotes (A) or Archaea (B) with the novel strategy that combines both strategies in the synthetic hybrid lipid introduced here (C).

In nature, several strategies are used by organisms to address problems of membrane integrity. Eukaryotic organisms, for instance, manufacture free cholesterol to fill defects in bilayer lipid membranes, which lead to increased membrane stability (Figure 3.1A).[14] Archaea, on the other hand, generate lipids with ether linkages and tethered lipid tails (Figure 3.1B) that result in chemically stable membrane-spanning lipids that make it possible for the organisms to thrive in extreme environments.[15]

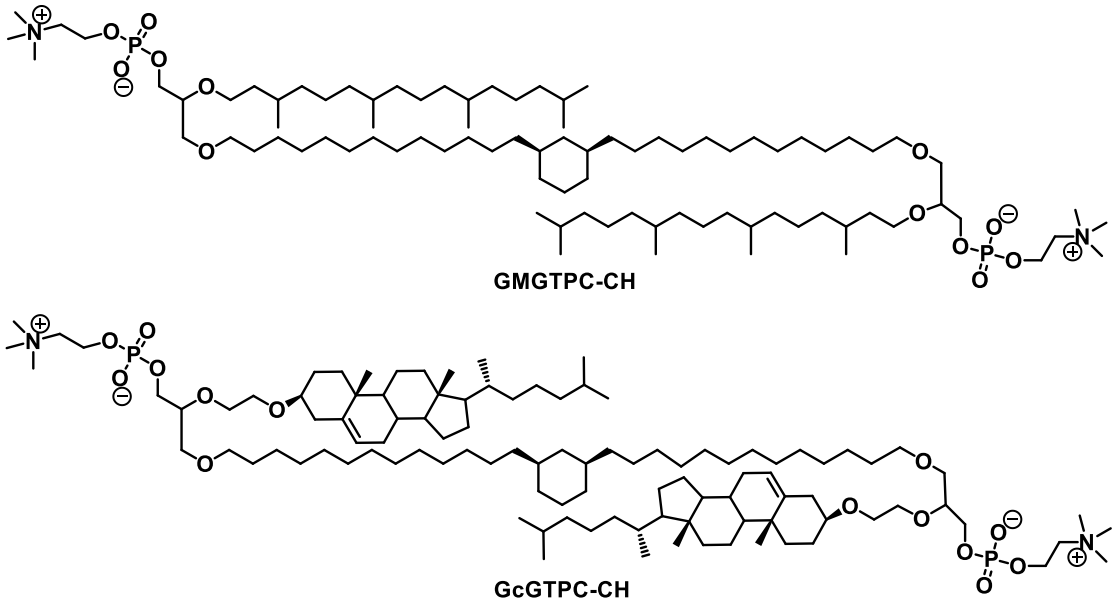

Figure 3.2. Structures of Archaea-inspired tetraether lipids with (**GcGTPC-CH**) or without (**GMGTPC-CH**) covalent cholesterol integration.

To develop liposomes with reduced leakage properties, we have designed Archaea-inspired tetraether lipids, **GMGTPC-CH** (synthesized in Chapter 2 of this dissertation), that incorporate structural features that are believed to increase membrane properties (Figure 3.2). This newly developed synthetic tetraether lipids readily formed stable liposomes and exhibited reduction of small ion membrane leakage by ~2 orders of magnitude when compared with leakage properties of membranes formed from commercially available diacyl lipids, EggPC (see chapter 2).[16] In contrast, the addition of free cholesterol to diacyl lipid formulations (using the strategy invoked by Eukaryotes) has been a common practice used by research groups to decrease membrane leakage by improving membrane integrity. However, free cholesterol has been observed to leach out from liposomes after injection into serum

containing environment, resulting in liposomal destabilization leading to premature loss of cargo.[17] One solution developed by Szoka's group, has been to covalently attach cholesterol to the glycerol backbone, which has been shown to eliminate cholesterol leaching from liposomes.[18–20]

In our design to synthesize lipids with further improved membrane properties, we explored the possibility to combine these two strategies used by nature for generating robust membranes by creating a hybrid lipid that incorporates covalent cholesterol integration into a tethered tetraether lipid (Figure 3.1C). Extracting the best structural features that reduces membrane permeability from our previously synthesized Archaea-inspired tetraether lipids from chapter 2, we preserved the cyclohexane integrated tethered tetraether lipid with phosphocholine headgroups, while replacing the phytanyl groups with an ethylene glycol extended cholesterol (shown in Figure 3.2.). Following the synthesis, we compared the leakage properties of membranes composed of this hybrid lipid to membranes formed from commercial diacyl lipids and an Archaea-inspired lipid that did not comprise covalently attached cholesterol (both with and without incorporation of free cholesterol in the membranes). In addition, molecular dynamics (MD) simulations provided a molecular interpretation for the observed experimental differences in leakage properties between different lipid membrane compositions. Lastly, we examined the capability of liposomes made from this hybrid lipid to incorporate functional ion channels into membranes, explored the capability of these lipids to be

recognized as substrates by a membrane-active phospholipase-D (PLD) enzyme, assessed the stability of liposomes composed of these lipids in serum, and evaluated the uptake of such liposomes in cells.

*3.2. Design/Synthesis of **GcGTPC-CH***

Several synthetic strategies of **GcGTPC-CH** were tested to maintain the olefin of the added cholesterol appendage. First, shown in Scheme 3.1A, we initially examined the possibility of synthesizing the glycerol backbone with epichlorohydrin following a previously published synthesis by Benvegnu's group that reported ~50% product conversion to a hemicyclic lipid scaffold.[21] However, when the crude material was analyzed *via* TLC and NMR after the reaction was mixed for 12 hours at 70 °C, only starting material diol **2.34** was recovered. To examine whether the initial coupling of diol **2.34** with epichlorohydrin takes place, the same reaction was repeated with an excess of epichlorohydrin (12 eq. from 2.1 eq.), however, no product formation was observed *via* ^{1}H-NMR. The lack of transformation observed for this reaction could be explained by the poor solubility of diol **2.34** in hexane, which may differ in solubility properties to the diol used by Benvegnu's group.

Next, we examined the possibility of starting the reaction of the glycerol scaffold from solketal (shown in Scheme 3.1B). Initial alkylation of alkyldibromo **2.36** by the free alcohol on solketal afforded tethered lipid precursor **3.1**. Following an acid catalyzed ring opening of the acetals forming tetraol **3.2**, the

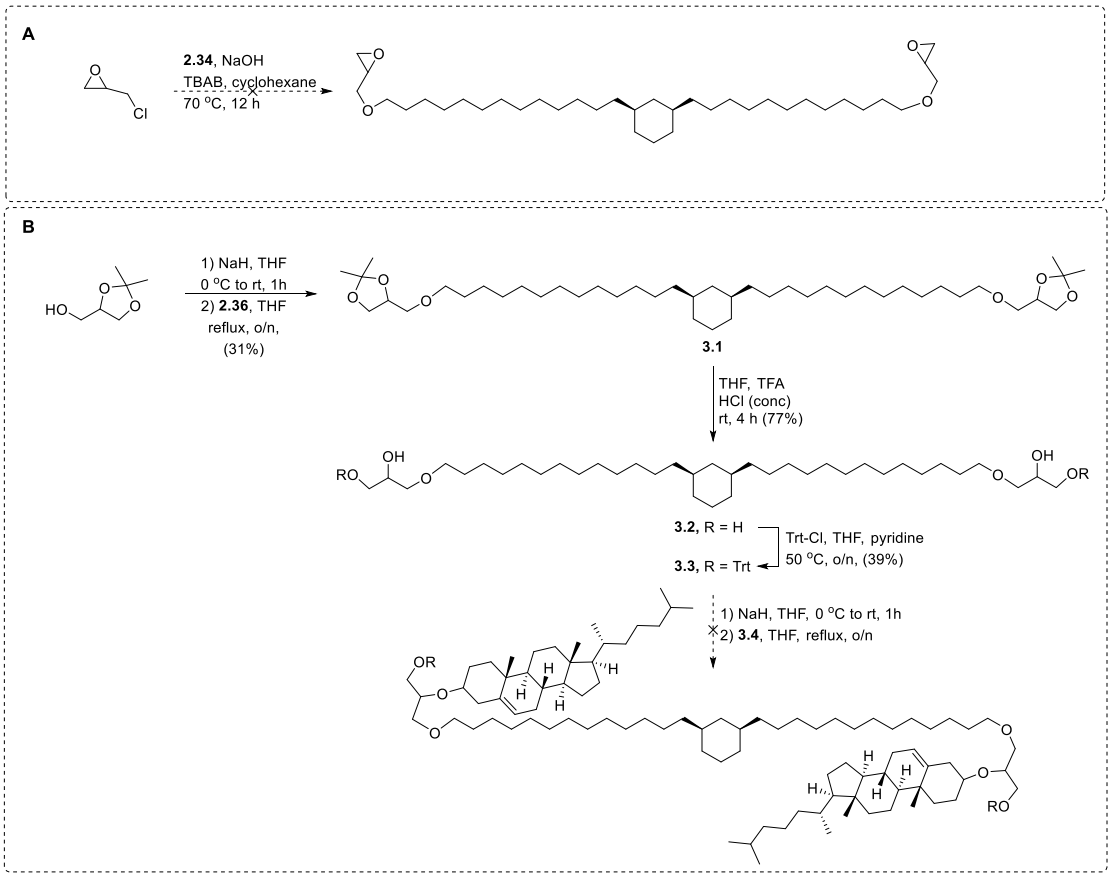

Scheme 3.1. Unsuccessful synthesis employed for **GcGTPC-CH.** A) Synthetic strategy of **GcGTPC-CH** using epichlorohydrin. B) Synthetic strategy of **GcGTPC-CH** using solketal.

terminal alcohols were protected by trityl groups affording protected lipid precursor **3.3**. Following a previously published protocol by Benvegnu's groups[21], alkylation of tosylated cholesterol was attempted with the free secondary diols of **3.3** under basic conditions in THF by heating the reaction to reflux while allowing the solvent to evaporate at 130 °C. However, after the reaction was stirred at 130 °C overnight (effectively neat), no product or starting material was isolated (black degradation products were observed). Believing the degradation occurred because the reaction was performed neat, the same reaction was performed in DMF. After the initial addition of NaH, however, the

reaction became black and turbid. The suspension in DMF was stirred for 24 hours at 130 °C, but the suspension never became homogenous and degradation products were observed. The synthetic scheme was not further optimized because of the low yields associated with the reactions steps up to that point (9% over 3 steps).

For our third synthetic approach to **GcGTPC-CH**, we attempted a similar strategy used for our previously synthesized tetraether lipids (shown in chapter 2) as our starting point. As shown in Scheme 3.1B, we initially designed the **GcGTPC-CH** lipid to comprise a cholesterol group directly attached to the glycerol lipid backbone without an ethylene glycol spacer. However, alkylation with the glycerol alcohol to the tosylated cholesterol was not achieved, but rather, the alcohol of the glycerol became tosylated instead. From this result, we decided to increase access of the nucleophile to the tosylated electrophile by synthetically modifying the cholesterol to include an ethylene glycol spacer on the 3β alcohol. The new plan to synthesize **GcGTPC-CH** began with a tosylation of the 3β alcohol on cholesterol followed by substitution of the tosyl group with ethylene glycol that afforded modified cholesterol **3.5** with retention of stereochemistry on cholesterol (shown in Scheme 3.2).[22] The free terminal alcohol in **3.5** was then converted to the corresponding tosylate to form **3.6**,

which successively reacted with 2-phenyl-1,3-dioxan-5-ol. The acetal of the

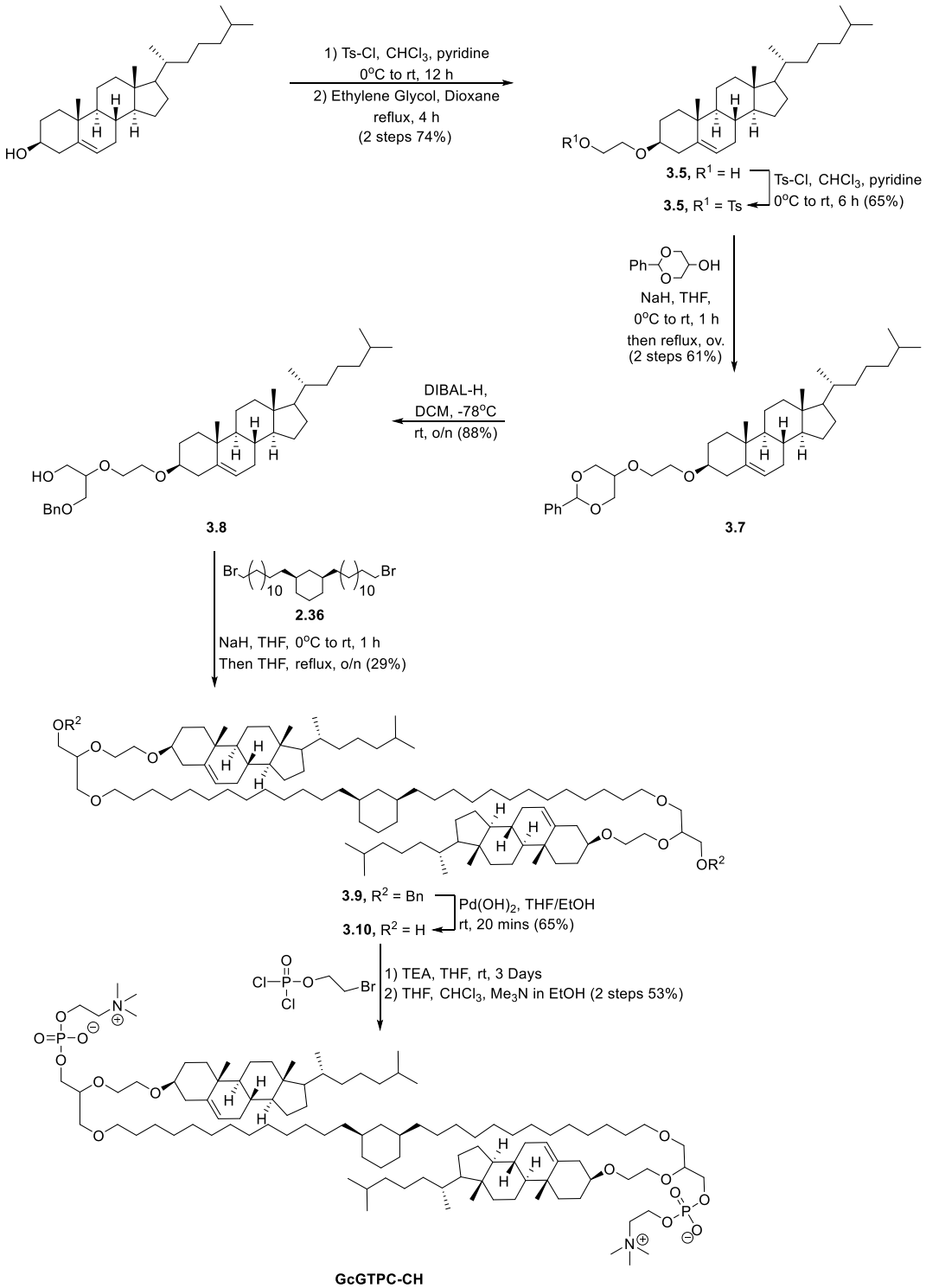

Scheme 3.2. Successful synthesis of **GcGTPC-CH**

newly formed cholesterol integrated glycerol scaffold **3.7** was deprotected using DIBAL-H to form the benzyl protected glycerol backbone **3.8**. Next, the cyclohexane integrated diibromoalkane **2.36**, from chapter 2, was alkylated by glycerol **3.8** under basic conditions to generate benzyl-protected lipid **3.9**. Notably, to obtain the diol **3.10** without reducing the olefins associated with the cholesterol, several conditions were screened (i.e. reaction time, amount of Pd, reaction concentration). Ultimately, we were able to optimize the reaction conditions for debenzylation without reducing the olefin by reducing the reaction time (to 20 minutes compared to our previous conditions that required 5 hours to 16 hours of mixing at room temperature) and using less Pd (5% w/w vs. 10% w/w used in previous conditions) and diluting the reaction (4.6 times) in THF:EtOH (1:1) to generate the desired diol **3.10** with the olefins intact. The formation of **GcGTPC-CH** was completed in a series of reactions that involved reacting diol **3.10** with 2- bromoethyl dichlorophosphate, which was followed by the displacement of bromides by trimethylamine (i.e., an analogous synthetic strategy as described in chapter 2).

*3.3. Physical Characterization of Liposomes Made from Pure **GcGTPC-CH, GMGTPC-CH,** and Diacyl Lipids*

After successfully synthesizing **GcGTPC-CH**, we examined whether we can form stable liposomes with pure **GcGTPC-CH** lipids. Dynamic light scattering (DLS) measurements demonstrated that we could generate liposomes with an average hydrodynamic diameter of ~150 nm by extrusion

through a 100 nm polycarbonate membrane (see Figure 3.3A). We then probed the physical characteristics of **GcGTPC-CH** and examined whether replacing the phytanyl group (which prevents natural archaeal tetraether lipids from undergoing a phase transition between 0 to 80 ºC)[23] in **GMGTPC-CH** with a cholesterol moiety would still maintain a fluid phase for liposomes within a useful temperature range. Differential scanning calorimetry (DSC) measurements (taken by David Onofrei) revealed that **GcGTPC-CH** lipid remained in a liquid phase from 5 to 65 °C (see Figure 3.3B). This result was in agreement with

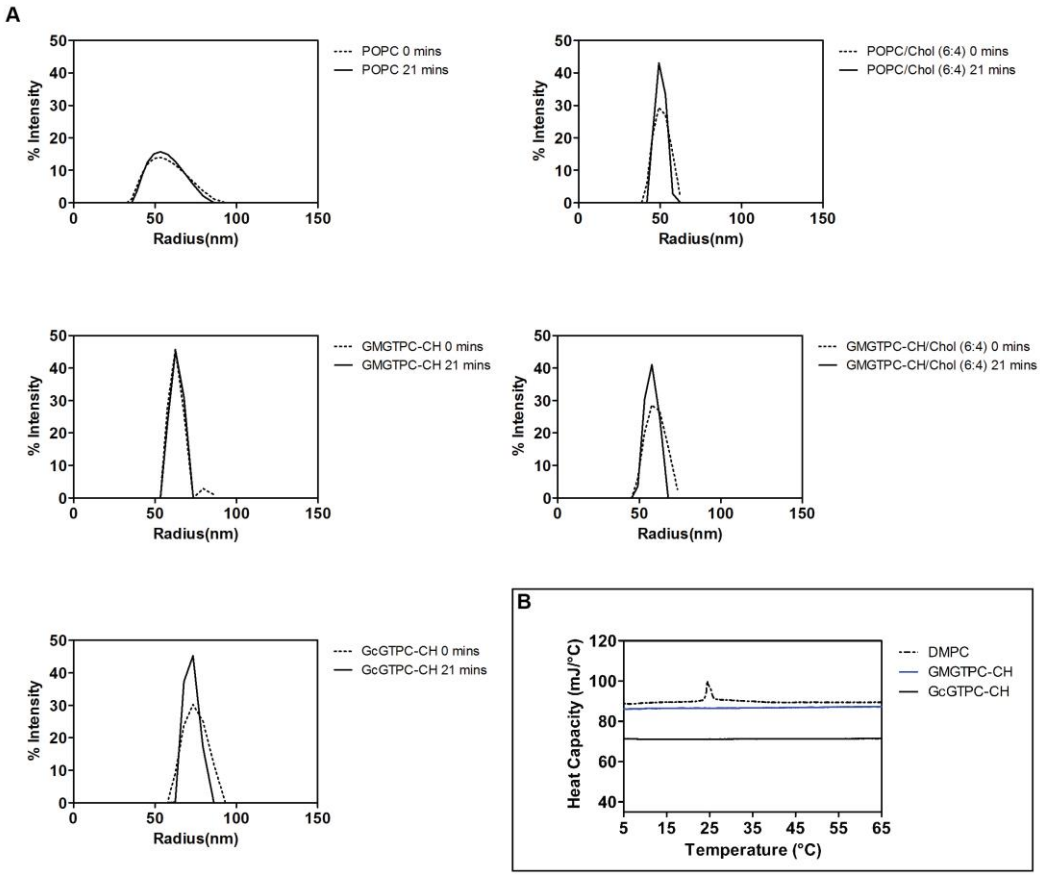

Figure 3.3. Physical characterization of lipids. A) DLS measurements of varying liposomal formulations. B) DSC measurements taken of synthetic and diacyl lipids. DSC measurements taken by David Onofrei.

previous reports, which showed that adding 40-50 mol% of free cholesterol to diacyl lipids[24] maintains a fluid phase and diminishes its phase transition. Furthermore, liposomes remained structurally stable throughout the time frame of leakage experiments and we did not observe any measurable changes in size by DLS (see Figure 3.3A).

*3.4. Investigation of Membrane Leakage Across Membranes Composed of **GcGTPC-CH** and Diacyl Lipid*

3.4.1. Comparison of Small Ion Leakage Rates Across Membranes Composed of Synthetic and Diacyl Lipids

Liposomes were formed using the same protocol as described in Chapter 2 (section 2.5.9). Using a previously described pH equilibration method (section 2.5.10) to estimate initial rates of leakage of small ions from liposomes,[16,25] we evaluated the observed rates of small ion membrane leakage to study whether the addition of free cholesterol (40 mol%) to POPC, **GMGTPC-CH**, or **GcGTPC-CH** liposomal formulations affected membrane permeation of small ions (see Figure 3.4). As expected, the addition of free cholesterol to POPC resulted in a beneficial decrease (10-fold) in observed rate of small ion membrane leakage compared with cholesterol-free POPC membranes[26] (Figure 3.5.). However, the addition of free cholesterol to **GMGTPC-CH** or **GcGTPC-CH** did not have a significant effect on the observed rate of small ion membrane leakage compared

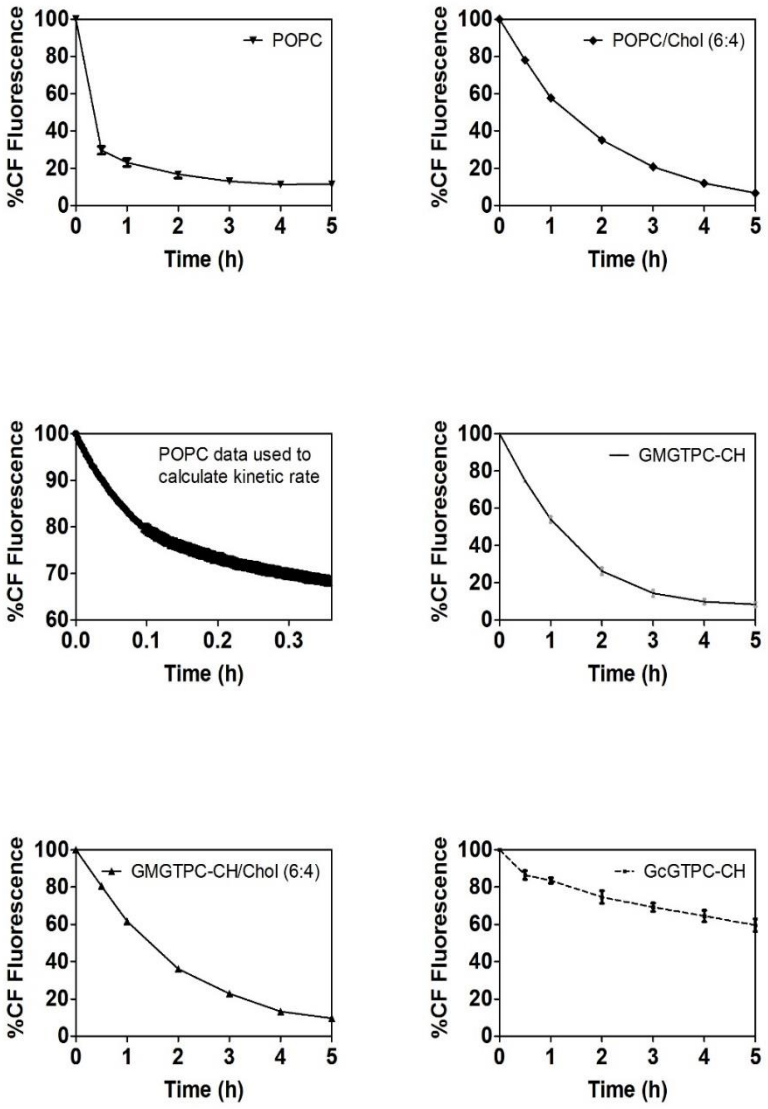

Figure 3.4. Normalized average plot of % CF fluorescence vs. time (h). (N = 9) fluorescence intensity (monitored at λ(Ex/Em) = 485/517 nm)

to the same lipid without added free cholesterol. To further probe this result, we examined whether free cholesterol was capable of integrating into the membranes composed of **GMGTPC-CH** or **GcGTPC-CH**. The presence of free cholesterol in **GMGTPC-CH** liposomes was confirmed by titration of both total phosphorus content and free total cholesterol using a Bartlett assay[27] and an

Amplex® Red cholesterol assay, respectively. The result showed a presence of 31 ± 10 mol% of free cholesterol in **GMGTPC-CH** liposomes, which is within the expected range of cholesterol concentration for liposomal formulations made by extrusion.[28] However, no free cholesterol was detected in **GcGTPC-CH** liposomes by the same analysis used for **GMGTPC-CH** liposomes. The absence of free cholesterol incorporated in **GcGTPC-CH** lipid membranes is in agreement with previous reports that suggest that the maximum incorporation

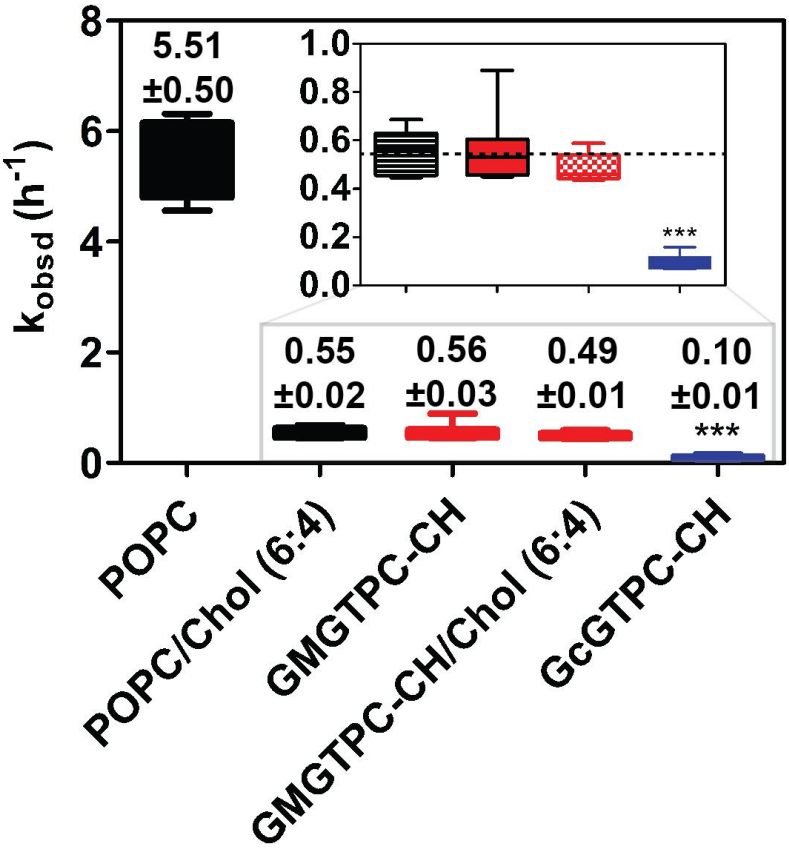

Figure 3.5. Membrane leakage results of small ions from liposomes formed from synthetic or POPC lipids with/without added free cholesterol. Comparison of the observed initial rates of decreased carboxyfluorescein (CF) fluorescence intensity (monitored at λ(Ex/Em) = 485/517 nm) from CF-encapsulated liposomes comprised of **GMGTPC-CH**, **GcGTPC-CH**, or POPC lipid with/without added 40 mol% cholesterol during liposome formation with averaged observed initial rates of membrane leakage noted over each box (unit = h^{-1};N=9).

of total cholesterol in fluid lipid membranes is ~50 mol% for liposomes prepared by extrusion.[28] Remarkably, despite the absence of membrane benefits associated with the addition of free cholesterol to liposomes, liposomes composed of pure **GcGTPC-CH** displayed a five-fold decrease in the observed rate of small ion membrane leakage compared with liposomes made of pure **GMGTPC-CH** (Figure 3.5). This observed reduction in small ion membrane leakage from **GcGTPC-CH** is consistent with the hypothesis that covalently attaching cholesterol to the glycerol backbone in **GcGTPC-CH** allows cholesterol to appropriately orient within the membrane and results in tighter lipid packing than **GMGTPC-CH** (with or without added free cholesterol).

3.4.2. Comparison of Small Molecule Leakage Rates Across Membranes Composed of Synthetic and Diacyl Lipids

When deciding on a FDA approved drug that will be used to probe membrane leakage properties of small molecules, we limited our options of drugs to neutrally charged molecules instead of charged molecules based on our previously published data that showed very little leakage from liposomes made from **GMGTPC** lipids for charged molecules.[29] From the list of drug candidates to screen for membrane leakage (shown in Figure 3.6), we began with 5-FU (5-fluorouracil). Initially, we passively encapsulated 5-FU in liposomes made with POPC/chol, **GMGTPC-CH**/chol or **GcGTPC-CH** and used a dialysis

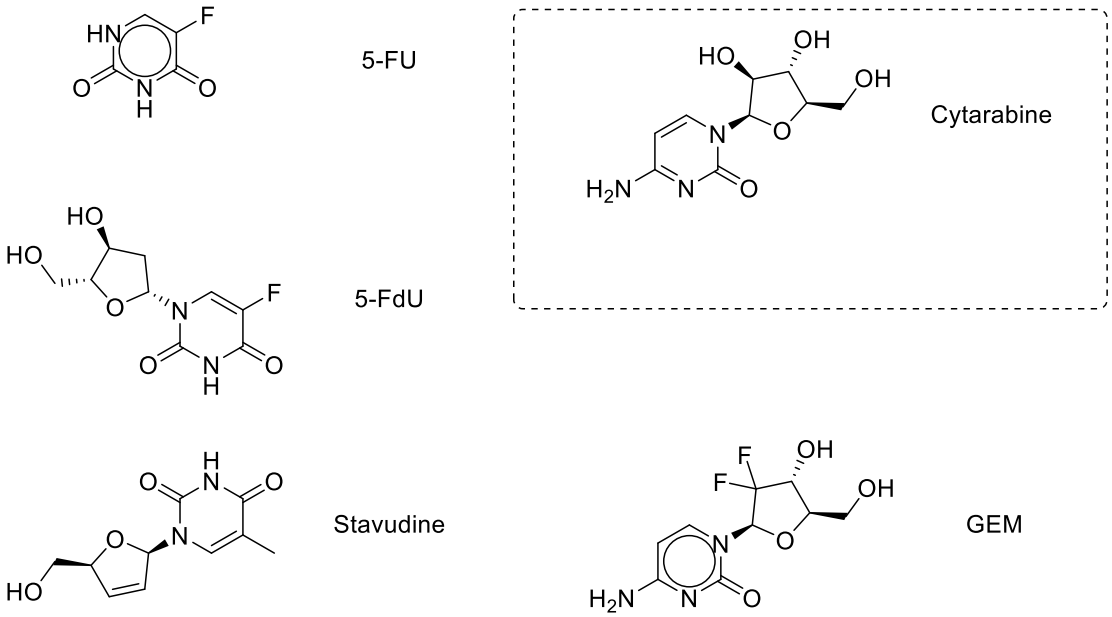

Figure 3.6. FDA approved drugs screened for membrane leakage.

assay to compare the leakage of 5-FU over a 48 hour incubation at 37 °C (see section 3.9.4. for more details). However, after the liposomes were purified using Sephadex®, no free 5-FU was detected *via* HPLC for liposomes made with either POPC/chol or **GMGTPC-CH**/chol. Liposomes made with **GcGTPC-CH**, on the other hand, had detectable free drug after purification, but the rate of leakage was too fast and did not appear to significantly differ from leakage of free drug through the dialysis membrane. Thinking the fast leakage from liposomes was due to the small size of 5-FU (130 g/mol), we examined the leakage of 5-FdU (246 g/mol), which has a molecular weight of ~ 2 times larger. Unfortunately, although the free drug was detectable using HPLC for POPC/chol liposomes after purification, the observed rate of leakage was too fast and the leakage rate was similar to the rate of leakage of the molecule through the dialysis membrane in the absence of liposome encapsulation. This

conclusion arose from having two separate batches of POPC/chol liposomes made sequentially with a 15 minute waiting period between the time it required for the Sephadex® to be washed, while the second batch of liposomes loaded with 5-FdU was equilibrating with the buffer (leaking). When we compared the two initial HPLC signals, the area measured for 5FdU was effectively baseline for the initial time point for the second batch (suggesting complete leakage while the Sephadex® was being cleaned). After concluding that the fast rate of leakage of 5-FdU from POPC/chol liposomes would be a challenge to interpret kinetically, we decided to screen a different drug instead of trying to tease out small differences that will most likely be masked by signal noise/error. Trying to understand why the molecules tested, thus far, had a fast rate of leakage, we hypothesized the fast leakage was caused by the fluorine substituent. Fluorine groups have been added to pharmaceutical molecules to enhance permeation through stomach linings, as such, may contribute to the rapid membrane leakage.[30] The next drug that was screened was Stavudine, (shown in Figure 3.6), an FDA approved drug that resembles a reduced 5-FdU without the fluorine substituent. However, similar fast leakage profile of 5FU was observed for Stavudine. From the membrane leakage results obtained for Stavudine, our hypothesis of the fluorine substituent driving the fast leakage was dismissed.

Therefore, we decided to probe another drug, gemcitabine (shown in Figure 3.6), an FDA drug most similar to cytarabine (an FDA approved drug that has been shown to be retained (80%) inside liposomes made with **GMGTPC**

lipids after 48 hours at 37 °C[29]). We passively encapsulated gemcitabine (GEM)[31] in liposomes to compare permeability of a neutrally charged molecule across membranes composed of POPC/chol, **GMGTPC-CH**/chol or pure **GcGTPC-CH**. When we compare the leakage of GEM over a 48 hour incubation at 37 °C (see section 3.9.4. for more details), we were able to observe retention of free drug inside liposomes long enough to measure leakage rates. Remarkably, in contrast to the results obtained from the small ion membrane leakage assay (Figure 3.5) that did not show a significant difference between POPC/chol and **GMGTPC-CH**/chol, all 3 liposomal compositions exhibited significantly different leakage profiles for encapsulated GEM (Figure 3.7). Notably, liposomes made from pure **GcGTPC-CH** retained 69.1 ± 4.1% of GEM after 48 hours, while liposomes made from POPC/chol (2.3 ± 0.1% retained GEM) or **GMGTPC-CH**/chol (7.1 ± 1.2% retained GEM) exhibited almost complete loss of encapsulated GEM over the same period of time. These contrasting results between small ion versus small molecule leakage profiles for the different lipids could reflect differences in mechanisms of leakage, where small ions are believed to leak through transient membrane pores and neutral molecules could leak through both membrane pores and membrane partitioning.[32]

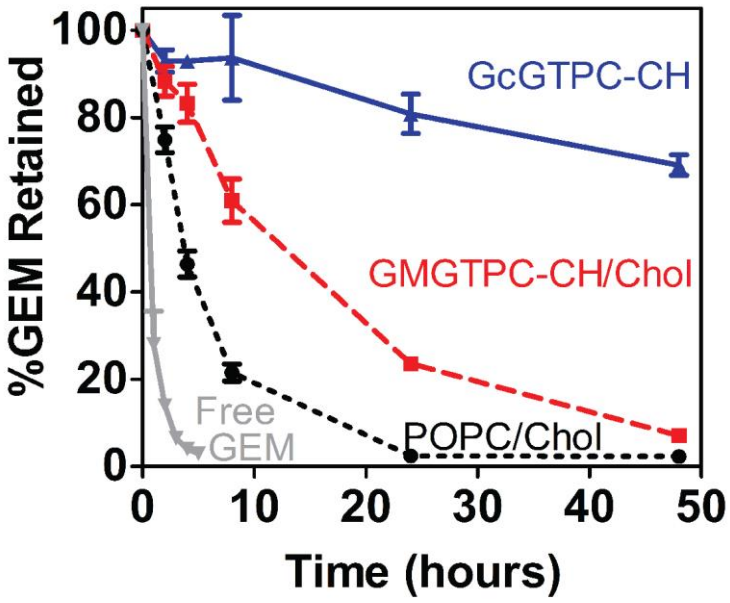

Figure 3.7. Membrane leakage results of gemcitabine (GEM, a neutrally charged drug) from liposomes formed from synthetic or POPC lipids with/without added free cholesterol. Graph of percent retention versus time of GEM encapsulated inside liposomes made from **GcGTPC-CH**, **GMGTPC-CH** with 40 mol% of free cholesterol, POPC with 40 mol% of free cholesterol, or free GEM (i.e., no liposomes) across a dialysis membrane upon incubation at 37 ºC for 48 hours.

3.4.3. Molecular Dynamics Simulations of Membranes Composed of Synthetic and Diacyl Lipids

In order to provide a molecular interpretation for the observed experimental trend in membrane permeability for POPC, **GMGTPC-CH**, and **GcGTPC-CH**, we performed molecular dynamics (MD) simulations of pure lipids

in membranes (see section 3.9.5. for details). Figure 3.8A shows overlaid

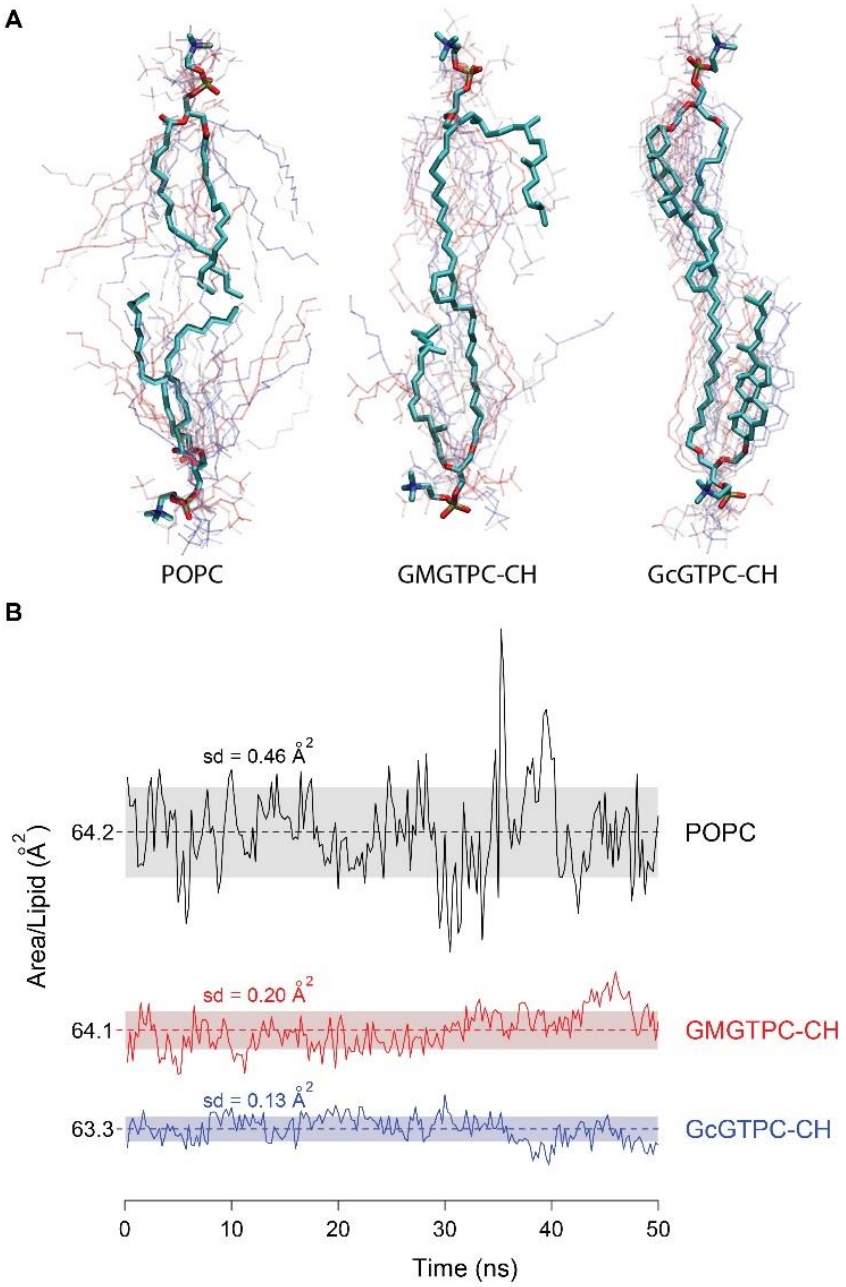

Figure 3.8. Results from molecular dynamics (MD) simulations of a membrane composed of pure POPC, **GMGTPC-CH**, or **GcGTPC-CH** lipids. A) Overlay of 10 snapshots of individual lipids (taken in 5 ns intervals from MD simulations of pure lipid membranes) highlighting the increased ordering of the lipid tails from POPC to GMGTPC-CH to GcGTPC-CH. B) Graph of the area occupied by individual lipids (within membranes comprised of pure lipids) over a 50 ns membrane simulation highlighting the variance in area per lipid (represented quantitatively as standard deviation (sd)). Experiments performed by Prof. David Sept.

snapshots of the same individual lipids at 5 ns intervals revealing the conformational space explored by each lipid over 50 ns (experiments performed by Prof. David Sept). The results highlight striking differences in the order of the lipid tails between these lipids. The reduced flexibility of lipid tails in the tetraether lipids translated to a decreased variance in the area occupied per lipid (Figure 3.8B), which could be represented quantitatively by the standard deviation (sd) around the mean area/lipid ($Å^2$). These calculations are in good agreement with the observed experimental trends for leakage of small ions and molecules across lipid membranes (Figure 3.5 and 3.7), supporting the concept that decreased variance in area per lipid leads to tighter lipid packing and lower

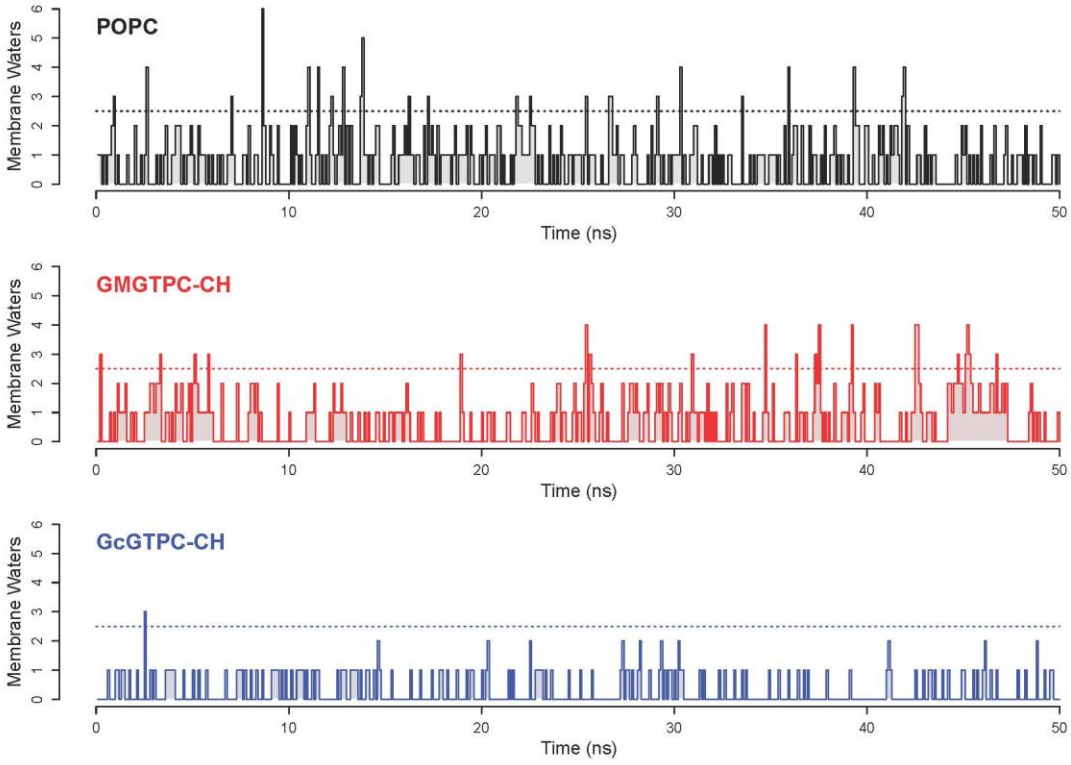

Figure 3.9. Total number of waters within the membrane for each snapshot over the final 50 ns of the trajectory. Experiments performed by Prof. David Sept.

permeability.[33] Furthermore, MD simulations (experiments performed by Prof. David Sept) shows an estimate of membrane water penetration for the different lipids[34] where we found 24 penetration events (i.e., transient events where 3 or more water molecules resided anywhere within the hydrophobic region of a membrane over a 50 ns MD simulation) for pure POPC membranes, 20 events for **GMGTPC-CH** and only 1 event for **GcGTPC-CH** under the same conditions (see Figure 3.9). These differences in the number of observed water penetration events presumably reflect variations in both composition and conformational freedom between the different lipids tails, since all lipids contained the same phosphocholine headgroups.

*3.5. Investigation of Functional Membrane Properties of **GcGTPC-CH** Membranes*

To explore whether membranes composed of **GcGTPC-CH** lipids retained useful membrane properties for potential biological applications currently using diacyl lipids, we examined whether 1) **GcGTPC-CH** lipid membranes can act as a membrane support for natural ion channel forming peptides such as gramicidin A (gA),[35,36] 2) **GcGTPC-CH** lipids can serve as a substrate for membrane active enzymes such as phospholipase-D (PLD),[37–39] 3) liposomes derived from **GcGTPC-CH** can remain sufficiently stable in serum-containing buffers,[3,40,41] and 4) small molecules encapsulated in **GcGTPC-CH** liposomes can be delivered to living cells.[42–44]

*3.5.1. Investigation of **GcGTPC-CH** Lipid Membrane to Support Gramicidin A Formation*

Gramicidin A (gA) is an antibiotic peptide that forms well defined ion channels in membranes.[45] Proper nanopore formation of gA in liposomal membranes allows monovalent cations to selectively cross between the surrounding buffer and the intra-liposomal buffer. Using the pH equilibration assay that we used to measure passive membrane leakage, we added gA to a buffered solution at pH 5.8 containing **GcGTPC-CH** liposomes with encapsulated carboxyfluorescein (CF) and an intra-liposomal pH of 7.2. To determine whether gA was functional upon incorporation into the membrane, pH-dependent fluorescence emission of CF was monitored for a flux of monovalent cations (predominantly H^+ ion flux) into the liposome, causing an accelerated reduction of CF fluorescence when compared with liposomes without the addition of gA. Similar to previously reported results that used diacyl lipids,[35,36] the addition of gA to **GcGTPC-CH** liposomes reduced 95% of the fluorescence of CF after 30 minutes (Figure 3.10A), suggesting that the ion channels were functional within the membrane. In addition, liposomes with just DMSO (without gA) was added to measure fluorescence changes to CF to confirm liposomal stability in the presence of DMSO (Figure 3.10A). Furthermore, to ensure the addition of gA does not cause the liposomes to rupture, the presence of stable liposomal structures throughout the experiment was confirmed using DLS measurements (see Figure 3.10B).

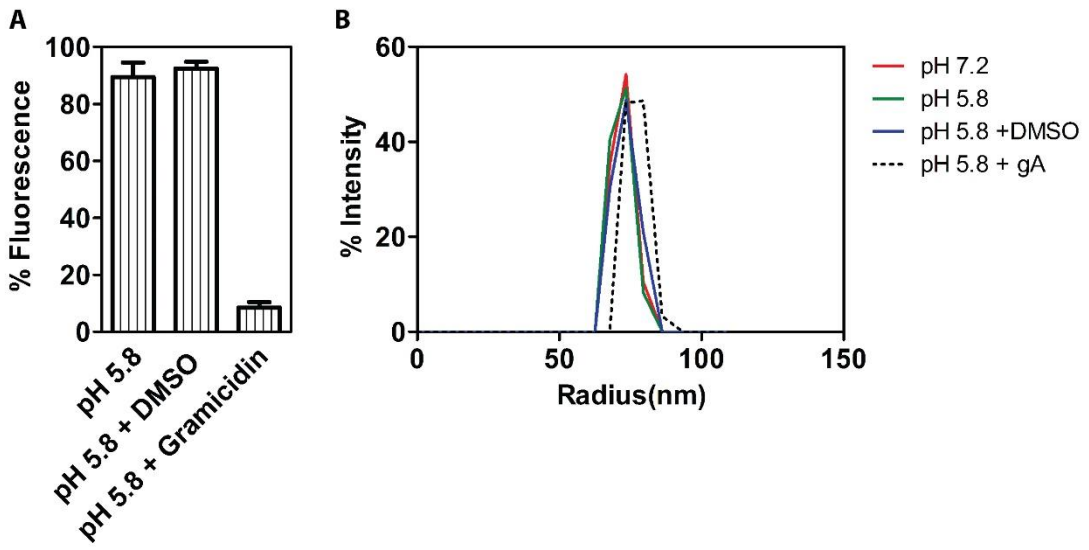

Figure 3.10. Effect of gramicidin A on **GcGTPC-CH** liposomes. A) Percent fluorescence of CF after incubation with or without gA at 37 ºC for 30 minutes. B) DLS measurements of **GcGTPC-CH** liposomes under different conditions.

*3.5.2. Investigation of **GcGTPC-CH** Lipid Membrane to Act as a Substrate for PLD*

We assessed whether phospholipase-D (PLD), a biological membrane-active enzyme that cleaves phosphodiester bonds in lipids, could recognize synthetic **GcGTPC-CH** lipids as a substrate. While phospholipase-C (PLC) requires an ester functionality on the C-2 carbon of the glycerol backbone for lipid recognition[46], the structural requirements necessary for PLD to recognize a lipid substrate are not known. Following reported protocols for probing the activity of PLD in liposomes composing commercial diacyl lipids,[37–39] PLD was added to a liposomal suspension composed of pure **GcGTPC-CH** lipids in the presence of Ca^{2+} ions at 37 °C. We observed a large morphological change in

the liposomes by DLS, beginning with liposomes with average diameter of ~150 nm with Ca^{2+} containing buffer without PLD and ending with ~1500 nm diameter objects after a 30 minute incubation of **GcGTPC-CH** liposomes with PLD (Figure 3.11 blue). This result is consistent with previous reports on the effect of PLD on liposomes composed of commercial phosphocholine (PC) diacyl lipids,[37–39] which is attributed to PLD-catalyzed cleavage of the choline group from the PC headgroup that is followed by a subsequent aggregation of liposomes upon interactions of phosphatidic acid (PA) headgroups with Ca^{2+} that is present in solution. Using a commercial choline detection assay, we also confirmed that PLD can cleave the choline appendage from the lipid headgroups in pure **GcGTPC-CH** liposomes, resulting in 76.5 ± 7.8% release

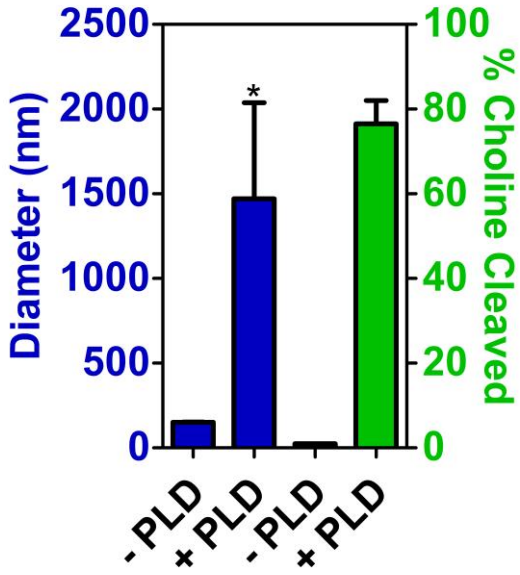

Figure 3.11**.** Effect of PLD on liposomes made with **GcGTPC-CH**. Liposome diameter measured using dynamic light scattering (DLS) after incubation with/without phospholipase-D (PLD) at 37 ºC for 30 min (blue, left axis; N = 10); Percent choline cleaved from GcGTPC-CH liposomes with/without the presence of PLD after 30 min incubation at rt (green, right axis; N = 2).

of choline from the lipid headgroups after 30 minutes at 37 °C, whereas no detectable free choline was cleaved from the lipids in the absence of PLD (Figure 3.11 green).

*3.6. Exploration of Serum Stability of **GcGTPC-CH** Liposomes*

In order to examine the potential advantage of **GcGTPC-CH** liposomes have over tetraether lipids that only contain structures from Archaea (**GMGTPC-CH**) for drug delivery system in protein-rich environments, a standard self-quenching leakage assay of CF from **GMGTPC-CH** (with or without added cholesterol) and **GcGTPC-CH** liposomes in serum-containing solutions were examined (see 3.9.8. for more details).[47] Briefly, liposomes were introduced into a buffered solution with fetal bovine serum (30% in PBS) at 37 °C and the increased fluorescence of CF upon leakage from liposomes was monitored over time. We observed an initial burst of CF fluorescence when CF-encapsulated **GMGTPC-CH** liposomes were incubated in serum-containing solutions (Figure 3.12). Whereas, CF-encapsulated **GMGTPC-CH** liposomes incubated with 40 mol% free cholesterol, exhibited a more gradual CF leakage profile than pure **GMGTPC-CH** liposomes that did not contain free cholesterol. After 5 days, the amount of CF leaked from **GMGTPC-CH** liposomes was similar, to the extent leaked with or without added free cholesterol. In contrast to these results from **GMGTPC-CH** liposomes, pure **GcGTPC-CH** liposomes exhibited a significantly reduced leakage profile of CF compared with **GMGTPC-CH** liposomes (with or

without added cholesterol), with an estimated 80% retention of encapsulated CF after 5 days of incubation in serum (Figure 3.12).

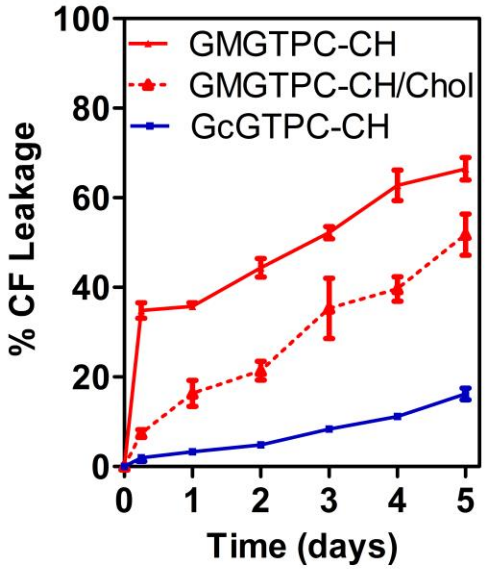

Figure 3.12**.** Percent liposomal leakage of CF after incubation with 30% serum in PBS at 37 ºC over 5 days (monitored at λ(Ex/Em) = 485/517 nm).

3.7. Small Molecule Delivery to Mammalian Cells

After observing that **GcGTPC-CH** liposomes were relatively stable in serum-containing solutions, we examined whether **GcGTPC-CH** liposomes could be used to deliver small molecule cargo into living mammalian cells. After confirming that **GcGTPC-CH** liposomes (without encapsulated cargo) were not toxic at total lipid concentrations up to 100 μM (see Figure 3.13; cell experiments were performed by Dr. Kevin Cao), we examined whether pure **GcGTPC-CH** liposomes could deliver liposome-encapsulated calcein to KB cells (a HeLa-

derived, epithelial-like cell line). We used calcein as a model for a small molecule drug in these studies because it is well known that calcein is not taken up by cells as a free molecule in cell medium, and the fluorescent properties of this molecule can be used to study its uptake in cells. In these studies, we also incorporated 0.5 mol% of a DSPE-PEG-folate (1,2-distearoyl-sn-slycero-3-phosphoethanolamine-polyethyleneglycol-folate) lipid into the liposomal membranes to facilitate folate-mediated endocytosis into KB cells (see section 3.9.9. for details).[48] The fluorescence micrograph in Figure 3.13B (taken by Dr.

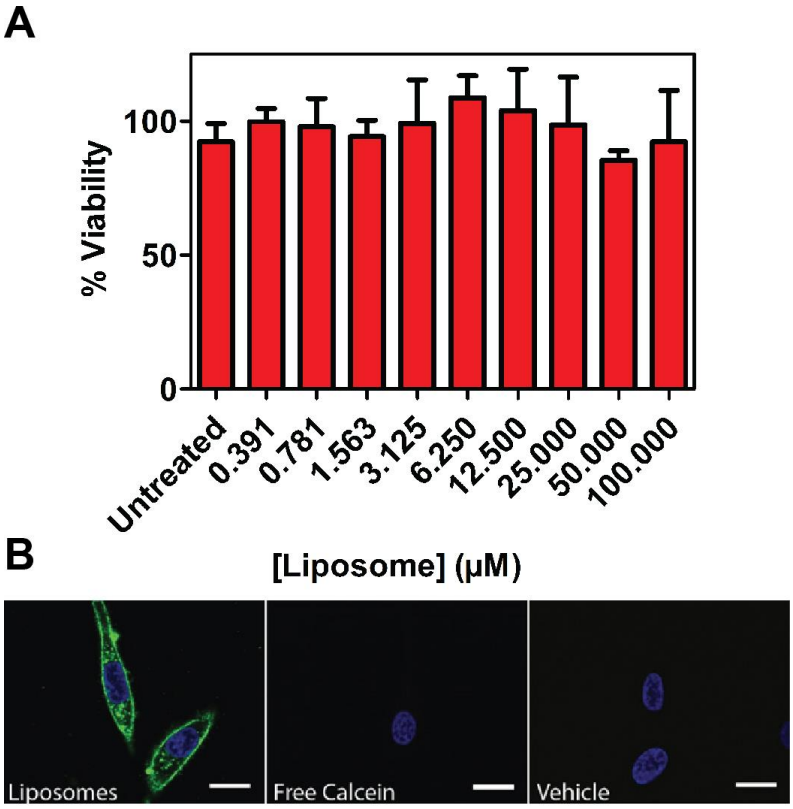

Figure 3.13**.** Cell uptake experiment with **GcGTPC-CH** liposomes. A) Cell viability assay of blank **GcGTPC-CH** liposomes against KB cells. B) Fluorescence microscopy image of KB cells after incubation with calcein (green)-encapsulated GcGTPC-CH liposomes with added 0.5 mol% of DSPE-PEG-folate lipid for 6 hours. Scale bar = 20 μm. Hoescht nuclear stain (blue) was added to stain the nuclei. Taken by Dr. Kevin Cao.

Kevin Cao) shows that calcein-encapsulated **GcGTPC-CH** liposomes are internalized into cells, demonstrating proof-of-concept that this synthetic lipid may have potential utility in liposomal drug formulations that exhibit good stability in serum-containing solutions.

3.8. *Conclusion*

We were successfully able to design and synthesize a hybrid **GcGTPC-CH** tetraether lipid that incorporates design elements inspired from two different strategies used by nature to improve membrane robustness through modifications of membrane composition and lipid structure. The new generation of tetraether lipid, **GcGTPC-CH,** exhibited a 50-fold reduction in membrane permeability to small ions when compared with membranes composed of a typical diacyl lipid, POPC, and a 5-fold reduction in membrane permeability compared with our previously reported best archaea-inspired tetraether lipid, **GMGTPC-CH**, that lacks a covalently attached cholesterol group.[16] Furthermore, pure **GcGTPC-CH** liposomes exhibited a ~30-fold reduction in leakage of a neutrally charged drug, gemcitabine, compared with POPC liposomes with 40 mol% added cholesterol, and a ~10-fold reduction in leakage of the drug compared with **GMGTPC-CH**/chol liposomes. These remarkable membrane stability data was in agreement with MD simulations that provided some mechanistic insight that both tethering of lipid tails and incorporation of covalently-attached cholesterol significantly increases the order of the lipid tails,

which decreases the variance in area per lipid and tightens lipid packing. These MD simulations also predict that the **GcGTPC-CH** lipids would exhibit the lowest water permeability of all 3 lipids examined. While **GcGTPC-CH** lipid membranes exhibit remarkably low permeability and exceptional stability in solution (with or without serum), the synthetic tetraether lipids can also retain properties that are typically found in natural membranes, such as the capability to incorporate functional biomolecules (ion channels formed from gramicidin A) and act as substrates for membrane-active enzymes (phospholipase-D). In addition, liposomes made of **GcGTPC-CH** can be used as a vehicle for cellular uptake of small molecule cargo (calcein was used as a model for a small molecule drug). While it remains to be seen whether the apparently advantageous properties of these lipids for drug delivery applications will translate to an *in vivo* setting, the results presented here support the concept that integrating covalently-attached cholesterol groups to a tethered tetraether lipid, which combines lipid design strategies exercised by eukaryotes and Archaea, leads to membranes with significantly improved stability and reduced permeability compared with membranes formed from common bilayer-forming lipid formulations.

3.9. Materials and Methods

3.9.1. Reagents and Instruments

All reagents were purchased from commercial sources and used without further purification. POPC lipid was purchased from Avanti Polar Lipids. The

POPC lipid was stored under Argon at -20°C and used within 3 months of purchase. Glassware was dried at 115°C overnight. Air and moisture-sensitive reagents were transferred using a syringe or stainless steel cannula. Intermediates were purified over silica (60Å, particle size 40-63 μm) purchased from Dynamic Adsorbents, Inc. Reactions were monitored by thin-layer chromatography (TLC) using 0.25 mm silica gel plates (60F-254) from Dynamic Adsorbents, Inc. Deuterated solvents were purchased from Cambridge Isotope Laboratories, Inc. ^{1}H, ^{13}C, ^{31}P NMR spectra were obtained on either JEOL ECA 500 spectrometer or Varian 400 MHz/500MHz spectrometer. Chemical shifts are reported in ppm relative to residual solvent. The FID file was analyzed using NMRnotebook version 2.70 build 0.10 by NMRTEC.

Dynamic Light Scattering (DLS) measurements were performed on a Wyatt DynaPro NanoStar (Wyatt Technology, Santa Barbara, CA) instrument using a disposable cuvette (Eppendorf UVette 220 nm – 1,600 nm) and data processed using Wyatt DYNAMICS V7 software. Each analysis involved an average of 10 measurements. The data was exported for final plotting using GraphPad Prism 5 (GraphPad Software, Inc., La Jolla, CA).

DSC experiments were performed in duplicate using a Thermal Analysis Q2000 DSC. Each experiment involved a 5 °C/min ramp from 0 °C to 67 °C under high purity N_2 at 50 mL/min. Samples were ~0.3 – 1.0 mg of liposomes dissolved in water at ~5% by weight. TA Universal Analysis was used to extract T_m for these samples.

Low resolution MS analysis was performed on a Micromass Quattro Ultima triple quadrupole mass spectrometer with an electrospray ionization (ESI) source. High resolution MS analysis was performed using Agilent 6230 Accurate-Mass TOFMS with an electrospray ionization (ESI) source by Molecular Mass Spectrometry Facility (MMSF) in the department of chemistry and biochemistry at University of California, San Diego.

Fluorescence decay measurements were taken on a Perkin Elmer Enspire© multimode plate reader (excitation 485 nm, emission 517 nm and 75 flashes); each measurement was taken with a 10 sec delay with 125 repeat (total acquisition time = 21 min). Costar EIA/RIA plates were used (96 well half area, no lid, flat bottom, non-treated black polystyrene). The data were exported for final plotting using GraphPad Prism 5 (GraphPad Software, Inc., La Jolla, CA).

HPLC analyses were performed using an Agilent 1100 Series HPLC and an analytical reverse-phase column (Eclipse XDB-C18 Agilent, 5 µm, 150 x 4.6 mm). Flow: 1 mL/min. Injection volume = 50 µL. Detection: 254 and 280 nm. Mobile phase: water/acetonitrile containing 0.1% (v/v) trifluoroacetic acid (TFA). *Method A*: Linear gradient from 5% to 95% of ACN in 10 minutes followed by 2 minutes of re-equilibration at 5% of ACN.

3.9.2. General Synthetic Procedures

(1R,3S)-1,3-bis(13-((2,2-dimethyl-1,3-dioxolan-4-yl)methoxy)tridecyl)cyclohexane (**3.1**)

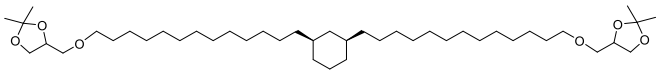

To a solution of solketal (0.26 g, 1.96 mmol) in 25 mL of dry THF, NaH (0.07g, 2.8 mmol)) was added at 0 °C and stirred for 1 hour at room temperature. Next, 0.56 g (0.94 mmol) molecule **2.36** was added and then heated at reflux for 16 hours. The reaction was quenched with water and the solvent was removed under vacuum. The residue was extracted with DCM, washed successively with water and brine, then dried over $MgSO_4$ and purified by column chromatography on silica gel using Hexane/EtOAc (9:1) as the eluent. Compound **3.1** was obtained as a clear oil (0.206 g, 31%).

Rf: 0.35 (Hexane/EtOAc 9:1); ^{1}H NMR (500 MHz, $CDCl_3$-d_1) δ 4.21 (m, *J* = 6.0 Hz, 2H), 4.00 (dd, *J* = 8.3, 6.0 Hz, 2H), 3.67 (dd, *J* = 8.3, 6.0 Hz, 2H), 3.48-3.35 (m, 8H), 1.68-1.61 (m, 4H), 1.55-1.50 (m, 4H), 1.37 (s, 6H), 1.31 (s, 6H), 1.25-1.08 (m, 47H), 0.74-0.66 (m, 2H), 0.46-0.39 (m, 1H); ^{13}C NMR (126 MHz, $CDCl_3$-d_1) δ 109.5, 77.5, 77.2, 77.0, 74.9, 72.0, 72.0, 67.1, 40.7, 38.0, 37.9, 33.6, 30.2, 29.9, 29.9, 29.8, 29.7, 29.6, 27.1, 26.9, 26.6, 26.2, 25.6; ESI-MS: 731.61 $[M+Na]^+$; HRMS 731.6160 calcd for $[C_{44}H_{84}O_6Na]^+$, found 731.6158.

3,3'-((((1R,3S)-cyclohexane-1,3-diyl)bis(tridecane-13,1-diyl))bis(oxy))bis(propane-1,2-diol) (**3.2**)

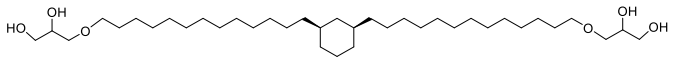

To a solution of **3.1** (0.206g, 0.29 mmol) in 0.4 mL of THF and 0.12 mL of TFA, 0.06 mL of conc. HCl (aq) was added and stirred at rt for 4 hours. Solvent was removed under vacuum and dried further using a high vac. overnight. **3.2** (141 mg, 77%) was obtained as a white solid.

^{1}H NMR (500 MHz, MeOD-d_4/$CDCl_3$-d_1 1:1) δ 3.47-3.43 (m, 2H), 3.28-3.21 (m, 2H), 3.20-3.09 (m, 10H), 1.36-1.33 (m, 4H), 1.25-1.21 (m, 4H), 0.92-0.78 (m, 47H), 0.45-0.37 (m, 2H), 0.17-0.10 (m, 1H).

3,3'-((((1R,3S)-cyclohexane-1,3-diyl)bis(tridecane-13,1-diyl))bis(oxy))bis(1-(trityloxy)propan-2-ol) (**3.3**)

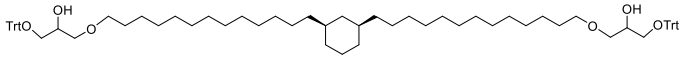

To a solution of **3.2** (0.139 mg, 0.22 mmol) in 1.2 mL of dry THF and 0.142 mL of dry pyridine, trityl chloride (0.15 g, 0.55 mmol) was added and stirred at 50 °C overnight. The reaction was cooled to rt and then the solvent was removed under vacuum, extracted with EtOAc 10 mL three times, washed with water then brine, and dried over $MgSO_4$. The crude oil was purified by column chromatography on silica gel using Hexane/EtOAc (9:1) as the eluent. Compound **3.3** was obtained as a clear oil (0.096 g, 39%).

Rf: 0.48 (Hexane/EtOAc 4:1); ^{1}H NMR (500 MHz, $CDCl_3$-d_1) δ 7.48-7.46 (m, 12H), 7.33-7.24 (m, 18H), 4.00-3.96 (m, 2H), 3.56-3.42 (m, 8H), 3.23-3.19 (m, 4H), 2.53-2.50 (m, 2H), 1.75-1.71 (m, 4H), 1.58-1.54 (m, 4H), 1.32-1.18 (m, 51.5H extra protons most likely from EtOAc), 0.82-0.74 (m, 2H), 0.55-0.48(m, 1H); ^{13}C NMR (126 MHz, $CDCl_3$-d_1) δ 144.0, 128.8, 128.0, 127.2, 86.7, 72.2, 71.8, 70.0, 64.7, 40.7, 37.9, 37.9, 33.6, 30.2, 29.8, 29.8, 29.7, 27.1, 26.6, 26.2.

(3S,8S,9S,10R,13R,14S,17R)-10,13-dimethyl-17-((R)-6-methylheptan-2-yl)-2,3,4,7,8,9,10,11,12,13,14,15,16,17-tetradecahydro-1H-cyclopenta[a]phenanthren-3-yl 4-methylbenzenesulfonate (**3.4**)

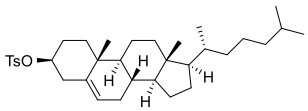

Molecule **3.4** was synthesized as previously reported.[49]

2-(((3S,8S,9S,10R,13R,14S)-10,13-dimethyl-17-((R)-6-methylheptan-2-yl)-2,3,4,7,8,9,10,11,12,13,14,15,16,17-tetradecahydro-1H-cyclopenta[a]phenanthren-3-yl)oxy)ethan-1-ol **(3.5)**

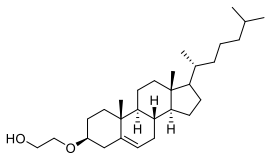

Compound **3.5** was prepared following a previously reported protocol.[22]

2-(((3S,8S,9S,10R,13R,14S)-10,13-dimethyl-17-((R)-6-methylheptan-2-yl)-2,3,4,7,8,9,10,11,12,13,14,15,16,17-tetradecahydro-1H-cyclopenta[a]phenanthren-3-yl)oxy)ethyl 4-methylbenzenesulfonate (**3.6**)

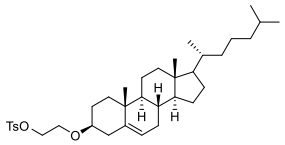

Compound **3.6** was prepared following a previously reported protocol.[22]

5-(2-(((3S,8S,9S,10R,13R,14S)-10,13-dimethyl-17-((R)-6-methylheptan-2-yl)-2,3,4,7,8,9,10,11,12,13,14,15,16,17-tetradecahydro-1H-cyclopenta[a]phenanthren-3-yl)oxy)ethoxy)-2-phenyl-1,3-dioxane (**3.7**)

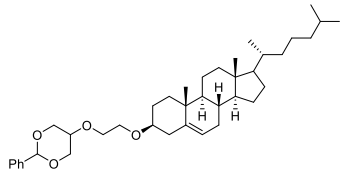

To a cooled suspension of 0.27 g (11 mmol) of NaH in 5 mL of dry tetrahydrofuran (THF), 0.67 g (3.7 mmol) of *cis*-1,3-O-Benzylideneglycerol was added drop wise and reacted for 1 hour at room temperature. Next, 1.97 g (4.1 mmol) molecule **3.6** was added and then heated at reflux for 16 hours. The reaction was quenched with water and the solvent was removed under vacuum. The residue was extracted with DCM, washed successively with water and brine, then dried over $MgSO_4$ and compound **3.7** was obtained as a white solid and then engaged to the next step.

3-(benzyloxy)-2-(2-(((3S,8S,9S,10R,13R,14S)-10,13-dimethyl-17-((R)-6-methylheptan-2-yl)-2,3,4,7,8,9,10,11,12,13,14,15,16,17-tetradecahydro-1H-cyclopenta[a]phenanthren-3-yl)oxy)ethoxy)propan-1-ol **(3.8)**

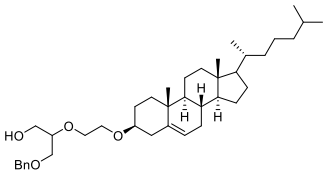

1.57 g (2.7 mmol) of **3.7** was dissolved in 7.5 mL of dry dichloromethane (DCM) then cooled to -78 °C. 7.7 mL of DIBAL-H in DCM (1 M) was added dropwise and the reaction was slowly brought back to room temperature and reacted for 16 hours. The reaction was quenched with methanol and 27 mL of (5 M) NaOH was added. The solution was then extracted with diethyl ether, washed successively with water and brine, then dried over $MgSO_4$ and purified by column chromatography on silica gel using Hexane/EtOAc (1:1) as the eluent. Compound **3.8** was obtained as a white oily solid (1.39 g, 88%).

Rf: 0.59 (Hexane/EtOAc 1:1); ^{1}H NMR (500 MHz, $CDCl_3$-d_1) δ 7.28-7.17 (m, 5H), 5.27-5.26 (m, 1H), 4.46 (s, 2H), 3.82-3.80 (m, 1H), 3.63-3.38 (m, 9H), 3.18-3.08 (m, 1H), 2.34-2.27 (m, 1H), 2.17-2.11 (m, 1H), 1.96-1.72 (m, 5H), 1.51-1.18 (m, 11H), 1.09-0.78 (m, 22H), 0.61 (s, 3H); ^{13}C NMR (126 MHz, $CDCl_3$-d_1) δ 140.5, 138.1, 128.3, 127.6, 127.6, 121.7, 80.2, 80.2, 79.5, 73.4, 70.3, 70.2, 70.1, 67.6, 67.5, 62.7, 56.7, 56.2, 50.1, 42.3, 39.8, 39.5, 38.9, 37.1, 36.8, 36.2, 35.8, 31.9, 31.8, 28.3, 28.0, 24.3, 23.9, 22.9, 22.6, 21.1, 19.4, 18.8, 11.9; ESI-MS: 617.53 $[M+Na]^+$; HRMS 617.4540 calcd for $[C_{39}H_{62}O_4Na]^+$, found 617.4534.

(3R,8R,9R,10S,13S,14R)-3-(2-((1-(benzyloxy)-3-((12-((1S,3R)-3-(13-(3-(benzyloxy)-2-(2-(((3S,8S,9S,10R,13R,14S)-10,13-dimethyl-17-((R)-6-methylheptan-2-yl)-2,3,4,7,8,9,10,11,12,13,14,15,16,17-tetradecahydro-1H-cyclopenta[a]phenanthren-3-yl)oxy)ethoxy)propoxy)tridecyl)cyclohexyl)dodecyl)oxy)propan-2-yl)oxy)ethoxy)-10,13-dimethyl-17-((S)-6-methylheptan-2-yl)-2,3,4,7,8,9,10,11,12,13,14,15,16,17-tetradecahydro-1H-cyclopenta[a]phenanthrene **(3.9)**

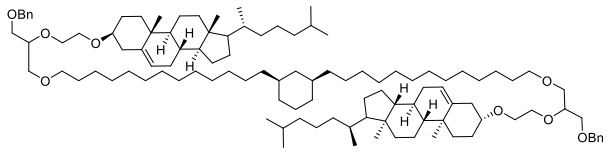

To a cooled suspension of 0.08 g (3.2 mmol) of NaH in 34 mL of dry THF, 1.39 g (2.3 mmol) of **3.8** was added drop wise and reacted for 1 hour at room temperature. Next, 0.64 g (1.1 mmol) molecule **2.36** was added and then heated at reflux for 16 hours. The reaction was quenched with water and the solvent was removed under vacuum. The residue was extracted with DCM, washed successively with water and brine, then dried over $MgSO_4$ and purified by column chromatography on silica gel using Hexane/EtOAc (9:1) as the eluent. Compound **3.9** was obtained as a clear oil (0.441 g, 29%).

Rf: 0.15 (Hexane/EtOAc 9:1); ^1H NMR (500 MHz, $CDCl_3$-d_1) δ 7.33-7.25 (m, 10H), 5.32-5.31 (m, 2H), 4.55 (s, 4H), 3.76-3.74 (m, 4H), 3.72-3.58 (m, 2H),

3.63-3.49 (m, 12H), 3.42 (t, *J* = 6.7 Hz, 4H), 3.22-3.14 (m, 2H), 2.38-2.35 (m, 2H), 2.21-2.16 (m, 2H), 2.03-1.81 (m, 10H), 1.72-1.68 (m, 4H), 1.55-1.42 (m, 14H), 1.31-0.74 (m, 105 H), 0.67 (s, 6H), 0.51-0.44 (m, 1H); ^{13}C NMR (126 MHz, $CDCl_3$-d_1) δ 141.2, 138.6, 128.5, 127.8, 127.7, 121.7, 79.6, 78.7, 73.6, 71.9, 70.9, 70.5, 70.2, 68.2, 67.7, 57.0, 56.4, 50.4, 42.5, 40.8, 40.0, 39.7, 39.3, 38.0, 37.9, 37.4, 37.1, 36.4, 36.0, 33.6, 32.1, 32.1, 30.3, 30.0, 29.9, 29.7, 28.6, 28.4, 28.2, 27.2, 26.6, 26.3, 25.8, 24.5, 24.0, 23.0 ,22.8, 21.3, 19.6, 18.9, 12.1; ESI-MS: HRMS 1656.3883 calcd for $[C_{110}H_{184}O_8Na]^+$, found 1656.3879.

2-(2-(((3S,8S,9S,10R,13R,14S)-10,13-dimethyl-17-((R)-6-methylheptan-2-yl)-2,3,4,7,8,9,10,11,12,13,14,15,16,17-tetradecahydro-1H-cyclopenta[a]phenanthren-3-yl)oxy)ethoxy)-3-((13-((1R,3S)-3-(13-(2-(2-(((3R,8R,9R,10S,13S,14R)-10,13-dimethyl-17-((S)-6-methylheptan-2-yl)-2,3,4,7,8,9,10,11,12,13,14,15,16,17-tetradecahydro-1H-cyclopenta[a]phenanthren-3-yl)oxy)ethoxy)-3-hydroxypropoxy)tridecyl)cyclohexyl)tridecyl)oxy)propan-1-ol **(3.10)**

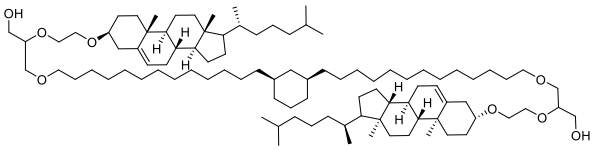

35 mg (0.022 mmol) of **3.9** and 1.8 mg (5% w/w) of $Pd(OH)_2$ was added to 4 mL of solvent mixture THF/EtOH (1:1). The suspension was purged with N_2 gas for 10 seconds and repeated 3 times. The suspension was then purged using

H_2 for 10 seconds and repeated 3 times. The reaction was stirred at room temperature for 20 mins. The suspension was then immediately filtered over celite and purified using column chromatography on silica gel using Hexane/EtOAc (7:3) as the eluent. Compound **3.10** was obtained as a white viscous oil (20.3 mg g, 65%).

Rf: 0.13 (Hexane/EtOAc 7:3); ^{1}H NMR (500 MHz, $CDCl_3$-d_1) δ 5.27-5.26 (m, 2H), 3.86-3.81 (m, 2H), 3.64-3.34 (m, 20H), 3.18-3.11 (m, 2H), 2.32-2.27 (m, 2H), 2.18-2.11 (m, 2H), 1.96-1.73 (m, 10H), 1.65-1.59 (m, 4H), 1.50-1.38 (m, 14H), 1.27-0.65 (m, 105H), 0.59 (s, 6H), 0.44-0.38 (m, 1H); ^{13}C NMR (126 MHz, $CDCl_3$-d_1) δ 140.9, 122.0, 80.3, 80.3, 79.8, 72.0, 71.2, 70.4, 70.4, 67.8, 67.7, 63.3, 57.0, 56.4, 50.4, 42.5, 40.8, 40.0, 39.7, 39.1, 39.1, 38.0, 38.0, 37,4, 37.1, 36.4, 36.0, 33.7, 32.1, 32.1, 30.3, 30.0, 29.9, 29.8, 29.7, 28.5, 28.5, 28.4, 28.2, 27.2, 26.6, 26.3, 24.5, 24.0, 23.0 22.8, 21.3, 19.6, 18.9, 12.1; ESI-MS: 1476.28 $[M+Na]^+$; HRMS 1476.2944 calcd for $[C_{96}H_{172}O_8Na]^+$, found 1476.2952.

2-(2-(((3S,8S,9S,10R,13R,14S)-10,13-dimethyl-17-((R)-6-methylheptan-2-yl)-2,3,4,7,8,9,10,11,12,13,14,15,16,17-tetradecahydro-1H-cyclopenta[a]phenanthren-3-yl)oxy)ethoxy)-3-((13-((1R,3S)-3-(13-(2-(2-(((3R,8R,9R,10S,13S,14R)-10,13-dimethyl-17-((S)-6-methylheptan-2-yl)-2,3,4,7,8,9,10,11,12,13,14,15,16,17-tetradecahydro-1H-cyclopenta[a]phenanthren-3-yl)oxy)ethoxy)-3-((oxido(2-

(trimethylammonio)ethoxy)phosphoryl)oxy)propoxy)tridecyl)cyclohexyl)tridecyl) oxy)propyl (2-(trimethylammonio)ethyl) phosphate **(GcGTPC-CH)**

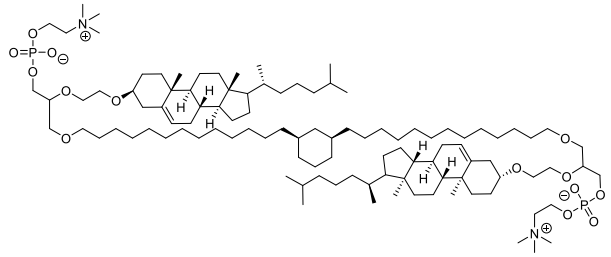

To a solution of 81 mg (0.34 mmol) of bromoethyldichlorophosphate in 1.5 mL of dry THF, a solution of 61 mg (0.04 mmol) of **3.10** and 64 µL of Et_3N (0.46 mmol) in 1.5 mL of dry THF was added dropwise. After stirring the mixture for 3 days in the dark at room temperature, toluene was added to precipitate triethylammonium chloride. Then, the solution was filtered through a small pad of celite and the filtrate was concentrated. The resulting residue was dissolved in a mixture of THF/$NaHCO_3$ (sat) (2.8 mM) and the reaction was stirred for 16 hours at room temperature. THF was evaporated under vacuum and the resulting aqueous solution was acidified to pH 1 using a dilution solution of hydrochloric acid (1M) and extracted using several portions of DCM/Methanol (MeOH) (8:2). The organic layers were combined, dried over Na_2SO_4 and concentrated under reduced pressure.

To a solution of the previous crude in a mixture of 3.5 mL of chloroform ($CHCl_3$) and 4 mL of Me_3N (33% in EtOH) was added and the reaction was stirred in a sealed tube at room temperature for 5 days. The reaction mixture was concentrated to dryness, purified on sephadex LH-20 using DCM/MeOH (1:1)

as eluent and purified by column chromatography on silica gel using DCM/MeOH/Water (70:30:5) as the eluent. **GcGTPC-CH** was obtained as a white (viscous oil) (40 mg, 53%).

Rf: 0.15 (Hexane/EtOAc 9:1); ^{1}H NMR (500 MHz, MeOD-d_4/$CDCl_3$-d_1 1:1) δ 4.99-4.95 (m, 2H), 3.92-3.85 (m, 4H), 3.57-3.52 (m, 4H), 3.43-3.33 (m, 6H), 3.29-3.05 (m, 16H), 2.97-2.94 (m, 2H), 2.85-2.84 (m, 18H), 2.00-1.77 (m, 4H), 1.67-1.44 (m, 10H), 1.34-1.32 (m, 4H), 1.19-1.07 (m, 15H), 0.98-0.32 (m, 110H), 0.16-0.08 (m, 1H); ^{13}C NMR (126 MHz, $CDCl_3$-d_1) δ 140.2, 121.4, 79.1, 78.3, 78.2, 71.3, 70.3, 69.6, 67.1, 66.0, 64.8, 64.8, 58.6, 58.6, 56.5, 55.9, 53.5, 49.9, 41.9, 40.2, 39.5, 39.1, 38.7, 37.4, 36.8, 36.4, 35.8, 35.5, 33.1, 31.6, 31.5, 29.7, 29.4, 29.3, 29.2, 28.0, 27.8, 27.6, 26.6, 26.0, 25.8, 23.9, 23.4, 22.1, 21.9, 20.7, 18.8, 18.1, 11.3; ^{31}P NMR (202 MHz, MeOD-d_4/$CDCl_3$-d_1 1:1) δ 0.12; HRMS 1784.4235 calcd for $[C_{106}H_{197}N_2O_{14}P_2]^+$, found 1784.4264.

3.9.3. General Buffer Preparation Procedures

Preparation of Buffer A- 4.18 g of Bis Tris (10 mM) and 11.68 g of NaCl (100 mM) was dissolved in 2 L of Milli-Q filtered deionized water. The pH was then adjusted to 7.2 by minimal addition of 2 M HCl.

Preparation of Buffer B - 4.18 g of Bis Tris (10 mM) and 11.68 g of NaCl (100 mM) was dissolved in 2 L of Milli-Q filtered deionized water. The pH was then adjusted to 5.8 by minimal addition of 2 M HCl.

Preparation of Buffer C – 5.2 g of 2-[4-(2-hydroxyethyl)piperazin-1-yl]ethanesulfonic acid (HEPES) (10 mM) and 17.5 g of NaCl (150 mM), were dissolved in 2 L of Milli-Q filtered deionized water. The pH was then adjusted to 7.4.

Preparation of Buffer D – 0.46 g of 2-[(2-Hydroxy-1,1-bis(hydroxymethyl)ethyl)amino]ethanesulfonic acid, N-[Tris(hydroxymethyl)methyl]-2-aminoethanesulfonic acid (TES) (2 mM), 5.84 g of NaCl (100 mM), 0.029 g of ethylenediaminetetraacetic acid (EDTA) (0.1 mM), and 0.31 g of histidine (2 mM) was dissolved in 1 L of Milli-Q filtered deionized water. The pH was then adjusted to 7.4.

Preparation of Buffer E – 0.23 g of TES (2 mM), 2.11 g of NaCl (72.23 mM), 0.62 g of CaCl2 (11.11 mM), 0.015 g of EDTA (0.1 mM), and 0.16 g of histidine (2 mM) was dissolved in 0.5 L of Milli-Q filtered deionized water. The pH was then adjusted to 7.4.

3.9.4. Gemcitabine Leakage Experiment Procedures

The *in vitro* leakage of the gemcitabine (GEM) from liposomes was measured using a dialysis assay. GEM encapsulated liposomes were made by weighing 10 mg of lipid and 40 mol% of cholesterol (only for POPC and **GMGTPC-CH**) into a 5 mL round bottom flask and dissolved in 1:1 chloroform/methanol. The solvent was evaporated *via* vacuo to form a lipid film and hydrated with 500 µL of 60 mM GEM in Buffer C. 50 µL of the stock liposomal formulation (20 mg/mL) was diluted with buffer C to 500 µL and purified using Sephadex® G-25 to prepare a 1 mL working solution. The purified liposomal suspensions were placed in a dialysis device (Slide-A-Lyzer® Mini dialysis, ref 88405, Thermo Scientific) with a molecular weight cutoff of 20 kDa and dialyzed against 42.5 mL of buffer C at 37 °C and shaken on an orbital shaker (50 rpm). At various time points, aliquots (40 µL) were withdrawn from the dialysis compartment and retention of encapsulated drug was measured by HPLC.

For HPLC measurements analysis, to a vial, 40 µL of a Triton solution (0.5 % w/v in HBS) was added to 40 µL of liposomal suspension. The samples were vortexed and analyzed by HPLC using method A for the detection of GEM. Data was analyzed using Agilent analysis software (Chemstation®). For each time point, the percentage of drug remaining in the liposomes was calculated using the following equation (1):

$$Retained\ drug\ (\%) = 100 \times \frac{Area(t)}{Area\ (t0)} \quad (1)$$

Molecular Dynamics Simulations and Analysis Procedures

Lipids were first constructed using Maestro (Schrödinger LLC, New York, NY). Membranes containing 729 lipids were then built and solvated using TIP3P water using VMD5. Each system was minimized and heated in 75 K steps, reaching a final temperature of 300 K. Following about 20 ns of equilibration, MD simulations for all membrane systems were performed for 100 ns under isothermal-isobaric (NpT) conditions. The temperature was maintained by using the Nose-Hoover chain method and the pressure was maintained at 1 atm. The CHARMM36 force field was used with a 10 Å cut-off for van der Waals with an 8.5 Å switching distance, and Particle Mesh Ewald for long-range electrostatics. All the simulations were carried out using NAMD6, and post-simulation trajectory analysis was carried out using both VMD, R (http://www.r-project.org), and the Bio3D package.[50,51]

To identify the number of water molecules in the core of the membrane, we used methods described previously[34]. In short, we identified water molecules that penetrated past the head groups and into the carbon-rich region of the membrane, i.e. between the ether or ester oxygens of the head groups on either side of the membrane. The calculation was performed in a grid fashion across the full membrane and the results reported were the total number of waters within the membrane for each snapshot over the final 50 ns of the trajectory.

3.9.5. General Procedure for Monitoring Gramicidin A Activity in Liposomes

GcGTPC-CH liposomes were prepared as described in general procedures for liposome extrusion. The general procedure to measure pH equilibrium of CF was used with a small modification. After the liposomes were prepared, a solution of gA was prepared 225 µM in DMSO. To each tube (i.e. pH 7.2, pH 5.8, pH 5.8 + nigericin) 2 µL of buffer A was added to control the volume. Additional solution containing 2 µL of DMSO (vehicle) or 2 µL gA (final concentration of 1 µM) was incubated at 37 ºC with liposomes for 30 minutes and CF fluorescence was measured and analyzed.

3.9.6. General Procedure for Phospholipase-D Induced Cleavage of Choline

GcGTPC-CH liposomes were prepared as described in chapter 2, section 2.5.9. The liposomes were first hydrated in buffer D, then the liposome formulation was incubated in buffer E with or without 5 units of PLD from cabbage (Sigma Aldrich) at 37 ºC for 30 minutes. After incubation, the liposome size was measured using dynamic light scattering (DLS) to study whether a morphology change occurred.

Additionally, PLD activity was confirmed using a commercially available phosphorus assay kit (Sigma, MAK122) according to the manufacturer's protocol. We estimated the percent choline released, which is directly correlated

with the phosphorus concentration, by normalization to the phosphorus concentration obtained by the Bartlett assay[27].

3.9.7. General Procedure for Self-Quenched CF Liposomal Release Assay in Serum

Liposomes prepared as described in chapter 2, section 2.5.9. Using the method of self-quenched CF loaded (100 mM in PBS) leakage assay[47], liposomes comprised of **GcGTPC-CH** (using general procedure for liposome extrusion) were incubated in PBS with 30 % fetal bovine serum (FBS) at 37 ºC (final liposome dilution of 1000 times from stock extruded solution) and CF fluorescence was monitored (Ex 485 nm/Em 517) nm for up to 5 days.

*3.9.8. General Procedure for Cellular Uptake of Small Molecules Entrapped in **GcGTPC-CH** Liposomes*

*3.9.8.1. Cell Toxicity Studies of **GcGTPC-CH** Liposomes*

KB cells were plated onto a fibronectin-treated 96 well plate at 5000 cells/well in folate deficient Roswell Park Memorial Institute (RPMI) 1640 medium (Invitrogen). The cells were incubated for 24 hours under a humidified atmosphere of 95% air and 5% CO_2 at 37 °C. After 24 hours of incubation, the cells were dosed with various concentrations of the liposomes, in triplicate. The cells were incubated with the liposomes for 24 hours, and then washed to

remove unbound compound. After incubation with the liposomes, the cells were carefully washed three times with 200 µL phosphate buffered saline (PBS) buffer and fixed with a solution of 200 µL PBS and 50 µL of 50% trichloroacetic acid. The cells were allowed to fix at 4°C for 1 hr. After fixation, the cells were washed five times with water and allowed to dry. After the plates are dried, 100 µL of a 0.4 % sulforhodamine B (SRB, Sigma Aldrich, S1402) solution in 1% acetic acid was added to each of the wells and incubated for 30 minutes at room temperature on a shaker. The SRB-treated cells were then washed five times with 1 % acetic acid and allowed to dry. Tris base solution (100 mM, 200 µL) was then added to each well and the plates were placed on an orbital shaker for 30 minutes. The plates were then read on a microplate reader at 515 nm. The absorbance values were used to create cell-toxicity curves.

*3.9.8.2. Fluorescence Microscopy of **GcGTPC-CH** Liposomal Uptake*

To a dry lipid film of **GcGTPC-CH** lipid with added 0.5 mol % of DSPE-PEG2000-folate lipid, 10 mM calcein in buffer A was then used to hydrate the lipid film. Liposomes were then prepared as described in chapter 2, section 2.5.9.

KB cells were plated with folate deficient RPMI-1640 media supplemented with 10% fetal bovine serum (FBS) on 10mm glass bottom plates and incubated for 12 hours. Media was then removed and a solution containing 10 µM of liposomes, free calcein, or PBS control was added to the cells and

incubated for 6 hours. Cells were then rinsed with media once, and a fresh media containing 2 μg/mL Hoescht nuclear stain was added. The living cells where then immediately imaged with an Olympus FluoView FV1000 deconvolution IX81 inverted confocal microscope equipped with a 405, 488, and 543 laser line. Fluorescence images were processed with ImageJ.

3.10. Acknowledgements

Chapter 3 is adapted, in part, from Takaoki Koyanagi, Kevin J. Cao, Geoffray Leriche, David Onofrei, Gregory P. Holland, Michael Mayer, David Sept, and Jerry Yang, “Hybrid Lipids Inspired by Extremophiles and Eukaryotes Afford Serum-Stable Membranes with Low Leakage.” *Chem. - Eur. J.* 2017, 6757–6762. Copyright 2017 Wiley. Permission to use copyrighted images and data in the manuscript was obtained from Kevin J. Cao, Geoffray Leriche, David Onofrei, Gregory P. Holland, Michael Mayer, David Sept, and Jerry Yang. The dissertation author is the first author of this manuscript.

3.11. References

(1) Torchilin, V. P. *Nat. Rev. Drug Discov.* **2005**, *4* (2), 145–160.

(2) Lasic, D. D. *Angew. Chem., Int. Ed. Engl.* **1994**, *33* (17), 1685–1698.

(3) Senior, J.; Gregoriadis, G. *Life Sci.* **1982**, *30* (I), 2123–2136.

(4) Spuch, C.; Navarro, C. *J. Drug Deliv.* **2011**, *2011*, 1–12.

(5) Cheng, J.; Teply, B. A.; Sherifi, I.; Sung, J.; Luther, G.; Gu, F. X.; Levy-Nissenbaum, E.; Radovic-Moreno, A. F.; Langer, R.; Farokhzad, O. C. *Biomaterials* **2007**, *28* (5), 869–876.

(6) Malam, Y.; Loizidou, M.; Seifalian, A. M. *Trends Pharmacol. Sci.* **2009**, *30* (11), 592–599.

(7) Colby, A. H.; Liu, R.; Schulz, M. D.; Padera, R. F.; Colson, Y. L.; Grinstaff, M. W. *Sci. Rep.* **2016**, *6* (November 2015), 18720.

(8) Tiwari, G.; Sriwastawa, B.; Pandey, S.; Bannerjee, S.; Tiwari, R.; Bhati, L.; Pandey, P. *Int. J. Pharm. Investig.* **2012**, *2* (1), 2.

(9) Danhier, F.; Feron, O.; Préat, V. *J. Control. Release* **2010**, *148* (2), 135–146.

(10) Ercole, F.; Whittaker, M. R.; Quinn, J. F.; Davis, T. P. *Biomacromolecules* **2015**, *16*, 1886–1914.

(11) Allen, T. M.; Cullis, P. R. *Adv. Drug Deliv. Rev.* **2013**, *65* (1), 36–48.

(12) Mura, S.; Nicolas, J.; Couvreur, P. *Nat. Mater.* **2013**, *12* (11), 991–1003.

(13) Benvegnu, T.; Réthoré, G.; Brard, M.; Richter, W.; Plusquellec, D. *Chem. Commun.* **2005**, 5536–5538.

(14) van Meer, G.; Voelker, D. R.; Feigenson, G. W. *Nat. Rev. Mol. Cell Biol.* **2008**, *9* (2), 112–124.

(15) Chong, P. L.-G.; Ayesa, U.; Daswani, V. P.; Hur, E. C. *Archaea* **2012**, *2012*, 1–11.

(16) Koyanagi, T.; Leriche, G.; Onofrei, D.; Holland, G. P.; Mayer, M.; Yang, J. *Angew. Chemie Int. Ed.* **2016**, *55* (5), 1890–1893.

(17) Haines, T. H. *Prog. Lipid Res.* **2001**, *40* (4), 299–324.

(18) Huang, Z.; Jaafari, M. R.; Szoka, F. C. *Angew. Chem., Int. Ed. Engl.* **2009**, *48* (23), 4146–4149.

(19) Foglia, F.; Barlow, D. J.; Szoka, F. C.; Huang, Z.; Rogers, S. E.; Lawrence, M. J. *Langmuir* **2011**, *27* (13), 8275–8281.

(20) Kohli, A. G.; Kierstead, P. H.; Venditto, V. J.; Walsh, C. L.; Szoka, F. C. *J. Control. Release* **2014**, *190*, 274–287.

(21) Jacquemet, A.; Lemiègre, L.; Lambert, O.; Benvegnu, T. *J. Org. Chem.* **2011**, *76* (23), 9738–9747.

(22) Bajaj, A.; Kondiah, P.; Bhattacharya, S. *J. Med. Chem.* **2007**, *50* (10), 2432–2442.

(23) Blöcher, D.; Gutermann, R.; Henkel, B.; Ring, K. *BBA - Biomembr.* **1984**, *778* (1), 74–80.

(24) Mabrey, S.; Mateo, P. L.; Sturtevant, J. M. *Biochemistry* **1978**, *17* (12), 2464–2468.

(25) Koyanagi, T.; Leriche, G.; Yep, A.; Onofrei, D.; Holland, G. P.; Mayer, M.; Yang, J. *Chem. - A Eur. J.* **2016**, *22* (24), 8074–8077.

(26) Papahadjopoulos, D.; Nir, S.; Oki, S. *Biochim. Biophys. Acta - Biomembr.* **1972**, *266*, 561–583.

(27) Bartlett, G. R. *J. Biol. Chem.* **1959**, *234* (3), 466–468.

(28) Ibarguren, M.; Alonso, A.; Tenchov, B. G.; Goñi, F. M. *Biochim. Biophys. Acta - Biomembr.* **2010**, *1798* (9), 1735–1738.

(29) Leriche, G.; Cifelli, J. L.; Sibucao, K. C.; Patterson, J. P.; Koyanagi, T.; Gianneschi, N. C.; Yang, J. *Org. Biomol. Chem.* **2017**, *15* (10), 2157–2162.

(30) Swallow, S. *Prog. Med. Chem.* **2015**, *54* (2), 65–133.

(31) Kroep, J. R.; Pinedo, H. M.; van Groeningen, C. J.; Peters, G. J. *Ann Oncol* **1999**, *10 Suppl 4*, 234–238.

(32) Paula, S.; Volkov, G.; Van Hoek, N.; Haines, T. H.; Deamer, D. W. *Biophys. J.* **1996**, *70* (1), 339–348.

(33) Nagle, J. F.; Scott, H. L. *BBA - Biomembr.* **1978**, *513* (2), 236–243.

(34) Schroeder, T. B. H.; Leriche, G.; Koyanagi, T.; Johnson, M. A.; Haengel, K. N.; Eggenberger, O. M.; Wang, C. L.; Kim, Y. H.; Diraviyam, K.; Sept, D.; Yang, J.; Mayer, M. *Biophys. J.* **2016**, *110* (11), 2430–2440.

(35) Ingólfsson, H. I.; Andersen, O. S. *Assay Drug Dev. Technol.* **2010**, *8* (4), 427–436.

(36) Capone, R.; Blake, S.; Restrepo, M. R.; Yang, J.; Mayer, M. *J. Am. Chem. Soc.* **2007**, *129* (31), 9737–9745.

(37) Ichikawa, S.; Walde, P. *Langmuir* **2004**, *20* (3), 941–949.

(38) Blackwood, R. A.; Smolen, J. E.; Transue, A.; Hessler, R. J.; Harsh, D. M.; Brower, R. C.; French, S. *Am. J. Physiol.* **1997**, *272* (4 Pt 1), C1279–C1285.

(39) Leventis, R.; Gagné, J.; Fuller, N.; Rand, R. P.; Silvius, J. R. *Biochemistry* **1986**, *25* (22), 6978–6987.

(40) Jones, M. N.; Nicholas, A. R. *Biochim. Biophys. Acta - Biomembr.* **1991**, *1065* (2), 145–152.

(41) Huang, Z.; Szoka, F. C. *J. Am. Chem. Soc.* **2008**, *130* (46), 15702–15712.

(42) Leamon, C. P.; Low, P. S. *Drug Discov. Today* **2001**, *6* (1), 44–51.

(43) Yang, G.; Yang, T.; Zhang, W.; Lu, M.; Ma, X.; Xiang, G. *J. Agric. Food Chem.* **2014**, *62* (10), 2207–2215.

(44) Wang, S.; Low, P. S. *J. Control. Release* **1998**, *53*, 39–48.

(45) Mayer, M.; Yang, J. *Acc. Chem. Res.* **2013**, *46* (12), 2998–3008.

(46) Snyder, W. R. *Biochim. Biophys. Acta (BBA)/Lipids Lipid Metab.* **1987**, *920* (2), 155–160.

(47) Weinstein, J. N.; Yoshikami, S.; Henkart, P.; Blumenthal, R.; Hagins, W. a. *Science* **1977**, *195* (4277), 489–492.

(48) Cao, Y.; Yang, J. *Bioconjug. Chem.* **2014**, *25* (5), 873–878.

(49) Ju, J.; Huan, M.-L.; Wan, N.; Qiu, H.; Zhou, S.-Y.; Zhang, B.-L. *Int. J. Mol. Sci.* **2015**, *16* (3), 5666–5681.

(50) Grant, B. J.; Rodrigues, A. P. C.; ElSawy, K. M.; McCammon, J. A.; Caves, L. S. D. *Bioinformatics* **2006**, *22* (21), 2695–2696.

(51) Skjærven, L.; Yao, X.-Q.; Scarabelli, G.; Grant, B. J. *BMC Bioinformatics* **2014**, *15* (1), 399.

Chapter 4

Thiol-Responsive Hybrid Tetraether Lipid for Drug Delivery

4.1. Introduction

Liposomes have been extensively studied as a drug delivery system for their low toxicity, good biocompatibility, high entrapment efficiency and the ease of chemical structural modifications.[1–6] Specifically, stimuli-responsive liposomes have gained interest for their utility to deliver drugs that can selectively release drugs at a specific target site, and therefore, reducing side effects and overcoming drug resistance.[1,7–9] Examples of stimuli-responsive liposomes include lipids that integrate cleavable linkers sensitive to acid, UV, enzyme, biological thiols and redox.[10,11] In particular, thiol-responsive liposomes have garnered interest as a delivery system to cancer cells, in which the intracellular thiol level (i.e. thioredoxin, thioredoxin reductase, cysteine, dihydrolipoic acid and glutathione) is found to be significantly higher than the extracellular fluid that allows retention of cargo in the extracellular fluid and liposomal release of cargo upon cellular uptake (shown in Figure 4.1).[12,13] Liposomal technologies responsive to thiol are traditionally mixed with other lipids that acts as the liposomal foundation to form stable liposomes.[1] However,

one disadvantage of doping triggerable lipid analogs into diacyl lipids is the instability of liposomes in the presence of serum.[14] We are the first to demonstrate a thiol-responsive cleavable tetraether lipids that are capable of forming stable liposomes pure.

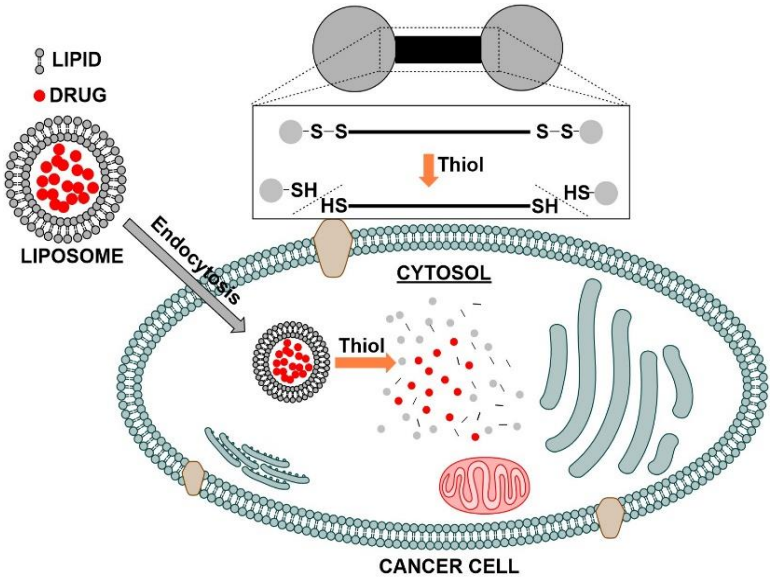

Figure 4.1. Schematic illustration of intracellular liposomal drug release triggered by thiol.

To address liposomal stability in serum, we have previously designed a synthetic hybrid lipid, namely, glycerol cholesterol-integrated glycerol tetraether lipid with phosphocholine headgroups (**GcGTPC-CH**), that incorporate structural features derived from both Eukaryotes (covalently attaching cholesterol to the glycerol lipid backbone) and Archaea (integration of cyclohexane ring to the hydrophobic core and tethering of lipid tails)[15] that showed ~50 times reduction of small ion membrane permeability and ~35 times increased retention of a neutral small molecule (gemcitabine) after 48 hours when compared with a commercial diacyl lipid while remaining stable in serum

(Chapter 3 of this dissertation). However, despite the enhanced stability and robustness, **GcGTPC-CH** liposomes lack the ability to be responsive towards stimuli, which would be advantageous for drug delivery.

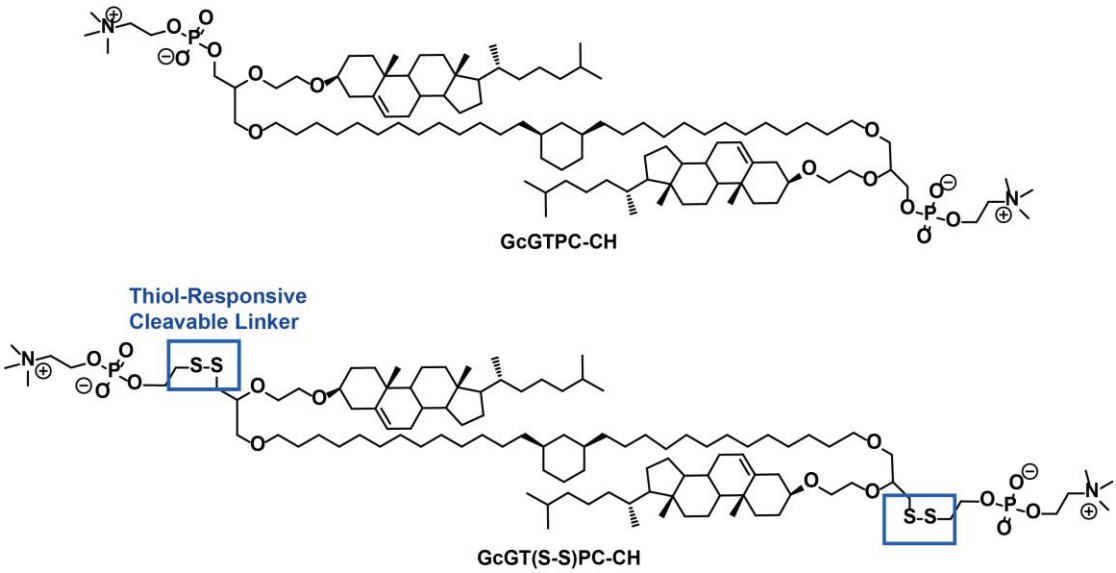

Figure 4.2. Molecular design of thiol responsive hybrid lipid **GcGT(S-S)PC-CH**.

Over the course of my PhD studies, we have designed and structurally optimized tetraether lipids, **GcGTPC-CH**, to have significantly reduced permeability to small ions and small molecules compared with commercial diacyl lipids. Consequently, we want to minimize addition of new structural features to the optimized lipid molecule to maintain the low permeability properties of **GcGTPC-CH** lipid, while making it responsive. After consideration of different possible stimuli-responsive cleavable groups, we chose to add a disulfide linker under the hypothesis that the relatively small addition to a larger lipid core will not perturb membrane packing of the lipid, rather than, for instance, the addition of H_2O_2/UV/acid cleavable linkers that typically involve the addition

of bulky aromatic groups (boronic acid conjugated to phenyl rings, nitrobenzene) or heteroatoms (orthoesters, acetals), respectively, that can disrupt lipid-membrane organization.[16–18] We began the design of the thiol responsive lipid analog by focusing the chemical modifications to a solvent accessible location, near the polar lipid headgroup, instead of the hydrophobic portion of the lipid to allow access of free thiols to the disulfide bonds. Further support to target near the headgroup of the lipid is shown in chapter 3, in which MD simulations suggests low variability in area per lipid tail that limits water molecules from entering the hydrophobic region of **GcGTPC-CH** lipid membrane. We envision that a disulfide linker between the polar lipid headgroup and the glycerol backbone will minimally affect membrane packing of the hydrophobic region of the lipid and, hence, nominally affect membrane permeability (shown in Figure 4.2). This hypothesis is further supported by our previous results that displayed a low dependence of changes in polar lipid headgroup on membrane leakage to small ions for tetraether lipid analogs (Chapter 2 of this dissertation).[19] By using this strategy, we envisioned synthesizing a cleavable lipid that would be stable and robust enough to form liposomes in pure form without the need of mixing with other lipids.

Herein, we present the synthesis of **GcGT(S-S)PC-CH** (Figure 4.2) and examined whether pure **GcGT(S-S)PC-CH** lipids can form stable liposomes. We next examined the effect of free thiols on triggered liposomal release of encapsulated cargo. Lastly, we examine the efficacy of Doxorubicin (DOX)

loaded liposomes made with **GcGT(S-S)PC-CH** lipids to kill mammalian cancer cells.

*4.2. Design/Synthesis of **GcGT(S-S)PC-CH***

We envision the most difficult step in the synthesis of **GcGT(S-S)PC-CH** lipid (Scheme 4.1) would be the formation of the disulfide bonds. We, thus, dissected the molecule into two fragments: 1) a dithiol lipid core and 2) a thiol conjugated phosphocholine. The retrosynthetic strategy for generating the thiol lipid core follows a similar synthetic strategy used for our previous tetraether lipid analogs that uses alkylation of a cyclohexane integrated dibromoalkane by a S-protected cholesterol functionalized mercaptoglycerol backbone. The addition of the cholesterol appendage to the mercaptoglycerol could then be accomplished by alkylation to the tosylated cholesterol derivative (from chapter 3) with a terminally diprotected mercaptoglycerol that can be formed by a selective terminal protection of mercaptoglycerol. Next, we focus our retrosynthetic attention to the thiol conjugated phosphocholine analog, which can be formed by alkylation of chlorophospholane by a S-Boc protected ethanolamine, followed by ring opening of the phospholane by trimethylamine.

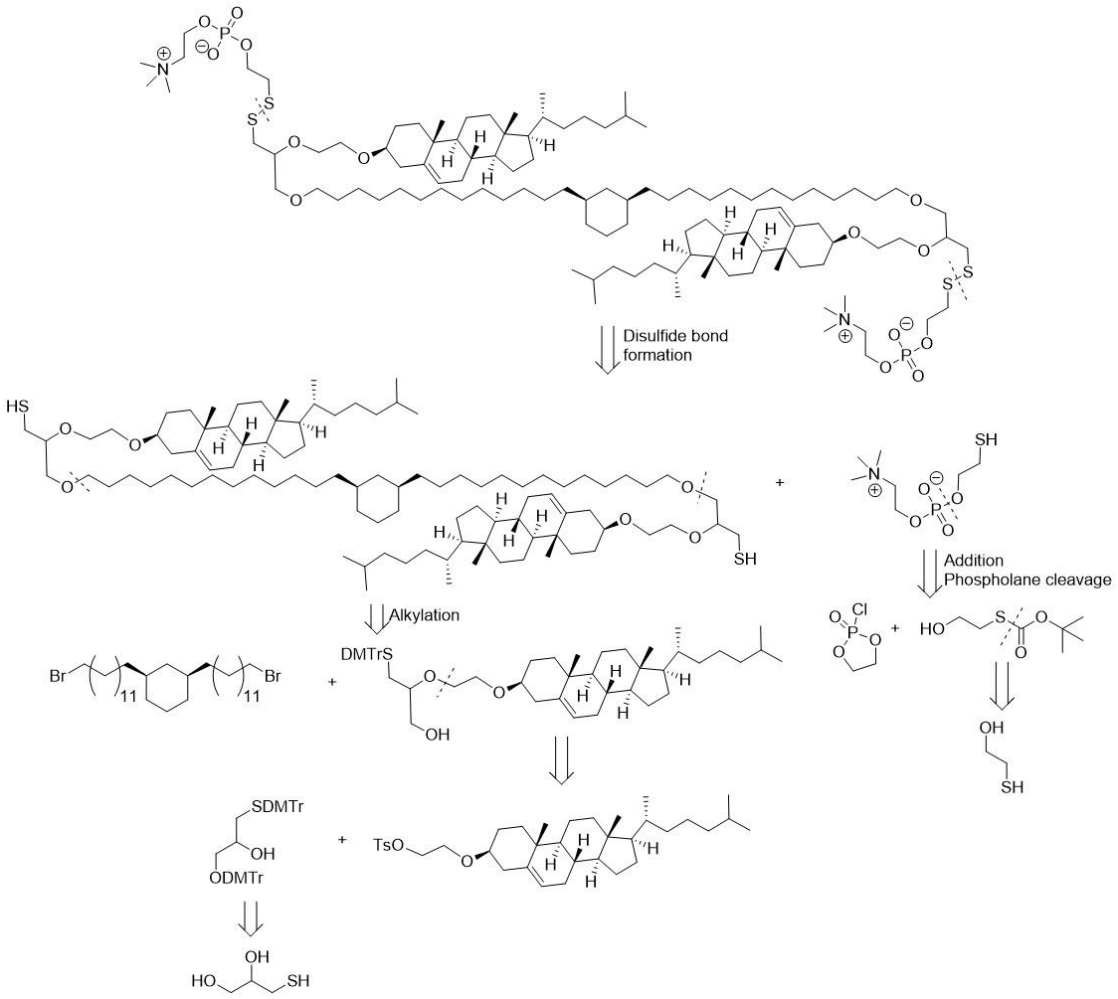

Scheme 4.1. Retrosynthetic design of **GcGT(S-S)PC-CH** lipid.

The synthesis of **GcGT(S-S)PC-CH** lipid (shown in Scheme 4.2) began by first synthesizing the phosphocholine derivative **4.2** by a selective thiol Boc-protection of 2-mercaptoethanol to form **4.1**. A nucleophilic substitution of **4.1** to 2-choloro-2-oxo-1,3,2-dioxaphospholane followed by a ring opening of phospholane with the addition of trimethylamine afforded the Boc-protected phophocholine derivative **4.2**. In parallel, the lipid core was synthesized by selectively protecting the terminal alcohol and terminal thiol of 3-mercaptopropane-1,2-diol to afford dimethoxytrityl protected glycerol derivative

4.4. The free secondary alcohol of **4.4** was reacted with tosylated cholesterol derivative **3.6** under basic conditions to afford the protected glycerol scaffold **4.5**. The glycerol scaffold **4.5** was selectively O-deprotected[20] with 80 % aqueous acetic acid to form **4.6**, in which the free alcohol successively reacted with dibromoalkane **2.36** under basic alkylating conditions to form the dimethoxytrityl protected thiol lipid **4.7**. Both protected thiol derivatives **4.2** and **4.7** were deprotected in the presence of acid, purified, dried briefly under vacuum and immediately reacted together to afford **GcGT(S-S)PC-CH** in a series of reactions involving activation of thiols on the lipid scaffold **4.8** by 4-phenyl-1,2,4-triazoline-3,5-dione (PTAD) and concluding the synthesis with the formation of the disulfide bond with thiol integrated phosphocholine **4.3** (see section 4.7.2. for details on the synthesis and characterization).

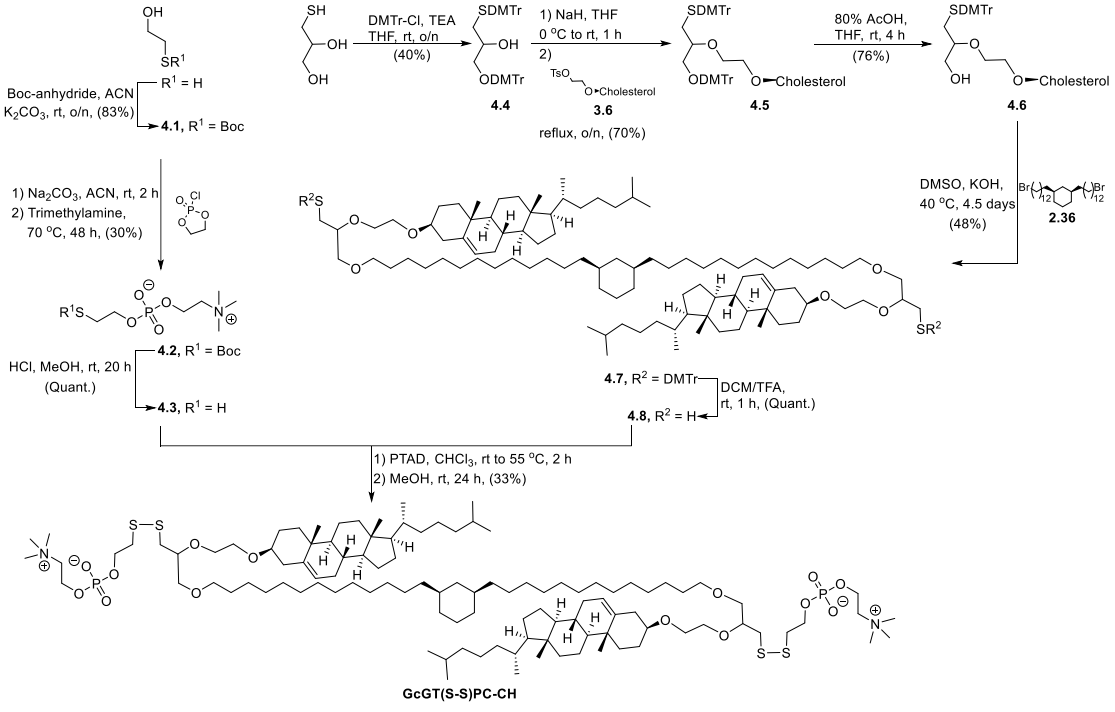

Scheme 4.2. Synthesis of **GcGT(S-S)PC-CH** lipid.

4.3. *Physical Characterization of Liposomes Made from Pure **GcGTPC-CH, GcGT(S-S)PC-CH,** and Diacyl Lipids*

Next, we examined whether the addition of the disulfide bonds would allow for stable liposome to form within a useful temperature range. Liposomes were successfully made using **GcGT(S-S)PC-CH** lipid by extrusion at room temperature following the protocol described in section 2.5.9. Furthermore, Differential scanning calorimetry (DSC) measurements revealed the lipid remains in a liquid phase from 5 to 65 °C and did not exhibition a phase transition (DMPC was used as a positive control, see Figure 4.3A). In addition, dynamic light scattering (DLS) measurement of lipids extruded through a 100 nm polycarbonate membrane successfully exhibited liposomes with an average diameter of ~160 nm (see Figure 4.3B).

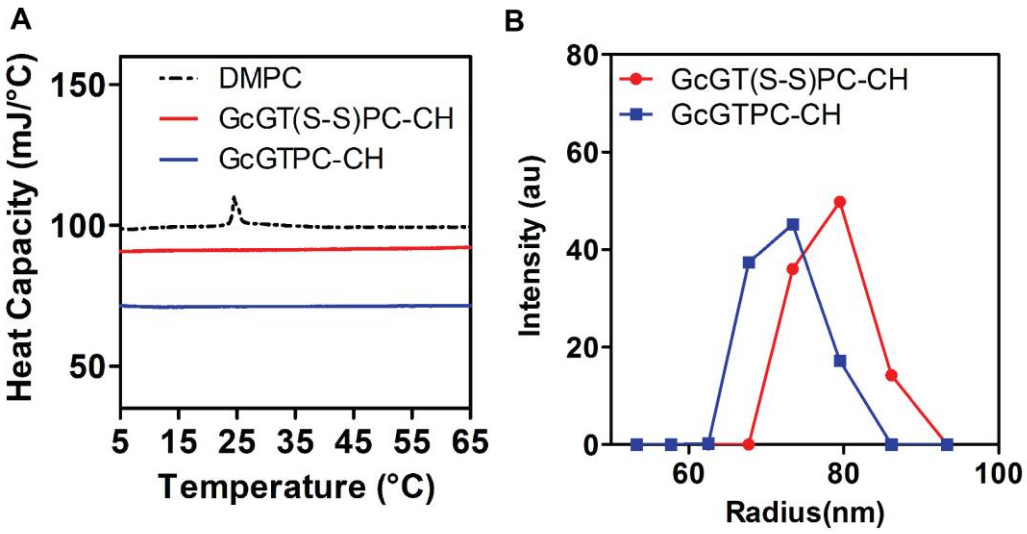

Figure 4.3. Physical characterization of lipids. A) DSC measurements of lipids. B) DLS measurements of synthetic lipids.

*4.4. Investigation of Membrane Leakage Properties of **GcGT(S-S)PC-CH, GcGTPC-CH** and Diacyl Lipid*

*4.4.1. Examination of Serum Stability of **GcGT(S-S)PC-CH, GcGTPC-CH** and Diacyl Liposomes*

Serum stability of liposomes made with either **GcGTPC-CH**, **GcGT(S-S)PC-CH** or POPC was examined. Following the same protocol used in chapter 3 (section 3.9.8.) that measures membrane stability by monitoring the leakage of CF in serum containing HEPES buffer (pH 7.4), liposomes made from palmitoyloleoylphosphatidylcholine (POPC) lost ~80 % of the CF cargo in 2 hours, whereas, both **GcGTPC-CH** and **GcGT(S-S)PC-CH** liposomes remained stable in serum for up to 48 hours at 37 ºC(shown in Figure 4.4). The serum stability of **GcGT(S-S)PC-CH** liposomes in serum supports the hypothesis that

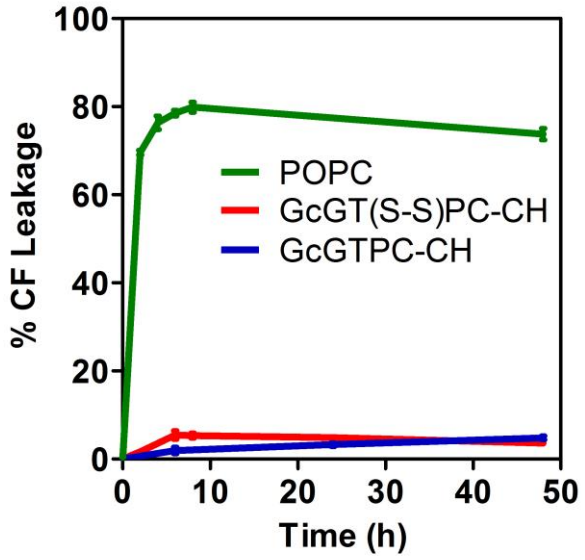

Figure 4.4. Serum induced leakage of CF from liposomes vs. time (h).

the addition of disulfide linkers did not cause a dramatic effect on membrane stability when compared to liposomes made with **GcGTPC-CH** lipids.

*4.4.2. Examination of Thiol Responsive Release of **GcGT(S-S)PC-CH** Liposomes*

In order to examine the liposomal cargo release efficacy of **GcGT(S-S)PC-CH** liposomes triggered by free thiols, a standard self-quenching leakage assay of carboxyfluorescein[21] (CF) was used (see section 4.7.3 for more details) with HEPES buffer (pH 7.4) containing varying concentration of dithiothreitol (DTT) at 37 °C for 1 hour (shown in Figure 4.5 {solid red bars}, further details including raw data can be found in section 4.7.3.) As anticipated, a dose dependent leakage of CF was observed when the concentration of DTT was increased from 0 mM to 20 mM caused by the destabilization of liposomes after cleavage of the polar lipid headgroup from the glycerol lipid backbone. To determine whether the destabilization of **GcGT(S-S)PC-CH** liposomes were caused by the reduction of the disulfide bonds rather than the high concentration of DTT, liposomes made with pure **GcGTPC-CH** (lacks cleavable disulfides) were incubated in a solution of 20 mM DTT under the same conditions. Gratifyingly, Figure 4.5 reveals that liposomes made from pure **GcGTPC-CH** remained stable in the presence of buffer containing 20 mM DTT (see Figure 4.5 {solid blue bar}). Additionally, DLS measurements demonstrates liposomes made with **GcGT(S-S)PC-CH** lipids after incubation in HEPES buffer (pH 7.4)

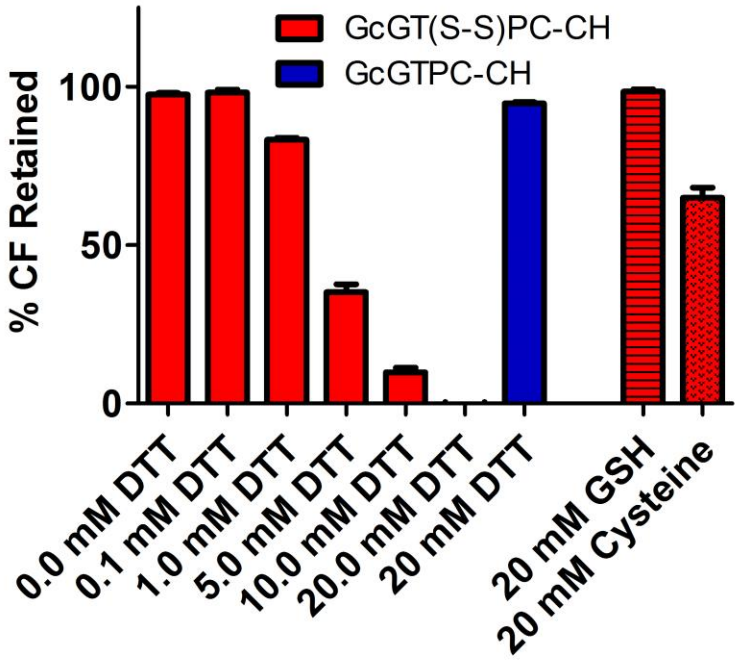

Figure 4.5. In vitro assay of thiol triggered response of liposomes made with **GcGT(S-S)PC-CH** {red} or **GcGTPC-CH** {blue}. CF triggered by DTT in HEPES buffer (pH 7.4) at 37 °C over 1 hour (monitored at λ(Ex/Em) = 485/517 nm); effect of 20 mM GSH and 20 mM cysteine in HEPES buffer at 37 °C over 2 hours (monitored at λ(Ex/Em) = 485/517 nm)

containing 20 mM DTT at 37 ºC for 60 minutes underwent a change in morphology, while the morphology of liposomes made from **GcGTPC-CH** lipids remained static under the same conditions (Figure 4.6). Next, to probe whether biologically relevant thiols could trigger the release of cargo from **GcGT(S-S)PC-CH** liposomes, **GcGT(S-S)PC-CH** liposomes were introduced to buffers containing cysteine and glutathione. After **GcGT(S-S)PC-CH** liposomes were incubated in buffer containing 20 mM of cysteine for 2 hours at 37 °C, ~ 45% of CF was released (see Figure 4.5). On the other hand, when **GcGT(S-S)PC-CH** liposomes were incubated in buffer containing 20 mM of glutathione, no

significant amount of CF was released after 2 hours at 37 °C (see Figure 4.5). This phenomena may be explained by either the lower reducing potential of glutathione[22,23] when compared with DTT or the increased negative charges on the cell impermeable glutathione compared with cysteine that results in a limited access to the disulfide bonds.[24] While these experiments using different thiols in cell free assays produced mixed results regarding the capability of thiols to trigger the release of encapsulated cargo from **GcGT(S-S)PC-CH** liposomes, we hypothesized that the complex mixture of different thiol-containing molecules within a cell may offer enough reducing potential to cause accelerated release of intraliposomal content.

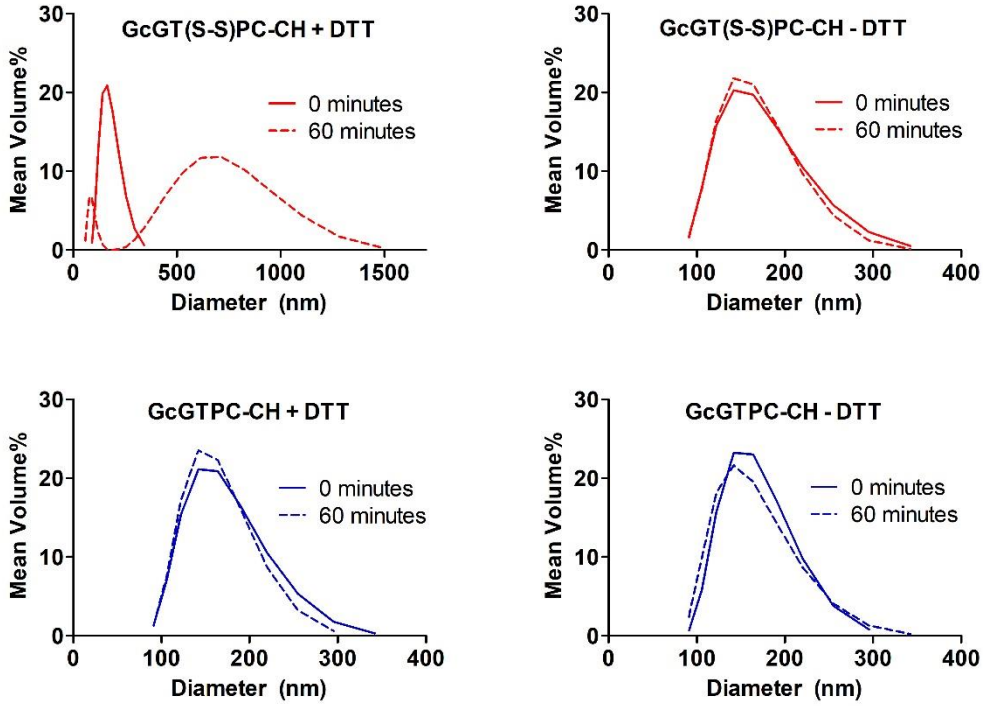

Figure 4.6. DLS traces of liposomes made with **GcGT(S-S)PC-CH** or **GcGTPC-CH** before and after incubation in HEPES buffer pH 7.4 with/without 20 mM DTT after 60 minute incubation at 37 ºC.

*4.4.3. Exploration of DOX Encapsulated **GcGT(S-S)PC-CH** and **GcGTPC-CH** Liposomes*

To probe whether thiol-responsive **GcGT(S-S)PC-CH** liposomes could form stable liposomes using active loading of drugs, we examined whether DOX could be actively loaded inside liposomes using a previously reported method employing an acid gradient (see section 4.7.4. for more details).[25] Briefly, 300 mM citrate buffer was passively encapsulated inside ~160 nm diameter extruded liposomes and incubated in a solution of DOX at 60 °C for 15 minutes. Unencapsulated DOX was removed by filtration using Sephadex® G-100 and the DOX loaded liposomes were used immediately. The encapsulation efficiency of DOX inside **GcGT(S-S)PC-CH** lipid and **GcGTPC-CH** liposomes was 86% (3.5% w/w DOX/lipid) and 84% (3.9% w/w DOX/lipid), respectively (DOX concentration was determined using HPLC and lipid concentration was

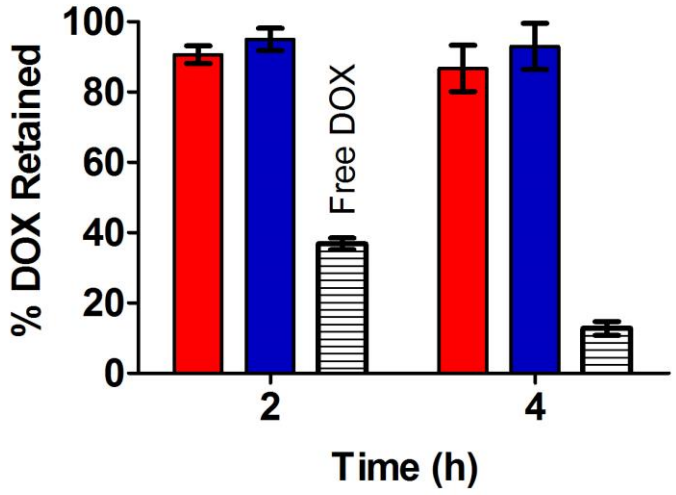

Figure 4.7. Percent leakage of DOX from liposomes after incubation at 37 °C over 4 hours. Free drug released through dialysis shown in grey (monitored at λ_{abs} = 280 nm).

determined using the Bartlett assay[26]). In addition, no significant difference in DOX leakage was observed from **GcGTPC-CH** and **GcGT(S-S)PC-CH** liposomes for 4 hours incubated at 37 °C in HEPES buffer (pH 7.4) by HPLC using a dialysis method[27] (shown in Figure 4.7).

4.5. Small Molecule Liposomal Delivery to Mammalian Cells

Before investigating the efficacy of liposomes made with **GcGT(S-S)PC-CH** lipids for accelerated release of cargo after cell-uptake, we first confirmed that both **GcGTPC-CH** and **GcGT(S-S)PC-CH** liposomes (without encapsulated cargo) were non-toxic for up to 300 µM of total lipid concentration against HeLa cancer cells (see Figure 4.8, all cellular experiments were performed by Dr. Jessica L. Cifelli). Next, when DOX-loaded liposomes were incubated with HeLa cells for four hours, confocal imaging of native DOX fluorescence revealed that liposomes readily internalized into cells (shown in Figure 4.9A; additional

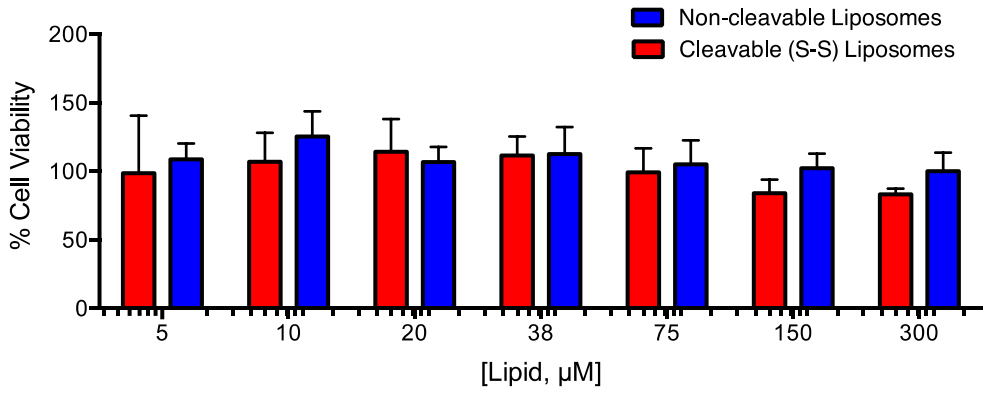

Figure 4.8. Cell viability of HeLa cells incubated for 48 h after short-term exposure (4h) to cleavable (**GcGT(S-S)PC-CH,** red) and non-cleavable (**GcGTPC-CH,** blue) liposomes. n ≥ 3, All concentrations are n.s. from control cells as determined by unpaired-t test. Data taken by Dr. Jessica L. Cifelli.

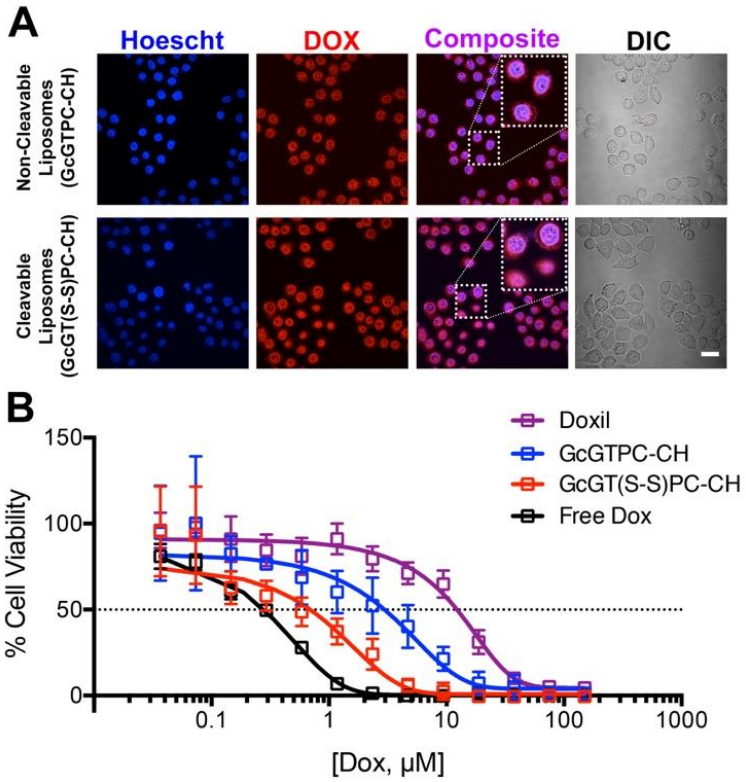

Figure 4.9. Cellular assay of DOX-loaded liposomes delivered to HeLa cells. A) Cellular uptake of doxorubicin (DOX) into Hela cells after short-term (4h) exposure of **GcGT(S-S)PC-CH** and **GcGTPC-CH** liposomes encapsulated with doxorubicin. Scale bar = 25 microns B) Cellular toxicity of DOX as either the free drug or encapsulated into various liposomal delivery systems on HeLa cells after short-term exposure (4h) and 48 h total incubation. n ≥ 3 for each concentration. The data is shown normalized to the total concentration of

images of cellular uptake of liposomes made with Doxil or free DOX are shown in section 4.7.5.1). After confirming successful cell uptake of DOX-loaded liposomes after 4 hours, a cell viability assay was performed to investigate whether **GcGT(S-S)PC-CH** liposome loaded with DOX exhibited improved efficacy for cellular toxicity compared with DOX-loaded **GcGTPC-CH** liposomes (which lack reducible disulfide bonds, see section 4.7.5.2. for more details). Briefly, the HeLa cells were incubated with various concentrations of DOX-loaded **GcGTPC-CH** liposomes, DOX-loaded **GcGT(S-S)PC-CH** liposomes,

DOXIL (a Food and Drug Administration [FDA] approved liposomal formulation of DOX), or free DOX for four hours. The cells were then washed and incubated at 37 °C for 48 hours, followed by analysis using an MTT cell viability assay. As shown in Figure 4.9B, DOX-loaded **GcGT(S-S)PC-CH** liposomes exhibited good toxicity towards HeLa cells with an IC_{50} of 0.5 μM, which was comparable to the toxicity observed for free DOX (IC_{50} of 0.2 μM). The DOX-loaded **GcGTPC-CH** liposomes (lacking disulfide bonds) displayed an IC_{50} of 1.9 μM, which is an order of magnitude less toxic than the free drug under these experimental conditions. DOXIL, on the other hand, displayed an IC_{50} value of 9.8 μM, which is ~20 times less toxic than the DOX-loaded **GcGT(S-S)PC-CH** liposomes. These results support the hypothesis of the natural reducing environment within the HeLa cancers is sufficient to accelerate the release of DOX from **GcGT(S-S)PC-CH** liposomes containing a thiol-cleavable linker when compared with DOX-loaded **GcGTPC-CH** liposomes or DOXIL, which contain lipids that do not contain disulfide groups.

4.6. *Conclusion*

We have, thus, successfully designed and synthesized the first tetraether lipid that contains disulfide cleavable linker that are stable enough to form liposomes in pure form, while maintaining optimized structural features explored in chapter 2 & 3 to allow stability in serum-containing buffer. Moreover, DOX-loaded **GcGT(S-S)PC-CH** liposomes were capable of delivering and promoting

accelerated intracellular release of DOX in HeLa cells with an IC_{50} value similar to free DOX and ~4 and ~20 times more toxic than our previous generation of **GcGTPC-CH** lipid and Doxil, respectively. Through synthetic exploration of the structure-function relationship of chemical groups found in natural (archaeal and eukaryotic) lipids, we were able to design a new **GcGT(S-S)PC-CH** lipid that has shown to form stable and robust liposomes with low inherent leakage. The liposomes were capable of delivering DOX to cancer cells with similar toxicity as for free DOX, which holds promise as an new class of drug delivery system for cancer therapy. This work represents a first step towards development of stimuli-responsive tetraether lipids, which may offer advantages of improved stability and reduced passive leakage of weakly basic and charged drugs compared with current liposomal drug delivery formulations used for cancer therapy and other systemically treated diseases.

4.7. Materials and Methods

4.7.1. Reagents and Instruments

All reagents were purchased from commercial sources and used without further purification. Glassware was dried at 115°C overnight. Air and moisture-sensitive reagents were transferred using a syringe or stainless steel cannula. Intermediates were purified over silica (60Å, particle size 40-63 μm) purchased from Dynamic Adsorbents, Inc. Reactions were monitored by thin-layer chromatography (TLC) using 0.25 mm silica gel plates (60F-254) from Dynamic

Adsorbents, Inc. Deuterated solvents were purchased from Cambridge Isotope Laboratories, Inc.

HeLa cells (human epithelial cervix carcinoma, Product No: CCL-2) and 3-(4,5-dimethylthiazolyl-2)-2, 5-diphenyltetrazolium bromide (MTT) cell proliferation assay (Product No: 30-1010K) were purchased from American Type Culture Collection (ATCC) (Manassas, VA). Doxil (DOX HCl liposome injection, 20mg/mL) was a generous gift from Dr. Stephen B. Howell of Moores Cancer Center (Lot: 600120P1).

^{1}H, ^{13}C, ^{31}P NMR spectra were obtained on either JEOL ECA 500 spectrometer or Varian 400 MHz/500MHz spectrometer. Chemical shifts are reported in ppm relative to residual solvent. The FID file was analyzed using NMRnotebook version 2.70 build 0.10 by NMRTEC.

Dynamic Light Scattering (DLS) measurements were performed on a Wyatt DynaPro NanoStar (Wyatt Technology, Santa Barbara, CA) or Malvern Zetasizer (Zen 3690, model Zs90) instrument using a disposable cuvette (Eppendorf UVette 220 nm – 1,600 nm) and data processed using Wyatt DYNAMICS V7 software. Each analysis involved an average of 10 measurements. The data was exported for final plotting using GraphPad Prism 5 (GraphPad Software, Inc., La Jolla, CA).

Low resolution MS analysis was performed on a Micromass Quattro Ultima triple quadrupole mass spectrometer with an electrospray ionization

(ESI) source. High resolution MS analysis was performed using Agilent 6230 Accurate-Mass TOFMS with an electrospray ionization (ESI) source by Molecular Mass Spectrometry Facility (MMSF) in the department of chemistry and biochemistry at University of California, San Diego.

Fluorescence decay measurements were taken on a Perkin Elmer Enspire© multimode plate reader (excitation 485 nm, emission 517 nm and 75 flashes); each measurement was taken with a 10 sec delay with 125 repeat (total acquisition time = 21 min). Costar EIA/RIA plates were used (96 well half area, no lid, flat bottom, non-treated black polystyrene). The data were exported for final plotting using GraphPad Prism 5 (GraphPad Software, Inc., La Jolla, CA).

HPLC analyses were performed using an Agilent 1100 Series HPLC and an analytical reverse-phase column (Eclipse XDB-C18 Agilent, 5 µm, 150 x 4.6 mm). Flow: 1 mL/min. Injection volume = 50 µL. Detection: 254 and 280 nm. Mobile phase: water/acetonitrile containing 0.1% (v/v) trifluoroacetic acid (TFA).

Method A: Linear gradient from 5% to 95% of ACN in 10 minutes followed by 2 minutes of re-equilibration at 5% of ACN.

4.7.2. General Synthetic Procedures

O-(tert-butyl) S-(2-hydroxyethyl) carbonothioate **(4.1)**

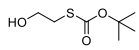

Compound **4.1** was prepared following a previously reported protocol.[28]

2-((tert-butoxycarbonyl)thio)ethyl (2-(trimethylammonio)ethyl) phosphate **(4.2)**

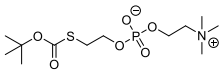

To a solution of 0.38 g (0.002 mol) **4.1** and 0.30 g (0.002 mol) of 2-chloro-1,3,2-dioxaphospolane 2-oxde in 6.5 mL of acetonitrile, 0.02 g (0.00018 mol) of Na_2CO_3 was suspended and stirred at rt for 2 hours. The salt was removed by filtration over a small pad of celite. The filtrate was then transferred to a pressure tube and 2 mL of trimethylamine was added at 0 ºC. After the addition, the reaction was warmed to rt, then heated to 70 ºC for 48 hours. Volatile solvents were removed *via* vacuum and the crude residue was purified over SiO_2 using a gradient of MeOH and water in DCM starting with 80/20 (DCM/MeOH), 80/20/2 (DCM/MeOH/H_2O), 70/30/5 (DCM/MeOH/H_2O), to 60/40/10 (DCM/MeOH/H_2O). Compound **4.2** was obtained as a clear oil (205 mg, 30%).

Rf: 0.40 (DCM/MeOH/$H_2$0 60:40:10); ^{1}H NMR (400 MHz, MeOD-d_4) δ 4.33-4.25 (2H, m), 4.02-3.95 (2H, m), 3.68-3.66 (2H, m), 3.25 (9H,s), 3.05 (2H, t, *J* = 6.79 Hz), 1.48 (9H, s); ^{13}C NMR (100 MHz, MeOD-d_4) δ 169.0, 84.9, 66.3, 64.4 (d, *J* = 5.55 Hz), 59.3 (d, *J* = 4.95 Hz), 53.6, 31.2 (d, *J* = 8.07 Hz), 27.3; ^{31}P NMR

(161 MHz, MeOD-d_4) δ 0.44; ESI-MS: 344.08 $[M+H]^+$; HRMS 344.1291 calcd for $[C_{12}H_{27}NO_6PS]^+$ found 344.1290.

2-mercaptoethyl (2-(trimethylammonio)ethyl) phosphate **(4.3)**

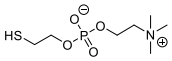

0.060 g (0.17 mmol) of **4.2** was dissolved in 3 mL of HCl in MeOH (3 M) then stirred at rt for 20 hours. Volatile solvents were removed to recover Compound **4.3** as a white oily solid (0.043 g, Qt).

ESI-MS: 244.16 $[M+H]^+$; HRMS 244.0767 calcd for $[C_7H_{19}O_4PS]^+$ found 244.0764.

1-(bis(4-methoxyphenyl)(phenyl)methoxy)-3-((bis(4-methoxyphenyl)(phenyl)methyl)thio) propan-2-ol **(4.4)**

To a solution of 1 g (9.2 mmol) of thioglycerol and 6.6 g (19.3 mmol) 4,4'-dimethoxytrityl chloride (DMTr-Cl) in 20 mL of dry THF, 12.8 mL (92 mmol) of triethylamine was added drop wise and stirred at rt overnight. Volatile solvents were removed *via* vacuum and purified by column chromatography on silica gel using Hexane/EtOAc (7:3) as the eluent. Compound **4.4** was obtained as a violet solid (2.6 g, 40 %).

Rf: 0.65 (Hexane/EtOAc 1:1); ^{1}H NMR (500 MHz, MeOD-d_4) δ 7.38-6.76 (18H, m), 6.79-6.76 (8H, m), 3.74 (6H, s), 3.71 (6H, s), 3.60-3.56 (1H, m), 3.02-2.99 (1H, m), 2.89-2.86 (1H, m), 2.54-2.51 (1H, m), 2.31-2.27 (1H, m); ^{13}C NMR (126 MHz, MeOD-d_4) δ 160.2, 159.8, 147.3, 146.6, 138.8, 138.7, 137.5, 132.2, 132.1, 131.5, 130.7, 129.5, 129.0, 128.8, 127.8, 127.7, 114.2, 114.1, 101.5, 87.4, 71.4, 68.0, 66.8, 61.7, 55.8, 38.1, 21.0, 14.6; ESI-MS: 735.19 $[M+Na]^+$; HRMS 735.2751 calcd for $[C_{45}H_{44}O_6S\ Na]^+$, found 735.2746.

2-(((3S,8S,9S,10R,13R,14S)-10,13-dimethyl-17-((R)-6-methylheptan-2-yl)-2,3,4,7,8,9,10,11,12,13,14,15,16,17-tetradecahydro-1H-cyclopenta[a]phenanthren-3-yl)oxy)ethyl 4-methylbenzenesulfonate (**3.6**)

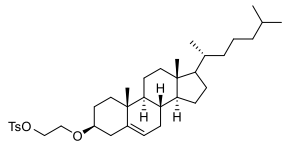

Compound **3.6** was prepared following a previously reported protocol.[29]

(3-(bis(4-methoxyphenyl)(phenyl)methoxy)-2-(2-(((3S,8S,9S,10R,13R,14S,17R)-10,13-dimethyl-17-((R)-6-methylheptan-2-yl)-2,3,4,7,8,9,10,11,12,13,14,15,16,17-tetradecahydro-1H-cyclopenta[a]phenanthren-3-yl)oxy)ethoxy)propyl)(bis(4-methoxyphenyl)(phenyl)methyl)sulfane **(4.5)**

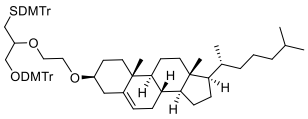

In a pressure tube, 500 mg (0.70 mmol) of **4.4** was dissolved in 3 mL of dry THF and 50 mg (2.1 mmol) was added at 0 ºC and stirred for 1 hour. 374 mg (0.77 mmol) of **3.6** was added and heated to 65 ºC then stirred overnight. The reaction was cooled to 0 ºC and quenched with H_2O and THF was removed via vacuum. The residue was resuspended in EtOAc and washed with water, brine and dried over Na_2SO_4 then purified over SiO_2 using Hexane/EtOAc (9:1) as the eluent. Compound **4.5** was obtained as a white viscous oil (494 mg g, 65%).

Rf: 0.43 (Hexane/EtOAc 8:2); ^{1}H NMR (400 MHz, $CDCl_3$-d_1) δ 7.42-7.20 (18H, m), 6.82-6.78 (8H, m), 5.32-5.29 (1H, m), 3.79 (6H, s), 3.77 (6H, s), 3.56-3.51 (4H, m), 3.37-3.32 (1H, m), 3.20-3.11 (2H, m), 3.01-2.97 (1H, m), 2.47-2.34 (3H, m), 2.21-2.16 (1H, m), 2.06-1.96 (2H, m), 1.88-1.81 (2H, m), 1.61-1.25 (12H, m), 1.19-0.88 (22H, m), 0.70 (3H, s); ^{13}C NMR (100 MHz, $CDCl_3$-d_1) δ 158.6, 158.2, 145.8, 145.2, 141.2, 137.6, 136.4, 136.4, 131.2,, 131.0, 130.3, 129.7, 128.5, 128.0,, 127.9,, 126.8,, 126.6,, 121.7,, 113.3,, 113.2,, 86.2, 79.5,, 79.5,, 79.1, 79.1, 70.3, 70.3, 67.6, 67.5, 65.7, 65.3, 57.0, 56.4, 55.4, 50.4, 42.6, 40.0,

39.8, 39.3, 37.5, 37.1, 36.4, 36.0, 34.9, 34.9, 32.2, 32.1, 31.8, 28.6, 28.5, 28.3, 24.5, 24.1, 23.1, 22.9, 22.8, 21.3, 19.6, 19.0, 14.4, 12.1; ESI-MS: 1147.67 $[M+Na]^+$; HRMS 1147.6456 calcd for $[C_{74}H_{92}O_7S\ Na]^+$, found 1147.6446.

3-((bis(4-methoxyphenyl)(phenyl)methyl)thio)-2-(2-(((3S,8S,9S,10R,13R,14S,17R)-10,13-dimethyl-17-((R)-6-methylheptan-2-yl)-2,3,4,7,8,9,10,11,12,13,14,15,16,17-tetradecahydro-1H-cyclopenta[a]phenanthren-3-yl)oxy)ethoxy)propan-1-ol **(4.6)**

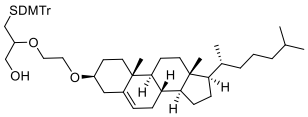

494 mg (0.44 mmol) of **4.5** was dissolved in minimal THF and 10 mL of 80% AcOH (aq) was added dropwise then stirred at rt for 4 hours. The acid was neutralized with a solution of sat. $NaHCO_3$ (aq), then extracted with DCM and dried over $MgSO_4$. The solvent was removed *via* vacuo and purified over SiO_2 using Hexane/EtOAc (9:1) as the eluent. Compound **4.6** was obtained as a clear oil (271 mg, 76%).

Rf: 0.15 (Hexane/EtOAc 8:2); ^{1}H NMR (500 MHz, $CDCl_3$-d_1) δ 7.49-7.25 (9H, m), 6.87 (4H, d, *J* = 8.64 Hz), 5.41-5.40 (1H, m), 3.83 (6H, s), 3.79-3.76 (1H, m), 3.63-3.41 (5H, m), 3.27-3.22 (2H, m), 1.68-1.31 (12H, m), 1.23-0.94 (22H, m), 0.76 (3H, s); ^{13}C NMR (126 MHz, $CDCl_3$-d_1) δ 158.1, 145.4, 140.6, 137.1, 130.8, 129.5, 127.9, 126.6, 121.8, 113.2, 80.7, 80.6, 79.5, 70.1, 70.1, 67.4, 67.4, 66.0, 64.6, 56.8, 56.2, 55.2, 50.2, 42.4, 39.8, 39.6, 39.0, 38.9, 37.2, 36.9, 36.3, 35.9,

33.4, 32.0, 31.9, 28.3, 28.1, 24.4, 23.9, 22.9, 22.7, 21.1, 19.4, 18.8, 11.9; ESI-MS: 845.33 $[M+Na]^+$;HRMS 845.5149 calcd for $[C_{53}H_{74}O_5S\ Na]^+$, found 845.5152.

(1R,3S)-1,3-bis(14-bromotetradecyl)cyclohexane **(2.36)**

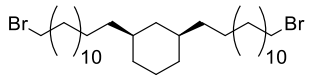

Compound **2.36** was prepared following a previously reported protocol.[15]

(1R,3S)-1,3-bis(13-(3-((bis(4-methoxyphenyl)(phenyl)methyl)thio)-2-(2-(((3S,8S,9S,10R,13R,14S,17R)-10,13-dimethyl-17-((R)-6-methylheptan-2-yl)-2,3,4,7,8,9,10,11,12,13,14,15,16,17-tetradecahydro-1H-cyclopenta[a]phenanthren-3-yl)oxy)ethoxy)propoxy)tridecyl)cyclohexane **(4.7)**

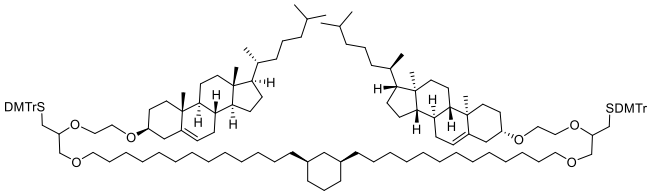

176 mg (0.21 mmol) of **4.6** and 34 mg (0.60 mmol) of KOH were suspended in 6 mL of dry DMSO and stirred at rt for 30 minutes. To the reaction, 46 mg (0.08 mmol) of **2.36** was added and stirred at rt overnight. After the reaction was stirred at rt overnight, the reaction was heated to 40 ºC and stirred for 4 days. 500 mL of water was added and extracted with EtOAc. The combined organic layers were back extracted with water, brine and dried over $MgSO_4$ and purified

over SiO_2 using Hexane/EtOAc (9:1) as the eluent. Compound **4.7** was obtained as a clear oil (76 mg, 48%).

Rf: 0.54 (Hexane/EtOAc 8:2); ^{1}H NMR (400 MHz, $CDCl_3$-d_1) δ 7.41-7.19 (18H, m), 6.82-6.78 (8H, m), 5.31 (2H, m), 3.81-3.77 (12H, s), 3.53-3.13 (20H, m), 2.42-0.69 (147H, m), 0.54-0.45 (1H, m), ; ^{13}C NMR (100 MHz, $CDCl_3$-d_1) δ 158.2, 145.7, 141.2, 137.5, 131.3, 131.0, 130.3, 129.9, 129.8, 129.4, 128.0, 126.7, 121.8, 121.7, 113.4, 113.3, 79.5, 79.5, 78.8, 78.7, 72.4, 71.8, 69.9, 69.8, 67.5, 65.9, 57.0, 56.4, 55.4, 55.3, 50.4, 42.6, 40.8, 40.0, 39.8, 39.3, 38.1, 38.0, 37.5, 37.1, 36.4, 36.0, 33.7, 33.6, 32.2, 32.1, 30.4, 30.0, 30.0, 29.9, 29.8, 28.6, 28.5, 28.3, 27.2, 26.7, 26.4, 24.5, 24.1, 23.1, 22.8, 21.3, 19.6, 19.0, 12.1; ESI-MS: Not detectable.

3,3'-((((1R,3S)-cyclohexane-1,3-diyl)bis(tridecane-13,1-diyl))bis(oxy))bis(2-(2-(((3S,8S,9S,10R,13R,14S,17R)-10,13-dimethyl-17-((R)-6-methylheptan-2-yl)-2,3,4,7,8,9,10,11,12,13,14,15,16,17-tetradecahydro-1H-cyclopenta[a]phenanthren-3-yl)oxy)ethoxy)propane-1-thiol) **(4.8)**

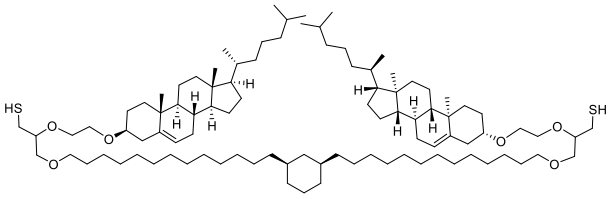

76 mg (0.036 mmol) of **4.7** and 30 mg (0.19 mmol) of triisopropylsilane were dissolved in 1.9 mL of DCM and 0.1 mL of TFA was added dropwise and stirred at rt for 1 hour. The acid was neutralized by the addition of sat. $NaHCO_3$ (aq)

and extracted with DCM. The combined organic layers were dried over MgSO4 and purified over SiO_2 using Hexane/EtOAc (9:1) as the eluent. Compound **4.8** was obtained as a clear oil (54 mg, Qt)

Rf: 0.30 (Hexane/EtOAc 9:1); ^{1}H NMR (400 MHz, $CDCl_3$-d_1) δ 5.34-5.33 (2H, m), 3.74-3.41 (18H, m), 3.23-3.16 (2H, m), 2.73-2.66 (4H, m), 2.39-0.44 (146H, m); ^{13}C NMR (100 MHz, $CDCl_3$-d_1) δ 141.1, 121.8, 80.2, 79.7, 71.9, 71.4, 70.2, 67.7, 57.0, 56.4, 50.4, 42.5, 40.0, 39.7, 39.3, 38.0, 38.0, 37.5, 37.1, 36.4, 36.0, 33.7, 32.2, 32.1, 30.3, 30.0, 29.9, 29.7, 28.7, 28.6, 28.5, 28.2, 27.2, 26.7, 26.6, 26.4, 24.5, 24.1, 23.1, 22.8, 21.3, 19.6, 19.0, 12.1 ; ESI-MS: 1502.92 $[M+NH_3]^+$; HRMS 1508.2488 calcd for $[C_{96}H_{172}O_6S_2\,Na]^+$, found 1508.2463.

((((((1R,3S)-cyclohexane-1,3-diyl)bis(tridecane-13,1-diyl))bis(oxy))bis(2-(2-(((3S,8S,9S,10R,13R,14S,17R)-10,13-dimethyl-17-((R)-6-methylheptan-2-yl)-2,3,4,7,8,9,10,11,12,13,14,15,16,17-tetradecahydro-1H-cyclopenta[a]phenanthren-3-yl)oxy)ethoxy)propane-3,1-diyl))bis(disulfanediyl))bis(ethane-2,1-diyl) bis(2-(trimethylammonio)ethyl) bis(phosphate) **(GcGT(S-S)PC-CH)**

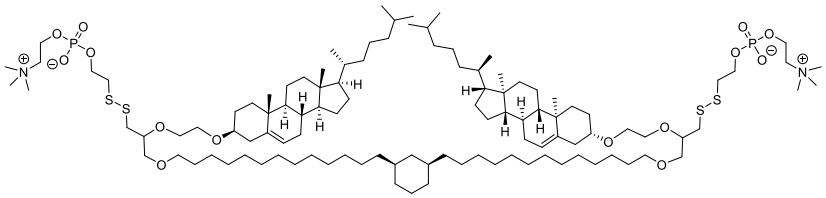

37 mg (0.025 mmol) of **4.8** and 9 mg (0.052 mmol) 4-phenyl-1,2,4-triazole-3,5-dione (PTAD) were dissolved in 1 mL degassed $CHCl_3$ and stirred at rt for 30

minutes. The mixture was next heated to 55 ºC and stirred for 2 hours until the red color disappeared. The reaction was cooled to rt and a solution of 32 mg (0.17 mmol) of **4.3** in 0.4 mL of degassed MeOH was added and stirred at rt for 3 days. The volatile solvent was removed and purified over SiO2 using DCM/MeOH/H_2O (60:40:10) as the eluent and Sephadex LH20 as the eluent DCM/MeOH (1:1). **GcGT(S-S)PC-CH** was obtained as a viscous oil (16 mg, 33%)

Rf: 0.44 (DCM/MeOH/H_2O 60:40:10); ^{1}H NMR (500 MHz, MeOD-d_4/$CDCl_3$-d_1 1:1) δ 5.00-4.99 (2H, m), 3.93-3.89 (4H, m), 3.80-3.76 (4H, m), 3.42-3.10 (24H, m), 2.86 (18H, s), 2.61-2.53 (8H, m), 2.04-2.01 (2H, m), 1.87-1.81 (2H, m), 1.66-0.34 (139H, m), 0.14-0.12 (1H, m); ^{13}C NMR (126 MHz, MeOD-d_4/$CDCl_3$-d_1 1:1) δ 140.2, 121.4, 79.2, 71.4, 71.2, 69.5, 67.0, 66.0, 66.0, 63.2, 63.1, 58.7, 58.7, 56.4, 55.8, 53.5, 49.9, 41.9, 40.2, 40.1, 39.5, 39.1, 38.7, 38.3, 38.2, 37.4, 37.4, 36.8, 36.4, 35.8, 35.5, 33.1, 31.6, 29.7, 29.4, 29.3, 29.3, 29.2, 28.0, 27.9, 27.6, 26.6, 25.8, 23.9, 23.4, 22.2, 21.9, 20.7, 18.8, 18.1, 11.3; ^{31}P NMR (202 MHz, MeOD-d_4/$CDCl_3$-d_1 1:1) δ 0.53; ESI-MS: 1991.20 $[M+Na]^+$;HRMS 1968.3743 calcd for $[C_{110}H_{205}N_2O_{14}P_2S_4]^+$, found 1968.3715.

4.7.3. General Procedure for Thiol Triggered Self-Quenched CF Liposomal Release Assay

Liposomes were prepared as described in general procedures for liposome extrusion. Using the method of self-quenched CF loaded (100 mM in HEPES buffer, pH 7.4) leakage assay[30], self-quench CF loaded liposomes comprised of **GcGTPC-CH** or **GcGT(S-S)PC-CH** lipids were subjected to varying concentration of dithiothreitol (DTT; 20 mM, 10 mM, 5.0 mM, 1.0 mM, 0.1 mM, and 0 mM of DTT), 20mM cysteine and 9.0 mM/ 20 mM glutathione (GSH) containing HEPES buffer shown in Figure 4.10.

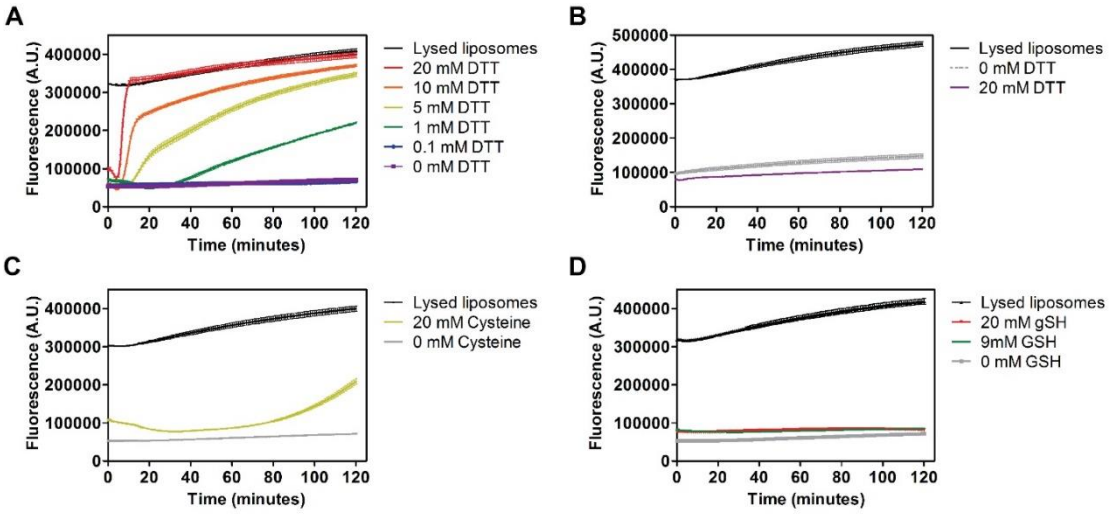

Figure 4.10. Raw kinetic traces of increased CF fluorescence from liposomal leakage. A) Dose dependent effect of DTT on self-quench loaded **GcGT(S-S)PC-CH** lipid liposomes. B) Effect of 20 mM DTT on liposomes made with **GcGTPC-CH**. C) Effect of 20 mM Cysteine on liposomes made with **GcGT(S-S)PC-CH** lipid. D) Effect of 9/20 mM of GSH on liposomes made with **GcGT(S-S)PC-CH** lipid. (Fluorescence of CF monitored at λ(Ex/Em) = 485/517 nm)

Membrane permeability of CF from liposomes was measured by monitoring the increase in fluorescence of CF using Perkin Elmer Enspire©

multimode plate reader (λ(Ex/Em) = 485/517 nm). Before each assay, 10 µL of the stock extruded lipid solution was diluted in 500 µL of HEPES buffer. Free CF was removed using a PD miniTrap™ G-25 Sephadex™ column from GE Healthcare ending in 100 times dilution from the stock extruded solution (0.1 mg/mL). 50 µL of purified liposome solution was next added into three 0.5 mL Protein Lo-Bind tubes for each lipid solution. In one tube, 450 µL of HEPES Buffer containing either DTT (shown in Figure 4.10A and 4.10B), cysteine (shown in Figure 4.10C) or GSH (shown in Figure 4.10D) was added. In the second tube, 450 µL of HEPES buffer containing Triton X-100 (0.5% v/v) was added to obtain 100% liposomal releases of CF. In the third tube, 450 µL of HEPES buffer without added thiols. 150 µL was added to each well of the plate three times for each tubes resulting in three measurements with three replicates with a total of 9 measurements per lipid solution.

4.7.4. General Procedure for DOX Loaded Liposomal Release Assay

The *in vitro* leakage of Doxorubicin (DOX) from liposomes was measured using a dialysis assay[27]. Briefly, DOX encapsulated liposomes were made by weighing 10 mg of lipid into a 5 mL round bottom flask and dissolved in 1:1 chloroform/methanol. The solvent was evaporated *via vacuo* to form a lipid film and hydrated with 500 µL of 300 mM citrate dissolved in Milli Q filtered water. 150 µL of the stock liposomal formulation (20 mg/mL) was diluted with HEPES buffer (pH 7.4) to 500 µL and purified using Sephadex™ G-25 to prepare a 1

mL working solution. Immediately after free citrate was removed, 35.1 µL of 6 mM DOX solution dissolved in Milli Q filtered water was added to the liposomal solution and heated at 60 °C for 15 minute. Unencapsulated free DOX was removed by filtering the liposomal solution over Sephadex^{TM} G-100. The purified liposomal suspensions was placed in a dialysis device (Slide-A-Lyzer® Mini dialysis, ref 88405, Thermo Scientific) with a molecular weight cutoff of 20 kDa and dialyzed against 42.5 mL of buffer C at 37 °C and shaken on an orbital shaker (50 rpm). At various time points, aliquots (40 µL) were withdrawn from the dialysis compartment and retention of encapsulated drug was measured by HPLC (λ_{abs} of DOX was monitored at 280 nM).

To a vial, 40 µL of a Triton solution (0.5 % w/v in HEPES buffer) was added to 40 µL of liposomal suspension. The samples were vortexed and analyzed by HPLC using method A for the detection of DOX. Data was analyzed using Agilent analysis software (Chemstation®). For each time point, the percentage of drug remaining in the liposomes was calculated using the following equation (1):

$$Retained\ drug\ (\%) = 100 \times \frac{Area(t)}{Area\ (t0)} \qquad (1)$$

4.7.5. General Procedure for Cellular Uptake of DOX Entrapped in Liposomes

4.7.5.1. Confocal Microscopy of the Cellular Uptake of Doxorubicin

HeLa cells were cultured on 35 mm dishes (MatTek) and incubated overnight in DMEM supplemented with 10% FBS. The growth medium was removed and solutions containing either free doxorubicin, or various liposomal encapsulated doxorubicin solutions (10 μM, final concentration of DOX for all), or HBS (UT control) were added. The cells were then incubated for 4 hours (37 °C, 5% CO_2). MatTeks were then rinsed (3x, ice cold-PBS) and nuclei were stained with Hoescht 33258 (10 minutes, 37 °C). Cells were rinsed again (2x, PBS) immediately prior to imaging. Cellular uptake of doxorubicin was imaged

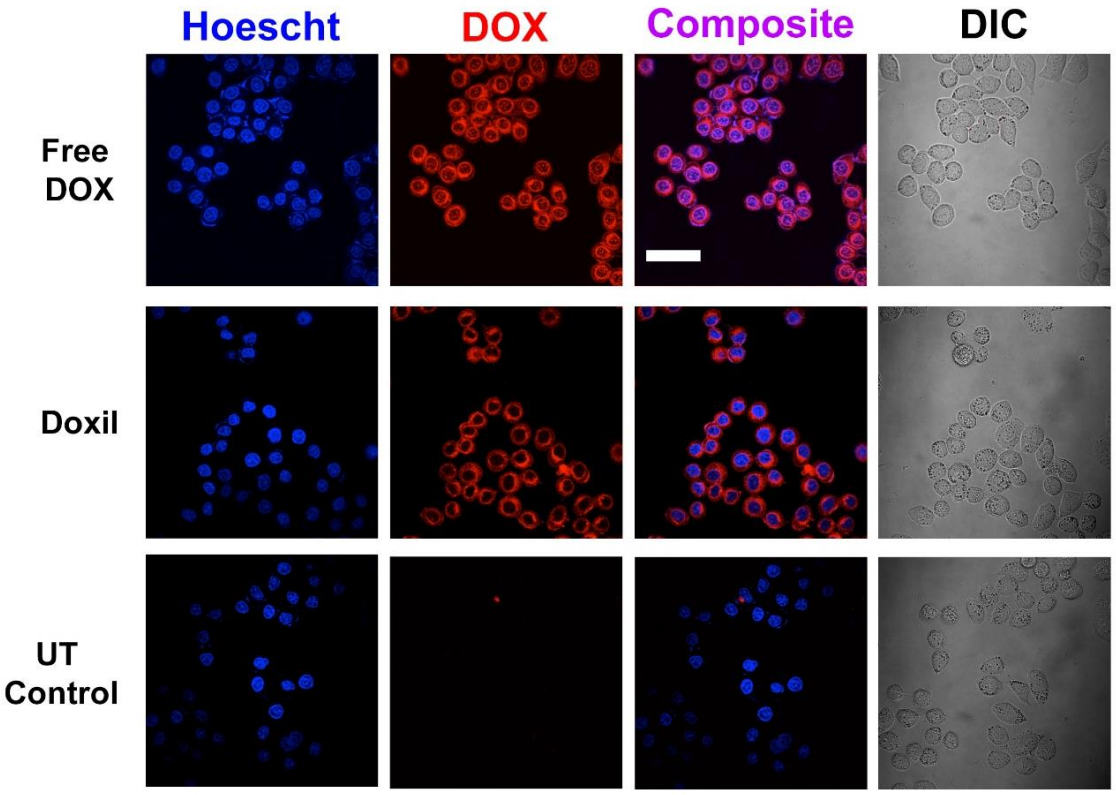

Figure 4.11. Cellular uptake of DOX into HeLa cells after 4h exposure with free DOX, Doxil, and untreated (UT) control (HBS). Scale bar = 50 μm, Data taken by Dr. Jessica L. Cifelli.

with an Olympus FV1000 spectral deconvolution confocal system equipped with an Olympus IX81 inverted microscope. Cell images were analyzed using ImageJ. The images shown in Figure 4.11 are fluorescence micrographs of representative z-slices from within the cells.

4.7.5.2. MTT Cell Proliferation Assay in HeLa Cells

An MTT cell proliferation assay was performed as previously reported with noted changes[27]. Briefly, cells were plated in 96-well dishes at a density of 10,000 cells/well in 100 µL of DMEM supplemented with 10% FBS. After adhering overnight, the medium was replaced with 100 µL of solutions containing various concentrations of either free doxorubicin, or various liposomal formulations of encapsulated doxorubicin (Doxil, cleavable (**GcGT(S-S)PC-CH** Lipid), and non-cleavable (**GcGTPC-CH**) liposomes: see general procedures for liposomes extrusion for details) with final concentrations of doxorubicin (0-150 µM). As controls, cells were also exposed to the cleavable and non-cleavable liposomes without DOX. Cells were exposed to these various solutions for 4 hours at 37 °C. Following, in which cells were rinsed (cold PBS), fresh complete medium was added (200 µL) and cells were let incubate. After 48 h of incubation, an MTT cell viability assay was then used to determine cell viability. Briefly, the MTT reagent (10 µL of the solution from the commercial kit) was added to each well and the cells were incubated for 3 additional hours. All solutions were then removed and the formazan crystals were subsequently

solubilized with DMSO (100 µL). The cell viability was determined by measuring the absorbance at 570 nm using a Perkin Elmer EnSpire© multimode plate reader. All results, shown in Figure 4.7, were expressed as percent reduction of MTT relative to untreated controls (defined as 100% viability) and the average absorbance value for each treatment was blanked with the absorbance reading of media control blanks. Each concentration was done in at least triplicate.

4.8. Acknowledgements

Chapter 4 is adapted, in part, from Takaoki Koyanagi, Jessica L. Cifelli, Geoffray Leriche, David Onofrei, Gregory P. Holland, and Jerry Yang, “Thiol-triggered release of intraliposomal content from liposomes made of extremophile-inspired tetraether lipids.” *Bioconjugate Chem.* 2017, ASAP. Copyright 2017 American Chemical Society. Permission to use copyrighted images and data in the manuscript was obtained from Jessica L. Cifelli, Geoffray Leriche, David Onofrei, Gregory P. Holland, and Jerry Yang. The dissertation author is the first author of this manuscript.

4.9. References

(1) Torchilin, V. P. *Nat. Rev. Drug Discov.* **2005**, *4* (2), 145–160.

(2) Clark, a P. *Cancer Pract. 6*, 251–253.

(3) Lasic, D. *Trends Biotechnol.* **1998**, *16* (7), 307–321.

(4) Chrai, S. S.; Murari, R.; Ahmad, I. *Biotech Trends* **2002**, No. April, 30–34.

(5) Allen, T. M.; Cullis, P. R. *Adv. Drug Deliv. Rev.* **2013**, *65* (1), 36–48.

(6) Tiwari, G.; Sriwastawa, B.; Pandey, S.; Bannerjee, S.; Tiwari, R.; Bhati, L.; Pandey, P. *Int. J. Pharm. Investig.* **2012**, *2* (1), 2.

(7) Wen, H.; Li, Y. *Med. Chem. (Los. Angeles).* **2014**, *4* (11), 748–755.

(8) Connor, J.; Yatvin, M. B.; Huang, L. *Proc. Natl. Acad. Sci. U. S. A.* **1984**, *81* (6), 1715–1718.

(9) Mura, S.; Nicolas, J.; Couvreur, P. *Nat. Mater.* **2013**, *12* (11), 991–1003.

(10) Lee, Y.; Thompson, D. H. *Wiley Interdiscip. Rev. Nanomed. Nanobiotechnol.* **2017**, *e1450*, 1–40.

(11) Danhier, F.; Feron, O.; Préat, V. *J. Control. Release* **2010**, *148* (2), 135–146.

(12) Lockwood, T. D. *Antioxid. Redox Signal.* **2002**, *4* (4), 681–691.

(13) Saito, G.; Swanson, J. A.; Lee, K. D. *Adv. Drug Deliv. Rev.* **2003**, *55* (2), 199–215.

(14) Jones, M. N.; Nicholas, A. R. *Biochim. Biophys. Acta - Biomembr.* **1991**, *1065* (2), 145–152.

(15) Koyanagi, T.; Leriche, G.; Onofrei, D.; Holland, G. P.; Mayer, M.; Yang, J. *Angew. Chem., Int. Ed.* **2016**, *55*, 1890–1893.

(16) De Gracia Lux, C.; Joshi-Barr, S.; Nguyen, T.; Mahmoud, E.; Schopf, E.; Fomina, N.; Almutairi, A. *J. Am. Chem. Soc.* **2012**, *134* (38), 15758–15764.

(17) Barbeau, J.; Belmadi, N.; Montier, T.; Le Gall, T.; Dalençon, S.; Lemiègre, L.; Benvegnu, T. *Tetrahedron Lett.* **2016**, *2*, 1–5.

(18) Mueller, A.; Bondurant, B.; O'Brien, D. F. *Macromolecules* **2000**, *33* (13), 4799–4804.

(19) Koyanagi, T.; Leriche, G.; Yep, A.; Onofrei, D.; Holland, G. P.; Mayer, M.; Yang, J. *Chem. - Eur. J.* **2016**, *22* (24), 8074–8077.

(20) Z. Huang, S. A. B. *Synlett* **1993**, 83–84.

(21) Weinstein, J.; Yoshikami, S.; Henkart, P.; Blumenthal, R.; Hagins, W. *Science.* **1977**, *195* (4277), 489–492.

(22) Banerjee, R. *J. Biol. Chem.* **2012**, *287* (7), 4397–4402.

(23) Brülisauer, L.; Gauthier, M. A.; Leroux, J. *J. Control. Release* **2014**, *195*, 147–154.

(24) Chompoosor, A.; Han, G.; Rotello, V. M. *Bioconjug. Chem.* **2008**, *19* (7), 1342–1345.

(25) Gubernator, J. *Expert Opin. Drug Deliv.* **2011**, *8* (5), 565–580.

(26) Bartlett, G. R. *J. Biol. Chem.* **1959**, *234* (3), 466–468.

(27) Leriche, G.; Cifelli, J. L.; Sibucao, K. C.; Patterson, J. P.; Koyanagi, T.; Gianneschi, N. C.; Yang, J. *Org. Biomol. Chem.* **2017**, *15* (10), 2157–2162.

(28) Temperini, A.; Annesi, D.; Testaferri, L.; Tiecco, M. *Tetrahedron Lett.* **2010**, *51* (41), 5368–5371.

(29) Bajaj, A.; Kondiah, P.; Bhattacharya, S. *J. Med. Chem.* **2007**, *50* (10), 2432–2442.

(30) Weinstein, J. N.; Yoshikami, S.; Henkart, P.; Blumenthal, R.; Hagins, W. *Science.* **1977**, *195* (4277), 489–492.